Poznan University of Technology

FACULTY OF ARCHITECTURE

The Future of Housing Buildings; Optimizing Natural Ventilation Strategies in Polish Housing: Simulation-Based Design for Thermal Comfort in a Changing Climate

Author: mgr. inż . arch. Mohammad Mahdi Mohammadi

Supervisor: dr hab. inż. arch Maciej Janowski

A dissertation submitted to attain the degree of

Doctor of Philosophy in

Architecture and Urban Planning

Poznan 2026

Acknowledgment

To My parents

Dad, even if you no longer remember me,

I will always remember that I stand where I am today because of your sacrifices, and unwavering support.

Mom, as you face your challenges with courage,

I continue to draw strength from your resilience and learn from the truth and determination with which you live your life.

تقدیم به پدر و مادرم

بابا، حتی اگر دیگر مرا به یاد نیاوری،

من همیشه به یاد خواهم داشت که به خاطر فداکاری‌ها و حمایت‌های بی‌دریغ تو در جایگاهی که امروز هستم ایستاده‌ام.

مامان، همانطور که تو با شجاعت با چالش‌هایت روبرو می‌شوی،

من همچنان از انعطاف‌پذیری تو نیرو می‌گیرم و از حقیقت و عزمی که در زندگی‌ات داری، می‌آموزم.

I am deeply grateful to my supervisor, Professor Janowski, for his invaluable guidance and expertise throughout this project. Their insightful feedback and discussion of the finer aspects of this research significantly contributed to the development and completion of this work.

Table of contents

Chapter 03

Chapter 04

Chapter 05

Chapter 06

Table of figures

Chapter 02

Chapter 03

Chapter 04

Chapter 05

Chapter 06

Table of tables

Chapter 02

Chapter 03

Chapter 04

Chapter 05

Chapter 06

Abstract

Climate change and the increasing frequency of summer heatwaves are creating new overheating risks in residential buildings located in climates such as Poland. At the same time, growing cooling demands challenge current sustainability goals and increase dependence on mechanical air-conditioning systems. Natural ventilation offers a low-energy alternative; however, its effectiveness in multi-family housing remains insufficiently understood, particularly under varying wind directions, window configurations, shading strategies, and future climate conditions.

This doctoral research investigates and optimizes cross-ventilation and corner-ventilation strategies in Polish multi-family residential buildings using a simulation-based approach. The study combines architectural analysis, climate assessment, Computational Fluid Dynamics (CFD), solar exposure evaluation, and thermal comfort modelling to examine the influence of building orientation, window size, shading systems, floor level, and wind direction on indoor airflow and thermal conditions. Two representative apartment typologies commonly found in Polish housing were selected as case studies. A validated CFD workflow was developed and verified against experimental data, achieving acceptable accuracy.

A total of 48 simulation scenarios were analyzed, covering two ventilation typologies, two window sizes, three shading configurations, and eight wind directions. The results demonstrate that building orientation is the most influential design parameter, with wind direction producing indoor temperature differences of up to 14.3 °C throughout all cases. Increasing window width by 30 cm reduced indoor temperatures by approximately 1.65°C in bedrooms and 2.1°C in living rooms while improving airflow velocities by up to 0.22 m/s. Larger windows consistently enhanced passive cooling performance, whereas appropriately designed shading devices further reduced overheating risks under high solar exposure. Cross ventilation generally achieved superior thermal performance; however, optimized corner-ventilation configurations also demonstrated significant potential for passive cooling in compact urban housing.

The research further integrated CFD outputs with Standard Effective Temperature (SET) analysis to evaluate occupant thermal perception under present and future climatic conditions. The findings reveal that conventional comfort assessments based solely on weather-file wind speeds may underestimate local discomfort conditions, while high-resolution CFD-based assessments provide a more realistic representation of indoor thermal environments. Simulations conducted under projected 2050 climate conditions indicate a substantial reduction in the effectiveness of passive cooling strategies, highlighting the need for climate-responsive architectural design.

The study contributes to building science by bridging architecture, building physics, and computational modelling through the development of evidence-based design recommendations for naturally ventilated residential buildings. The findings provide practical guidance for architects, engineers, and policymakers seeking to improve thermal comfort, reduce overheating risk, and enhance climate resilience in Polish housing and similar temperate-climate regions.

Keywords: Natural ventilation, cross ventilation, corner ventilation, thermal comfort, CFD, Standard Effective Temperature (SET), passive cooling, overheating, residential buildings, Poland, climate change.

Streszczenie

Zmiany klimatyczne i rosnąca częstotliwość letnich fal upałów stwarzają nowe zagrożenia przegrzania w budynkach mieszkalnych zlokalizowanych w klimatach takich jak polski. Jednocześnie rosnące zapotrzebowanie na chłodzenie stanowi wyzwanie dla obecnych celów zrównoważonego rozwoju i zwiększa zależność od mechanicznych systemów klimatyzacji. Wentylacja naturalna oferuje energooszczędną alternatywę; jednak jej skuteczność w budownictwie wielorodzinnym pozostaje niedostatecznie poznana, szczególnie w przypadku zmiennych kierunków wiatru, konfiguracji okien, strategii zacieniania i przyszłych warunków klimatycznych.

Niniejsza rozprawa doktorska bada i optymalizuje strategie wentylacji poprzecznej i narożnej w polskich budynkach wielorodzinnych, wykorzystując podejście oparte na symulacji. Badanie łączy analizę architektoniczną, ocenę klimatu, obliczeniową mechanikę płynów (CFD), ocenę nasłonecznienia i modelowanie komfortu cieplnego, aby zbadać wpływ orientacji budynku, wielkości okien, systemów zacieniania, poziomu podłogi i kierunku wiatru na przepływ powietrza i warunki termiczne w pomieszczeniach. Jako studia przypadków wybrano dwa reprezentatywne typy mieszkań powszechnie spotykane w polskim budownictwie mieszkaniowym. Opracowano i zweryfikowano z danymi eksperymentalnymi sprawdzony proces pracy CFD, uzyskując akceptowalną dokładność. Przeanalizowano łącznie 48 scenariuszy symulacyjnych, obejmujących dwie typologie wentylacji, dwa rozmiary okien, trzy konfiguracje zacieniania i osiem kierunków wiatru. Wyniki pokazują, że orientacja budynku jest najważniejszym parametrem projektowym, a kierunek wiatru powoduje różnice temperatur wewnętrznych sięgające 14,3°C we wszystkich przypadkach. Zwiększenie szerokości okien o 30 cm obniżyło temperaturę wewnętrzną o około 1,65°C w sypialniach i 2,1°C w salonach, jednocześnie poprawiając prędkość przepływu powietrza nawet o 0,22 m/s. Większe okna konsekwentnie poprawiały wydajność pasywnego chłodzenia, a odpowiednio zaprojektowane urządzenia zacieniające dodatkowo zmniejszały ryzyko przegrzania przy dużym nasłonecznieniu. Wentylacja poprzeczna generalnie zapewniała lepszą wydajność termiczną; jednak zoptymalizowane konfiguracje wentylacji narożnej wykazały również znaczny potencjał pasywnego chłodzenia w kompaktowych budynkach miejskich.

Badania dodatkowo zintegrowały wyniki CFD z analizą Standardowej Temperatury Efektywnej (SET), aby ocenić percepcję termiczną mieszkańców w obecnych i przyszłych warunkach klimatycznych. Wyniki badań ujawniają, że konwencjonalne oceny komfortu oparte wyłącznie na danych pogodowych dotyczących prędkości wiatru mogą niedoszacować lokalnych warunków dyskomfortu, podczas gdy oceny o wysokiej rozdzielczości oparte na CFD zapewniają bardziej realistyczne odwzorowanie środowiska termicznego wewnątrz budynków. Symulacje przeprowadzone w prognozowanych warunkach klimatycznych na rok

2050 wskazują na znaczne obniżenie skuteczności pasywnych strategii chłodzenia, co podkreśla potrzebę projektowania architektonicznego uwzględniającego zmiany klimatu.

Badanie wnosi wkład do nauki o budownictwie, łącząc architekturę, fizykę budowli i modelowanie obliczeniowe poprzez opracowanie opartych na dowodach rekomendacji projektowych dla budynków mieszkalnych z wentylacją naturalną. Wyniki badań dostarczają praktycznych wskazówek architektom, inżynierom i decydentom dążącym do poprawy komfortu termicznego, zmniejszenia ryzyka przegrzania i zwiększenia odporności na zmiany klimatu w polskim budownictwie mieszkaniowym i podobnych regionach o klimacie umiarkowanym.

Słowa kluczowe: wentylacja naturalna, wentylacja poprzeczna, wentylacja narożna, komfort termiczny, CFD, Standardowa Temperatura Efektywna (SET), chłodzenie pasywne, przegrzanie, budynki mieszkalne, Polska, zmiany klimatu.

List of abbreviations

WWR: Window to Wall Ratio

NV: Natural Ventilation

CV: Cross Ventilation

CFD: Computational Fluid Dynamics

HVAC: Heating, Ventilation, and Air Conditioning

LCC: Life Cycle Cost

IEQ: Indoor Environmental Quality

DHW: Domestic Hot Water

PEB: Plus Energy Buildings

PH: Passive House

PV: Photovoltaic

EPC: Energy Performance Certificates

EP: Energy Performance

BPS: Building Performance Simulations

BES: Building energy Simulation

BEM: Building Energy Modeling

DSF: Double-Skin Facade

RMSE: Root Mean Square Error

CV-RMSE: Coefficient of Variation of the Root Mean Square Error

H: Height

L: Length

V: Velocity

T: Temperature

TMY: Typical Meteorological Year

DSY: Design Summer Year

IPCC: Intergovernmental Panel on Climate Change

SET: Standard Effective Temperature

MRT: Mean Radiant Temperature

EPW: Energy Plus Weather

RH: Relative Humidity

GF: Ground Floor

FF: First Floor

Author contribution statement

This thesis is an original work by the author and has not been previously published in its entirety.

Small portions of this work may have appeared in the following publications, for which the author holds the copyright:

- *Mohammadi, M.M. and M. Janowski, The impact of size in fenestration design on the airflow and temperature in natural cross ventilation, case study: A two-bedroom Polish multifamily home. BUILDER, 2023. 315(10): p. 74-83.*
- *Mohammadi, M.M. and M. Janowski, Evaluating the Impact of Horizontal Louvers on Natural Ventilation and Thermal Comfort in Polish Multi-Family Homes: A CFD Analysis, in 9th EACWE. 2025: Trondheim, Norway. p. 556-560.*
- *Bazazzadeh, H., et al., AI- aided surrogate model for prediction of HVAC optimization strategies in future conditions in the face of climate change. Energy Reports, 2025. 13: p. 1834-1845.*

Except for the aforementioned publications, no part of this thesis has been published or submitted for publication elsewhere. The research, analysis, and writing presented herein were conducted solely by the author as part of doctoral studies at Faculty of Architecture and Urban Planning at Poznan University of Technology.

Chapter 01: Overview

1 Introduction

Thermal comfort in European residential buildings is strongly influenced by both the window-to-wall ratio (WWR) and the use of shading strategies. Larger windows can increase daylight and views but also raise the risk of overheating and higher cooling loads, especially during summer or heatwaves [1, 2]. However, research consistently shows that when effective shading, such as external blinds, overhangs, or dynamic systems, is combined with optimized WWR, it is possible to achieve better thermal comfort without sacrificing daylight or energy efficiency [3, 4]. This interaction allows for larger windows while mitigating overheating risks, particularly when paired with high-performance glazing and passive cooling measures [5]. The optimal balance depends on climate, orientation, glazing type, and occupant behavior, but integrated design approaches that consider both WWR and shading are key to resilient and comfortable homes in Europe.

2 Research hypothesis and scientific problem

Contemporary residential buildings in cold climates, such as those in Poland, are increasingly vulnerable to overheating due to climate change and heatwaves [6, 7]. Existing natural ventilation strategies, particularly in cross and corner ventilation scenarios [8], are often inadequately applied or poorly understood in terms of their real-world performance under variables like wind directions, solar exposure, and building geometries [9]. Furthermore, the use of simplified models in prior studies fails to capture the complex interactions between airflow, thermal loads, shading design, and building floor levels, etc. leading to design decisions that may be scientifically imprecise and inefficient.

The configuration of openings, specifically window size [10, 11], orientation, and shading design [12] has a measurable and optimizable impact on reducing overheating and improving airflow in residential buildings with cross ventilation potential. Accurate simulation-based analysis using realistic geometries and actual climate conditions will reveal that larger windows, when properly oriented and shaded, enhance passive cooling performance. This approach will challenge the limitations of generic shoebox models and supports the development of a constructional viable and climate-responsive ventilation strategies.

3 Purpose of research

The purpose of this research is to investigate and optimize natural ventilation strategies (cross & corner ventilation) in residential buildings under current and future climate conditions. Through the use of detailed computational simulations and realistic architectural models, the study aims to assess how window size, placement, shading devices, and wind direction influence indoor air temperature and airflow. The goal is to provide scientifically validated **design guidelines** and **methodology** that improve thermal comfort, reduce overheating, and support energy-efficient, real-scale practical solutions for retrofitting or designing housing in Poland.

The research also seeks to bridge the gap between simulation practices that traditionally focused on engineering aspect, airflow behavior, energy performance; and architectural design needs, which prioritize spatial functionality, aesthetics, human comfort, and construction feasibility. By integrating advanced Computational Fluid Dynamics (CFD) simulations into the architectural design process and applying them to a realistic, full-scale residential layouts rather than abstract or simplified models, this study provides architects with practical, evidence-based tools to make early-stage design decisions. This interdisciplinary approach enables more accurate prediction of thermal and airflow performance under real-world conditions, supporting the creation of housing that is not only efficient but also adaptive to future climate scenarios. Ultimately, the research tries to contribute to more resilient and climate-responsive residential environments by aligning performance-driven design strategies with the practical and creative demands of architecture.

4 Concept and description of scientific research

This research addresses the growing challenge of overheating in residential buildings in different climates, particularly in countries like Poland, where climate change has intensified summer heatwaves. The study focuses on evaluating and optimizing passive cooling strategies through natural ventilation (specifically in cross and corner ventilation layouts) which are often underutilized or poorly implemented in current residential designs.

Using a combination of literature review, real-world case analysis, and advanced Computational Fluid Dynamics (CFD) simulations, the research investigates how key architectural variables such as **shape, orientation, building porosity, window size, shading devices** (overhangs, side fins, and louvers), **wind direction, solar exposure, and building floor level** affect indoor temperature and airflow. The methodology involves modeling realistic multi-room apartment layouts instead of simplified shoebox geometries, allowing for more accurate assessment of ventilation performance in both standard and corner-apartment typologies.

The scientific aim is to quantify the thermal and airflow impact of different design scenarios under varying climatic and spatial conditions. A special focus is placed on identifying critical areas for overheating and evaluating how strategic design interventions can mitigate thermal discomfort.

The findings will support the development of practical design strategies for architects and urban planners by offering detailed, simulation-based evidence for improved window configurations and ventilation planning.

5 Research method used and methodology

This research follows a two-phase methodology combining **qualitative** and **quantitative** approaches. The first phase includes a literature review and typological analysis of over 300 residential units across seven Polish cities. This stage focuses on identifying common architectural features, indoor spatial layout, window configurations, and ventilation strategies in both cross and corner apartments. These findings inform the selection of two representative case studies (one for normal cross ventilation and one for corner ventilation) for in-depth simulation analysis.

The second phase employs advanced numerical simulations using Computational Fluid Dynamics (CFD). Autodesk CFD is used for the main simulation work, while selected cases are validated through cross-platform comparison with OpenFOAM via the Butterfly plugin for Grasshopper. Each case study is modeled in 3D with realistic architectural geometry including some minor simplifications and tested under 8 wind directions, 2 window sizes (baseline and large), and 3 shading strategies (Baseline, with overhang and sidefins, and with louvers). Key environmental variables including temperature, airflow velocity, and wind behavior pattern are extracted at multiple indoor points across two floors.

Raw simulation data are cleaned, averaged, and categorized by room type (living room and bedroom) and floor level (ground and first floor). Differences in temperature and velocity between scenarios are analyzed to identify patterns and critical zones affected by overheating or poor ventilation. The results are further interpreted in relation to thermal comfort targets. The methodology emphasizes accuracy and architectural relevance by avoiding oversimplified box models, enabling practical conclusions that align with real design contexts.

6 Description of expected results of scientific research

The expected results of this research include a comprehensive evaluation of how window size, orientation, and shading configurations influence indoor thermal conditions and airflow in cross and corner-ventilated residential buildings. Through detailed CFD simulations and scenario analysis, the study anticipates confirming that larger window areas, when appropriately oriented with effective shading strategies, significantly reduce indoor temperatures and improve natural airflow, especially during the summer months under changing climate conditions and heatwaves.

The research also expects to identify specific wind directions and opening combinations that lead to critical overheating or poorly ventilated zones, especially on upper floors and in sun-exposed façades. It is anticipated that ground floor units will show relatively lower temperatures due to shading from surrounding structures, but will exhibit reduced airflow compared to upper floors. First-floor spaces are expected to demonstrate stronger ventilation rate but also increased vulnerability to overheating, especially in sun-facing layouts.

Another key result is the validation of corner ventilation as a viable but underutilized passive cooling strategy. The study aims to provide quantified evidence showing that strategic window placement in corner configurations can match or even exceed traditional cross-ventilation performance under certain conditions. These findings will contribute to better-informed decisions in both new residential design and energy-efficient retrofitting of existing housing stock.

7 Innovation, importance and influence of research

The innovation of this research lies in its architectural application of advanced simulation tools to evaluate realistic building typologies under climate change conditions, moving beyond oversimplified models traditionally used in engineering-based ventilation studies. By integrating corner ventilation as a focus (an under-researched yet constructional relevant strategy) the study introduces a novel perspective on natural ventilation in compact urban housing.

The expected results contribute significantly to the development of science by combining CFD with architecture, offering a multidimensional understanding of how window configurations, shading, and wind behavior interact within actual residential spaces. This interdisciplinary approach bridges gaps between building physics, environmental design, and housing research.

From a societal perspective, the findings offer practical, low-cost strategies to improve thermal comfort in dwellings, particularly in existing multi-family buildings vulnerable to overheating. As energy demand for cooling continues to rise globally, especially in cool and temperate regions facing more frequent heatwaves, such research supports public health, housing resilience, and energy equity.

In the broader context of civilization and climate adaptation, this work contributes to the discourse on sustainable urban living by empowering architects, engineers, and policymakers with evidence-based design guidelines. These strategies promote comfort and energy efficiency without relying on mechanical systems aligning with global sustainability goals and EU climate directives for the building sector.

8 Opening

The following chapters continue the research in the same logical sequence embedded in the title and central objective of this dissertation. The journey begins by establishing the theoretical foundation of natural ventilation. In the second chapter, the literature development of natural ventilation research is explored, along with its principles, mechanisms, and typologies. This review traces how natural ventilation evolved from traditional passive strategies to contemporary simulation-based approaches and identifies the major research gaps that shaped the direction of this study.

Following this, the discussion narrows to the context of multi-family housing in Poland, examining the architectural characteristics, limitations, and environmental challenges of building typology. Finally, chapter three investigates the specific literature and current condition of natural ventilation in Polish apartments, highlighting why this topic remains rather underexplored despite increasing cooling demands caused by climate change.

Chapter Four translates these theoretical discussions into a practical research framework. It explains the full methodological process of the study, including the selection of representative case studies, classification of housing typologies, development of simulation scenarios, and the modeling workflow. This chapter describes the process of creating realistic architectural models and explains the CFD, solar radiation, and environmental simulation methods used throughout the research.

Chapter Five moves into the analytical phase of the research. First, simulation models are validated under repeated and controlled conditions to ensure the accuracy of the process and setting. Following validation, the results are presented systematically through a detailed spatial analysis of each case. The performance of the strategies is examined room-by-room, floor-by-floor, and case-by-case to identify how variables such as wind direction, window size, and shading systems influence airflow behavior and indoor temperature distribution.

Finally, Chapter Six expands the discussion beyond CFD outputs alone. While airflow simulations form the technical foundation of this research, air velocity by itself cannot fully explain human comfort. Therefore, CFD results are integrated into thermal comfort simulations to evaluate how occupants actually experience indoor environments. This chapter translates engineering outputs into a more understandable human-centered scale by examining perceived temperature under both current and future climate scenarios. The use of future morphed weather files further highlights the urgency of climate-responsive housing design and demonstrates how strategies that perform adequately today may become insufficient in future conditions.

Together, these chapters reflect the overall progression of the dissertation: from theory, to methodology, to simulation, and finally to synthesis and future adaptation.

Chapter 02: Natural ventilation

1 Introduction

Natural ventilation is a crucial area of study in contemporary building design, with a growing body of literature recognizing its vital role in indoor air quality (IAQ), thermal comfort, and building energy consumption [13]. Natural ventilation can improve indoor environments and reduce reliance on mechanical systems [14-16]. A comprehensive literature review in this chapter reveals various methodologies, airflow patterns, ventilation models, and influencing parameters associated with natural ventilation, especially cross ventilation.

2 Literature summary

The co-occurrence network of terms for a period of 95 years (1930-2025) and the overlay visualization were produced following scientific mapping using VOSviewer [17]. The visual represents a keyword co-occurrence network map generated from literature related to natural ventilation, thermal comfort, and energy efficiency in buildings. Each cluster of colored nodes indicates a thematic grouping of research topics: yellow focuses on natural ventilation and passive design, blue on thermal comfort and environmental conditions, green on indoor air quality and occupant behavior, and red on energy use, climate change, and building systems. The central terms like natural ventilation, thermal comfort, ventilation, serve as bridges between clusters, indicating the relevance and interdisciplinary connections. This visualization illustrates the complexity and interdependence of key research themes in sustainable building design and highlights the growing integration of airflow modeling, comfort studies, and energy performance in current architectural research.

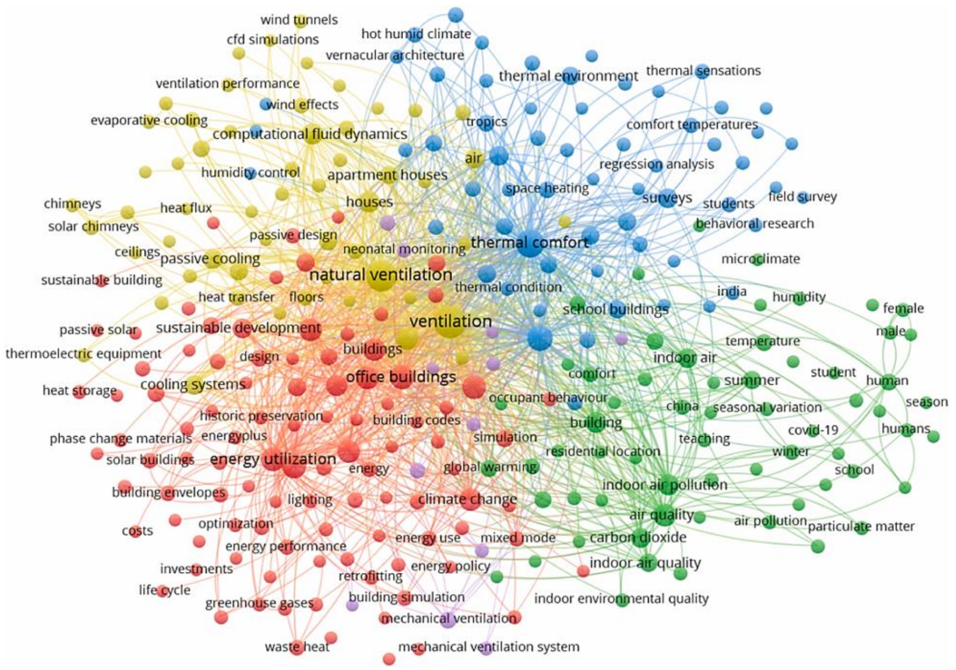

Fig. 2- 1: Co-occurrence network of keywords (Source: Created by the authors using VOSviewer and Scopus data).Benefits and Significance [17].

By narrowing down and limiting the search scope to the keywords on window to wall ratio (WWR), shading and thermal comfort in residential buildings in the period 2015 to 2025, 212 relevant researches were found, which is demonstrated below. The graph below also shows the distribution of the papers over these years.

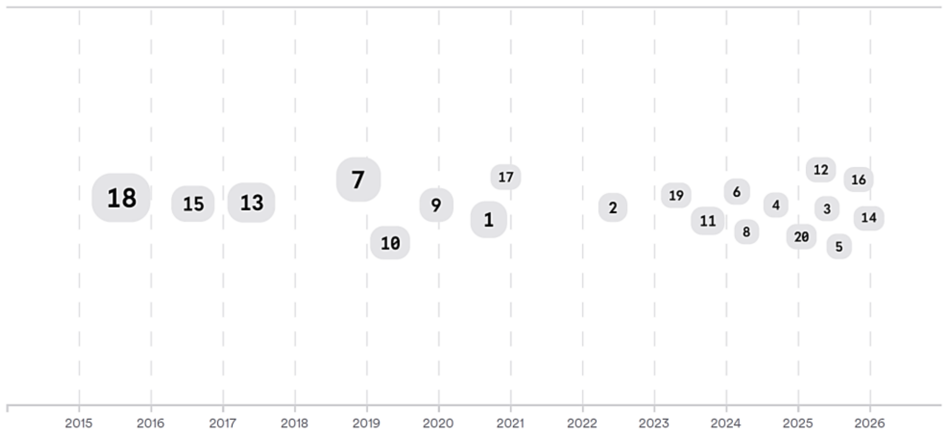

Fig. 2- 2: Timeline (2015-2025) of 212 key studies on window to wall ratio (WWR) and shading interaction for thermal comfort. Larger markers indicate more citations.

To identify the research gap and establish the scientific foundation of this study, a structured literature review process was first conducted at the beginning of the doctoral research in 2021. The review focused on publications between 2015 and 2021 using combinations of keywords related to natural ventilation parameters, window-to-wall ratio (WWR), shading devices, thermal comfort, and residential buildings (building program). After applying database filters and manually screening titles, abstracts, and study relevance, approximately 90 articles were identified as directly relevant to the research topic. This initial review played a critical role in defining the scope of the dissertation and identifying underexplored intersections between façade design variables, airflow performance, and indoor thermal comfort.

During the completion of this doctoral research, the same review process was repeated and updated to include studies published between 2021 and 2025. The updated review revealed that approximately 120 additional studies were published during this relatively short period. As illustrated in Figure 2-2, this increase demonstrates that research on thermal comfort, and passive cooling strategies has become an important global research trend, particularly in response to climate change, overheating risks, and growing cooling demands in buildings. The rapid expansion of literature also confirms the relevance and timeliness of this dissertation, as the research directly aligns with a fast-growing scientific field.

Topic/Outcome	Simulation Studies	Field Studies	Residential Focus	Office/Educational
Overheating risk	24	4	14	11
Optimal WWR range	20	2	12	11
Shading device effectiveness	22	4	12	14
Thermal comfort	11	3	4	3

Table 2- 1: Showing where research is focused and the gap based on key topics related to WWR, shading, and thermal comfort in different scenarios in 2015-2021.

To better illustrate existing research concentrations and identify unresolved gaps, Table 2-1 summarizes the dominant directions of previous studies. The table demonstrates that most research has focused heavily on simulation-based investigations of overheating risk, optimal WWR ranges, and shading performance. While residential buildings receive considerable attention, many studies remain concentrated on office and educational buildings. More importantly, thermal comfort appears significantly underrepresented compared to other performance indicators, particularly in residential applications. This imbalance highlights a critical research gap: many studies evaluate façade variables such as windows and shading systems primarily through energy or temperature metrics, while fewer investigate how these design decisions influence occupant comfort through integrated airflow and thermal analysis. This gap directly informs the methodology of the present study.

This section presents the most relevant, recent, and methodologically significant studies identified through this review process. To improve clarity, these studies are categorized based on their primary themes, including natural ventilation performance, window design, shading strategies, thermal comfort assessment, and climate adaptation. This thematic structure helps position the current research within existing knowledge while clearly demonstrating how this dissertation extends previous studies through a more integrated architectural and simulation-based approach.

3 Types of natural ventilation

Several natural ventilation strategies can be employed in building design, each with its own characteristics and applicability:

Cross Ventilation (CV): Cross ventilation is considered the most efficient type of natural ventilation, involving airflow through a building via different inlet and outlet openings driven by pressure differences [13, 14, 18] from different sides of the building.

Single-Sided Ventilation (SSV): Single-sided ventilation relies on air exchange through a single opening, making it less effective than cross ventilation [18, 19] but still viable in certain contexts.

Mixed-Mode Ventilation (MM): Mixed-mode ventilation combines natural and mechanical systems to optimize indoor conditions [17].

Natural ventilation (NV) operates based on different driving forces and is typically classified as wind-driven [20], buoyancy-driven [21], or a combination of both [22]. Depending on the placement and configuration of openings, NV can be further categorized into four main strategies: cross ventilation (CV) [20], corner ventilation (CRV) [23], stack ventilation (SV) [24], and single-sided ventilation (SSV) [25], as illustrated in Fig. 2-3.

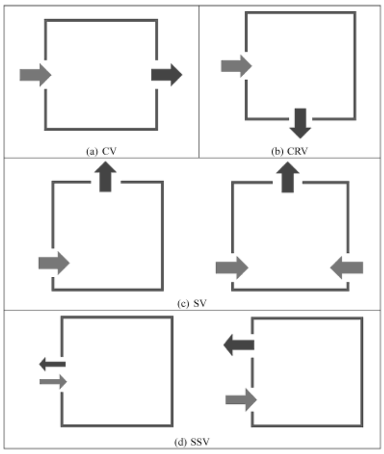

Fig. 2- 3: Classification of NV strategies: (a) cross ventilation (CV) and (b) corner ventilation (CRV) on the horizontal plane; (c) stack ventilation (SV) on the vertical plane; (d) single-sided ventilation (SSV) on the vertical/horizontal plane [8].

Different types of ventilation from different sources are demonstrated:

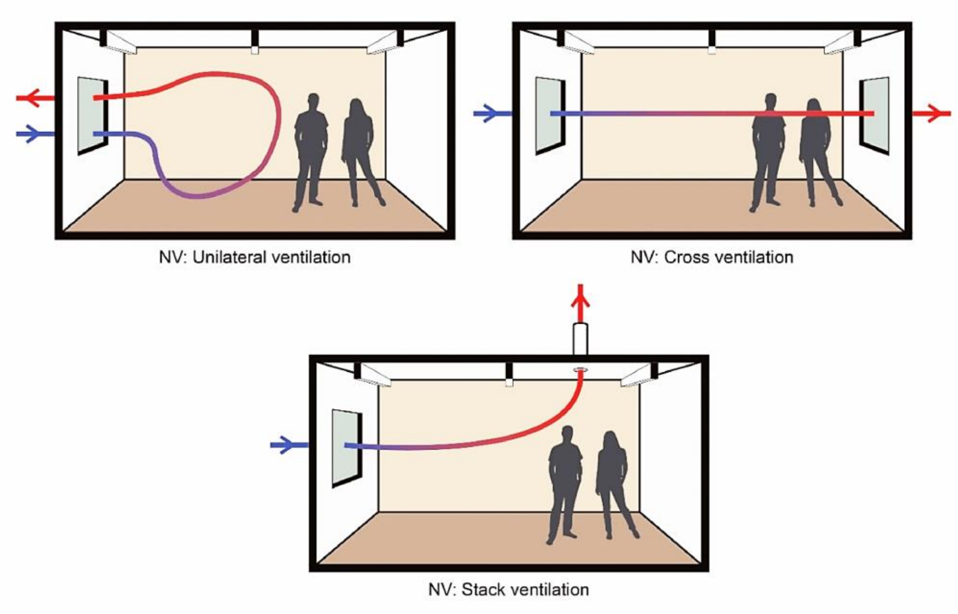

Fig. 2- 4: Schematically shows the principles of these classes of NV [17].

Natural ventilation offers several key advantages:

Improved Indoor Air Quality: Natural ventilation can effectively prevent airborne contagion and reduce the risks associated with Sick Building Syndrome. Research indicates that good natural ventilation design lowers carbon dioxide concentration and improves thermal comfort, leading to increased occupant productivity [13, 26, 27].

Thermal Comfort: Natural ventilation helps maintain comfortable indoor temperatures by facilitating the movement of air, which can have a positive impact on health [18].

Energy Efficiency: By harnessing natural forces like wind and thermal buoyancy, natural ventilation reduces the energy consumption associated with mechanical ventilation systems [14, 28].

3.1 Parameters influencing natural ventilation (CV)

Before discussing cross ventilation, it is important to briefly mention single-sided ventilation, which is the most common natural ventilation strategy in residential buildings. This method relies on openings located on only one façade, where airflow is driven by wind pressure fluctuations and buoyancy effects. Although widely applied in apartment buildings due to structural limitations, its effectiveness is often restricted by shallow airflow and the formation of stagnant indoor zones, therefor it is dominant in this field of study and the most important influencing elements are listed in Fig. 2-5.

Cross ventilation (CV) is also a widely studied and applied natural ventilation technique. Jiang et al. [13] note that it is the most efficient natural ventilation type. The investigation of the mechanisms and phenomena behind CV can aid in gaining a more profound comprehension of the principles of natural ventilation [13, 19, 29, 30].

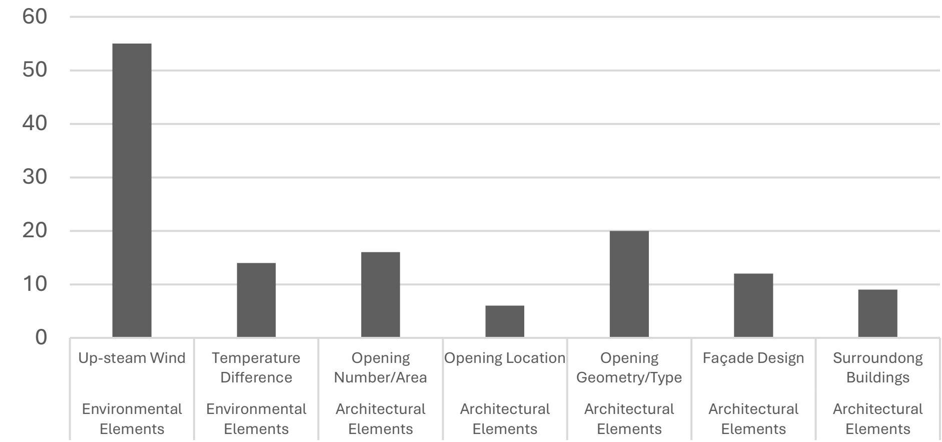

Fig. 2- 5: Proportion of different influencing elements considered in the reviewed SSV papers [8].

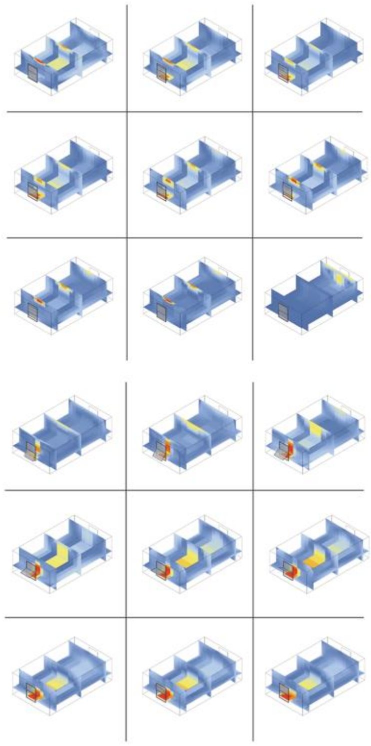

Cross ventilation, a highly effective form of natural ventilation, is driven by pressure differences across a building created by wind, allowing for the exchange of indoor and outdoor air through openings on opposing facades. This process is crucial for enhancing indoor air quality by removing pollutants, improving thermal comfort by dissipating heat, and significantly reducing building energy consumption associated with mechanical ventilation systems. The performance of cross ventilation is significantly influenced by factors such as wind speed and direction (airflow pattern), the size and location of openings, and the internal layout of the building and some other parameters:

- Airflow patterns: Cross ventilation involves air entering a building through an opening on one side and exiting through an opening on the opposite side [15, 16, 31-33]. The resulting airflow helps remove indoor pollutants and regulate temperature.
- Ventilation models: Various models are used to simulate and analyze cross-ventilation, including power balance models and local dynamic similarity models [34-36].
- Influencing parameters: Parameters such as opening size, location, wind direction, and internal layout affect the efficiency of cross ventilation [18, 37, 38].

Several other factors affect the performance and effectiveness of natural ventilation systems [39-41] these parameters are the main focus for this specific study:

Building Design and Orientation: The layout and orientation of a building significantly impact how natural ventilation performs. Optimizing building design to capture prevailing winds and facilitate airflow is essential [18, 38].

Opening Size and Configuration: The size and configuration of openings, such as windows and vents, affect ventilation rates. Larger openings generally allow for greater and better airflow patterns, but strategic placement is also critical [18]. Zhang et al. display that two-opening configurations proved to be tremendously efficient for cross-ventilation [18]. Using a larger opening on the windward or leeward surface, the two-opening window configuration achieves higher ventilation rates and better indoor wind circulation than both the three- and four-opening window configurations [18]. The other research regarding the opening configurations is presented in Fig. 6, 7, & 8.

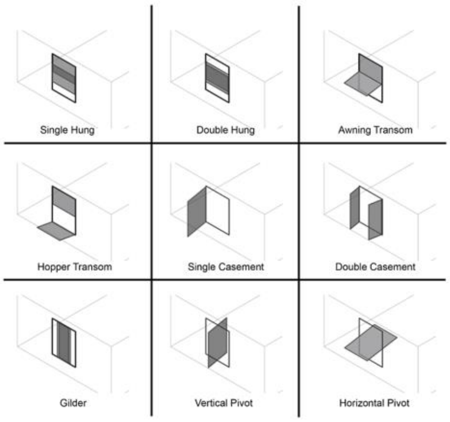

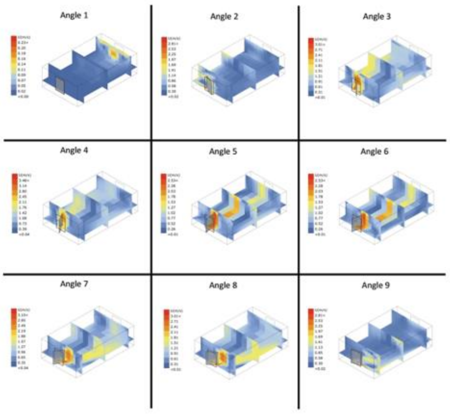

Fig. 2- 6 (Left) Matrix of 9 window design [42, 43].

Fig. 2- 7 (Right): CFD simulation of window 8 (vertical pivot) with 9 different opening positions, resulting in large variation in airflow velocity, direction and zoning [43].

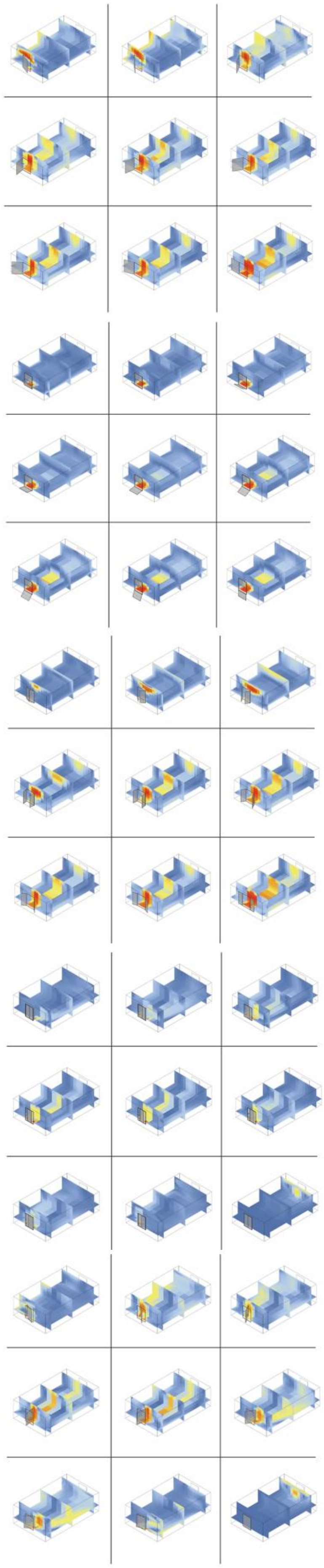

Fig. 2- 8 (Top to bottom): CFD simulation and airflow pattern of double sliding widow, hopper transom window, single casement window, awing transom widow, double casement window, gliding window, horizontal pivot window, vertical pivot window [43].

Location: The location of openings influences airflow patterns and ventilation efficiency. Openings in the upper part of windward walls tend to provide higher airflow velocity [18].

Window Type: The type of window or vent can also play a role. For example, windows with louvers can help control airflow and prevent rain infiltration [18], however this statement is also being examined though out this study in order to better evaluate the effect of louvers on natural ventilation.

Wind speed and direction: Wind speed and direction are critical determinants of natural ventilation performance. High wind speeds can enhance ventilation rates, but the direction must align with building openings for effective cross ventilation [39].

Urban context: The surrounding urban environment can either impede or facilitate natural ventilation [9, 44-49]. Buildings in densely built areas may experience reduced wind speeds due to blocking effects from adjacent structures [37, 50, 51].

Pollution: High levels of outdoor air pollution can negate the benefits of natural ventilation unless appropriate filtrations are in place [13, 19].

Noise: Excessive noise from external sources can also be a deterrent to natural ventilation, especially in urban environments [52-55].

Temperature and humidity: Climatic conditions significantly influence the viability of natural ventilation. In warm climates, natural ventilation can reduce cooling loads, but it may struggle to maintain thermal comfort during heatwaves [19].

Seasonal variations: Seasonal variations in temperature and wind patterns also affect the performance of natural ventilation [9, 49, 56, 57].

Internal layout and obstructions: The internal layout of a building and the presence of obstructions can significantly modify indoor wind fields and reduce ventilation rates [18].

In conclusion, cross ventilation stands as a cornerstone of sustainable building design, offering a natural means to achieve healthy and comfortable indoor environments by leveraging wind-driven airflow. While significant progress has been made in understanding its fundamental principles and influencing factors, ongoing research continues to explore optimal design strategies, considering diverse building configurations, environmental conditions, and the integration with other passive and active systems to fully realize its potential in creating resilient and high-performance buildings.

4 Natural ventilation in specific building types

The application of natural ventilation varies depending on the building type and its specific requirements [18, 38, 58]. In residential buildings natural ventilation is commonly used to improve indoor air quality and reduce energy consumption [17, 58]. Effective strategies include optimizing window placement and promoting cross ventilation [17, 38].

In office buildings natural ventilation can enhance thermal comfort and reduce cooling loads in [17, 18, 59-63]. However, careful design is needed to address issues such as noise and air pollution.

In healthcare facilities like hospitals, natural ventilation must be carefully managed to minimize the risk of infection transmission. Design parameters and slight positive pressure in critical areas are essential considerations [39].

In educational buildings, while natural ventilation can be beneficial, it may not always maintain adequate CO_2 levels [58]. Therefore, hybrid or mechanical systems might be necessary [58, 64].

Natural ventilation in underground spaces requires specific design considerations to ensure adequate airflow and air quality. Optimizing the integration of aboveground and underground spaces is crucial [49, 65, 66].

5 Challenges and Limitations

Despite its advantages, natural ventilation faces several challenges and limitations:

Adverse ambient conditions: Natural ventilation can introduce adverse ambient conditions such as deteriorating air quality, street noise, and excessive heat gain or loss [13]. High ventilation rates can lead to local draughts, wind noise, and interruptions to indoor activities due to excessive airflow [13].

Heatwaves and climate change: During heatwaves and in future climate scenarios, natural ventilation alone may not suffice to maintain thermal comfort [19, 67, 68]. Ahmed et al. [19] note that single-sided ventilation demonstrates the poorest ability to provide thermal comfort, while cross ventilation highlights better performance in terms of reducing indoor air temperatures compared to outdoor. However, windcatchers and solar chimneys displayed even better performance by producing relatively high ventilation rates [19].

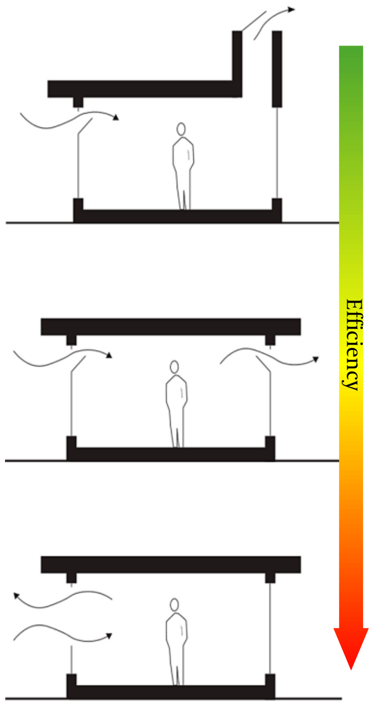

Fig. 2- 9: Natural ventilation: stack ventilation (top), cross ventilation (middle) and single-sided ventilation (bottom) [58]. Edited by author.

Indoor air quality: In urban areas or regions with high pollution levels, natural ventilation can compromise indoor air quality by drawing in pollutants [69, 70].

External factors: Natural ventilation's effectiveness is highly dependent on external factors such as wind speed, direction, and temperature differences, which can be unpredictable [39].

Design: Designing effective natural ventilation requires considerable expertise, which can hinder their widespread application [13].

Building regulations and standards: Compliance with building regulations and ventilation standards can pose additional challenges [71].

6 Tools and techniques for assessing NV

Various tools and techniques are employed to assess and optimize natural ventilation in buildings:

Computational Fluid Dynamics (CFD): CFD simulations are used to model airflow patterns and predict ventilation performance [18, 28, 49, 71]. These simulations can help visualize airflow and identify potential issues in building design [18, 49]. These simulations employ numerical analysis and turbulence models to solve the complex equations governing fluid motion, thereby providing detailed insights into how air moves within and around buildings. By simulating airflows, CFD can quantify crucial ventilation metrics such as airflow rates, air change per hour (ACH), age of air (AOA), and wind velocity distributions. Different CFD techniques, including RANS, LES, and DNS, offer varying levels of accuracy and computational cost, with LES being particularly useful for capturing wind flow fluctuations. Furthermore, CFD can be integrated with other simulation tools like Building Energy Simulation (BES) and Airflow Network Models (ANM) through coupling methods, offering a more holistic understanding of building performance by considering both ventilation and energy consumption.

These detailed simulations enable designers to visualize complex three-dimensional airflow patterns using tools like velocity vectors and streamlines, which is essential for comprehending how air interacts with the building's geometry and internal layout. This visualization capability allows for the identification of potential issues that might hinder effective ventilation. For instance, CFD can reveal areas with poor air mixing, the occurrence of short-circuiting where fresh air bypasses occupied zones, and the negative impacts of internal walls or surrounding buildings on airflow. By conducting parametric studies, where design variables are systematically altered, CFD can help optimize building designs to enhance natural ventilation performance, such as determining the most effective placement and size of openings or the ideal configuration of internal partitions. Ultimately, while requiring validation against experimental data, CFD simulations offer a powerful means to analyze and improve ventilation strategies in buildings. This tool is used for this study and will explore more detailed about it in the future chapters.

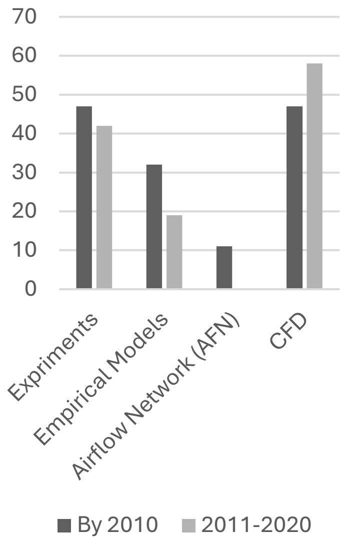

Fig. 2- 10: Proportion of different methodologies applied in the reviewed papers [8]. Graph by author.

Wind tunnel experiments: Wind tunnel experiments provide valuable data on airflow around buildings and the effectiveness of different ventilation strategies [18, 19, 37]. These experiments, which can be conducted at both full and reduced scales (as for buildings normally reduced scale), allow for controlled investigation of wind properties like direction and velocity, and building parameters such as opening configurations. Reduced-scale experiments are particularly advantageous due to their repeatability and cost-effectiveness, making them applicable in the building design stage. Wind tunnels enable researchers to measure wind pressure distributions on building surfaces and airflow characteristics within and around the models under various conditions. The data obtained from experiments is vital for validating CFD simulations, assessing the impact of building geometry, opening size and location, internal partitions, and even the influence of surrounding urban environments on ventilation performance. Techniques like velocity integration and tracer gas methods are employed in wind tunnels to quantify ventilation rates, and innovative approaches like rotating building models are used to simulate the effects of fluctuating wind conditions on cross-ventilation.

Airflow network models: Airflow network models are integrated with building energy simulations to evaluate the energy savings potential of natural ventilation [28, 49, 72-74].

Tracer gas techniques: Tracer gas methods measure ventilation rates and air exchange effectiveness within buildings [71, 75, 76].

On-site measurements: Field measurements in real buildings provide empirical data on ventilation performance and thermal comfort [18, 77].

Several strategies focusing on optimized building design can significantly enhance the performance and applicability of natural ventilation. Proper building orientation is a crucial factor, as aligning a building to effectively capture prevailing winds can maximize the potential for wind-driven natural ventilation. Studies have shown that wind direction relative to the openings significantly affects cross-ventilation performance, with perpendicular winds generally resulting in the highest ventilation rates. Several other strategies can enhance the performance and applicability of natural ventilation:

- Building orientation: Proper building orientation to capture prevailing winds can maximize natural ventilation [38, 71, 78-80].
- Window placement: Strategic placement of windows to facilitate cross ventilation can significantly improve airflow [18, 38].
- Building shape: Aerodynamic building shapes can enhance wind-driven ventilation [18].

Furthermore, strategic placement of windows is essential to facilitate effective airflow within the building. Designing for cross-ventilation, which involves having openings on opposite sides, is a particularly efficient natural ventilation strategy as it allows large volumes of air to flow through, effectively removing indoor pollutants and heat. The size, location, and number of openings play a critical role in the ventilation rate and indoor airflow patterns. For example, having a larger opening on the leeward side in a two-opening configuration can increase cross-ventilation. Finally, the aerodynamic shape of a building can also be designed to enhance wind-driven ventilation. While there are sources provide more specific details on elements like roof shape and eaves [81] influencing airflow, the general principle is that building forms can be optimized to better interact with wind patterns and promote natural airflow in architecture design.

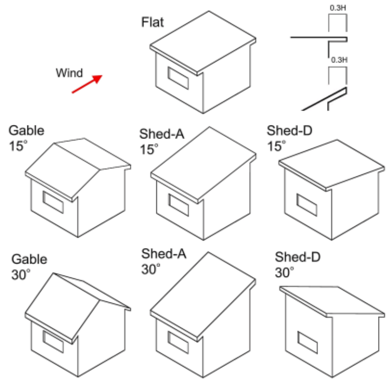

Fig. 2- 11: Building configurations (with eaves) considered in this study [81].

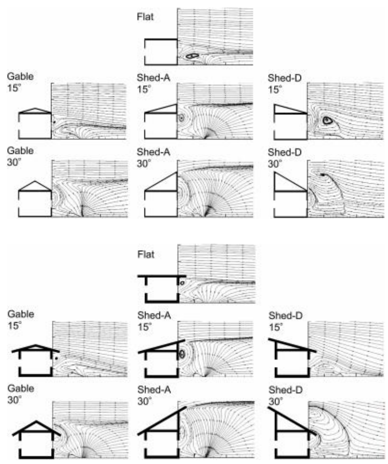

Fig. 2- 12: Streamlines behind building at vertical center plane for various roof shapes and pitches (top). Streamlines behind buildings with eaves (bottom) [81].

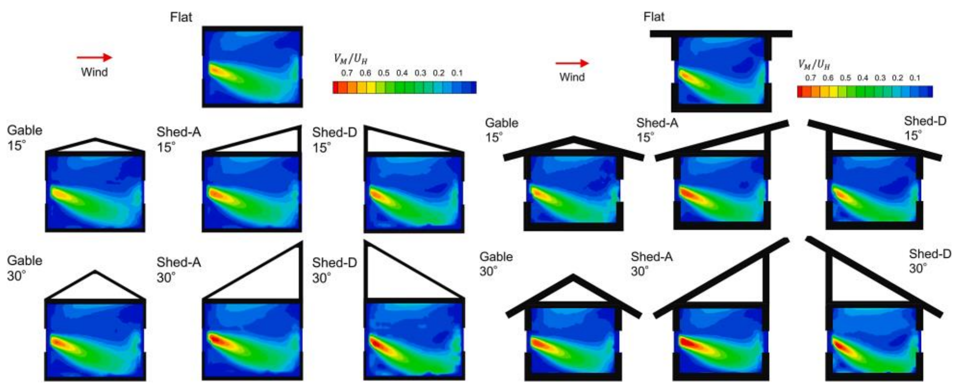

Fig. 2- 13: Contours of dimensionless velocity magnitude on vertical center plane inside buildings without eaves (left). Contours of dimensionless velocity magnitude on vertical center plane inside buildings with eaves (right) [81].

Zhai et al. [71] reviewed both analytical and empirical models and commonly used network airflow models. The analytical and empirical methods were found to be the ones with minimal contributions to the literature in the last decades; although they are classified as simplified methods, they are useful tools, validated with experiments [82, 83]. Despite the fact that the multizone models are the main tool to predict the ventilation performance on an entire building, the authors concluded that the CFD models were the most popular ones, being found in 70% of the reviewed literature [15, 84].

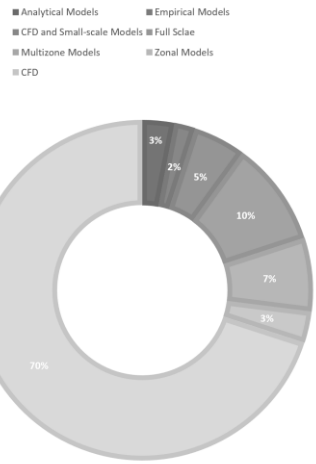

Fig. 2- 14: The share of different models in for predicting ventilation in buildings [15]. Graph by author.

7 Natural ventilation potential

As NV efficiency relies on local climate, quantitative data about its potential is fundamental in providing designers information to properly use the natural forces of wind and buoyancy at the preliminary stage of building design [71, 85, 86]. To provide such data, researchers have been studying the Natural Ventilation Potential (NVP) across different climate zones worldwide [61, 87, 88]. For instance, the NVP from wind was compared with the airflow required to restore indoor thermal comfort using meteorological data in studies from Aynsley, Haase and Amato, and Pesic et al., all aimed at hot and humid climates [71]. The latter also accounted for the potential under different ventilation modes [89]. Luo et al. included the indoor air quality issues when developing a revised mathematical model to estimate the potential for naturally ventilated buildings in China [90]. Later on, Yin et al. proposed another model taking into account solution multiplicity, window opening percentage, air velocity, and humidity [71]. Withal, Constanzo and Donn showed in their study how natural ventilation could be successfully applied to existing office buildings in many different urban climates, including hot dry/humid, mixed humid, marine and cold [91]. Yin et al. [38] note that metrics used in assessing natural window ventilation significantly impact the design of windows and interior layouts. These indicators include Airflow (velocity, flow pattern, and pressure), T (temperature/heat gained), TC (thermal comfort), IAQ (indoor air quality), and EC (energy consumption) [38].

7.1 Window layout parameters

The performance of NV is significantly influenced by both window and indoor layout parameters:

- Geometry and design: Factors such as window geometry, opening ratio, number of openings, location, type, orientation, and shading systems play a crucial role [18]. Proper window designs can maintain thermal comfort, reduce cooling loads, extend ventilation periods, and improve IAQ.
- Orientation: The orientation of windows impacts the amount of solar radiation admitted and the potential for capturing prevailing winds [38].
- Location: The location of windows affects airflow patterns and ventilation efficiency. High window positions may capture more wind, while lower positions may provide better airflow distribution [18, 38].
- Opening Size/WWR: The window-to-wall ratio (WWR) and opening size determine the amount of air that can enter a building [38].

Optimizing these parameters can balance ventilation with energy efficiency [38].

- Type: Window types, such as awning, casement, or sliding windows, influence how effectively they capture and direct airflow [38].
- Shading: Shading devices like louvers, overhangs, and blinds can control solar heat gain while allowing for ventilation [38].

7.2 Indoor layout parameters

- Geometric and thermal properties: The geometric and thermal properties of indoor obstructions influence local thermal comfort and airflow patterns [38].
- Arrangement of interior spaces: The arrangement of interior spaces can either facilitate or impede airflow. Open layouts generally promote better ventilation compared to highly compartmentalized spaces [38].
- Furniture placement: The placement of furniture can affect airflow patterns and create stagnant zones. Strategically positioning furniture can help improve ventilation [38].
- The integration of facade and interior arrangement is critical for achieving effective NV. Integrated design ensures that window parameters and interior layouts work together to optimize ventilation performance.

Understanding airflow dynamics in diverse architectural designs and environments is crucial for harnessing the benefits of natural ventilation. Recent research into the cross-ventilation flow in two-layered models, representative of terraced houses in tropical climates like Malaysia, reveals the significant impact of inlet opening positions and the alteration of indoor flow patterns due to multi-zoning [37]. This emphasizes the need for detailed investigations into how building configuration influences ventilation performance, extending beyond single-story or single-zone models in Poland. Furthermore, innovative architectural projects such as The Interlace in Singapore and Wave Culture City in Hangzhou, China, demonstrate the potential for optimizing natural airflows in underground spaces by strategically integrating aboveground and subterranean areas facilitate natural airflows [49]. These examples underscore the importance of considering both the specific design of individual buildings and the broader integration of spaces to effectively leverage natural ventilation principles.

8 Future research directions

Several avenues for future research hold promise in further enhancing the understanding and application of natural ventilation. While the sources extensively discuss the benefits and current state of natural ventilation, they also identify numerous areas where further investigation is needed to overcome limitations, optimize performance, and expand its applicability in diverse contexts. These research gaps span from addressing the impact of climate change and urbanization on natural ventilation potential to refining simulation tools and exploring the integration of natural ventilation with other passive and active building systems. Furthermore, a deeper understanding of the interplay between indoor and outdoor environments, occupant comfort, and the effectiveness of various natural ventilation strategies under different conditions remains crucial for maximizing the benefits of this sustainable approach. Several avenues for future research can further enhance the understanding and application of natural ventilation [19, 38, 71, 92]:

8.1 Performance in extreme climates:

Further evaluation is needed to determine the effectiveness of natural ventilation in extreme climates, especially during heatwaves and under future climate scenarios [19, 93]. This includes studying innovative combinations of passive cooling techniques, such as solar chimneys or windcatchers with water evaporation cooling.

8.2 Impact of air pollution:

With increasing air pollution levels, further research is urgently required to investigate filter-enabled natural ventilation, particularly with solar chimney/windcatcher incorporation [19, 94].

8.3 Integration with renewable energy systems:

More studies are needed on how to integrate natural ventilation with renewable energy systems like solar and geothermal to achieve optimal building energy performance [19, 92, 95].

8.4 Urbanization effects:

Additional investigation is necessary to understand how urbanization and changes in the built environment affect natural ventilation potential [37, 45]. This involves studying the impact of building density, street canyons, and urban heat islands on wind and ventilation effectiveness [13, 37, 49].

8.5 Health and well-being:

More comprehensive research is required to assess the relationship between natural ventilation, indoor air quality, and occupant health [27, 55, 96]. This includes investigating the impact of different ventilation strategies on reducing indoor pollutants, allergens, and pathogens.

8.6 Advanced modeling techniques:

Continued development and refinement of advanced modeling techniques, such as CFD and machine learning, are essential to improve the accuracy of ventilation performance predictions [18, 71].

8.7 Technology-economics and Life Cycle Costs (LCC):

Comprehensive technology-economics and life cycle cost analyses are necessary to demonstrate the long-term benefits of combined window systems and passive strategies [97]. These analyses should consider energy savings, maintenance costs, and environmental impacts to provide a holistic assessment of sustainability [19, 98].

8.8 Indoor environment studies:

More studies are needed on the effects of interior conditions on natural window ventilation, as it is a crucial issue for ensuring accurate results [38].

This includes investigating how geometric and thermal properties of indoor obstructions affect local thermal comfort and airflow patterns.

8.9 Buoyancy-driven and corner ventilation:

High volume of studies has been conducted to identify the key design factors that have a substantial impact on wind-driven cross-ventilation and single-sided ventilation [38]. Limited attention has been given to the potential benefits of buoyancy-driven window ventilation and wind-driven corner ventilation.

9 Natural ventilation and thermal comfort

Simultaneous study of various parameters such as the combination of natural ventilation systems and their physical layout in achieving and improving the thermal comfort is important [77]. The extensive literature review of the effects of natural ventilation systems in buildings indicates that the majority of available studies are limited to low-rise buildings with simple geometries, and few studies can be found on high-detailed buildings [99]. On the other hand, the effects of cross-natural ventilation and Double-Skin Façade (DSF) systems as well as their configuration in improving the thermal comfort conditions have not been studied [18]. Therefore, examining the impact of the configuration of natural ventilation systems and the positions of inlet and outlet openings on airflow and temperature patterns in indoor spaces is important.

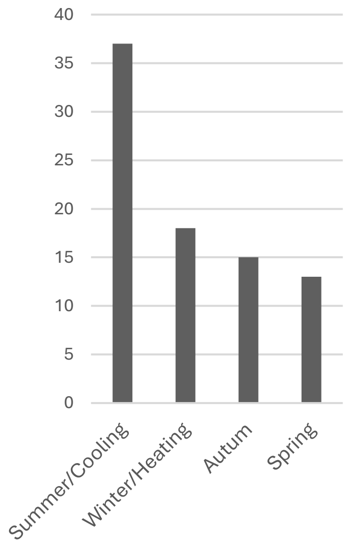

Fig. 2- 15: The frequency of thermal comfort study in the determined investigated seasons [100]. Graph by author.

The two bar charts illustrate the focus areas of existing research articles related to thermal comfort and indoor climate strategies. The first chart shows that the highest number of studies address summer conditions and cooling strategies, followed by winter heating, with significantly fewer articles focusing on autumn and spring. This suggests that extreme seasonal conditions receive the most academic attention. The second chart reveals a strong emphasis on HVAC systems in the literature, with notably fewer studies exploring personal control strategies and natural ventilation. This indicates a research gap and underrepresentation of low-energy, occupant-driven solutions like natural ventilation, highlighting the need for more studies in these areas, such as the current thesis.

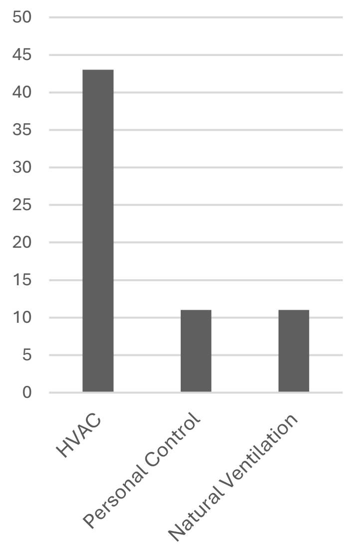

Fig. 2- 16: The frequency of thermal comfort study in the operation modes of the investigated buildings [100]. Graph by author.

Simultaneous study of various parameters in natural ventilation systems and their physical layout is indeed crucial for effectively achieving and improving thermal comfort in buildings. The sources highlight that many factors influence natural ventilation performance, including window geometry, opening ratio, number of openings, location, type, orientation, and shading systems. Furthermore, the internal layout, including the presence and arrangement of furniture and partitions, also plays a significant role in airflow patterns and thermal comfort. Investigating these elements in isolation may not provide a complete understanding of their interactive effects on the indoor environment. The majority of existing research on natural ventilation has predominantly focused on low-rise buildings with simple geometries. This leaves a significant gap in our understanding of how natural ventilation performs in more complex architectural designs, particularly in housing apartments which are increasingly common in modern urban environments.

The interaction between different natural ventilation strategies and building envelope technologies also warrants further investigation. For instance, the effects of cross-natural ventilation in conjunction with façade systems and the optimal configuration of these systems for enhanced thermal comfort remain largely unstudied. For example, DSFs themselves present a complex heat transfer process, and their integration with natural ventilation needs careful consideration, especially in varying climates. Therefore, it is essential to thoroughly examine the impact of the configuration of natural ventilation systems, specifically the positions of inlet and outlet openings, on airflow patterns and temperature distribution within indoor spaces. Understanding these relationships is vital for developing effective natural ventilation designs that can contribute to both energy efficiency and occupant comfort in a wider range of building types and climatic conditions.

10 Impact of opening positions on thermal comfort

Studies on the effect of the height of the openings on the internal natural airflow in one-story buildings can be found in many studies; However, studies on the effect of this important factor on providing thermal comfort in buildings equipped with double-skin façade are not available [101]. Studies focus on natural-ventilated buildings based on wind-driven and buoyancy-driven forces [18]. The aim of these studies is to use passive strategies in buildings in hot and dry climates. In this research, two methods of field studies and numerical modeling have been used in order to provide accurate results [18]. In order to achieve optimal patterns in the design of natural-ventilated buildings; CFD simulation and PMV thermal comfort index have been used in the evaluation of various configurations [102, 103]. The results of the present study show that although the cooling energy demand in residential buildings in hot climates is high and the use of natural ventilation systems is beneficial, but these systems alone are not able to provide thermal comfort conditions [104]. However, the accurate and correct location of the openings is effective in improving thermal comfort by increasing the volume flow.

11 Conclusion

Natural ventilation, particularly cross ventilation, is a sustainable and effective strategy for enhancing indoor air quality, thermal comfort, and energy efficiency in buildings [13, 14, 71]. While natural ventilation offers numerous benefits, it also presents challenges related to climate, air quality, noise, and building design [13, 19]. However, by addressing these challenges through careful design, advanced technologies, and informed policies, the full potential of natural ventilation can be realized, leading to more sustainable, healthy, and comfortable built environments [19, 38]. Continued research, and practical implementation are essential to promote the adoption of natural ventilation and its contribution to a more sustainable future [19, 38, 71].

Natural ventilation, especially cross ventilation, stands out as a sustainable and effective strategy for significantly enhancing indoor air quality, thermal comfort, and energy efficiency in buildings. By harnessing natural forces like wind pressure and temperature differences, natural ventilation replenishes indoor spaces with fresh outdoor air without relying on energy-intensive mechanical systems. This can lead to a substantial reduction in cooling demand and energy consumption, with studies suggesting potential energy savings of 20% to 40% depending on the local climate. Furthermore, natural ventilation contributes to improved indoor air quality by diluting and removing indoor pollutants, and it has been shown to help prevent airborne contagion and reduce the risks of Sick Building Syndrome. Occupants in naturally ventilated buildings may also experience greater thermal comfort and a wider tolerance of temperatures compared to those in air-conditioned environments, particularly when they have control over airflow through operable windows.

Despite its numerous advantages, the widespread adoption of natural ventilation faces several challenges related to varying climatic conditions, potential issues with outdoor air quality, noise pollution, and the complexities of building design. For instance, in urban environments, natural ventilation can introduce undesirable dust and street noise, and extreme weather events can limit its effectiveness. Moreover, designing effective natural ventilation systems often requires significant expertise and careful consideration of factors like building orientation, window placement, and internal layout. To overcome these limitations and fully leverage the potential of natural ventilation, continued research and innovation are essential. This includes refining design strategies, developing advanced technologies like hybrid ventilation systems, and implementing informed policies that promote its use. By proactively addressing these challenges, we can realize the full benefits of natural ventilation, leading to more sustainable, healthy, and comfortable built environments.

Chapter 03: Polish housing

1 Introduction

The Polish housing sector is undergoing significant transformation, driven by both internal economic growth and external pressures from the European Union to improve energy efficiency and reduce carbon emissions. This review examines the current state of apartment and multi-family housing in Poland, focusing on building categories, typologies, and conditions. The review draws from various sources including journal articles, reports, and conference proceedings, which provide insights into the complexities and challenges facing the Polish residential sector.

2 Categories of residential buildings

The Polish residential building stock is generally classified into four main categories [105]:

- Single-family houses (SFH): These are detached houses, often found in rural and low-density areas. Many of these rely on solid fuels like coal, biomass, and waste for heating and hot water [105, 106].
- Terraced houses (TH): These are houses joined together in a row [107].
- Multi-family houses (MFH): These are buildings with multiple separate housing units, often found in urban areas [105, 107].
- Apartment blocks: These are larger buildings with many apartments, typically found in cities [105, 107].

These categories are further subdivided based on construction periods, reflecting the evolution of building standards and insulation requirements over time. The classification organizes buildings by vintage, corresponding to the introduction of new U-value requirements for building envelopes. The defined periods are: before 1945, 1946-1957, 1958-1982, 1983-1991, 1992-2002, 2002-2009, 2010-2013, 2014-2016, 2017-2020, and from 2021 onward [108].

2.1 Typology of apartments and multi-family housing

Two major archetypes dominate the Polish residential building stock: multi-family houses in urban areas and single-family dwellings in low-density areas[107]. Within multi-family housing, there are several typological variations, often influenced by historical and economic factors.

Historical buildings: Older buildings, especially those built before 1945, often have poor thermal insulation and high energy consumption [106]. Many of these are in need of significant renovation and modernization [105].

Post-socialist era buildings: Large housing estates, often referred to as "blokowiska[1]" were built during the socialist era and are characterized by repetitive designs and standardized construction techniques using prefabricated concrete panels [106, 109]. These buildings also frequently suffer from poor insulation and inadequate ventilation [105].

[1] Housing estates

Modern multi-family buildings: Newer multi-family buildings vary widely in design and construction. Some of these adhere to modern energy efficiency standards, while others are built to maximize profit, sometimes resulting in substandard living conditions. There is a trend toward "micro-apartments," which are small units that do not meet the technical requirements for standard apartments [109].

The typology of Polish apartments and multi-family housing has also been shaped by various socio-economic factors and shifts in housing policy. The dominance of private ownership and the commodification of housing have resulted in a focus on market value rather than user needs. This has led to the development of smaller, less functional apartments, often sold as investment properties [109].

3 Materials and construction techniques

The materials and construction techniques used in Polish apartments and multi-family housing have evolved considerably over time.

- Historical buildings: Older buildings often used traditional materials such as brick and stone, but these lack modern insulation, contributing to high energy consumption [105].
- Post-socialist era buildings: These buildings primarily used prefabricated concrete panels, a construction method that allowed for rapid building but often resulted in poor thermal performance and indoor comfort [109].
- Modern buildings: Modern construction utilizes a mix of materials as described below:

Concrete is widely used for foundations and load-bearing structures. Silicate blocks also is increasingly used for walls due to their good thermal properties [109]. Modern buildings include insulation materials like rock wool and polystyrene. The level of insulation is a key factor in achieving energy efficiency [110]. They often use large windows to maximize natural light and solar heat gains in the winter, but these can contribute to overheating in the summer [111, 112], however in this study I are going to evaluate this matter. Mechanical ventilation systems are becoming more common in new buildings to ensure adequate air exchange. However, their adoption in existing buildings is challenging [113].

The selection of materials and technologies in building construction is influenced by multiple factors, including economic constraints, energy performance standards, [114] and regulatory requirements [105]. Cost considerations play a significant role, as developers and builders seek to balance affordability with durability and performance. Energy efficiency requirements, driven by both environmental concerns and government policies, guide the choice of insulation, glazing, and HVAC systems to minimize energy consumption and operational costs.

3.1 Conditions in apartments and multi-family housing

The conditions within Polish apartments and multi-family housing vary widely based on the age, location, and construction standards of the buildings.

Energy efficiency: A significant portion of Polish residential buildings, especially older single-family homes, lack adequate thermal insulation. The average energy use in older buildings is around 175 kWh/m^2 per year, with heating accounting for more than 75% of total energy consumption [115, 116].

Heating systems: Many households still rely on coal-fired boilers, which contribute to high levels of particulate pollution (SO_2, NOx, PM10, and PM2.5) and CO_2 emissions [105, 117]. There is a growing movement toward district heating and renewable energy sources, particularly in urban areas [106, 115].

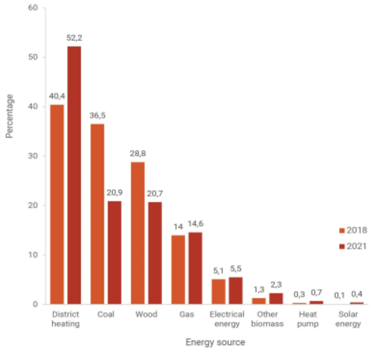

Fig. 3- 1: Shift in energy source in residential buildings in Poland between 2018 and 2021 [118].

Ventilation: Natural ventilation systems are common, but they are often inadequate, leading to poor indoor air quality [105, 119]. Mechanical ventilation systems with heat recovery are becoming more prevalent in new constructions. The effectiveness of ventilation is also influenced by the behavior of residents, such as their window-opening habits [119, 120].

Indoor air quality (IAQ): Studies show that indoor air quality in Polish homes can be poor, particularly in areas with high levels of outdoor pollution. Pollutants like nitrogen dioxide, benzene, toluene, ethylbenzene, and xylene (BTEX) are found in higher concentrations indoors compared to outdoors [121]. Inadequate ventilation and the use of solid fuels for heating can contribute to these issues as well.

Thermal comfort: Overheating in the summer is a major concern, especially in buildings with poor ventilation and large glazing areas [11, 111, 112]. Polish regulations focus on energy conservation but neglect indoor environmental issues [105]. There is a lack of detailed regulations regarding thermal comfort or overheating calculations [122]. Studies suggest that optimal insulation thicknesses are often higher than the minimum requirements for both life cycle costs and thermal comfort [111]. However, This increases the probability of overheating during warm seasons concerning global warming and this issue bring up the increase in cooling demand in close future.

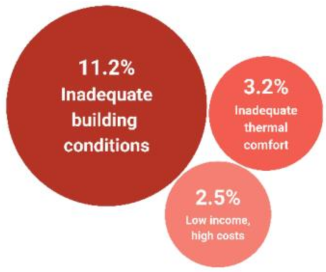

Fig. 3- 2: Indicators of energy poverty in Poland (%of households considered energy poor per indicator by 2021) [118].

The Polish housing sector is facing a complex set of challenges and opportunities as it strives to meet both national and EU targets for energy efficiency and sustainability. While the country has made progress in adopting new building standards, significant work remains to be done in retrofitting existing buildings and improving the overall quality and comfort of housing. The shift towards renewable energy, better thermal insulation, and improved ventilation will all be critical to meeting the demands of the 21st century. The growing interest in co-housing and housing cooperatives is a positive development towards more sustainable and community-oriented housing solutions. Continued research and innovation will be crucial to ensure that all residents in Poland can access safe, comfortable, and energy-efficient homes. The sources point to a need for continued policy development that will prioritize not only energy efficiency but also indoor air quality, thermal comfort, and the overall well-being of occupants in Polish housing. This literature review provides a broad overview of Polish housing in apartments and multi-family buildings, based on the provided sources. Further research may be required to fully explore the nuances and complexities of this important sector.

4 Energy use in Poland

The building energy use in Poland is among highest in the world with the number of 38% [123]. Energy consumption patterns in Poland's residential sector vary significantly based on housing type, with single-family homes consuming the most energy overall. The four main categories of Polish building stock (SFH, TH, MFH), and apartment blocks, has its own distinct characteristics that contribute to different energy consumption patterns. Single-family Houses (SFH) are the largest energy consumers in the residential sector [105, 106]. They predominantly rely on coal, biomass, and waste for heating and domestic hot water (DHW). In 2013, it was found that 70% of single-family residences used coal as their primary energy source [106]. A large proportion of single-family homes, about 70% (or 3.6 million), have inadequate or no thermal insulation. Heating demand constitutes over 75% of their total energy use, including DHW, cooling, lighting, and appliances [124].

More than 40% of Multi-family houses and apartment blocks, particularly those in urban areas, are connected to district heating systems [123]. Multi-family buildings are more energy-efficient per household due to shared walls and heating systems, but their overall consumption is significant because of their numbers. Studies on multi-family buildings have shown that a large percentage (56.7%-70.5%) of heat used in DHW systems is lost due to heat losses in older buildings [125].

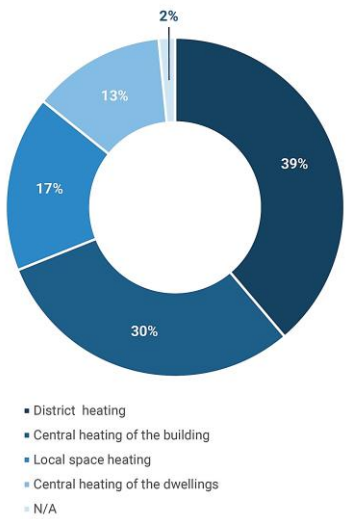

Fig. 3- 3: Types of heating systems in the Polish housing stock by the year 2022 [118].

Poland has one of the highest rates of energy consumption per square meter in buildings within the EU, exceeding 200 kWh/m²/year [106]. Due to Poland's transitional climate, with cold winters and warm summers, heating is a major factor in overall energy consumption. Buildings are heating-dominated [11, 105].

As mentioned before, the residential sector in Poland relies more on solid fuels than any other EU country, contributing to poor air quality and energy inefficiency. Although there has been a slight decrease in the use of coal in district heating, it is still the dominant fuel [105, 106]. Around 39% of the energy share for heating is from coal [126]. During 2008-2018, Polish houses improved energy efficiency at a rate of 1.13% per year, which was lower than the EU average and significantly below the pace obtained by Poland's industry [127].

A significant portion of Polish residential buildings have not undergone thermal modernization, especially those built before 1970 [106]. Buildings constructed before 1918 have the highest primary energy demand, with those built between 1945 and 1970 having a lower but still significant demand [106]. Newer buildings (2003-2010) have lower energy demands.

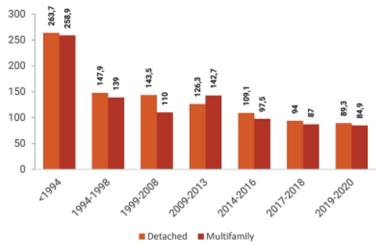

Fig. 3- 4: Median primary energy demand by year of building construction [118].

Year of building construction	Number of buildings	Unitary demand for non-renewable primary energy (kwh/m2 per year)	Unitary demand for final energy
Before 1918	405000	>350	>300
1918-1944	804000	300-350	260-300
1945-1970	1364000	250-300	220-260
1971-1978	660000	210-250	190-220
1979-1988	754000	160-210	140-190
1989-2002	671000	140-180	125-160

Table 3- 1: Demand for energy of building constructed before 2002 by the year of building construction [118].

Despite there is a lack of sufficient and reliable data related to energy use in buildings, which hinders the development of effective energy-saving measures [106], occupant behavior also plays a significant role in energy consumption [119].

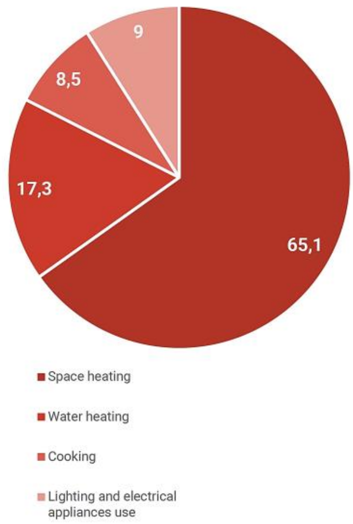

Fig. 3- 5: Percentage of energy consumption in residential building [118].

In summary, energy consumption in Poland varies across different types of housing, with single-family homes using the most energy, particularly when they rely on solid fuels for heating. Multi-family homes are more efficient per household but still contribute significantly to overall energy consumption. The age and insulation of buildings are also crucial factors in determining energy usage. The country's ongoing transition away from coal and towards renewable energy sources, coupled with improvements in building standards and insulation, will play a key role in reducing energy consumption in the future.

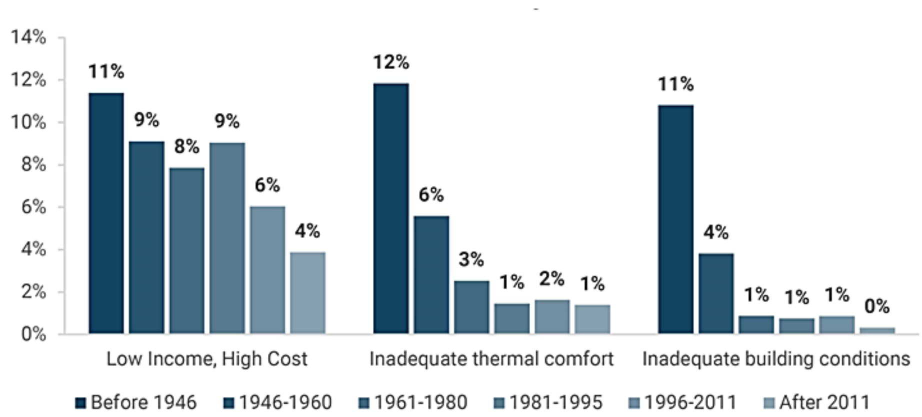

Fig. 3- 6: Risk of fuel poverty in multifamily housing by year of construction (%) [118].

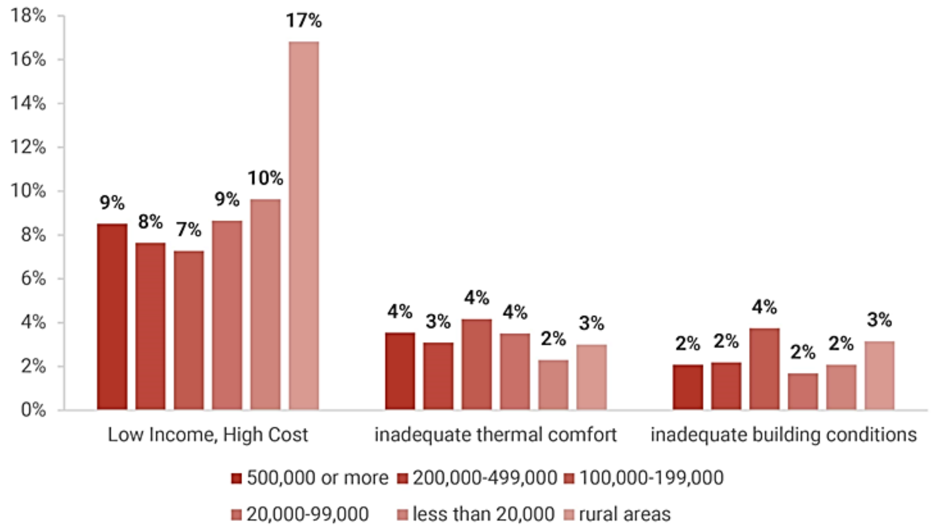

Fig. 3- 7: Percentage of risk of energy poverty by class of residence [118].

5 Poland's housing sustainability goals

Several challenges hinder Poland's housing energy efficiency goals, including a heavy reliance on coal, a lack of financial incentives for green technologies, and insufficient building standards and enforcement.

Poland's energy market heavily relies on coal, especially for heating. The residential sector in Poland depends more on solid fuels than any other EU country [105, 106]. A significant portion of Polish households use coal for heating and domestic hot water [106]. This reliance on coal contributes to air pollution and makes it difficult to reduce greenhouse gas emissions.

Although Poland plans to phase out coal by 2049, the demand for imported coal remains high [128]. The country imports coal from Russia, Chile, Colombia, the USA, and Kazakhstan [129]. Also the existing energy grid is old, with low energy production efficiency and high pollutant emissions. Studies have shown a lack of financial benefits for homeowners regarding medium-level thermal modernization. On the other hand, the high initial costs of Passive House (PH) certified homes are also a barrier [130].

Polish regulations do not always align with EU standards for energy efficiency [105, 106]. Although Poland has a long history of energy efficiency regulations [105, 106], the current building standards often lack specific requirements or are not enforced effectively. For instance, there is no specific overheating calculation method in the Polish Energy Performance of Buildings (EPB) method, the only related statement is that "*overheating should be avoided during summer periods*" [105]. However in cold seasons in 2022, approximately 5% of the Polish population lived in cold homes, while 35% lived in overcrowded apartments, indicating that a significant proportion are affected by unfit housing [118]. The availability of the most significant and cutting-edge technology for Poland and other technologically advanced EU nations is listed in table below:

	EU	Poland
Double-glazed low-e glass	Mature	Mature
Window films	Established	Established
Window attachments (e.g. shutters, shades, storm panel)	Mature	Mature
Highly insulating windows (e.g. triple-glazed)	Established	Established
Typical insulation	Mature	Mature
Exterior insulation	Mature	Mature
Advanced insulation (e.g. aerogel, VIPs)	Initial	Non-existent
Air sealing	Mature	Established
Cool roofs	Established	Initial
BIPV/ advanced roofs	Initial	Non-existent
Prefabricated envelope	Initial	Non-existent

Table 3- 2: Availability of most modern building technologies [124].

Overheating is a significant concern in Polish houses, especially in the context of increasing energy efficiency standards and climate change. While efforts are focused on reducing heating demand through increased insulation and passive solar gains, this can lead to uncomfortably high indoor temperatures during summer periods if proper cooling strategies and solar protection measures are not implemented. Current Polish regulations are noted to lack specific requirements and enforcement regarding overheating prevention and thermal comfort, often focusing more on energy conservation. Studies indicate that solely adhering to energy efficiency regulations may not guarantee thermal comfort in buildings, with issues like excessive glazing contributing to overheating. Addressing overheating is crucial to ensure the well-being of occupants and the overall sustainability of energy-efficient buildings in Poland.

There is also a lack of focus on indoor environmental quality [105]. While Polish regulations mention avoiding overheating, they do not provide specific guidance on thermal comfort. The Polish standard complies with EPB standards default recommendations, but the regulation neglects indoor environmental issues while enforcing energy conservation measures [131]. There is a need for a framework for nearly zero-energy buildings (nZEB) in Poland [105, 112]. The current Polish energy efficiency target for domestic hot water, ventilation, and heating in a single-family house is 70 kWh/m^2 per year, but this is difficult to achieve with just natural ventilation strategies [105]. The decisions about energy efficiency mechanisms and targets are sometimes politicized, and some ministers without technical backgrounds adopt ineffective measures or policies.

Poland's energy efficiency goals are hindered by a complex set of issues including a strong reliance on coal, financial obstacles, policy and regulatory weaknesses, and a lack of focus on the indoor environment, and workforce challenges. Addressing these issues is crucial for Poland to achieve its energy efficiency and carbon reduction targets.

6 Current Polish sustainability regulations

Here's a breakdown of how these regulations and policy’s function:

Early regulations: Formal guidelines for permissible heat losses were established as early as 1957, with heat transfer coefficients used to measure this [132]. Requirements for heat transfer in walls were updated in 1964, before the oil crisis in 1972, and again in 1974 and 1982, influenced by the energy challenges of the oil crisis [105, 106].

Evolution of requirements: The calculated energy usage for typical Polish buildings was 240-380 kWh/m^2 up to 1985, with subsequent requirements to reduce this, for example, to 160-200 kWh/m^2 in 1991-1992, and 90-120 kWh/m^2 by 1998 [133].

Adoption of EPBD: With Poland's entry into the EU in 2004, the European Energy Performance of Buildings Directive (EPBD) was adopted in 2009 [134]. This led to the requirement for Energy Performance Certificates (EPC) for new buildings, and buildings for sale or rent.

Nearly Zero Energy Buildings (nZEB): As of 2021, all newly built buildings in Poland must meet the nZEB standard, which is defined by national parameters and is challenging to meet [105, 112]. These requirements apply to the thermal insulation of the external casing of buildings, the primary energy indicator, and encourage the use of renewable energy sources [112, 135].

Thermal Comfort: Unfortunately, as mentioned till here, Polish regulations focus mainly on reducing energy demand, with less emphasis on detailed analysis of thermal comfort and protection against overheating [114]. While regulations require avoiding overheating in the summer, and that windows block some solar irradiation, they are not specific regarding thermal comfort calculations.

Polish regulations and policies have made strides in addressing energy efficiency, but there are still challenges related to implementation, enforcement, and the need to integrate energy efficiency with indoor environmental quality and broader decarbonization goals.

7 Challenges facing climate change

As climate change presents a significant and growing challenge, its impact on thermal comfort in Poland's residential buildings is becoming increasingly important. While Poland is actively pursuing energy efficiency in its building stock, often driven by European Union, the changing climate is leading to a notable increase in cooling demands and the risk of overheating in homes. This situation creates a complex challenge, as measures aimed at improving energy efficiency, such as enhanced insulation and airtightness, can inadvertently worsen indoor thermal comfort during warmer periods if not properly addressed. Ensuring comfortable living conditions alongside energy efficiency in Polish homes under the influence of climate change requires careful consideration and integrated design strategies. Climate change and thermal comfort present significant, interconnected challenges, particularly in the context of building design and energy consumption. Here's a breakdown of the main problems and challenges:

Increased cooling demand: Rising global temperatures lead to a significant increase in cooling energy demands in buildings. Studies project substantial increases in cooling energy needs, potentially by 210% from 1975 to 2085 [136]. In Poznan, Poland, simulations show a 135% average increase in cooling load by 2080 [106].

Decreased heating demands: While heating energy requirements are decreasing due to milder winters, the reduction is not uniform across all regions [137]. For example, Poznan is projected to see a 40% decrease in heating load by 2080 [106].

Shifting thermal loads: The balance between heating and cooling loads is shifting, with cooling becoming a more dominant factor in overall energy consumption [138]. In some building prototypes, the contribution of cooling loads is expected to surpass heating loads by 2080 [106].

Peak power demand: The increase in cooling demand may lead to a surge in peak power demand, potentially causing an energy crisis if not properly addressed [139].

Regional variations: The impact of climate change on building energy consumption varies depending on geographical and climatic conditions [140]. For example, countries with moderate climates may see increased cooling needs offset by lower heating needs, while hotter countries may experience more extreme summer energy demands [141].

Uncertainty in predictions: Climate change is complex, and predictions are influenced by factors such as greenhouse gas emissions, technological advancements, and global policies, making it difficult to create accurate energy models [142].

8 Thermal comfort challenges

There are many researches and reports focusing on optimizing Polish residential buildings' walls and roofs insulation thickness, and mechanical ventilation features [143]. Increased insulation and airtight building envelopes, while improving energy efficiency, can lead to overheating in the summer, particularly in buildings without proper cooling systems or solar protection [11, 111, 114]. Large south-facing glazing, often used to maximize solar gains, can also contribute to overheating [111, 112, 120]. Airtight buildings with insufficient ventilation can lead to poor indoor air quality and thermal discomfort [111, 144]. On the other hand, natural ventilation may not be enough to meet energy efficiency targets and thermal comfort needs [106].

There are different models for assessing thermal comfort [114]. Static models like Predicted Mean Vote (PMV) and Predicted Percentage of Dissatisfied (PPD) are commonly used, but adaptive models are more appropriate in naturally ventilated spaces because they consider occupant adaptation and behavioral adjustments [11, 114]. Occupant behavior can significantly impact thermal comfort and energy consumption [11, 105, 106, 114, 120]. For instance, wearing shorts in winter or improper use of shading can reduce the intended effectiveness of building design. The interaction between residents and their buildings can affect both internal conditions and energy consumption [119].

Obviously, there is a lack of consistent methods for assessing thermal comfort in technical regulations for buildings [114]. Some regulations focus on energy demand, neglecting thermal comfort. Improving energy efficiency through increased insulation may inadvertently worsen thermal comfort by leading to overheating. This requires a holistic approach that considers both energy and comfort requirements. Polish building standards do not always address overheating and thermal comfort adequately, leading to uncomfortable indoor conditions, and do not enforce mechanical ventilation for energy efficient targets. There is no overheating calculation method in the Polish EPB, and solar protection is only recommended prescriptively, and not as a design requirement.

The influence of the Soviet era on thermal comfort perception may hinder expected energy reduction [105]. The cost-optimality approach that should define the performance targets of the Polish EPB is not implemented. So, there is a need for more research on indoor thermal and air quality, alternative heating systems, and comparative studies that embrace the cost optimality approach. For instance, improving building energy efficiency without addressing thermal comfort can create uncomfortable conditions and lead to increased energy consumption if cooling or ventilation is needed to maintain comfort [111, 114, 120]. Solutions must consider energy efficiency, thermal comfort, and environmental impacts all together [11, 105, 106, 111, 114]. Addressing these challenges requires a comprehensive approach that integrates climate change mitigation strategies, energy-efficiency, and a focus on maintaining thermal comfort for occupants [11, 105, 106, 111, 114].

9 Polish regulations for comfort and ventilation in multi-family apartments

Polish regulations for comfort and ventilation in multi-family homes and their renovation are primarily focused on energy efficiency, with less emphasis on specific comfort requirements, often leading to a discrepancy between regulatory standards and actual living conditions [105, 114]. Here are a breakdown of the relevant regulations and their impact on multi-family homes:

9.1 Energy efficiency:

The regulations prioritize the reduction of energy demand and greenhouse gas emissions, particularly for heating, ventilation, and domestic hot water [114]. As of 2021, all new buildings must meet nearly Zero Energy Building (nZEB) standards, which focus on energy use rather than comfort. These standards include thermal insulation of the building envelope, a target for primary energy use, and the promotion of renewable energy sources [105, 112]. The present Polish energy efficiency objective for domestic hot water (DHW), and heating in a single-family dwelling is set at 70 kWh/m^2 per year and for multi-family houses 65 kWh/m^2 per year [145] as demonstrated in table below:

	Applicable from 1 January 2017	Applicable from 31 December 2020
Single-family houses	95	70
Multi-family houses	85	65
Healthcare buildings	290	190
Warehouses and farm buildings	90	70
Other non-residential buildings	60	45

Table 3- 3: Primary energy requirement for new buildings in Poland (kWh/m2 per year) [145].

Energy Performance Certificates (EPCs) are mandatory for new buildings and those for sale or rent, assessing energy efficiency using the primary energy use intensity indicator [105].

9.2 Thermal comfort regulations:

As discussed before, while regulations include a general provision to avoid overheating during summer, they lack specific requirements for thermal comfort or overheating calculations [105, 111]. There is a requirement about windows glazing being able to block some part of the irradiation. The regulations do not enforce a detailed analysis of thermal comfort, focusing mainly on reducing energy demand. The Polish regulation neglects indoor environmental issues while enforcing energy conservation measures.

9.3 Ventilation standards:

Polish ventilation regulations are based on European standards, allowing natural or gravitational ventilation in individual zones for buildings up to nine stories. Mechanical ventilation is required for taller buildings [144]. For houses, the required airflows are 70 m^3/h for the kitchen, 50 m^3/h for the bathroom, and 30 m^3/h for a separate toilet. Public buildings should provide at least 20 m^3/h of outdoor air for each person [144].

9.4 Renovation and retrofitting regulations:

The 1998 Thermo-modernization Law provides subsidies for building refurbishments aimed at reducing heat energy use. This includes replacing coal-fired boilers, insulating walls, and other upgrades [105, 111]. The law identifies three levels of thermo-modernization: low, medium, and deep, ranging from basic heat source upgrades to full building envelope renovations [105]. An estimated average renovation rate of 3% is necessary to achieve the Union's energy efficiency targets until 2050 (European Parliament, 2018) [118].

Target year	Building renovated	Average renovation rate	Share of thermally insulated residential buildings in the total housing stock	Coal phaseout
2030	2.4 Million	3.6%	70%	In cities
2040	5.2 Million	4.1%	n/a	All residential buildings
2050	7.5 Million	3.7%	65% of buildings with an EP<50 kWh/m^2 per year, and 22% between 50 and 90 kWh/m^2 per year	n/a

Table 3- 4: Polish long-term renovation strategy targets [146].

However, Poland has not fully implemented the EU's cost-optimal methodology for defining energy-efficient measures in buildings. There is a discrepancy between Poland's U-values for building envelopes and those suggested by the EU's cost-optimal approach.

9.5 Indoor Environmental Quality (IEQ):

There is also lack of focus on indoor air quality as well, particularly concerning ventilation. The Polish building standard still allows the use of solid fuels while focusing mainly on reducing indoor emissions. Polish regulations neglect indoor environmental issues while enforcing energy conservation measures [105]. In 2019, the Polish Building Energy Standard adopted the EN-16798-1 standard, which recommends specific criteria for CO_2 concentrations in living rooms and bedrooms [105].

9.6 Challenges in thermal comfort and ventilation standards:

Overheating can occur due to a focus on energy efficiency, like high levels of thermal insulation, especially in the absence of cooling systems. Large windows to maximize solar gain in winter can contribute to overheating in the summer if not properly shaded [105, 111, 112].

On the other hand, there is a lack of detailed analysis of thermal comfort or protection from overheating, as regulations do not force designers to conduct detailed analyses of these parameters [105, 111]. Regulations do not include requirements for vibratory comfort, which is important for the quality of internal environments [111]. The implementation of EPCs does not always ensure proper inspections of energy conservation measures. There is often a lack of design reviews and quality control for high-performance homes. Many buildings use low-quality mechanical ventilation systems with very low flow rates. And finally, cooling demands are not addressed in the EPB calculation method.

9.7 Recommendations:

First, Polish regulations should be updated to include more specific requirements for thermal comfort and indoor air quality. They should also include minimum requirements for solar protection, especially in buildings with large windows on the south side. The EU's cost-optimal methodology should be fully adopted to determine cost-effective energy efficiency measures for building renovation.

The adoption of high-performance natural and mechanical ventilation systems should be encouraged, particularly for new builds, given that primary energy demand targets cannot be met with natural ventilation. Then, there should be a focus on holistic design that considers both energy efficiency and occupant comfort, including thermal, acoustic, and visual elements. Last but not least, improve education and training for building professionals in the areas of energy efficiency, thermal comfort, and indoor air quality.

In summary, while Polish regulations aim to improve energy efficiency in multi-family homes, they often fall short in addressing specific comfort and ventilation parameters. Future revisions of building regulations should include a stronger focus on the holistic design of comfortable, healthy homes that include thermal comfort, indoor air quality, and occupant needs.

10 Creative solutions

Addressing the challenges of climate change and natural ventilation in multi-family residential buildings requires a combination of innovative design, technological upgrades, and policy changes.

Combining natural and mechanical ventilation can provide the benefits of both. Natural ventilation can be utilized when external conditions are favorable, and mechanical ventilation with heat recovery can ensure adequate airflow when needed [105, 119]. This approach balances energy efficiency and indoor air quality. Hybrid ventilation systems can be designed to adapt to changing weather conditions, utilizing natural ventilation when possible to reduce energy consumption, and switching to mechanical systems when necessary. Implementing decentralized mechanical ventilation systems that allow for individual control over air exchange in each apartment, which can be more effective than relying on a central system [105]. This can help overcome the challenges of integrating central systems in existing buildings, while providing better ventilation control. Designing buildings to maximize cross ventilation which can be achieved through strategic placement of windows and openings [144]. Integrating atria can improve natural ventilation and lighting in multi-story buildings [11]. Using building orientation to minimize solar heat gain [11]. By combining these ventilation related strategies, buildings can achieve optimal indoor comfort and energy efficiency while ensuring healthy air quality. A well-designed hybrid system leverages natural airflow when conditions allow and mechanical support when needed, creating a resilient and adaptive ventilation approach. Future research can explore smart ventilation controls that dynamically adjust based on occupancy, outdoor conditions, and real-time air quality monitoring, further enhancing sustainability and occupant well-being.

Using advanced glazing that reduces solar heat gain can help to prevent overheating during the summer [111]. Implementing external shading devices, such as blinds or louvers, is more effective than internal shading for reducing heat gain [120]. These can be automated or manually adjusted by residents. Dynamic shading can respond to changing solar angles and weather conditions to maximize thermal comfort and energy savings. Installing smart sensors and controls that monitor indoor air quality, temperature, and humidity, and automatically adjust ventilation and shading as needed [106, 120]. Smartphone applications can be used to collect data, and also allow occupants to control building systems such as ventilation and shading.

Upgrading insulation in walls, roofs, and floors can significantly reduce heat loss in the winter and heat gain in the summer, which reduces the need for both heating and cooling [114]. Using high-quality, airtight windows can minimize unwanted air infiltration, improving overall energy efficiency and comfort [144]. Addressing thermal bridges by properly insulating elements like windows, doors, and structural beams can help to further minimize heat loss or gain and airflow control.

Using machine learning models to analyze building characteristics and energy performance, helping to identify the most effective retrofit measures. Surrogate data-driven methods can overcome the limitations and data requirements of traditional energy audits [147]. These methods can use readily available data such as building age, weather, and utility bills.

Providing education and awareness programs for residents about the importance of proper ventilation, energy saving strategies, and the use of new technologies [119, 144]. As the occupant behavior plays a significant role in building energy use and indoor air quality. Solutions should account for user preferences, and educational programs should support optimal and effective use of implemented systems.

The most effective approach will likely involve an integration of several of these solutions. For example, combining improved insulation and airtightness with a hybrid ventilation system, smart controls, and optimized building orientation. This approach can maximize both energy savings and thermal comfort. By combining these solutions, it is possible to make multi-family residential buildings and apartments more resilient to climate change, while also improving indoor air quality and thermal comfort for residents.

11 Challenges hinder ventilation adoption in Poland

Several challenges hinder the widespread adoption of ventilation systems in Polish residential buildings, as detailed in the sources:

The initial investment cost of mechanical ventilation systems, including heat recovery units, is a significant barrier, making them less attractive than cheaper, less efficient alternatives [105]. The higher price of these systems increases the overall cost of building construction, which is a major consideration for developers and owners. Also, there is a lack of awareness among building professionals and occupants about the importance of ventilation for maintaining indoor air quality and thermal comfort [105]. Many people are unfamiliar with how these systems work and their benefits, which leads to resistance in adopting them.

Current standards do not mandate the use of mechanical and natural ventilation, allowing developers to manipulate air volume calculations using low-quality mechanical systems with inadequate flow rates [105]. The lack of high-quality control during the building permit process, including design and construction reviews, contributes to the problem.

There is a preference for natural ventilation, which is often seen as sufficient, despite its limitations in modern, airtight buildings [106, 119]. The habits and preferences of residents may not align with the requirements of energy-efficient buildings, potentially leading to misuse or underutilization of other types of ventilation systems. However, there is a common misconception that natural ventilation alone can ensure high indoor air quality and thermal comfort, which leads to a neglect of the need for mechanical ventilation, particularly in airtight buildings [14].

Integrating central mechanical ventilation systems with heat recovery in existing buildings is particularly challenging and expensive [105]. This is because retrofitting existing buildings with ductwork and other components of mechanical ventilation systems is difficult and often disruptive [105]. The need to retrofit older buildings to accommodate mechanical ventilation can result in added costs and complexities. On the other hand, many existing buildings are not designed to accommodate mechanical ventilation systems, which means that retrofitting can be difficult and expensive [119]. The design of some buildings may not facilitate easy installation of ductwork or ventilation units.

The challenges to widespread mechanical ventilation adoption in Poland include high costs, lack of awareness, weak regulations and enforcement, technical complexities, cultural preferences, integration difficulties, and a lack of comprehensive financial support. These factors collectively contribute to the relatively slow uptake of mechanical ventilation in Polish residential buildings.

Chapter 04: Methodology

1 Introduction

This study adopts a mixed-methods approach, combining both qualitative and quantitative methods to assess and optimize natural ventilation in Polish residential apartments. The first phase involves a literature review and graphical analysis, serving as the qualitative foundation for understanding the evolution of housing typologies, climate adaptation strategies, and ventilation practices in Poland. Over 300 housing units from different cities were examined through visual mapping and statistical categorization to identify representative building forms. This phase also included case study selection, where key prototypes were chosen for in-depth analysis based on their layout, relevance, frequency, and architectural diversity.

The second phase, centered on analytical and numerical simulations using CFD. This includes the creation of detailed 3D models, scenario testing (with different window sizes, shading devices, and wind directions), and environmental boundary settings. A validation process using Butterfly (OpenFOAM) was applied to ensure accuracy and reliability. The selected case studies were analyzed to evaluate airflow performance, cooling potential, and the influence of design variables on natural ventilation effectiveness under different climatic conditions.

Complementing the CFD simulations is a thermal comfort analysis (final chapter), which also follows a quantitative methodology. The study is grounded in real-world residential data and building typologies, making it contextually and practically applicable. Together, the combination of literature review, case study selection, numerical simulation, and thermal comfort assessment provides a comprehensive methodological framework to evaluate and enhance passive cooling strategies in Polish housing.

Based on what discussed, this is the overview of this chapter and general workflow. Two main steps:

1. Prototype selection (library and theoretical)
2. Simulation (analytical and numerical)

2 Prototype selection

The Polish housing stock is classified based on four types: Single-family houses, terrace houses, multi-family houses, apartment blocks [105], but the Polish residential building stock is dominated by two main archetypes: (1) multifamily houses in dense urban regions and (2) single-family houses in rural and low-density areas [115]. New house owners prefer smaller houses for affordable cost because a smaller surface area allows them to have lower taxes [105], less maintenance cost and less energy costs.

Unlike single-family homes, which face their own challenges, multi-family buildings in, often dependent on natural ventilation for cooling, require a more targeted approach. Enhancing thermal comfort and indoor air quality in these buildings calls for integrated solutions, including insulation improvements, upgraded ventilation systems, effective shading, and supportive financial and policy frameworks tailored to their unique urban context.

The amount of concentration committed to improving building energy efficiency and thermal comfort can be determined by comparing it to the number and the floor area of buildings currently in existence. This chart shows Poland's investment plan for energy efficiency in non-residential (public), residential multi-family and single-family buildings in size of the building market in Poland. The number of non-residential buildings is around 310,000 with a total area around 250 Mm^2. There are around 535,000 multifamily buildings (with a floor area of around 400 Mm^2) and 5 million single-family houses (occupying a floor area of 540 Mm^2) [148] by the year 2018. So, multi-family residential is the second in Polish building stock and based on the increasing future demand, requires more attention and research.

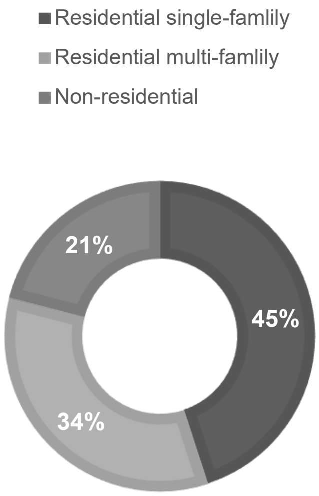

Fig. 4- 1: Share of building type by floor area. Calculation based on data from the Polish Statistic Office and BPIE report [148, 149].

The prototype selection process for the study on fenestration design and its impact on airflow and thermal comfort in Polish multi-family homes was a comprehensive, multi-faceted approach. It began with a broad survey of existing housing stock, progressed through detailed categorization and modeling, and culminated in simulations under specific environmental conditions. This systematic methodology ensured that the prototypes accurately represented the diversity of Polish housing while also allowing for focused analysis of key design parameters.

2.1 Initial Survey and Categorization

To initiate the case study selection process, a comprehensive graphical analysis was conducted on over 30 residential communities constructed between 1940 and 2020 across seven major Polish cities, including Warsaw, Gdańsk, and Poznań. This initial dataset encompassed over 320 residential units, with a focus on multi-family apartment buildings, a typology that remains prevalent in urban Polish contexts. The primary aim was to explore **spatial layouts**, ventilation strategies, and facade organizations across different architectural periods. The graphical analysis involved comparing floor plans, window placements, and orientation patterns, aiming to identify trends or recurring design logics that could influence thermal performance and natural ventilation potential. However, this purely visual method proved to be insufficient, as it lacked the depth and clarity needed to extract quantifiable parameters relevant to the research goals, particularly those concerning indoor climate behavior and energy performance.

As a result, the approach was refined by converting the architectural plans into structured statistical data, enabling a more analytical interpretation. Parameters such as ventilation type, window-to-wall ratio, floor area, and facade configuration were extracted and categorized, allowing for the generation of informative graphs and charts. This enhanced dataset provided a clearer foundation for selecting representative case studies that reflect the diversity of Polish housing stock and offer meaningful insights into natural ventilation effectiveness across building typologies and climatic conditions. Some of the main graphical analyses are shown here:

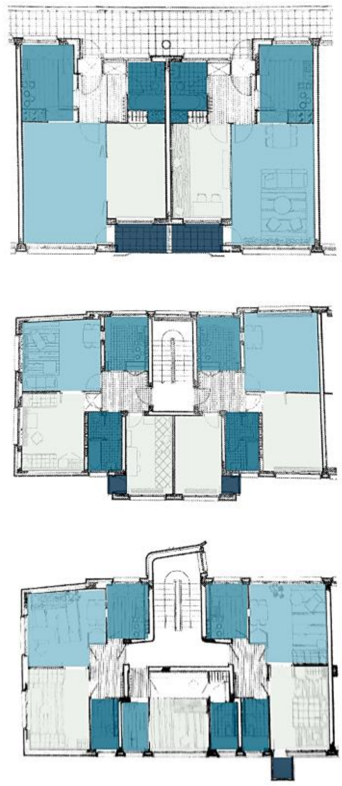

Fig. 4- 2: Kolo II WSM housing state 1947-1950 in Warsaw. A social housing estate based on the principles of the Athens Charter and the principles of C.A. Perry's neighborhood unit, using the polygonal "small prefabrication" technology of crushed concrete. From top to bottom: Plans of apartments in the gallery building and plan view of two units [150]. Edited by author.

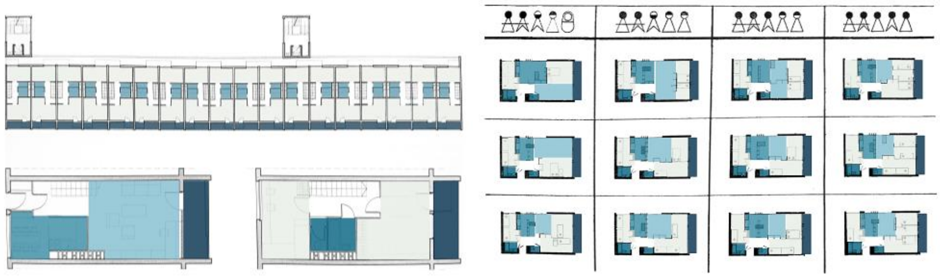

Fig. 4- 3: (Left) Mezonetowiec in Wrocław (designed by Jadwiga Grabowska-Hawrylak, Edmund Frąckiewicz, Marta and Igor Tawryczewscy, 1958-1960) A gallery-style building with two-level residential units stacked on top of each other in the Le Corbusier immeubles villas style, i.e. a tenement house with villas. Here, it is made using the monolithic technology of poured concrete with transverse walls filled with rubble concrete blocks [150]. Repeated floor plan at the level of apartment entrances and Floor plan of the lower and upper levels of the apartment color coded by author.

(Right) Sady Żoliborskie in Warsaw (designed by Halina Skibniewska, greenery design by Alina Scholtz, 1958-1963). Low point development using existing greenery and the possibility of flexible creation of the internal structure of individual apartments [150]. Apartment layouts depending on the family structure (5-person apartment, 57 m^2) showing the division of the interior using adjustable elements "wall units". Color coded by author.

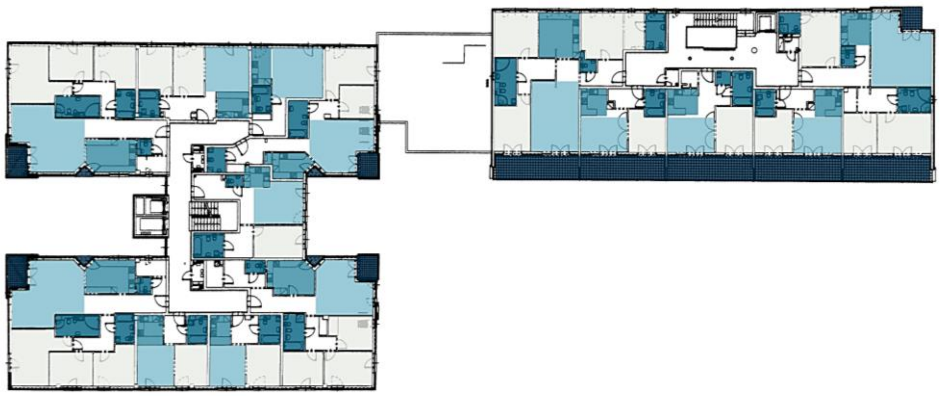

Fig. 4- 4: Office-Housing-Retail Buildings in Warsaw, 1998-2001. Site area 2567m^2 and building area 2128m^2 including 66 units [151]. Second floor plan, color coded by author.

Fig. 4- 5: "Kukurydze" in Katowice (designed by Henryk Buszko, Aleksander Franta, 1977-1979) One of the tallest tower megastructures in Poland with 8-9 apartments on each floor facing two different cardinal directions, services above the ground floor and an underground garage. Plan of one of the floors and two-bedroom apartment layout [150] color coded by author.

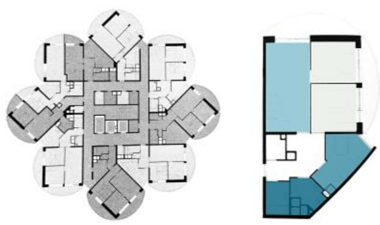

Fig. 4- 6: Winnica Housing Estate in Warsaw, 1998-2000. Total site area 16982m2 and building area 14300m2 including 240 apartment units between 50-150m2. The best building of Warsaw 2000-2001 (multi-family houses) in the LIFE IN ARCHITECTURE competition [152]. Ground floor plan of the multi-family building color coded by author.

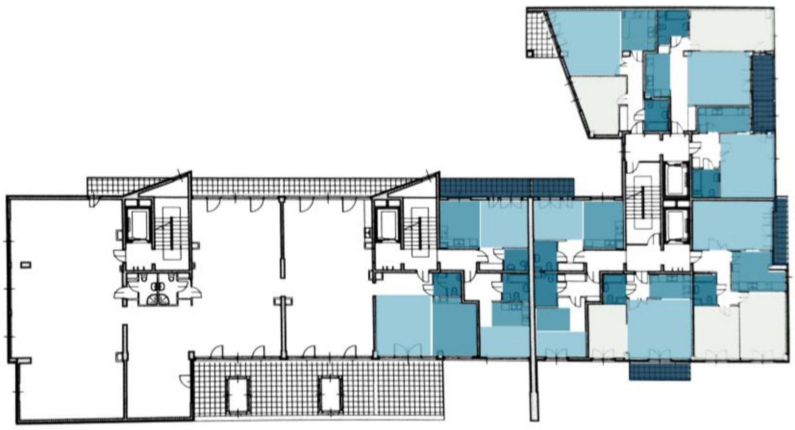

Fig. 4- 7: The Cotton House Apartment Building with Retail Area, Warsaw, 1998-2000. Site area 2009m2 and building area 1565m2 including 67 units in total [153]. Second floor plan color coded by author.

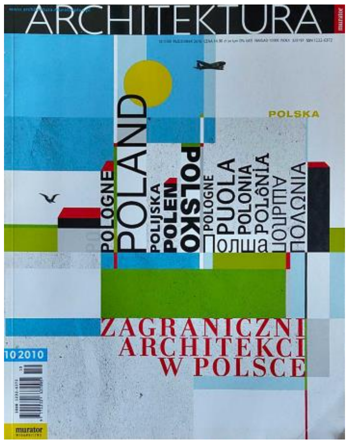

Fig. 4- 7: Cover of some ARCHITEKTURA magazines used for case study review.

These plans and cases were sourced from a variety of resources, including Polish architecture magazines, books, and reports dating from 1940 to 2020 (80 years period), specifically the "ARCHITEKTURA" series. This historical perspective allowed the researchers to understand how housing designs have evolved over time and to identify common archetypes. The categorization process was based on several key factors:

Size: The housing units were classified by the number of bedrooms, ranging from studios (no bedroom) to one-bedroom, two-bedroom, three-bedroom, and four-bedroom units. This is a critical factor, as the size of the unit directly impacts the layout and the potential for different ventilation strategies.

Ventilation type: The plans were assessed for their potential for natural ventilation, specifically whether they were suited for cross-ventilation or single-sided ventilation. As mentioned before, cross-ventilation, which involves airflow through a unit from one side to the other, is generally more effective for cooling than single-sided ventilation.

Facade organization: The organization of the building's facade, including the placement and size of windows, was another important factor. This affects how much solar radiation enters the building and how effectively natural ventilation can be utilized.

Fenestration type: Fenestration refers to the design and placement of windows in a building. The researchers categorized the window types based on their size, shape, and operational characteristics.

Location and year of construction/design: These factors provide context to the designs. Location affects climate exposure, while the year of construction/design reflects prevailing architectural styles and building codes.

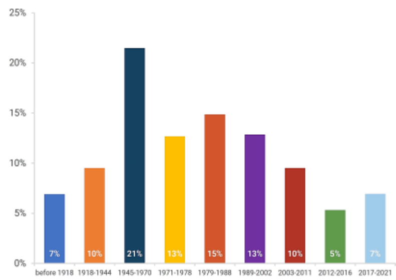

Fig. 4- 8: Share housing units in Poland by the year of construction (until 2022) [118].

After the initial categorization, since researchers identified two dominant archetypes in Polish residential buildings: multi-family houses in dense urban regions and single-family houses in rural and low-density areas [115]. Given the focus of the study on multi-family homes and thermal comfort, I only concentrated on the former archetype for further analysis.

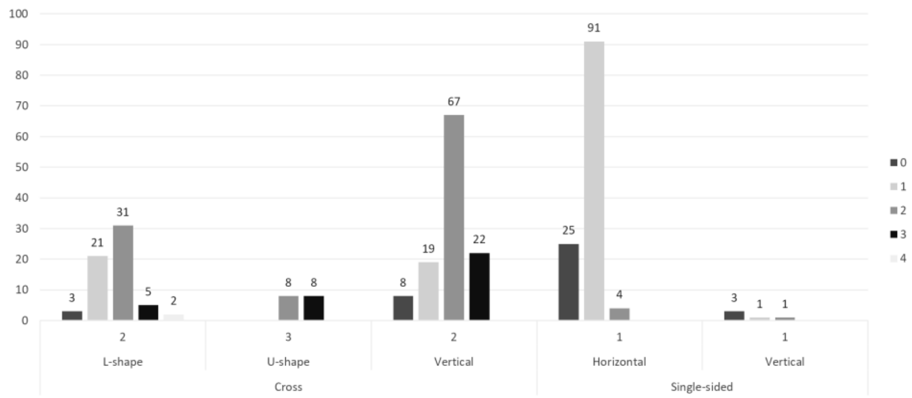

Fig. 4- 9: Distribution of the number of apartments surveyed based on the type and potential of ventilation and the number of rooms.

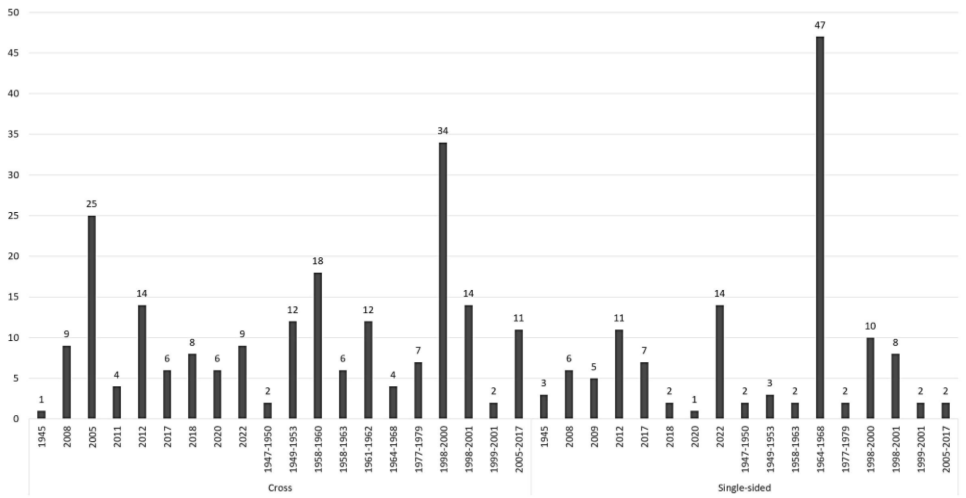

Fig. 4- 10: Distribution of the number of apartments based on the ventilation type and potential, year of design and construction.

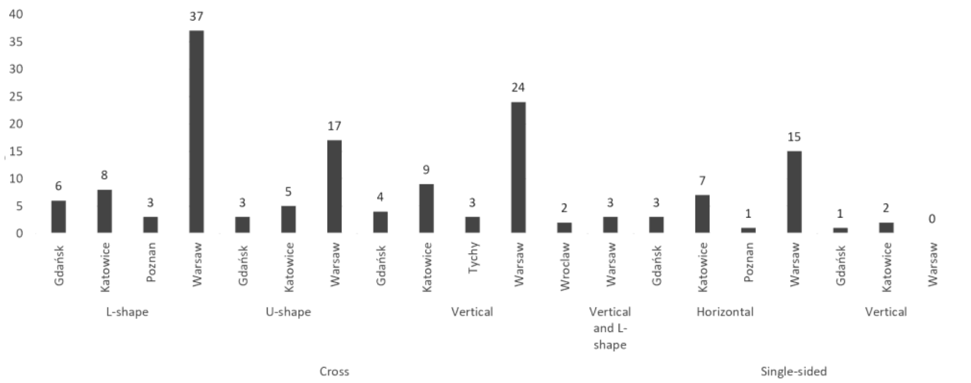

Fig. 4- 11: Distribution of the number of studied apartments based on the type and potential of ventilation and city.

Based on the analyzed data and statistical findings, although residential buildings constructed between 1945 and 1970 represent a larger portion of the housing stock, they were not prioritized for this study. Since the focus of this research is on optimizing cross ventilation, and the architectural characteristics required for effective natural ventilation, specifically cross-ventilation potential, were more prevalent in buildings constructed between 1995 and 2005. According to our dataset of 320 apartment units analyzed, cross-ventilated layouts were more commonly implemented during this period. However, after 2010, such designs became less frequent due to the increasing pressure to maximize land use, leading to more compact and less ventilated building forms. Since this change leads to single-side ventilation design (which is the most challenging type of ventilation), this gap has already been covered by many researchers [8, 25, 153].

Furthermore, considering the timing of this research, and the fact that major building renovations are typically recommended every 25-30 years [154], this period (1995-2005) presents an ideal time frame for intervention. Therefore, two residential complexes from this era were selected as case studies, representing not only relevant architectural features for natural ventilation but also a practical opportunity for energy-efficient retrofitting in the current decade. These two also represent two different types of cross ventilation and corner ventilation.

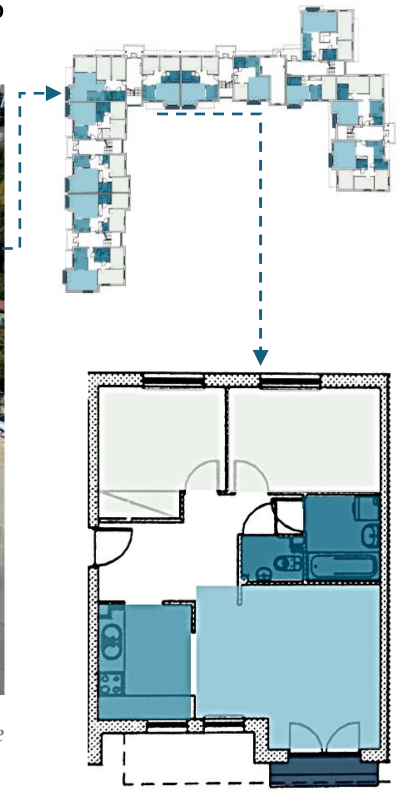

Fig. 4- 12: Warszawa Osiedle Winnica [155]. The process of selecting building block and the apartment unit (not scaled).

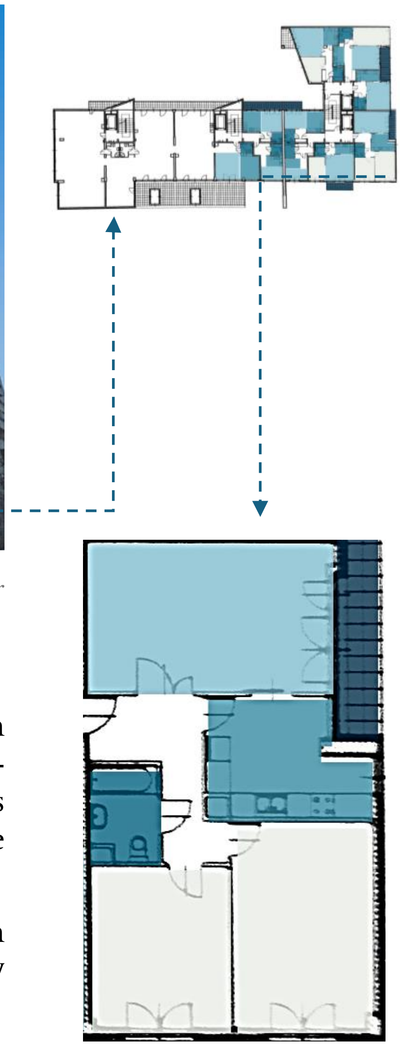

Fig. 4- 13: Cotton House, Warszawa [156]. The process of selecting the apartment unit for corner ventilation case study (not scaled).

2.2 Ventilation potential and window type selection

Ventilation Potential: An important observation was that two-bedroom housing units often have the potential for cross-ventilation, while single-bedroom units and flats are usually limited to single-sided ventilation. This distinction is significant because cross-ventilation is generally more effective at promoting airflow and reducing indoor temperatures.

Window Types: To ensure the models were realistic, I consulted with architects and experts to determine the most commonly used window types in Poland. Two window sizes were selected for further study: 120cm wide by 150cm high and 150cm wide by 150cm high. These sizes represent typical dimensions found in Polish multi-family homes.

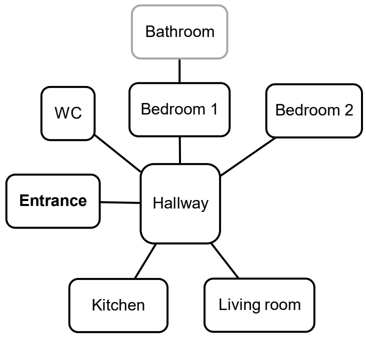

Fig. 4- 14: Graph diagram of the frequent spatial hierarchy in the two-bedroom units of the surveyed apartments.

The detailed approach to prototype selection ensured that the study's findings were relevant to the Polish context and could provide practical guidance for improving the thermal comfort and energy efficiency of multi-family homes. By considering a range of factors, from housing archetypes and ventilation strategies to window types and solar protection devices, the I was able to gain a nuanced understanding of the interplay between design and environmental performance. The results of this study can inform the design of new buildings and the renovation of existing ones, helping to create more comfortable and sustainable living environments in Poland.

3 Analytical and numerical study

Two main categories of CFD studies can be distinguished: (1) fundamental studies, which are typically conducted for simple, generic building configurations to obtain insight in the flow behavior, for parametric studies and for CFD validation, and (2) applied studies, which provide knowledge of the natural ventilation in specific and often much more complex case studies [157]. In the remainder of this section, only applied studies with natural cross-ventilation will be addressed.

CFD has undergone a significant evolution in Computational Wind Engineering (CWE) over the past 50 years, transitioning from an emerging field into an increasingly established one in research, practice, and education [157, 158]. This evolution has been driven by the improvement of computational power and the spread of commercial and open-source CFD codes [157, 159]. Early efforts in CWE focused on determining and analyzing wind velocity and pressure fields around buildings. A pivotal moment in its history was the organization of the International Symposium on Computational Wind Engineering (CWE) in 1992, which fostered interaction between wind engineers and aerodynamicists and marked the beginning of impressive growth in the field [160].

Recognized successes of CFD in CWE:

- **Establishment as a distinct field:** CWE is now recognized as an individual research and application area within wind engineering, evidenced by its successful conference series under the International Association of Wind Engineering (IAWE) [157, 158].
- **Broadening scope of applications:** The range of topics covered by CWE has significantly increased over time. Initially focused on wind loads, it now encompasses various environmental applications such as pedestrian-level wind conditions, natural ventilation of buildings, wind-driven rain on building facades, pollutant dispersion, urban microclimate, urban wind energy, and snow/sand erosion and accumulation [159, 161-164]. For instance,

CFD is increasingly used to simulate pedestrian wind comfort [163, 165], natural ventilation performance [50, 166], and the distribution of wind-driven rain on building facades [167, 168].

- **Development of best practice guidelines:** Recognizing the sensitivity of CFD results to various computational parameters, significant efforts have been made to develop best practice guidelines for CWE simulations [157, 161, 169, 170]. These guidelines aim to ensure more accurate and reliable CFD simulations, particularly for applications like pedestrian-level wind studies [171, 172].
- **Provision of detailed flow field data:** A key advantage of CFD over experimental testing is its ability to provide detailed information on relevant flow variables in the entire calculation domain (whole-flow field data) under controlled conditions and without similarity constraints [170, 173, 174]. This allows for a more comprehensive understanding of wind flow phenomena.
- **Growing acceptance in practice:** CFD is gaining increasing acceptance as a practical tool in wind engineering. The Dutch Wind Nuisance Standard, NEN8100, specifically allows the use of CFD alongside wind-tunnel testing for assessing pedestrian-level wind comfort and safety, marking a significant milestone in its acceptance [175, 176].
- **Advancements in turbulence modeling for environmental applications:** While challenges remain, steady Reynolds-Averaged Navier-Stokes (RANS) models have become the main tool for many environmental applications due to their robustness and computational efficiency [177, 178]. The strengths and weaknesses of different turbulence models for pollutant dispersion have also been clarified
- **Integration with design platforms:** The development of CFD plug-ins integrated into urban and building design platforms like Revit, Rhino/Grasshopper, and SketchUp is expanding the use of CFD in the early design stages for performance simulations [179-182].

Future directions of CFD in CWE:

Future efforts will focus on better modeling of complex factors such as **thermal effects and unresolved obstacles like trees** in urban environments [183-185], as well as improving the accuracy of turbulent scalar (heat) fluxes [186, 187]. There is a growing interest in utilizing the detailed information from CFD not just for prediction but for searching for optimal designs in urban environments and building shapes to mitigate adverse wind effects and improve environmental performance [188-190]. This involves integrating CFD with robust optimization techniques.

Coupling CFD with Building Energy Simulation (BES) is expected to increase for **improved prediction of building performance**, including airflow, thermal comfort, and energy consumption [49, 191, 192]. The development of faster and more accurate CFD plug-ins for design platforms will make CFD more accessible to architects and urban planners in the early design stages [179, 193, 194]. Integrating **fast CFD (FFD)**

methods with machine learning (ML) algorithms is seen as a crucial future trend for enhancing computational efficiency and providing immediate feedback [195].

Ensuring the **quality and reliability of CFD simulations** through rigorous verification and validation studies, including comparisons with high-quality wind-tunnel or on-site measurement data, remains crucial [169, 196]. Validation for simpler configurations when data for complex scenarios is unavailable will continue to be important [165, 197, 198]. Future research may delve into areas currently less explored by CWE, such as surface convective heat transfer, wind and acoustics, wind-borne debris, wind energy in the built environment, and sports aerodynamics.

Despite the progress, the CWE community acknowledges that **CFD is complementary to, but cannot replace, traditional methods like wind-tunnel testing and full-scale measurements** [199-201]. Exploiting the synergy between experiments and CFD simulations is considered the most promising approach for tackling complex wind engineering problems. The ultimate goal is to develop CFD into a more structured and reliable design tool for both environmental and structural aspects of building and urban design.

3.1 CFD tools

The application of Computational Fluid Dynamics (CFD) has seen rapid expansion in building design, driven by improvements in computational power and the wider availability of both commercial and open-source CFD codes. This has led to the development of a diverse range of CFD tools and plug-ins tailored for the architecture, engineering, and construction (AEC) industry, seamlessly integrating with popular design platforms such as Autodesk Revit, Rhinoceros/Grasshopper, and etc. These tools offer varying capabilities for simulating airflow, pollutant dispersion, thermal conditions, and other environmental aspects crucial for building performance evaluation and optimization. A comparative analysis of these CFD tools and plug-ins is essential for understanding their specific features, underlying solvers, integration methods, and suitability for different stages of the design process and various building performance analyses. The table below provides an overview of various CFD tools and plug-ins used in building design, highlighting their integration platforms, underlying solvers, and some key characteristics mentioned in the sources. Keep in mind that this is not an exhaustive list, but it covers the tools and plug-ins most prominently discussed in the recent researches.

CFD Tool/Plug-in	Design Platform(s)	CFD Solver(s) Used	Comfort study	Open source	Key Features/Notes
ANSYS Fluent	Standalone	ANSYS Fluent	✓	×	Requires high computer resources. Used for mesh generation and CFD simulations. Can be used for various building design applications.
OpenFOAM	Standalone, Grasshopper (via Butterfly)	OpenFOAM	✓	✓	Requires high computer resources. Used by Butterfly plug-in. Validated CFD software. Butterfly is extensively applied to predict airflow conditions in urban blocks.
Autodesk CFD	Standalone, Revit	Autodesk CFD	×	×	Has a friendly GUI and automatic meshing. Supports airflow, pollutant dispersion, and heat transfer simulations. Airflow simulation results can have lower accuracy than OpenFOAM. Popular plug-in for Revit.

Autodesk Flow Design	Standalone, Revit	(Not explicitly mentioned)	×	×	Performs rapid airflow simulations for forced convection and calculates drag coefficient. Exhibits lower accuracy than validated CFD software like OpenFOAM. User-friendly interface for architects.
RhinoCFD	Rhinoceros	PHOENICS	✓	×	Integrates airflow, pollutant dispersion, and heat/mass transfer analysis. Sufficient accuracy and high computational speed for outdoor airflow. Relatively wide variety of turbulence models. Used for optimizing natural ventilation.
Butterfly	Grasshopper	OpenFOAM	✓	✓	Extensively applied for predicting airflow in urban blocks. Uses external CFD solver (OpenFOAM). Requires establishing a simulation workflow by linking graphical nodes. Lacks a mature GUI. Cannot simulate porous media such as trees. Relatively wide variety of turbulence models.
Swift	Grasshopper	(Not explicitly mentioned)	×	✓	Concise GUI to simplify initial settings. Architect-friendly for airflow simulations. Supports parametric analysis.
Eddy3D	Grasshopper	OpenFOAM	✓	✓	Models box and cylindrical computational domain for multiple wind directions. Used for annual outdoor thermal comfort assessment. Used for wind factor calculation.
ProceduralCS	Grasshopper	OpenFOAM	×	✓	Uses cloud technology for parallel computation. Supports various simulations including energy. Has optimization functions.
ixCube CFD	Grasshopper	OpenFOAM	×	✓	Relatively new...
GH_Wind	Grasshopper	FFDSolver	×	×	Uses Fast Fluid Dynamics (FFD) method for increased simulation speed. Trade-off between speed and accuracy. Lacks a turbulence model Generates smaller wind speed values in low-height areas compared to others.
MicroFlo	SketchUp	IES(VE)	×	×	Focused on indoor and outdoor forced convection simulations. Sensitive to changes in window openings. Provides only the STKE turbulence model.
MacroFlow	SketchUp	ApacheSim	×	×	More capable of simulating natural convection, air infiltration, and thermal pressure ventilation. Provides only the STKE turbulence model. Used to input detailed wind speed data for energy performance simulation.

Table 4- 1: CFD simulation tools and capabilities.

Other researchers also developed the same chart with some different features:

	Energy demand	**Outdoor comfort**	**Urban environmental conditions**	**CFD**	**Open source**
(a) Software					
UWG [202]	×	×	✓	×	✓
SOLWEIG [203]	×	✓	✓	×	✓
Energy Plus [204]	✓	×	×	×	✓
CitySim [205]	✓	✓	✓	×	✓
TRNSYS [206]	✓	×	×	×	✓
ENVI-met [207]	×	✓	✓	✓	×
OpenFOAM (OpenFOAM)	×	×	×	✓	✓
FreeFem++ (FreeFEM)	×	×	×	✓	✓
ANSYS Fluent	×	×	✓	✓	×
Autodesk CFD [208]	×	✓	✓	✓	×
DesignBuilder [209]	✓	✓	×	✓	×
(b) Hybrid workflows					
ENVI-met + EnergyPlus [210]	✓	✓	✓	✓	×
Ladybug Tools [211-213]	✓	✓	✓	✓	✓
UMI [214]	✓	✓	✓	×	✓
ENVI-met + TRNSYS [215]	✓	✓	✓	✓	×
Ladybug Tools + ENVI-met [216]	✓	✓	✓	✓	×

Table 4- 2: Simulation tools and workflow capabilities[217].

3.2 Challenges of method and software

Applying CFD in building performance and environmental simulations presents several key challenges, and ensuring the accuracy and reliability of the results requires rigorous validation techniques [197, 218-220]. Here is a list of these challenges:

High Reynolds numbers in wind engineering applications necessitate high grid resolutions, especially near walls, and accurate wall functions [197]. The high grid resolutions will cause more computational demand, time and costs.

Complex 3D flow fields around bluff bodies with sharp edges, involving impingement, separation, and vortex shedding, pose difficulties not encountered in simpler flows [197]. Numerical difficulties arise from **flow at sharp corners** and their consequences for discretization schemes.

Inflow and outflow boundary conditions are particularly challenging, especially for Large Eddy Simulation (LES) [218]. Accurate simulation, especially with LES, can be **time-consuming and costly** [219]. Coupling CFD with BES can be computationally demanding, sometimes requiring simplified models [221, 222].

Accurate **turbulence modeling** remains a significant challenge. Reynolds-averaged Navier-Stokes (RANS) models might not accurately capture turbulent dispersion, especially for phenomena like wind-driven rain on high-rise facades [223]. LES, while more accurate, increases model complexity and sensitivity to input data [224, 225]. Modeling the interaction between **outdoor wind flow and indoor airflow** at ventilation openings is complex. Coupled and decoupled approaches exist, each with its own challenges [225].

Modeling the **dispersion of pollutants** in complex urban environments requires resolving individual buildings [178]. Simulating phenomena influenced by **atmospheric stability** (e.g., pollutant dispersion) poses challenges in turbulence modeling [226]. The treatment of peak structural wind loads and cladding pressures remains a major challenge [227]. Due to these factors, exploring all possible design variations using full CFD simulations can be inefficient, highlighting the need for robust optimization techniques alongside increasing computational power.

CFD results can be very **sensitive to the wide range of computational parameters** that users must set, including target variables, governing equations, turbulence model, computational domain, grid, boundary conditions, discretization schemes, and convergence criteria. The **selection of appropriate inflow boundary conditions**, particularly for simulating atmospheric boundary layers, is crucial [179]. Incorrect specifications can lead to inaccurate results.

For natural ventilation in complex urban environments, large differences in spatial scales (urban area to ventilation openings) demand high-resolution grids and increase computational cost [228, 229]. Scaling issues can arise when comparing reduced-scale wind tunnel measurements with full-scale scenarios, particularly for buoyancy-driven flows and ventilation openings [226].

Applying CFD for studies like natural ventilation in practice, especially in complex urban environments, has remained relatively limited due to computational cost and the expertise required [230]. As a result, although CFD has long been recognized as a powerful tool for visualizing and optimizing airflow in buildings, its practical application in architectural design and retrofitting projects has been slow to evolve. This research aims to address and bridge that gap by demonstrating the advancement of today's simulation platforms, increased accessibility to computational resources, and the integration of plugin-based tools such as Butterfly and Eddy3D within visual programming environments, CFD analysis is now more achievable than ever; even for early-stage design or renovation scenarios. By combining accurate 3D modeling, validated simulation workflows, and intuitive visualization outputs like airflow vectors and heatmaps, this study not only highlights the technical feasibility of using CFD in typical residential case studies but also provides a reproducible methodology that can be implemented by researchers, architects, and planners. It showcases that with today's software and hardware capabilities, CFD can move beyond academic or specialized engineering use and become a practical decision-making tool for improving natural ventilation and thermal comfort in real-world buildings.

3.3 Why Autodesk CFD?

Autodesk CFD is a strong candidate for research, particularly in the fields of urban and building design, due to its comprehensive simulation capabilities, user-friendly interface, and deep integration with common design platforms [231]. The following reasons justify choosing Autodesk CFD for research:

- Autodesk CFD is designed as a plug-in for Autodesk Revit (software used for 3D modeling).
- Unlike some other CFD plug-ins that focus only on airflow, Autodesk CFD supports a wide range of objectives like airflow and natural ventilation, pollutant dispersion, thermal and radiation Analysis.
- Another standout features are the ability to automatically generate unstructured tetrahedral meshes.
- It provides a concise **Graphical User Interface (GUI)** and guidance through simulation steps.
- In research involving multi-objective optimization (e.g., evaluating 1,600 urban block cases), Autodesk CFD's **fast simulation speed** has been cited as a key factor in improving workflow efficiency.
- While specialized software like OpenFOAM may offer higher precision in some scenarios, studies have found that Autodesk CFD provides **acceptable accuracy** for early design analysis.

In summary, Autodesk CFD should be chosen when the research requires a **high degree of integration with BIM**, the ability to simulate **multiple environmental factors** (heat, air, and pollutants) simultaneously, and a

fast, automated workflow suitable for early-stage design optimization [231].

3.4 Coupled wind-induced CFD simulation

Accurate design and evaluation of **natural cross-ventilation** in buildings require a robust simulation approach that can capture the complex interaction between **external wind flow** and **indoor airflow dynamics**. Computational Fluid Dynamics (CFD) is widely regarded as the most effective and precise method for modeling such scenarios, particularly due to its ability to resolve detailed spatial variations in pressure, velocity, and temperature. However, it is well recognized that CFD simulations are **highly sensitive to numerous user-defined parameters**, including boundary conditions, turbulence models, mesh resolution, and solver settings, all of which can significantly influence the accuracy and reliability of the results [225]. As noted by Chen [15], CFD has become the most common and suitable modeling technique for studies on **indoor air quality** and **natural ventilation**, as these complex phenomena are often difficult to analyze using analytical or empirical models alone.

In the context of cross-ventilation, one of the most effective forms of natural ventilation, CFD modeling can generally follow two main approaches: the **decoupled** method and the **coupled** method. The **decoupled method** involves conducting two separate simulations: one for the outdoor environment, where openings in the building are either removed or modeled as solid surfaces; and a second simulation for the indoor space, where the external simulation's pressure values at the openings are used as boundary conditions. While this method reduces computational demand, several studies have shown that it can introduce **significant inaccuracies**, particularly in capturing the dynamic pressure fluctuations and bidirectional airflow that occur at large openings [225, 232, 233].

To overcome these limitations, the **coupled CFD method** has become the preferred approach in current research. In this method, both the **indoor** and **outdoor environments** are modeled within the **same computational domain**, allowing for the simultaneous and interactive calculation of airflow patterns across building openings. This approach provides a **more realistic simulation of natural ventilation**, as it better reflects the complex exchange of air between the building's interior and exterior through façade openings. The openings are modeled as voids, enabling the simulation to resolve the airflow entering and exiting the building based on real-time pressure differentials, rather than relying on static boundary inputs [232]. This method requires very fine meshing process which will cause high computational demand and time.

The simulation process in this study was conducted using **Autodesk CFD**, a commercial CFD tool capable of handling steady-state, incompressible flow with built-in support for turbulence modeling and thermal analysis. The coupled simulation setup employed in this research ensures that the interaction between external wind forces and indoor airflow is accurately captured, providing a reliable basis for analyzing cross-ventilation performance and informing passive design strategies.

3.5 Validation methods and techniques

Ensuring the quality control of numerical results requires both **verification** (assessing numerical errors) and **validation** (determining if the model represents the physical flow accurately) [234].

High-quality full-scale or reduced-scale measurements (e.g., wind tunnel data, on-site measurements) are indispensable for validation. These measurements should satisfy important quality criteria. CFD results are compared with experimental data for various parameters such as velocity fields, pressure distributions, air exchange rates, and pollutant concentrations [229]. For LES validation, comparisons should be based not only on mean quantities but also on the frequency distributions of statistically representative ensembles [235]. Validation studies should be performed not only for isolated buildings but also for buildings in groups and complex urban environments [236].

The development and use of **best practice guidelines** for validating CFD in wind engineering are essential to address the sensitivity to computational parameters and promote reliable simulations [237]. Extensive best practice guideline documents have been compiled. These guidelines often focus on steady RANS simulations but also provide some information on Unsteady RANS (URANS), LES, and hybrid methods [161, 219]. For urban wind environment applications, best practice guidelines include verification and validation processes for predicting wind flow around buildings [18, 238].

Then, performing spatial and temporal **sensitivity analyses** to assess discretization errors is crucial. It is important to use CFD codes that are well documented and for which basic verification tests and validation studies have been successfully performed and reported [157, 184].

When experimental data for complex cases are unavailable, validation should be performed for **simpler configurations** that exhibit flow features resembling those expected in the case under study [239]. Comparing results from different CFD models or between CFD engines and other simulation types (e.g., zonal models, Airflow Network Models) can contribute to validation [240]. Validation studies are conducted for specific applications like natural ventilation (assessing airflow patterns, ventilation rates, air change per hour, age of air) [18, 241], wind-driven rain, and pollutant dispersion (comparing concentration fields) [242].

Applying CFD in building performance and environmental simulations is challenged by computational demands, the complexity of physical phenomena, sensitivity to user settings, and scale issues. Rigorous validation, primarily through comparison with experimental data, adherence to best practice guidelines, and comprehensive sensitivity analyses, is crucial to ensure the accuracy and reliability of CFD simulations in these fields.

3.6 3D modeling

To maintain a balance between simulation accuracy and computational feasibility, the apartment block model was strategically simplified in both form and scale. The overall shape of the building was reduced and streamlined to avoid excessive computational demands due to its originally large and complex footprint. However, to ensure realistic airflow interaction, the modeled unit was expanded on both lateral sides to represent neighboring apartments. This extension allowed the simulation to account for cross-ventilation dynamics and airflow obstruction that typically occur in continuous multi-family housing blocks, preserving the contextual behavior of wind flow across shared façades.

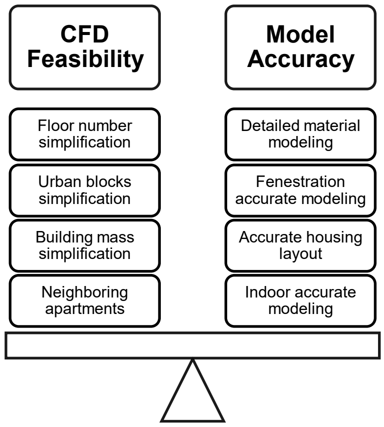

Fig. 4- 15: Balance between simulation accuracy and computational feasibility of CFD.

Regarding vertical complexity, the number of floors was limited to two, with each level carefully chosen to represent extreme conditions within the actual building. The ground floor stands in for the lowest levels, where wind velocity is typically reduced due to surface friction and obstructions, as confirmed by wind profile. In contrast, the top floor represents upper-level units exposed directly to the sun and prevailing winds, which often experience the most significant thermal loads and wind interactions. This two-level approach allows for targeted analysis of ventilation performance under the most contrasting conditions in the vertical profile, while minimizing the simulation's computational intensity.

3D model generation: Based on the categorized cases, I created two detailed 3D model of a typical two-bedroom multi-family home. The model included representations of the building's geometry, including internal walls and the placement of windows. The placement of internal walls can affect temperature and air velocity.

Fenestration: The 3D model incorporated different fenestration designs, including variations in window size and the incorporation of solar protection devices.

Window solar protection options: Then I created test models with different window protection options; a base model with no shading, horizontal louvers, and overhangs. These options represent common strategies used in Poland to mitigate solar heat gain.

3.7 Simulation scenarios

To evaluate the performance of natural ventilation and shading strategies under varying climatic conditions, a detailed scenario-based simulation framework was developed. Each selected case study apartment was tested under a combination of variables that reflect realistic summer conditions in Poland. The primary scenario setting included two window configurations, a smaller baseline opening and an enlarged version to test the impact of increased façade permeability (Fig. 4-16). The selection of two fully open different window sizes in this study was based on both architectural relevance and their impact on natural ventilation performance. The smaller window represents the typical size found in existing residential buildings, providing a realistic baseline for airflow and thermal analysis. The larger window reflects a feasible design intervention aimed at enhancing cross-ventilation potential without compromising structural or aesthetic integrity. By comparing these two sizes, the study evaluates how increasing the window-to-wall ratio affects indoor airflow patterns and thermal comfort, especially under summer conditions. This approach allows for a clear understanding of the trade-offs between natural ventilation effectiveness and design constraints, helping to inform retrofit strategies for improved passive cooling.

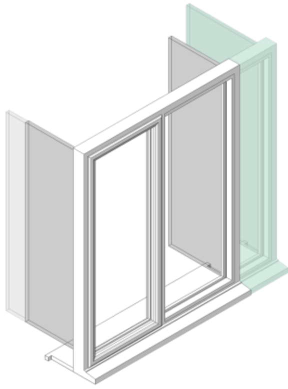

Fig. 4- 16: Two configurations of fully open windows in comparison to each other.

Additionally, three shading control options were integrated: (1) no shading (base model), (2) a 30 cm horizontal overhang with vertical side-fins, and (3) 10 cm deep horizontal louvers. These were applied to analyze their effect on indoor airflow, solar gain reduction, and thermal comfort. Furthermore, to account for Poland's variable wind patterns, simulations were conducted for eight prevailing wind directions (0°, 45°, 90°, 135°, 180°, 225°, 270°, and 315°). This comprehensive matrix of scenarios allowed for a nuanced understanding of how window sizing, shading devices, and wind orientation interact to influence ventilation effectiveness and cooling potential in residential settings.

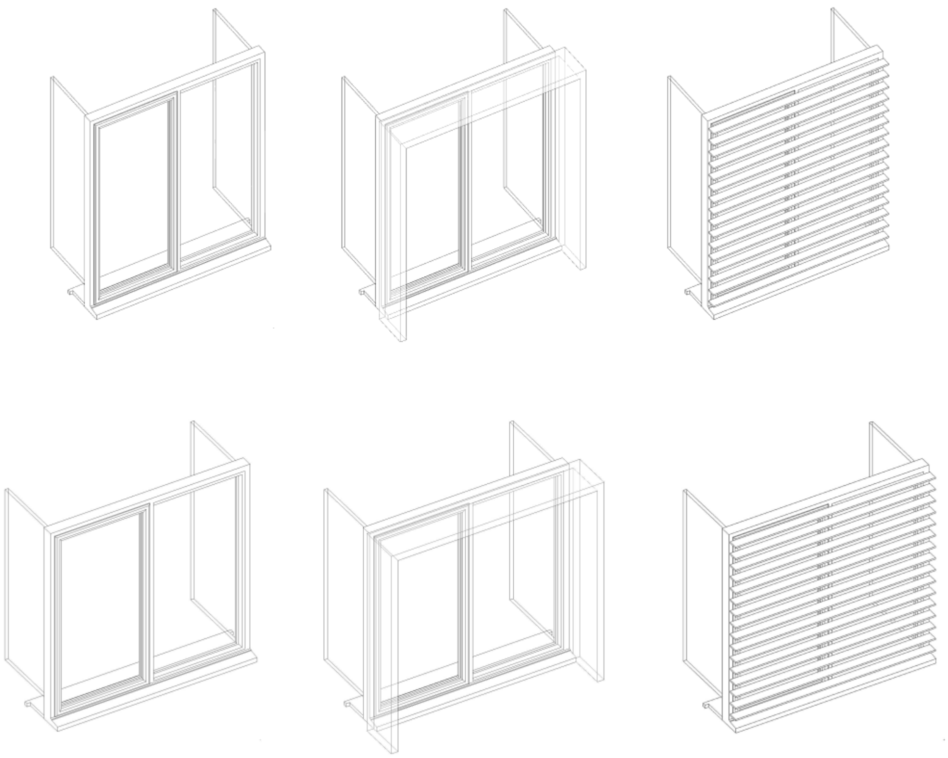

Fig. 4- 17: Different window size and solar protections; Small windows (top), large windows (bottom) with solar protections.

3.8 Model nomenclature:

To streamline the presentation of results, each model was assigned a concise name:

- **Window Size**: Small window or Base Model window (S), Big window (B)

- **Shading**: No shadings or Base Model (BA), Shading devices (SH), Louvers (LO)
- **Combined**: For example, a small window with the base model was designated as S-BA.

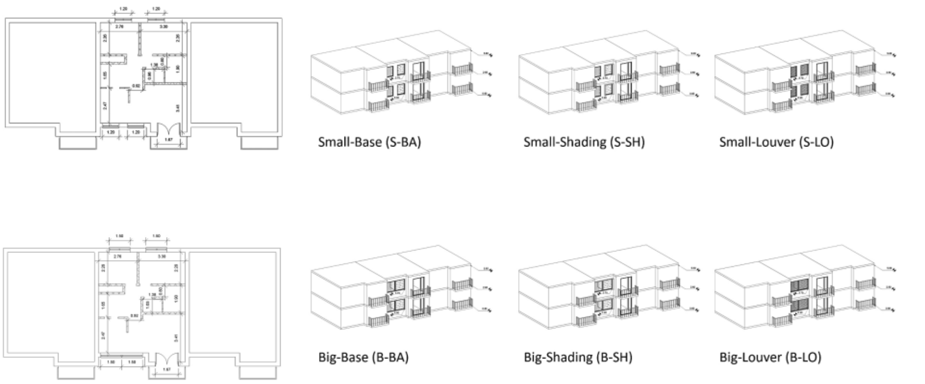

Fig. 4- 18: Full overview of the Cross Ventilation (CV) case study and scenarios.

1st row from left to right: cross ventilation case base model plan view, perspective views of base model (SBA), base window with shading (SSH) and base window with louvers (SLO). 2nd row from left to right: cross ventilation model with large windows plan view, perspective views of no shading with large window (BBA), then with shading (BSH) and last, with louvers (BLO).

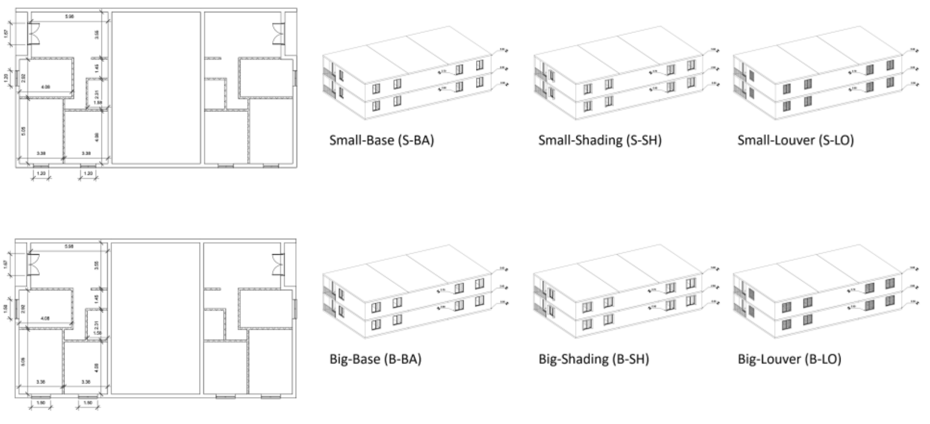

Fig. 4- 19: Full overview of the Corner Ventilation case study and scenarios.

1st row from left to right: corner ventilation case base model plan view, perspective views of base model (SBA), base window with shading (SSH) and finally, with louvers (SLO). 2nd row from left to right: corner ventilation model with large windows plan view, perspective views of no shading with large window (BBA), then with shading (BSH) and last, with louvers (BLO).

To simulate the effects of a dense urban context, two rows of surrounding building blocks were also introduced into the CFD domain. These blocks were modeled at the same height as the main building and placed based on recommended spacing ratios found in validated studies [243, 244]. Their inclusion ensures a more accurate representation of wind shading, redirection, Urban Heat Island (UHI), and turbulence commonly found in urban settings. By adopting these simplifications while retaining essential environmental and architectural parameters, the model achieves both realism and efficiency, making it suitable for iterative scenario testing and broader applicability in practical urban design evaluations. Since the primary focus of this study is on indoor airflow and thermal comfort, most of the simplifications were applied to outdoor and large-scale features such as building massing, surrounding context, and floor count, etc. ensuring accurate indoor results while maintaining simulation efficiency.

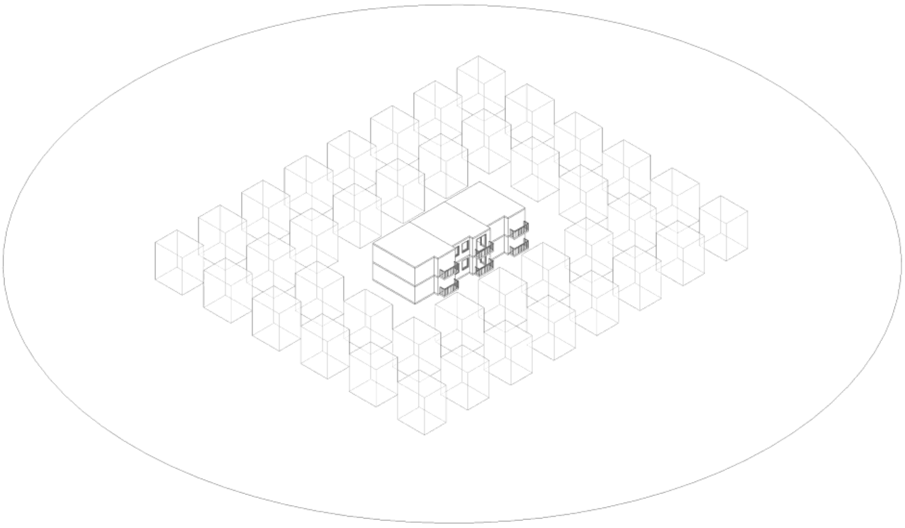

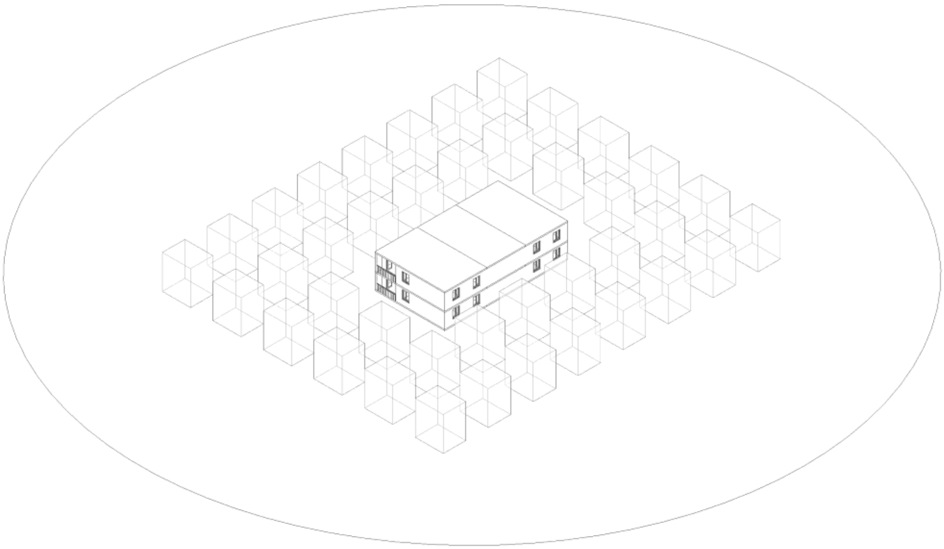

Fig. 4- 20: Cases in two floor blocks, surrounded with two rows of same height block simulating a dense urban area.

4 Boundary condition and domain

In order to ensure realistic and reliable simulation results, appropriate boundary conditions were defined based on both climatic data and best practices in CFD modeling for natural ventilation studies. The boundary conditions reflect hottest (the most extreme weather condition) in summer scenarios in Polish residential contexts, with a focus on capturing the airflow and thermal behavior under varying wind directions and facade configurations. The simulation domain includes conditions for airflow inlets and outlets, wall treatments, ground and sky boundaries, and solar heat influence on surfaces. These conditions were carefully selected to balance model accuracy with computational efficiency, while also aligning with the overall objective of evaluating cross-ventilation performance in representative apartment typologies.

4.1 Step 1. Climate Data:

To evaluate the performance of the prototypes under extreme conditions, the researchers used weather data from July 2022, which represented the worst (hottest) scenario for several major Polish cities. The analysis considered air temperatures in Warsaw (35°C), Poznan (37°C), Gdansk (35°C), and Krakow (36°C), as well as relative humidity (60-70%) and minimum wind speed (3-4m/s).

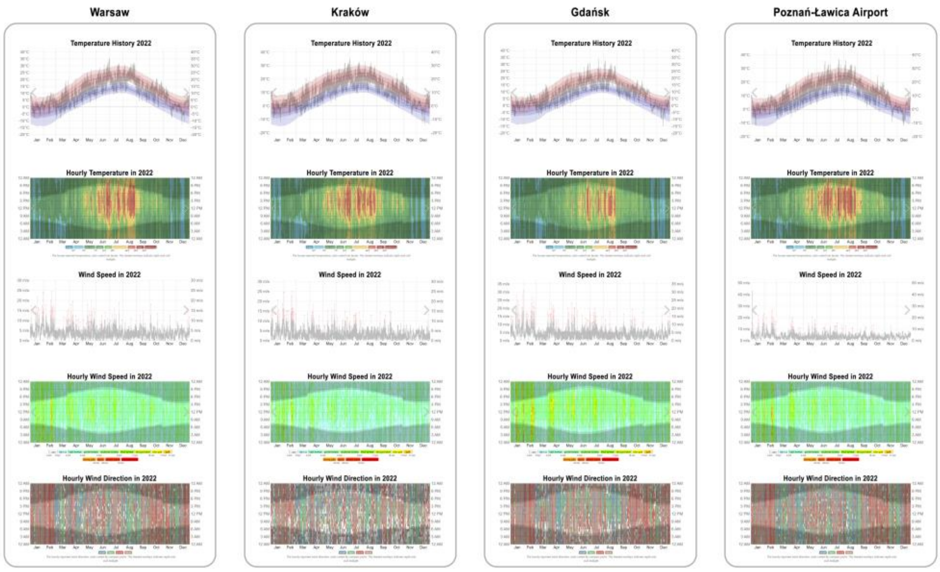

Fig. 4- 21: Air temperature, hourly temperature, hourly wind speed, and hourly wind direction in cities (left to right) in Warsaw, Krakow, Gdansk, and Poznan [245].

A second set of climate analyses was conducted to identify specific time periods during which natural ventilation (NV) would be most effective in improving thermal comfort. These periods are characterized by moderately high outdoor temperatures (typically ranging between 28°C and 32°C). This approach aimed to pinpoint windows of opportunity and potential where natural ventilation alone could be used to avoid mechanical cooling, particularly in late spring and summer afternoons. By targeting these thresholds (in the final chapter), the study highlights when NV has the highest potential to reduce indoor discomfort with minimal intervention, emphasizing its role as a low-energy cooling strategy during peak demand seasons. This analysis supported scenario selection and informed the timing of simulations to reflect the most relevant and realistic summer conditions in Polish apartments.

4.2 Step 2. Boundary Domain:

To ensure accuracy and minimize user-dependent errors in CFD simulations, many international research teams have developed best practice guidelines for setting up boundary conditions and simulation parameters (Fig. 4-22). Notably, these recommendations aim to standardize procedures and reduce inconsistencies in wind flow modeling across both external and internal building environments [246]. Following this approach, the current study begins with a CFD investigation of wind-induced airflow as the first simulation phase, addressing both outdoor wind behavior and its interaction with interior spaces through cross-ventilation openings.

For this purpose, simulations were conducted using both Autodesk CFD and OpenFOAM, applying Reynolds-Averaged Navier-Stokes (RANS) equations to resolve airflow patterns around and within the building geometry. The simulation setup was developed in accordance with guidelines established in prior work by Blocken et al. [247, 248], who performed validated CFD studies on cross-ventilated buildings. Their methodology includes detailed prescriptions on domain size, inlet conditions, meshing strategy, and validation protocols, serving as a reliable foundation for consistent CFD modeling.

The computational domain was scaled based on the building height (H), following the recommended ratios: 15H downstream, 5H upstream, and 5H laterally from the building's footprint to the outer domain boundaries [247]. This ensures undisturbed inlet flow and sufficient room for wake development, as well as symmetry and numerical stability. Accordingly, the full dimensions of the virtual wind tunnel for this simulation are approximately 260 meters in length, 190 meters in width, and 42 meters in height, as illustrated in Fig. 4-23 and derived from the domain scaling equations.

H ≈ 7m
l: 5H + Building + 15H = 260m
w: 5H + Building + 5H = 190m
h: H + 5H = 42m

The boundary domain used in the CFD simulations was intentionally set a little larger than standard recommendations to ensure accurate airflow behavior across all wind directions. This enlargement in width was particularly necessary because the building model is rotated to simulate different wind angles (45 and 90), causing its geometry to shift closer to the domain edges in certain orientations. To prevent any interference from boundary walls and to maintain a stable and undistorted airflow field, the upstream, downstream, and lateral boundaries were extended accordingly. This approach ensures that the results remain valid and unaffected by artificial pressure or velocity constraints near the domain limits, particularly in rotated scenarios.

The modeled building represents a contemporary multi-family residential building in Poland, constructed using common materials and techniques reflective of regional standards. External walls consist of conventional masonry with typical insulation, while the flat concrete roof aligns with modern urban housing practices in the Polish climate zone. To focus the analysis purely on ventilation effects, no vegetation, or extra balconies, or external shading devices were included in the base model. The windows are double-glazed, incorporating both single-hung and double-hung types, which are typical in local construction and provide a balanced trade-off between thermal insulation and controllable ventilation. These specifications ensure that the simulation results are not influenced by extraneous passive cooling measures, allowing for a clear assessment of the role of natural ventilation and airflow behavior under various design and environmental conditions.

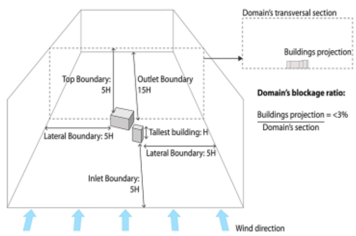

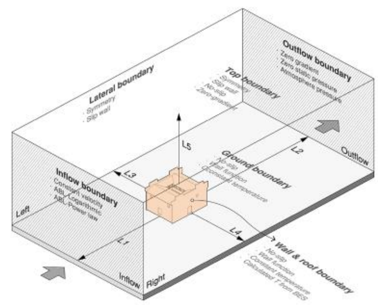

Fig. 4- 22: Selected domain's dimensions criteria (top) *[246]* and commonly used boundary conditions in CFD modeling of natural ventilation in vernacular architecture (bottom) *[249]*.

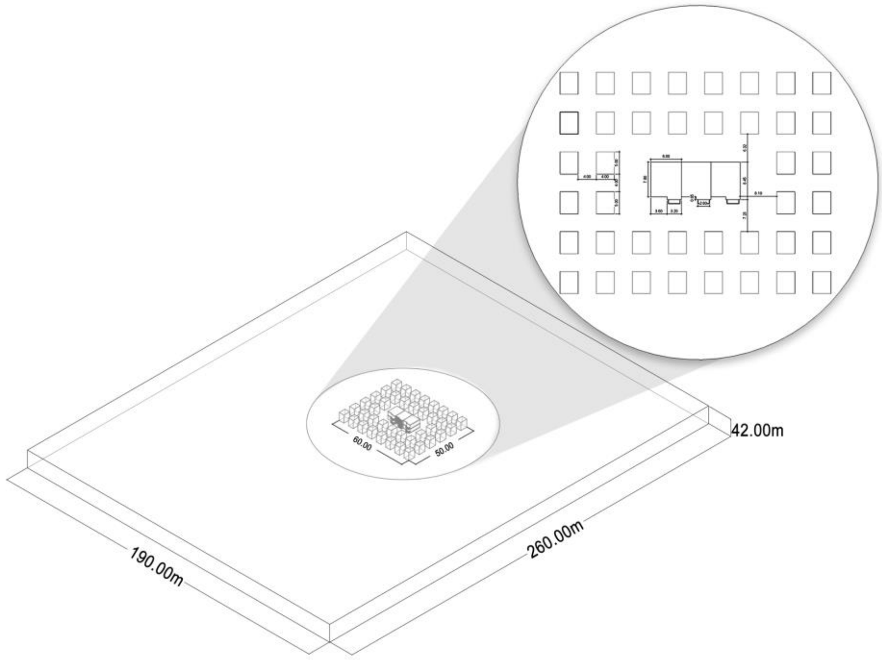

Fig. 4- 23: Boundary domain of this study in cross ventilation case.

4.3 Step 3. Boundary Conditions:

The model has been placed inside a volume of air with the inlet air velocity of 4m/s with the temperature of the hottest and the most extreme day (35°C) and relative humidity of 50%. The outlet gauge (Leeward Facade) pressure has been set to 0Pa and temperature not directly set (calculated by CFD simulation); the other four faces of the boundary domain (sides, top/sky, bottom/ground) has been set to be no-slip/symmetry (standard) with the temperature calculated from simulation. Just the ground was treated as adiabatic and given a fixed summer ground temperature.

Walls (building internal and external surfaces) are set to no-slip or standard, for their thermal condition set as calculated from simulation and solar radiation (solar gain). Interior surfaces (floor, furniture, ceiling) set to isothermal conditions or left with standard wall treatment. Glass material was used for the windows, and UPVC material for the window frames, wood material for balcony railings, and concrete construction elements were applied for the rest.

Boundary Type	Condition Type	Setting / Value
Inlet (Windward)	Velocity Inlet	Wind speed and direction based on 8 cardinal/intercardinal directions (0°-315°)
	Temperature	Fixed: 35°C (summer outdoor design conditions)
Outlet (Leeward)	Pressure Outlet / Outflow	Static pressure = 0 Pa (reference)
	Temperature	Not specified (solved by CFD engine)
Walls (Interior & Exterior)	No-slip wall	Standard CFD wall treatment
	Thermal Condition	Adiabatic or fixed temperature where needed
Ground (Building Base)	No-slip wall	Adiabatic or fixed at summer ground temp
Top (Sky Boundary)	Symmetry or Pressure Outlet	Neutral boundary (zero-gradient)
Side Boundaries (Wind Domain)	Velocity Inlet / Pressure	Matched to wind direction and domain size requirements

Table 4- 3: Bullet-point list of the boundary conditions used in the simulation.

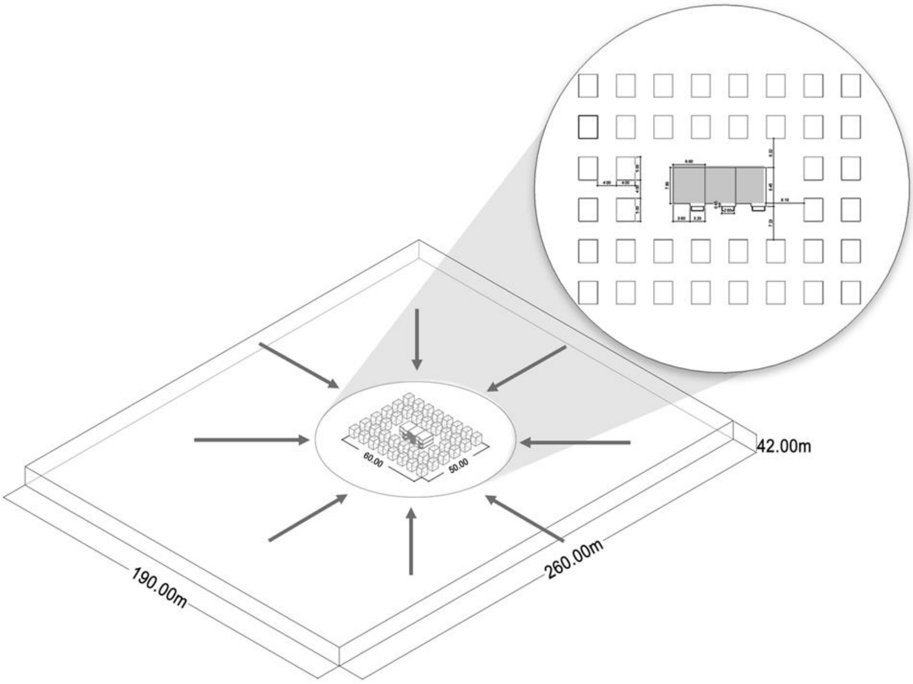

Fig. 4- 24: Boundary domain and all wind directions.

5 Mesh setting

The computational grid generated for all simulations shall resolve the flow features in the naturally ventilated spaces and around the development. The recommended grid sizes are as follows:

Location	Grid Size (m)
Within the functional spaces of interest	0.1 - 0.5
Building of interest	0.5 -1.0
Surrounding building	1.0 - 5.0
From ground surface to 10m height in vertical direction	0.5 - 1.0
From 10m height to H max height in vertical direction, (H max is the height of the tallest building among the group of buildings modelled explicitly)	1.0 - 5.0

Table 4- 4: The recommended grid sizes for each study scale [244].

To ensure a reliable representation of airflow dynamics while maintaining computational efficiency, the CFD simulation employs a base cell size of 0.5 meters across the computational domain. This resolution offers a practical balance between capturing detailed flow behavior and keeping simulation time and memory usage within reasonable limits. To allow for smoother transitions between coarse and fine mesh regions, a cell-to-cell growth rate of 1.30 is applied. This gradual expansion ensures numerical stability and mesh uniformity, particularly in zones where velocity gradients are expected to change rapidly.

The aerodynamic roughness length Z_0[2] for wind profile should be selected from the updated Davenport-Wieringa roughness classification as follows, to match the terrain category of the development site of interest, including the tree/greenery effect.

Z_0 (m)	Landscape Description

[2] Aerodynamic Roughness Length

0.0002 Sea	Open sea or lake (irrespective of the wave size), tidal flat, snow-covered flat plain, featureless desert, tarmac, concrete, with a free fetch of several kilometers.
0.005 Smooth	Featureless land surface without any noticeable obstacles and with negligible vegetation; e.g. beaches, pack ice without large ridges, morass, and snow-covered or fallow open country.
0.03 Open	Level country with low vegetation (e.g. grass) and isolated obstacles with separations of at least 50 obstacle heights; e.g. grazing land without windbreaks, heather, moor and tundra, runway area of airports.
0.10 Roughly open	Cultivated area with regular cover of low crops, or moderately open country with occasional obstacles (e.g. low hedges, single rows of trees, isolated farms) at relative horizontal distances of at least 20 obstacle heights.
0.25 Rough	Recently-developed young landscape with high crops or crops of varying height, and scattered obstacles (e.g. dense shelterbelts, vineyards) at relative distances of about 15 obstacle heights.
0.50 Very rough	Old cultivated landscape with many rather large obstacle groups (large farms, clumps of forest) separated by open spaces of about 10 obstacle heights. Also low large vegetation with small interspaces such as bush land, orchards, young densely-planted forest.
1.0 Closed	Landscape totally and quite regularly covered with similar-size large obstacles, with open spaces comparable to the obstacle heights; e.g. mature regular forests, homogeneous cities or villages.
≥ 2.0 Chaotic	Centers of large towns with mixture of low-rise and high-rise buildings. Also irregular large forests with many clearings.

Table 4- 5: Updated Davenport-Wieringa roughness classification [250].

In this study, an aerodynamic roughness length (Z_0) of 1.0 meters was selected to represent the surrounding landscape conditions in the CFD simulations. This value corresponds to a "closed" terrain classification, where the environment is densely and uniformly covered with large, similar-sized obstacles, such as homogeneous urban areas or mature, regular forests. This setting closely reflects the **compact urban fabric of Polish** cities, where multi-story residential buildings are arranged with limited open space between them. The chosen roughness length ensures that the simulation captures realistic **wind profiles** and turbulence characteristics typical of dense built environments.

The final mesh comprises approximately 1.8 million cells (1,806,508 elements) for the first case and over 2.3 million cells (2,381,750 elements) for the corner ventilation case, which has been verified as sufficient to resolve airflow patterns (next chapter), especially in areas critical for assessing cross-ventilation and corner ventilation flows. Special attention is given to the near-wall and opening mesh refinement, where layering techniques are employed to increase resolution in boundary layers. This allows the model to accurately simulate airflow interactions with building surfaces, which are essential for evaluating surface heat transfer, thermal comfort, and ventilation efficiency. Furthermore, snapping settings are enabled to enhance the adherence of mesh cells to curved and angled geometry boundaries, reducing mesh distortion and improving accuracy in complex architectural features.

These meshing strategies are designed in alignment with CFD best practices for building performance simulations. They collectively enhance the model's capability to predict realistic airflow patterns, pressure distributions, and temperature fields, providing a solid foundation for analyzing natural ventilation effectiveness and its impact on indoor environmental quality.

6 Run and solve setting

As previously discussed, the CFD simulation is configured using the Reynolds-Averaged Navier-Stokes (RANS) equations with k- ε turbulence model, a widely accepted approach for modeling airflow and turbulence in built environments. This model offers a robust and computationally efficient solution for capturing both large-scale air movements and turbulent mixing effects, making it particularly suitable for simulations of natural ventilation in architectural spaces. A steady-state simulation approach is adopted to assess ventilation performance under stable boundary conditions, reflecting typical daily scenarios rather than transient fluctuations.

Parameter	Case 1 (cross ventilation)	Case 2 (corner ventilation)
Air temperature	35 °C	35 °C
Relative humidity	50 %	50 %
Building surface temperature	By Autodesk CFD radiation	By Autodesk CFD radiation
Wind speed	Log-law profile	Log-law profile
Wind speed at reference height (10m)	4 m/s	4 m/s
Wind direction	0-360 (8 directions)	0-360 (8 directions)
Turbulence model	RNG k-epsilon	RNG k-epsilon
Turbulence kinetic energy	0.1 m^2/s^2	0.1 m^2/s^2
Turbulence dissipation rate	0.01	0.01
Reference temperature	35 °C	35 °C
Mesh cells	1,806,508 elements	2,381,750 elements
Refinement levels	4 (walls & openings)	4 (walls & openings)

Table 4- 6: Autodesk CFD simulation parameters summary.

To support high-resolution spatial analysis, the **result grid size is set to 0.5 meters**, matching the base cell size of the computational mesh. This configuration yields approximately **22,500** and **31,500 result points (every less than 20 centimeters)** distributed throughout the space of cross and corner ventilation models respectively, enabling detailed examination of airflow vectors, air temperature distribution, and ventilation performance across both indoor and outdoor zones. The simulation is performed in a **fully coupled method**, allowing the simultaneous calculation of indoor and outdoor airflow dynamics. This coupling is essential for accurately capturing the interaction between external wind forces (such as those acting in streets or canyons) and internal airflow patterns, which are driven by pressure differentials and façade by openings.

Convergence criteria are set to a residual threshold of **10^{-5}**, and convergence is achieved over **1000 iterations** in all cases. However it differs from case to case due to the different wind directions, and scenario in two cased. This level of convergence ensures both the **numerical stability** and **accuracy** of the results, indicating that flow variables (velocity, pressure, and temperature) have stabilized and are not changing significantly between iterations. The result is a reliable and precise dataset that can be confidently used for evaluating natural ventilation performance, assessing indoor thermal comfort, and guiding design decisions in later stages of the research.

7 Conclusion

The following are step by step guidance notes to help project keep track of natural ventilation design and simulation progress:

Guidelines	Description/Selection	Response & Criteria
Submission Details		Provide the project details (especially information on natural ventilated design, building massing/orientation, GFA of natural ventilated spaces, % of opening & windows, credible source of site information with surrounding buildings, vegetation and terrain, future development etc.)
Problem Statement	Objective & work scope	Describe natural ventilated challenges, proposed solution, desired outcome and work scopes from the simulation model. Whenever necessary, use the architectural drawing for explanation. Describe design stages and fix simulation details. Subsequent design change has to be supported by simulation results.
Site Information		Describe the site information, and illustrate how the geometrical info is incorporated into the simulation model. Terrain effect can be ignored if elevation is less than 10m.
CFD Approach	Simulation methodology	The CFD solver shall have the minimum capability of solving the Navier-Stokes fluid flow equations for a three-dimensional incompressible flow at steady state. Turbulence modelling shall also be included with the minimum requirement of using the standard k-ε turbulence model, coupled with standard wall function
	Assumption & simplification	Describe simulation model assumption, limitations and geometrical simplification. Whenever necessary, use the published literature data (including software manual) and comparison between architectural & CFD model for explanation
CFD Domain	Computational domain	Describe the domain decomposition methodology; and relevant meshing type for each domain within the site. Describe the domain that be modelled implicitly with Davenport Roughness classification
CFD Meshing	Mesh size, distribution and quality	To carry out proper domain decomposition. To use hexahedral cells in the rectangular domain of NV space. Tetrahedral cells can be used to model the surrounding site features of the NV space. As a guide, the dimension of the computational mesh should be set at 0.1 to 0.2 m within the functional space of interest, 0.5 to 1.0 m for building of interest and 1.0 - 5.0 m for surrounding buildings. The computational element size in vertical direction should be set at 0.5 - 1 m from ground surface to 10m height; followed by 1 - 5m to H max height.
CFD Model	Atmospheric boundary layer	1. To ensure horizontal ABL homogeneity in upstream and downstream 2. To ensure sufficiently high mesh resolution in vertical direction near ground (e.g. height of first cell < 1m) 3. To know the relationship between equivalent sand-grain roughness height (ks) and corresponding aerodynamic roughness height.
	Turbulence model	To use the steady Reynolds-Average Navier Stokes (RANS), with minimum requirement k-ε turbulence model equation for NV flow.
CFD Boundary Conditions	Inlet wind profile	To ensure the vertical profile for wind velocity and turbulence in the ABL should be modelled by assuming constant shear stress with height.
	Top & sides of domain	To use zero velocity gradients and zero normal gradients of all variables.
	Outlet plane	To use zero static pressure.
	Window modelling	To use actual window opening size. Attach window schedule and drawing for verification.
	Louver & shading	To use simplified porous zone with appropriate pressure drop components and directional effect.
	Heat source	To use aggregated heat load from heat sources
CFD numerical	Discretization scheme	To use 2nd order for momentum equations
	Convergence criteria	To ensure solution is converged and monitored points at functional space reach steady values
Documentation		Full documentation of parameters, readable scale
Design iteration	Baseline case Modified case Optimal case	Baseline case - fixed building massing and layout Modified case - to highlight improvement on NV design Optimal case - final design with incorporation of NV features or passive innovative ideas

Table 4- 7: Step by step guidance to help project keep track of natural ventilation design and simulation progress.

Chapter 05: Results

1 Introduction

This chapter outlines the validation process of the CFD methodology and presents the initial simulation results that establish a foundation for the full performance analysis. Validation is a critical step in ensuring the accuracy and reliability of computational simulations, particularly when applied to complex airflow and thermal comfort scenarios in real-world building environments. By replicating an experimentally tested model from existing literature and comparing the outcomes with measured data, the simulation setup was refined and calibrated to reflect realistic boundary conditions and airflow behavior. Following successful validation, the same simulation framework was applied to the case studies introduced earlier in the thesis. The early results presented here focus on airflow velocities and air temperature distributions across key scenario variations, offering a first look into how natural ventilation, window sizing, and shading strategies influence indoor thermal conditions. These results serve as a baseline for the more detailed comparative analyses and comfort evaluations that follow.

2 Input and outputs

In CFD studies focused on natural ventilation and indoor environmental quality, it is common practice to define a set of standardized inputs and outputs that guide both the simulation process and its evaluation. Typically, **inputs** include geometrical modeling of the physical space, boundary conditions such as wind speed, wind direction, outdoor air temperature, surface temperatures, and internal heat gains, along with solver settings, turbulence models, and mesh configuration. The corresponding **outputs** often consist of airflow velocity fields, temperature distributions, pressure maps, and sometimes thermal comfort or air change rates. These outputs provide critical insights into the effectiveness of ventilation strategies and overall indoor climate performance.

	Developing models for a group	Developing personal models	Aiming at optimized control of HVAC systems	Focusing on/predicting occupants' behavior	Total
Outdoor environment	18	7	3	6	34
Indoor environment	29	19	10	9	67
Personal/demographic	25	11	6	5	47
Contextual	10	5	1	3	19
Behavioral	4	6	1	6	17
Physiological	10	12	3	1	26
Lighting/visual	2	4	2	-	8
Time measure	10	5	2	5	22
CO_2 concentration	9	2	4	1	16
Occupancy status	5	1	3	2	11
Spatial/architectural	2	-	-	-	2
Noise	-	1	1	-	2
Expressed state	2	-	2	2	6
Vegetation	1	-	-	-	1

Table 5- 1: The frequencies of used input parameters in relation with the main objectives of the reviewed papers [100]. Graph by author.

In the context of this research, the simulations were driven by inputs such as 3D apartment geometry, two window configurations, three solar shading strategies, and eight wind directions representing typical urban airflow scenarios in Poland. Boundary conditions included inlet wind velocities, outdoor air temperature, RH, internal wall conditions, and the presence of adjacent buildings to mimic urban density. The CFD outputs generated for each scenario included air temperature and air velocity data, measured across various zones of the apartment, and categorized by floor level (ground and first floor). These outputs were carefully extracted and organized to allow for comparative analysis between different case configurations.

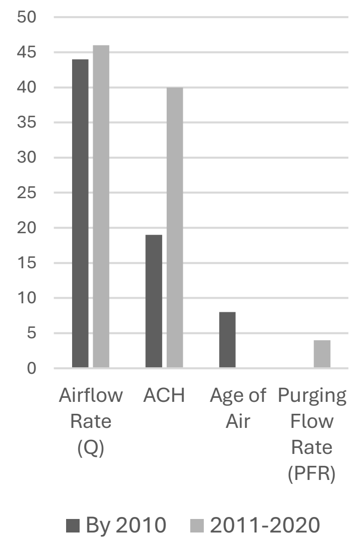

Fig. 5- 1: Proportion of different ventilation rate indices evaluated in the reviewed SSV papers [8]. Graph by author.

It is important to emphasize, however, that the data presented at this stage represent the raw outputs of the CFD simulations, objective numerical results that form the technical foundation for further interpretation. While these values provide clear physical indicators of airflow and thermal behavior, they are not yet assessed in terms of human thermal comfort or design performance. The comprehensive evaluation of these outputs, including discussions on their implications for energy efficiency, occupant well-being, and retrofit strategies, will be carried out in subsequent chapters. This approach ensures that the interpretation remains grounded in validated data while aligning with the broader objectives of the research.

3 Validation process

To determine the accuracy and reliability of the results of CFD simulations based on the 3D steady RANS equations, mesh calibration and results validation is needed. To validate the CFD process performed for this study, the methodology proposed and used by Kastner et.al [251] was followed. The validation of this study was carried out in two stages: Mesh Validation and Results Validation.

3.1 Mesh validation using Butterfly

According, the first stage of validation is sensitivity analysis in the meshing stage, which is carried out in three modes: (1) Coarse, (2) Medium and (3) Fine. The mesh size, mesh number, images, and other details for each refinement stage are illustrated and summarized in Table 5-2.

The mesh sensitivity was quantified using the relative percentage difference between mesh solutions using equations below and the results are reported in the table 5-2:

$$\mathrm{Error}_{21} = \frac{|U_2 - U_1|}{U_2} \times 100$$

$$\mathrm{Error}_{32} = \frac{|U_3 - U_2|}{U_3} \times 100$$

Where:

U_1 is the average indoor air velocity for the coarse meshing (for GF = 1.1, FF = 1.54);

U_2 is the average indoor air velocity for the medium meshing and (for GF = 1.08, FF = 1.52) ;

U_3 is the average air velocity of all indoor places for the fine meshing (for GF = 1.07, FF = 1.51) .

Parameter	1. Coarse mesh	2. Medium mesh	3. Fine mesh
Mesh and model illustration	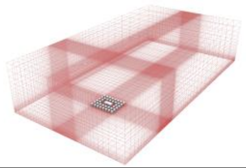	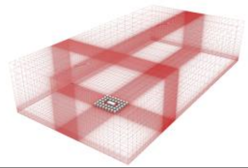	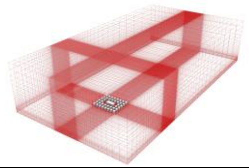
Cell number (M)	1.26 (-30%)	1.8	2.34 (+30%)
Relative difference (%)	Ground floor: 1.85 First floor: 1.31	-	Ground floor: 0.93 First floor: 0.66
$\frac{U_{Av.}}{U_{Ref.}}$	Ground floor: 0.275 First floor: 0.385	Ground floor: 0.27 First floor: 0.38	Ground floor: 0.268 First floor: 0.377
Minimum cell size (m)	~0.75	0.50	~0.40
Cell to cell ratio	1.30	1.30	1.30
Iteration	467	661	1760
Time (s)	+5000	+17500	+102000

Table 5- 2: Refined mesh sizes for the validation study in case cross ventilation.

Based on the table, the variation between coarse and medium mesh is less than 2% while between medium and fine meshes is below 1% ($error_{32} < error_{21}$), indicating that the solution is in the acceptable range and considered mesh independent. A **mesh-independence study** (comparing coarse, medium, and fine meshes) ensures that key quantities change by less than 1 % between successive refinements. This balances computational cost with accuracy and mirrors the careful grid convergence approaches recommended in the literature.

3.2 Result validation

To ensure the credibility of our CFD methodology, I begin by selecting a well-documented experimental case from Kosutova et al. (2024) [252] as our reference benchmark. By replicating this case in Autodesk CFD, I anchor simulation approach in empirical evidence before extending it to more complex apartment geometries.

Next, I recreate wind tunnel geometry and **computational domain** within Autodesk CFD. The experimental model is a 0.15 m^3 cubic enclosure at 1:20 scale, equipped with windward and leeward openings. To minimize blockage and interference effects, our CFD domain extends at least 6H downstream, 4H upstream, and 3H laterally, mirroring the open-circuit tunnel dimensions. This ensures that inlet and outlet boundaries do not unduly influence the internal flow field, faithfully emulating the physical setup.

Defining **boundary conditions** exactly as in the experiment is crucial. I prescribe a **uniform inlet velocity** of **2m/s** with at the windward opening, reflecting the measured atmospheric boundary layer profile. The inlet air temperature is fixed at 25°C, matching the ambient test condition. The leeward opening is modeled as a **zero-gauge-pressure outlet**, allowing temperature to be solved freely. All other surfaces are treated as **no-slip, adiabatic walls**.

I employ a **polyhedral mesh**, refining cell size near the openings, heated wall, and center plane to capture steep velocity and temperature gradients.

Other geometry and boundary settings:

1. **Reference Case**

- Two opening-size configurations from Kosutova et al. (2024):
  - **Large opening (LO)**: 0.07m × 0.04m (12.5% façade porosity)
  - **Small opening (SO)**: 0.04m × 0.035m (6.2% façade porosity)

2. **Recreate Geometry and Domain**

- Model the cubic enclosure (0.15 m^3 at 1:20 scale) with windward and leeward openings per the paper's dimensions (Fig. 5-2).
- Surround it by a rectangular CFD domain of at least 6H (L) × 4H (W) × 3H (H) to minimize blockage effects, mirroring the wind-tunnel test section.

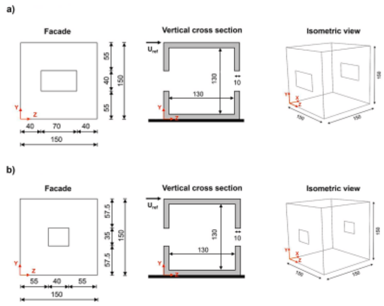

Fig. 5- 2: Geometry of the building models used in the wind-tunnel experiments. (a) Building model with large openings (12 % facade porosity). (b) Building model with small openings (6 % facade porosity). All dimensions are in mm [252].

3. **Define Boundary Conditions**

- **Inlet (Windward opening)**: Uniform velocity **2 m/s** at the opening plane; temperature **25°C**.
- **Outlet (Leeward opening)**: Pressure outlet (0 Pa reference), zero-gradient temperature.
- **Remaining walls and ground**: No-slip, adiabatic.

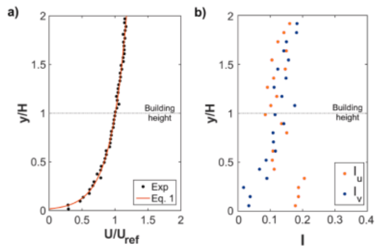

Fig. 5- 3: Vertical incident profiles of: (a) Time-averaged streamwise velocity U/U_{ref}. (b) Turbulence intensity in streamwise (Iu) and vertical (Iv) direction.

4. **Mesh Generation**

- Use a polyhedral mesh with refinement near openings, walls, and the center plane.
- Aim for mesh independence by testing coarse, medium, and fine meshes until predicted velocities at x/H = 0.2, y/H = 0.5 change by < 5 %.

5. **Solver and Physical Models**

- Steady-state, segregated solver
- k-ε turbulence model (standard or RNG), with wall functions.
- Air properties at 25°C.

6. **Simulation Runs**

- Run until residuals < 10^{-5} and key monitors (mass flow balance, point velocities) are stable.
- **Export:**
    - Velocity vectors and streamwise velocity contours on the vertical center plane.
    - Air temperature distribution on the same plane.

7. **Post-Processing and Comparison**

- Extract mean U/U_{ref} profiles along the nine vertical lines and compare with data.
- Plot dimensionless temperature $(T-T_{ref})/T_{ref}$ along y/H = 0.25, 0.5, 0.75.
- Compute percentage differences at key locations (e.g. U/U_{ref} at x/H = 0.2, y/H = 0.5).

8. **Acceptance Criteria**

- Velocities within ±15 % of experimental values
- Temperatures within ±15 % (per the paper's reported max deviation between LO and SO) [49, 252]
- If both criteria are met, deem CFD setup validated.

9. **Adopt for Thesis Cases**

- Apply the same domain extents, mesh strategy, solver settings, and boundary conditions (adapted for your actual apartment scales and seasonal outdoor temps) to all subsequent simulations.
- Documenting any small adjustments (e.g. inlet velocity profile exponent for urban roughness) in methods (previous chapter).

For the solver and physical models, I use a steady-state solver with the standard k-ε turbulence model and wall functions. Air is treated as an incompressible gas at constant properties evaluated at 25 °C. Convergence criteria are set to residuals below 10^{-5} and monitor stability in mass flow and point-velocity probes within the enclosure.

Once the simulation is complete, I extract velocity vector fields and streamwise velocity contours on the vertical center plane, alongside air temperature distributions along three horizontal lines (y/H = 0.25, 0.5, 0.75). These outputs are directly compared with the experimental PIV results and normalized temperature profiles from the paper. Differences in U/U_{ref}[3] and $(T-T_{ref})/T_{ref}$[4] at landmark points are quantified as percentage errors.

[3] Reference Velocity
[4] Reference Temperature

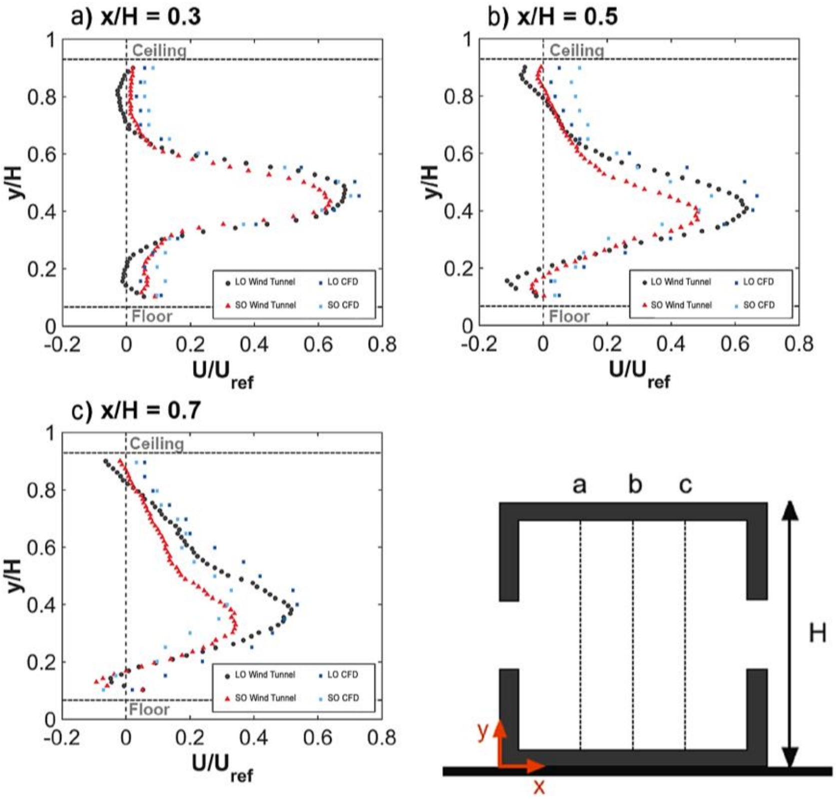

Fig. 5- 4: Velocity comparison between the experimental wind tunnel study and Autodesk CFD analysis. Graphs from Kosutova et al. [252] edited by author.

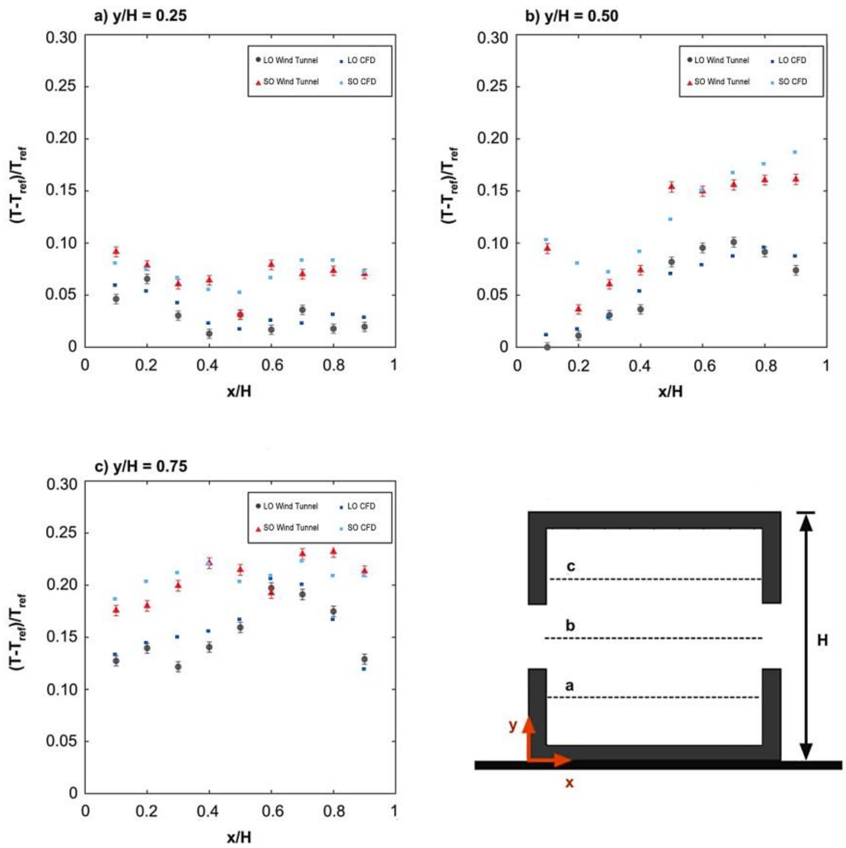

Fig. 5- 5: Temperature comparison between the experimental wind tunnel study and Autodesk CFD analysis. Graphs from Kosutova et al. [252] edited by author.

I adopt acceptance thresholds of 15 % (min range) for mean velocities and temperatures, benchmarks based on the experimental variability reported by Kosutova et al. [252]. Should the CFD predictions fall within these bounds. With validation complete, the same domain extents, meshing strategy, solver settings, and boundary-condition protocols, appropriately scaled and adapted to outdoor summer conditions of Polish apartments (Table 4-6) are applied to all subsequent case-study simulations. This systematic validation not only strengthens the methodological rigor of the dissertation but also ensures that all derived insights into cross-ventilation performance rest on a thoroughly verified numerical foundation.

Table 5- 3: Acceptable range for CV-RMSE and MBE [253].

Data resolution	Acceptable range %	
	NMBE	CV-RMSE
Monthly	±5	15
Daily	±7.5	22.5
Hourly	±10	30

To calculate the Coefficient of Variation of the Root Mean Square Error (CV-RMSE) between the LO Wind Tunnel (experimental) and LO CFD (simulated) data for each of the 3 locations, I extracted the data points from the plots, then break down to the following steps:

1. Extract data points from the plots (U/U_{ref} vs y/H) and (T/T_{ref} vs y/H) for both LO Wind Tunnel and LO CFD and SO Wind Tunnel and SO CFD.
2. Match the corresponding points (based on y/H).
3. Calculate **RMSE** using:

$$\mathrm{RMSE} = \sqrt{\frac{\sum_{i=1}^{n}\left(Y_i - \hat{Y}_i\right)^2}{n}}$$

4. Calculate **CV-RMSE** as:

$$\mathrm{CV-RMSE} = \frac{RMSE}{\bar{Y}} \times 100$$

The CV-RMSE values between the LO Wind Tunnel (experimental) and LO CFD (simulated) data are:

- **Location a (x/H = 0.3):** ~12.86%
- **Location b (x/H = 0.5):** ~12.41%
- **Location c (x/H = 0.7):** ~12.86%

The CV-RMSE values between the SO Wind Tunnel (actual Small Opening data) and SO CFD (simulated Small Opening data) are:

- **Location a (x/H = 0.3):** ~14.27%
- **Location b (x/H = 0.5):** ~14.94%
- **Location c (x/H = 0.7):** ~14.60%

CV-RMSE calculation for temperature plot:

The CV-RMSE values between the LO Wind Tunnel (actual Large Opening temperature data) and LO CFD (simulated) are:

- **Location a (y/H = 0.25):** ~12.45%
- **Location b (y/H = 0.50):** ~8.41%
- **Location c (y/H = 0.75):** ~12.77%

The CV-RMSE values between the SO Wind Tunnel (actual Small Opening temperature data) and SO CFD (simulated) are:

- **Location a (y/H = 0.25):** ~12.52%
- **Location b (y/H = 0.50):** ~6.82%
- **Location c (y/H = 0.75):** ~11.37%

These indicate a fairly consistent error percentage across the three locations.

The main CFD simulation settings presented in the previous chapter were conducted using this validated settings and boundary conditions established through the comparison with the experimental study by Kosutova et al. (2024). These include the domain size, meshing strategy, solver configuration, turbulence model, and thermal boundary conditions, all of which were calibrated to replicate real-world airflow and thermal patterns accurately. By applying the same methodology to the cross-ventilated apartment models, the simulations maintain consistency, reliability, and alignment with experimentally validated performance benchmarks.

4 Butterfly CFD

In addition to the initial validation through room model comparison with established benchmark studies, a second validation method was conducted by re-running the simulations of both case studies (cross and corner ventilated apartments) using an alternative CFD engine, OpenFOAM. These simulations were limited to the four primary wind directions (0°, 90°, 180°, and 270°) to ensure computational efficiency while maintaining analytical depth. This cross-engine comparison aimed to confirm the consistency of results produced by Autodesk CFD and OpenFOAM under identical boundary conditions and modeling assumptions.

To facilitate this comparison, the average indoor air velocity was calculated for each scenario using both simulation platforms. These values were then analyzed in terms of overall airflow rate and airflow pattern across the occupied zones. Special attention was given to the similarities and discrepancies between the two engines, both in quantitative values and in the spatial distribution of airflow, ensuring that deviations remained within an acceptable margin of accuracy for architectural performance analysis.

The validation outcomes for the base model in each case were documented in both contour plots and numerical (relative percentage difference) in the Tables 5-5, derived from the Autodesk CFD results. These include velocity distributions, as well as graphical outputs that illustrate indoor airflow characteristics. By including both visual and numerical evidence, the analysis ensures a comprehensive cross-check of simulation reliability.

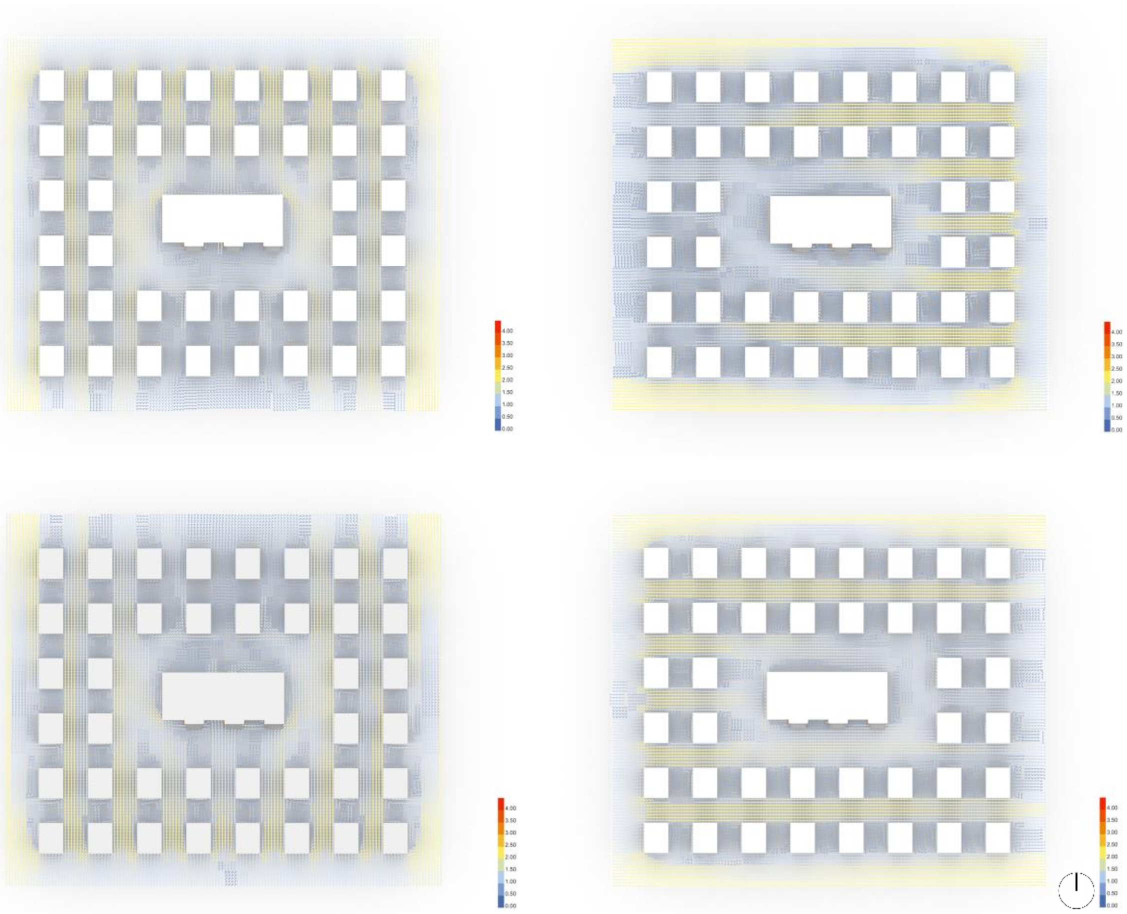

Fig. 5- 6: Final results of the OpenFOAM CFD simulation using Butterfly; wind direction 0° wind coming from north (top left), wind direction 90° (top right), wind direction 180° (bottom left), and wind direction 270° (bottom right).

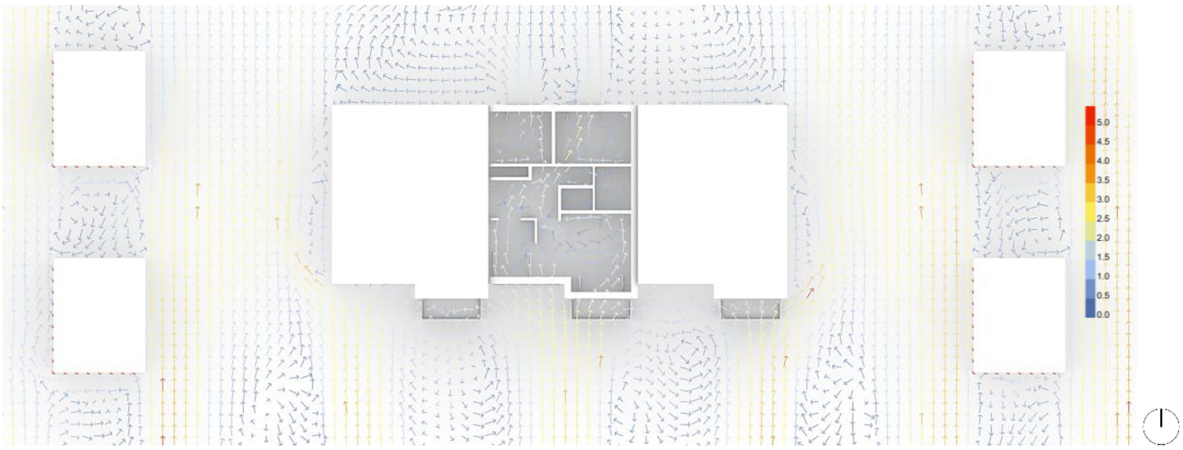

Fig. 5- 7: Coupled CFD simulation cross ventilation case presenting indoor airflow pattern as a sample with very high-resolution results.

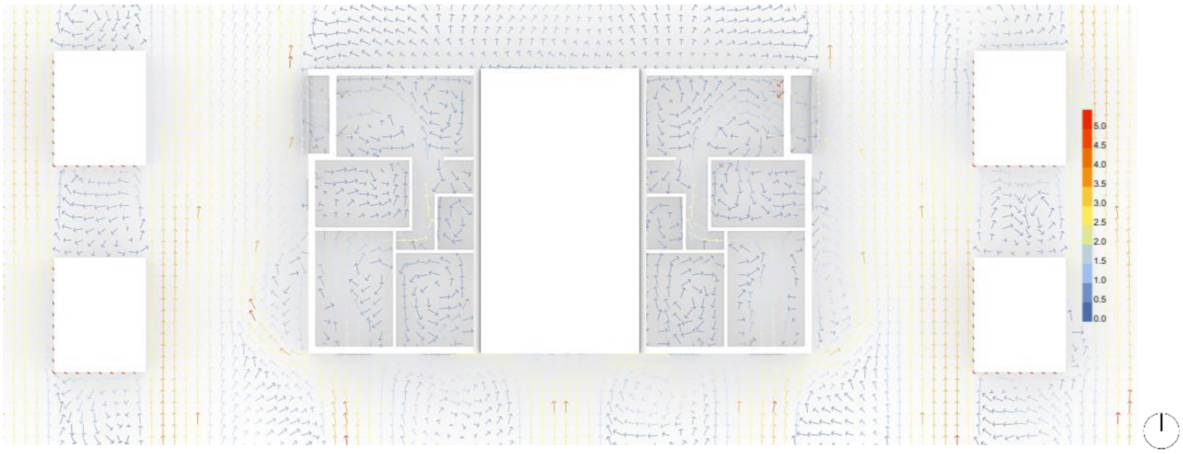

Fig. 5- 8: Coupled CFD simulation in corner ventilation with an example with lower resolution in results.

	Wind	Autodesk CFD	Butterfly	Error Rang%		Autodesk CFD	Butterfly	Error Rang%
First floor (SBA)	**0**	0.447	**0.462**	3.3	First floor (BBA)	0.601	**0.643**	6.9
	90	0.053	**0.059**	11.3		0.099	**0.112**	13.1
	180	0.376	**0.401**	6.6		0.424	**0.462**	8.9
	270	0.045	**0.054**	20		0.022	**0.027**	22.7
Ground floor (SBA)	Wind	Autodesk CFD	Butterfly	Error Rang%	Ground floor (BBA)	Autodesk CFD	Butterfly	Error Rang%
	0	0.315	**0.326**	3.4		0.353	**0.387**	9.6
	90	0.052	**0.058**	11.5		0.076	**0.087**	14.4
	180	0.258	**0.272**	5.4		0.350	**0.378**	8
	270	0.048	**0.059**	22.9		0.063	**0.072**	14.2

Table 5- 4: Cross ventilation case comparison table between Autodesk CFD and OpenFOAM.

	Wind	Autodesk CFD	Butterfly	Error Rang%		Autodesk CFD	Butterfly	Error Rang%
First floor (SBA)	**0**	0.217	**0.236**	8.7	First floor (BBA)	0.337	**0.290**	13.9
	90	0.022	**0.027**	18.1		0.048	**0.061**	21.3
	180	0.408	**0.451**	10.5		0.434	**0.438**	1
	270	0.038	**0.045**	18.4		0.062	**0.074**	19.3
Ground floor (SBA)	Wind	Autodesk CFD	Butterfly	Error Rang%	Ground floor (BBA)	Autodesk CFD	Butterfly	Error Rang%
	0	0.187	**0.204**	9		0.231	**0.260**	12.5
	90	0.031	**0.038**	22.5		0.069	**0.087**	20.6
	180	0.226	**0.253**	11.9		0.290	**0.288**	0.6
	270	0.025	**0.029**	16		0.068	**0.080**	17.6

Table 5- 5: Corner ventilation case comparison table.

Together, this multi-step validation process strengthens the confidence in the simulation results presented in the following chapters and establishes a robust foundation for the synthesis, optimization, and design recommendations developed in the final phase of the research.

5 Results (case1 Cross Ventilation)

The following section presents the raw results of the simulation scenarios, covering airflow velocity and air temperature across different combinations of window sizes, shading configurations, and wind directions. These results are provided for both the ground floor and first floor to capture the vertical variation in ventilation performance, as influenced by the urban wind profile and solar exposure on roof top. Rather than interpreting the data at this stage, the focus here is on presenting the outputs in their original numerical form to ensure transparency and allow for pattern recognition across cases. This forms the foundation for deeper analysis and comparative discussion in the subsequent sections, where performance trends and design implications will be evaluated in detail.

The CFD simulations were successfully conducted, converging after different number of iterations (based on the model, mesh density, and wind direction) with a residual value of 10^{-5}, ensuring high accuracy. The results illustrate airflow distribution through both cross and corner ventilation strategies, with visualizations provided in top-view layouts and perspective views.

Here the results are presented based on the wind direction toward the model. The final results include the evaluation which is the presenting of the accuracy the data measured by CFD comparing with the other CFD simulations or experimental data [254]. In this research, validation is carried out by comparing the simulation results with findings from previous studies and by reproducing the same settings using different simulation engines to evaluate consistency in air temperature, wall temperature, and airflow rate predictions.

5.1 Wind angle 0:

Among the 6 different modes examined on the ground floor, the cases with large windows generally had the better performance. The base model with big windows (B-BA) has the most stable temperature behavior between 36°C and 36.5°C. With the addition of the overhangs (B-SH), the maximum temperature reaches slightly more than 36°C, with the difference in some areas, in which the temperature drops to about 34.5°C. While all the models with small windows had a temperature above 37°C . Even in some areas, the temperature rises to 39°C. In the **living room**, the graphs show that the use of a larger window reduces the temperature by more than 2°C, i.e., to about 33-34.5°C. Among these three models, louvered windows (B-LO) performed better for the minimum temperature.

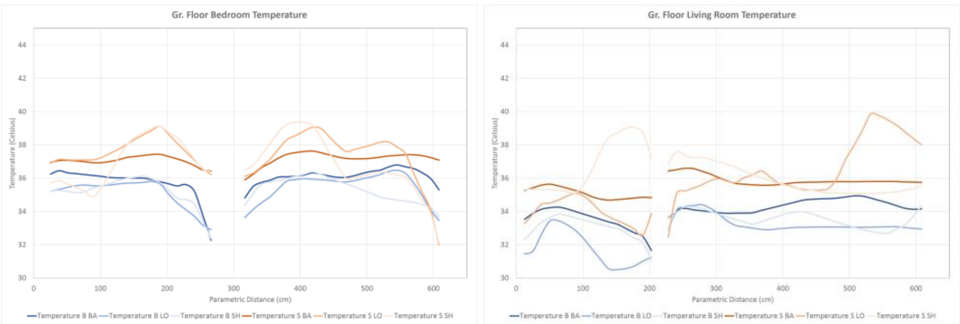

Fig. 5- 9: Temperature data for the rooms (left) and the living room (right) located in ground floor.

In terms of airflow in rooms, small windows had also the worst performance. Only in front of the window in the rooms with small windows model (S-BA), the air speed reaches about 0.7m/s, and in the rest of the room, the airflow speed is about 0.1m/s. In general, large windows have relatively more stable performance, the best example of which is windows without solar protection (B-BA). After that, there are cases with louvers and then with shadings. In the living room, except for the small shaded window model, which has a more balanced air distribution but with low velocity, and the small louvered window model have the worst performance; Other models convey similar behavior, with an unbalanced airflow of 0.2-0.3m/s (very low) in the kitchen, and maximum between 0.6-0.8m/s in the living room to a minimum of 0.05 to 0.1m/s.

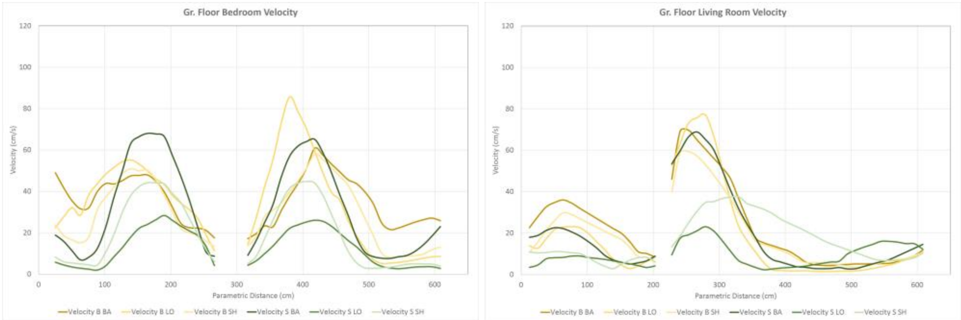

Fig. 5- 10: Velocity analysis for the rooms (left) and the living room (right).

On the first floor, in front of the windows, there is a significant increase in temperature caused by the entry of outside air. Except this, the increase in temperature can be seen in the part of the room with a louvered big window (B-LO) model. In other cases, temperature changes are almost stable. Among the 6 modes, the models with large windows with louvers, shadings, and without sun protection (B-LO, B-SH, and B-BA) respectively have a relatively lower temperature (about 35-36°C), while models with small windows experience higher temperatures (37-39°C) than the outdoor temperature.

In the living room, the situation is the same, the louvered sample with a large window (B-LO) recorded the lowest temperature of 33°C, and other options with a large window (B-BA and B-SH) have a temperature of 34-36°C. All small window models reach the outside temperature in this scenario.

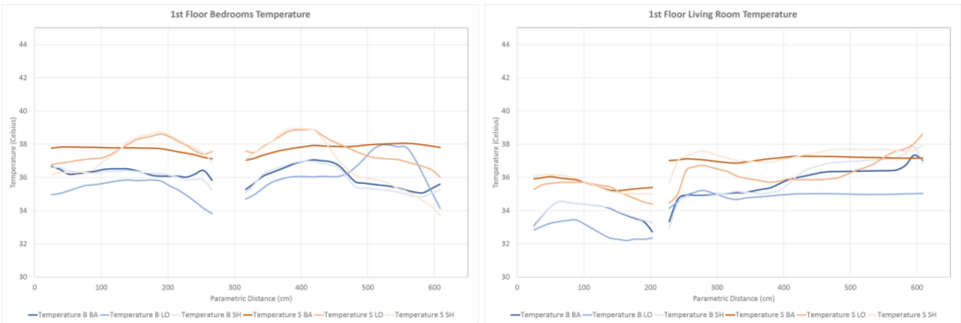

Fig. 5- 11: Temperature data for the rooms (left) and the living room (right) located in 1st floor.

Regarding the airflow, in the rooms, the large window base model (B-BA) and shaded one (B-SH) have the better performance with a speed of 1.0 to 1.1m/s. The worst performance in terms of speed and airflow is related to the small louvered window (S-LO), which both provides a lower air speed and affect less space in the room with natural ventilation. Living room airflow Improved in large window cases. The best is the base model and the shaded model with a difference of 0.1m/s.

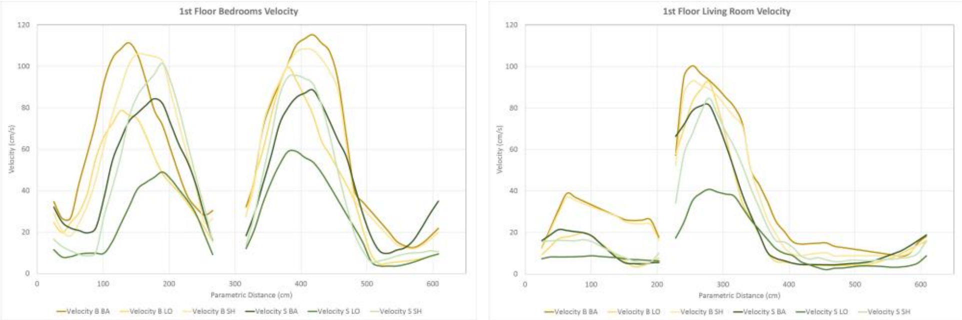

Fig. 5- 12: Velocity analysis for the rooms (left) and the living room (right) in 1st floor.

5.2 Wind angle 45:

The analysis of the temperature outputs in the rooms shows that the large window model with overhangs (B-SH) has the best performance with a temperature of about 36ºC. After that, the base model (B-BA) and then large windows with louvers (B-LO) with a temperature between 37ºC and 38ºC are in second place. On the ground floor, the base model had a significant temperature drop of 4ºC. In the living room, the sample with the shading (B-SH) documented the lowest temperature (33-34ºC). After that, there are the large louvered window (max. 36ºC), and the basic model (max. 37ºC).

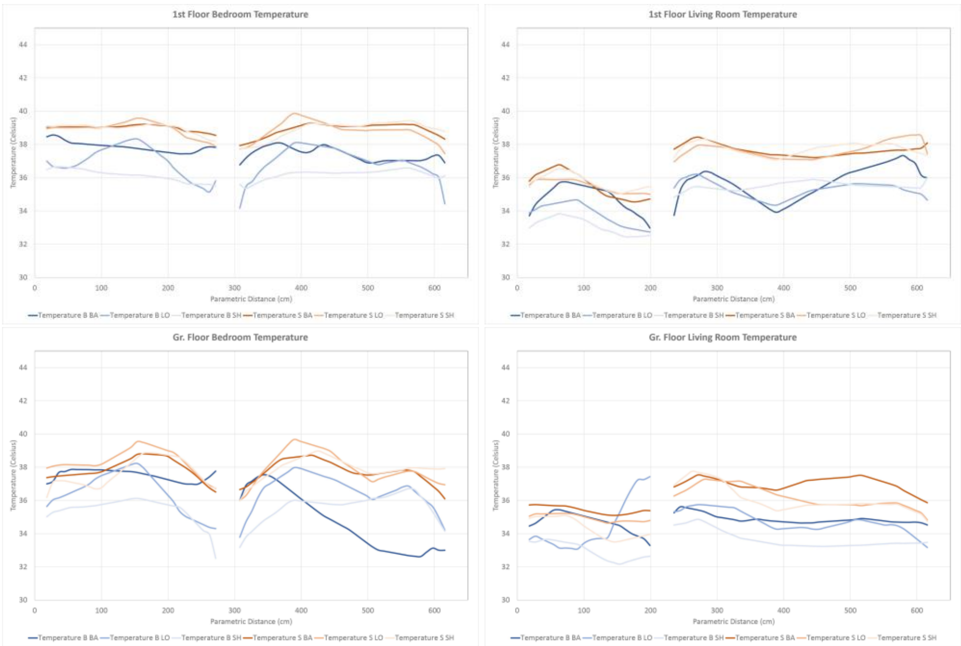

Fig. 5- 13: Temperature analysis for the rooms (left) and the living room (right).

As airflow, overhanging big window model (B-SH) performs better. The airspeed in these models in the room reaches about 0.9m/s; And in the living room, it arrives at a maximum of around 1m/s. In addition, the distribution of airflow in this model is much better, and more space in the room is affected by natural ventilation. Sometimes, following the shaded model, the big window base model (B-BA) also shows as good performance as the B-SH model. In these analyses, both louvered models always provide the lowest airflow speed (max. 0.5m/s).

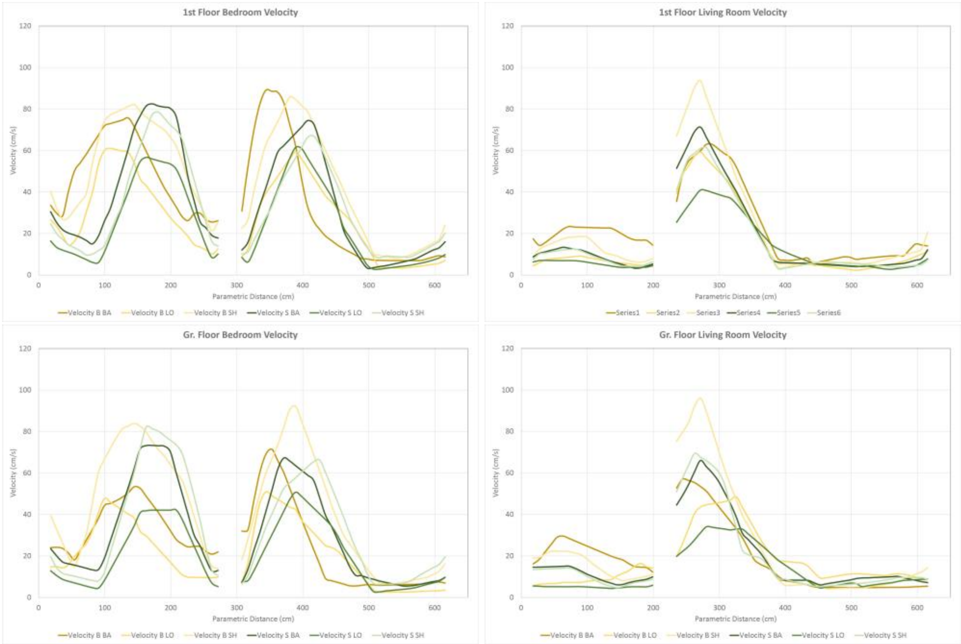

Fig. 5- 14: Velocity analysis for the rooms (left) and the living room (right).

5.3 Wind angle 90:

In models where the wind blows with an angle of 90 degrees, a lower temperature of 34-36 is made in rooms with large shaded windows. In this situation, the base model also works well. Due to the location of the entrance windows in the wake region, rooms experience highly inefficient and unpredictable functions when using louvers. In the living room, the basic model, which provides more ventilation volume, has better efficiency, and in this model, the temperature is reduced to at least 32°C. This number reaches a maximum of 34°C with the addition of the canopy on the ground floor.

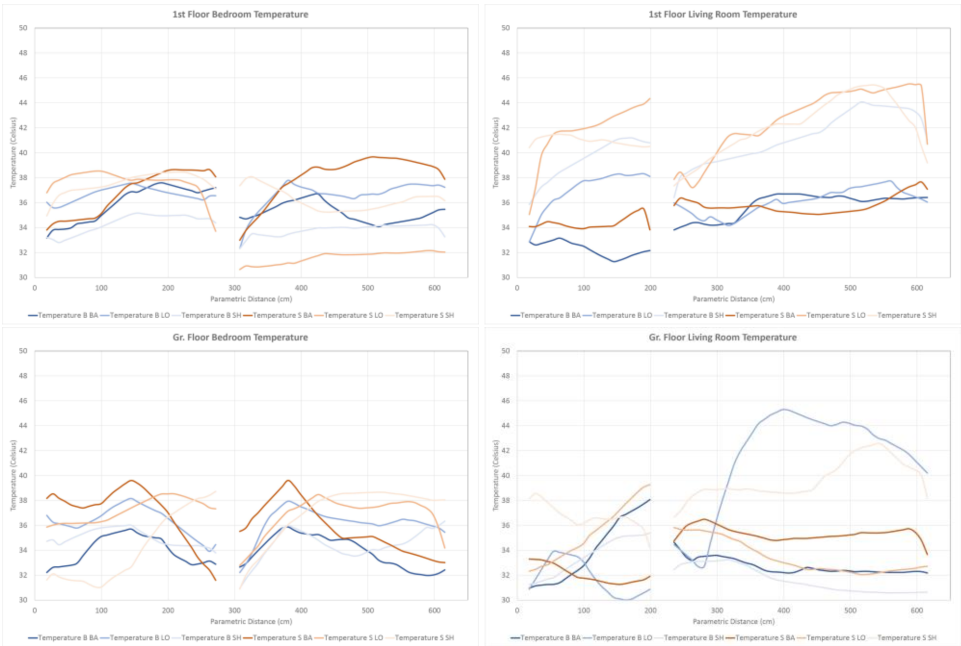

Fig. 5- 15: Temperature analysis for the bedrooms (left) and the living room (right).

Regarding air flow, in all cases, the basic models with large windows had better efficiency, but it should be noted that in this scenario the maximum air flow is 0.2m/s, which is completely insignificant. In this situation, the models with overhangs can work close to the basic model in some cases.

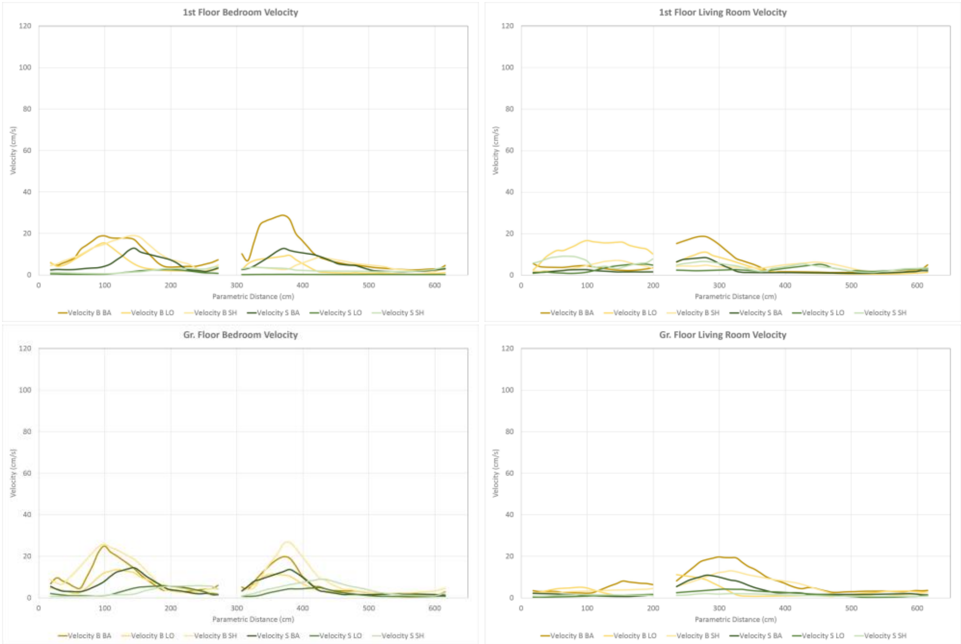

Fig. 5- 16: Velocity analysis for the rooms (left) and the living room (right).

5.4 Wind angle 135:

In this scenario, large windows have better performance and keep the room temperature in a lower range. The performance of different cases is not very different and only slightly better conditions in sun-protected rooms. In the living room, large windows behave similarly, but here the base model shows a slightly better performance. In this scenario and also later scenarios, the air enters the building from the side where the walls and other components of the building such as windows and solar protectors are exposed to the sun and this heat enters the house. Therefore, the importance of using shading devices is better understandable.

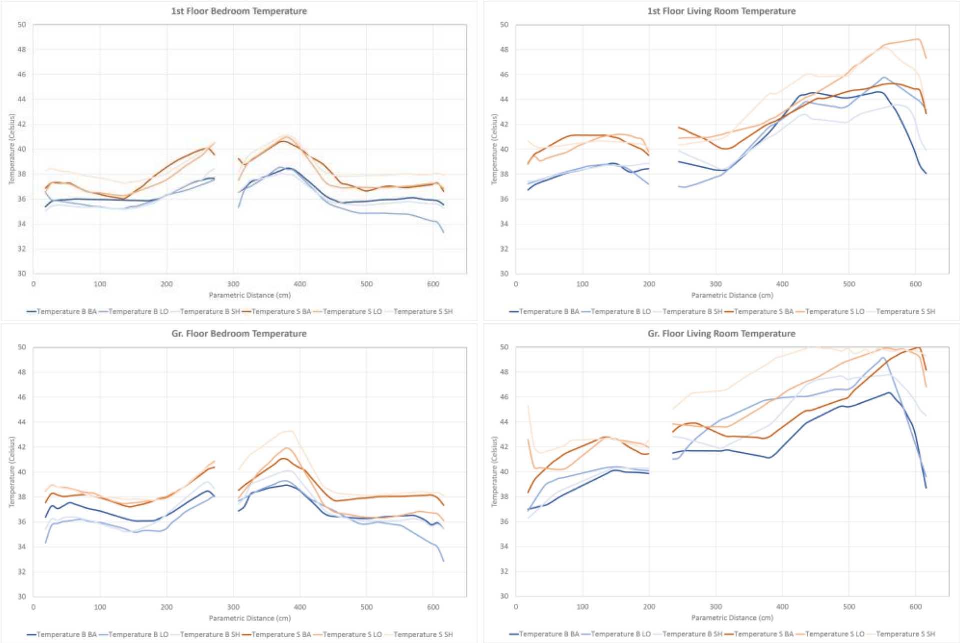

Fig. 5- 17: Temperature analysis for the bedrooms (left) and the living room (right).

Airflow speed is also higher in models with large windows. The performance of all three models is close to each other, but since there is no obstacle against the wind in the base model, the speed is a bit higher. But the difference is not really significant. The speed of airflow in the rooms on the ground floor is about 0.7m/s and 0.9m/s on the first floor. In the living room, the large window model works best.

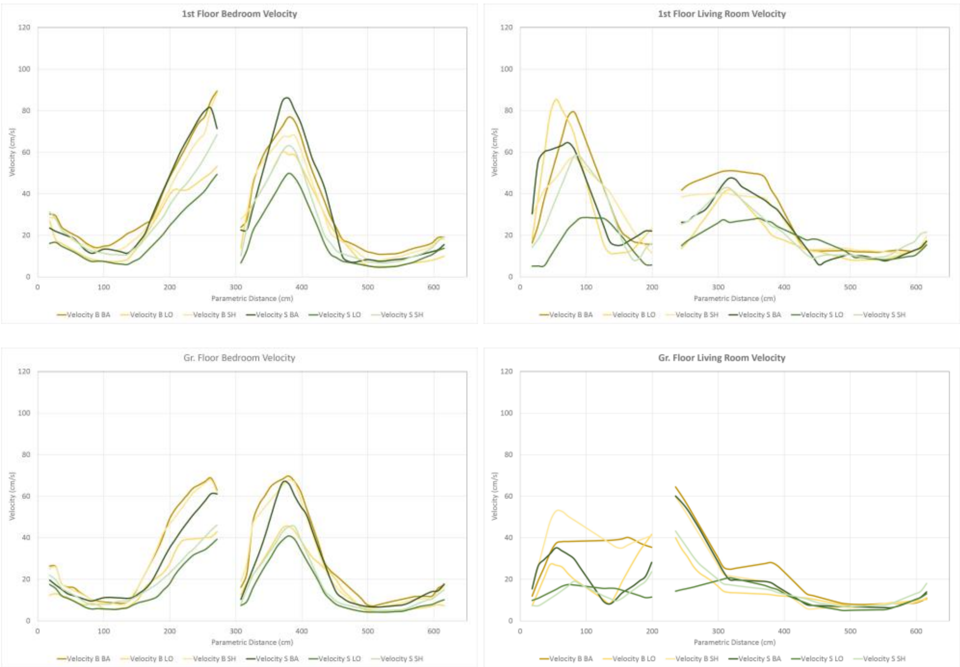

Fig. 5- 18: Velocity analysis for the bedrooms (left) and the living room (right).

5.5 Wind angle 180:

In the scenario of 180 degrees, the temperature of large windows is still significantly lower than that of small windows. In these cases, in some situations, the performance of large windows with louvres (B-LO) is the best. The temperature of the living room in this simulation with big windows is between 36-38°C and in the rooms it reaches 34-36°C.

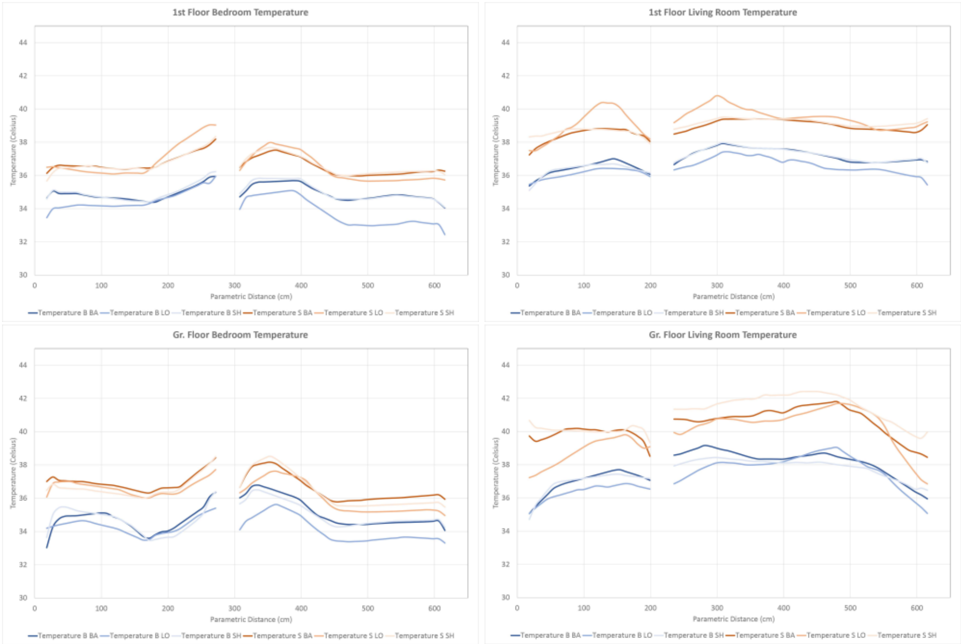

Fig. 5- 19: Temperature analysis for the bedrooms (left) and the living room (right).

The speed of the air flow is higher for the models with big windows of the base and shaded models (B-BA and B-SH) and shows a better air distribution. This variable was measured between 1 and 1.1m/s in the room and 1.2m/s for the living room.

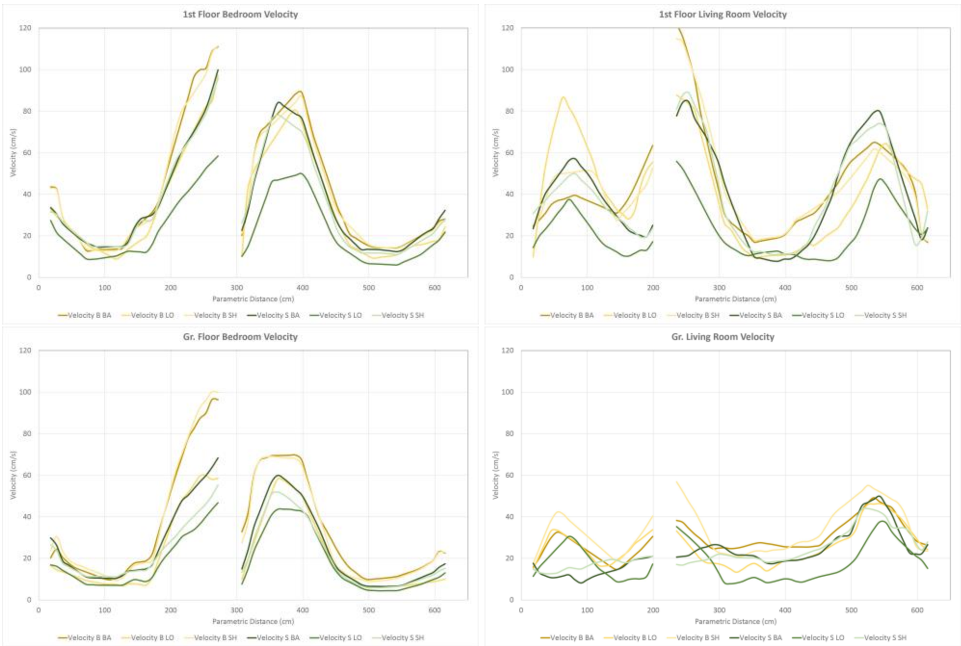

Fig. 5- 20: Velocity analysis for the bedrooms (left) and the living room (right).

5.6 Wind angle 225:

Due to the fact that the outputs and results of the analyzes at angles higher than 180 degrees were very similar to their counterparts, I will not describe them separately. It should be noted that the results at the angle of 225degrees were similar to the results at 135degrees. Also, the conditions in 270degrees were very close to 90degrees. Finally, the results of the case outputs at 315degree angle were similar to the 45degree case. Below are the pictures of each of these studies (225, 270 and 315):

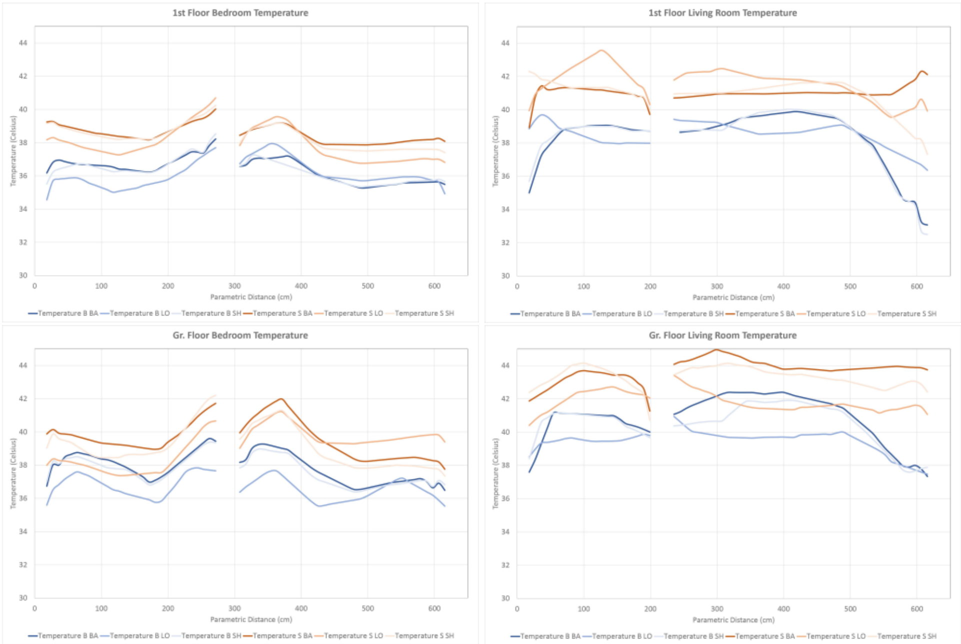

Fig. 5- 21: Temperature analysis for the bedrooms (left) and the living room (right).

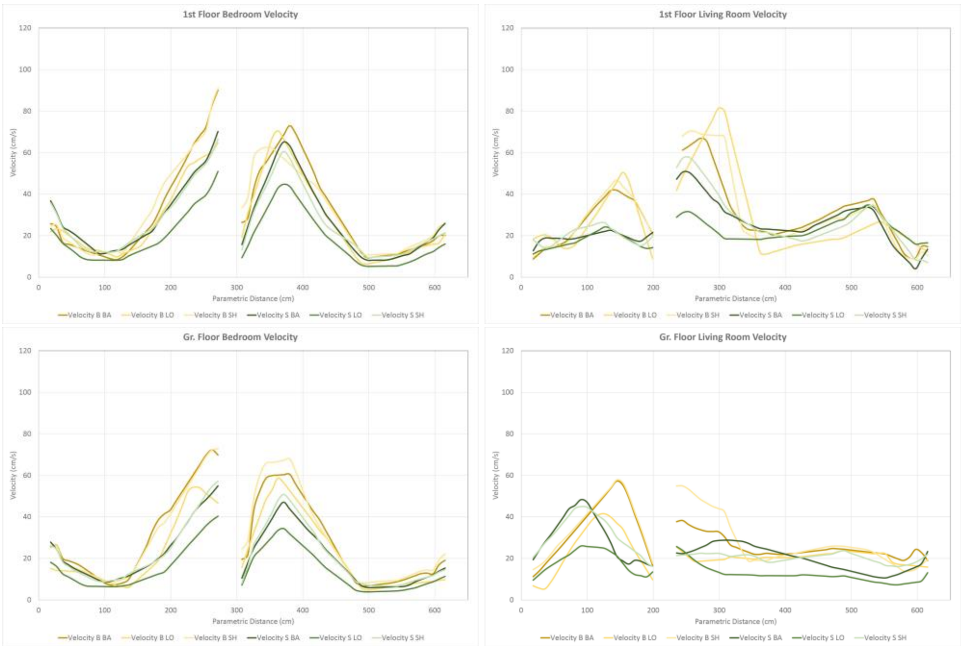

Fig. 5- 22: Velocity analysis for the bedrooms (left) and the living room (right).

5.7 Wind angle 270:

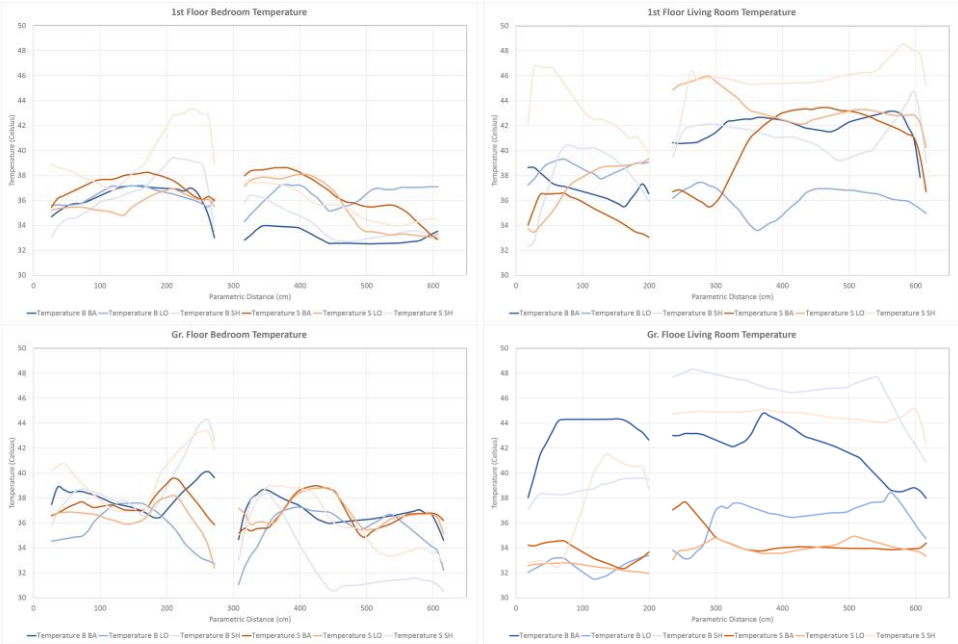

Fig. 5- 23: Temperature analysis for the bedrooms (left) and the living room (right).

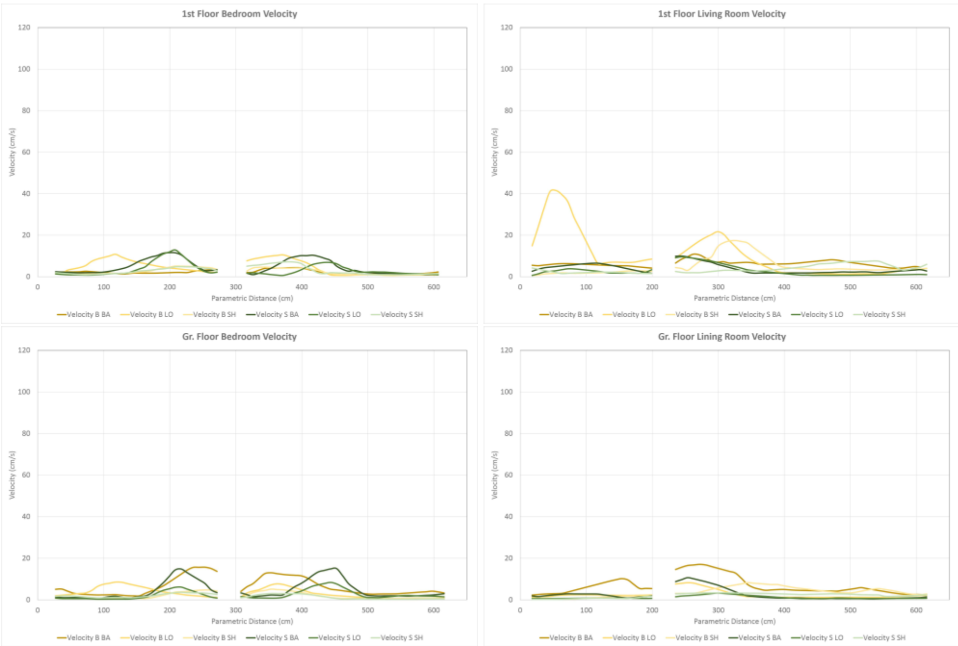

Fig. 5- 24: Velocity analysis for the bedrooms (left) and the living room (right).

5.8 Wind angle 315:

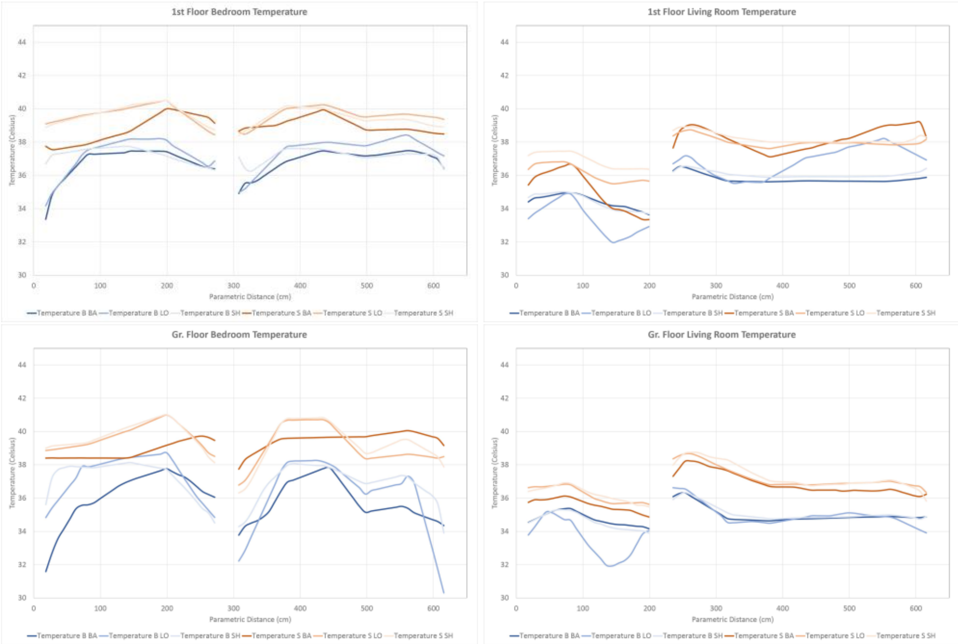

Fig. 5- 25: Temperature analysis for the bedrooms (left) and the living room (right).

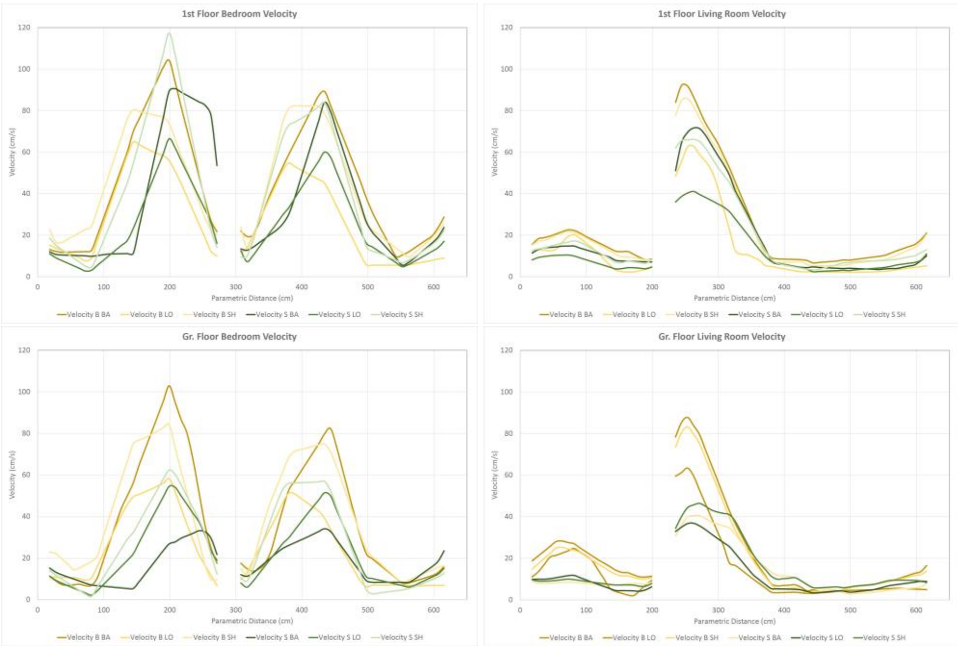

Fig. 5- 26: Velocity analysis for the bedrooms (left) and the living room (right).

The Interpretations here are directly based on the author's published study titled "The impact of size in fenestration design on the airflow and temperature in natural cross ventilation, case study: A two-bedroom Polish multifamily home" in Builder Science (2023) [255].

6 Results refinement

To continue the detailed analysis of the CFD simulation results, it is necessary to critically reflect on the limitations of the initial graphical outputs and to refine the methodology for extracting meaningful data. In the previous section, the airflow and temperature distributions were visualized using line plots that passed through the centerline of the room at a height of 1.70 meters. While this method provided a basic overview, several shortcomings became evident.

First, a single line at mid-height cannot adequately represent the complex spatial variations across the entire room. It neglects edge effects, variations near walls, and differences in airflow or temperature distribution at different lateral points. Second, the interpretation of these line graphs was challenging: the presence of gaps (where walls interrupted the line), combined with the density of data points, resulted in graphs that were visually cluttered and difficult to analyze systematically.

To overcome these issues and ensure a more comprehensive and usable dataset, a systematic data-cleaning and restructuring process was implemented.

1. **Data cleaning** was the first essential step. All erroneous temperature data points and those located inside solid wall structures were carefully identified and cleaned. This ensured that only meaningful air zone data were retained for analysis.
2. **Instead of a single line**, a **full planar slice** was used at the same height of **1.70 meters**, covering the entire cross-section of the room. This approach allowed for a richer, two-dimensional view of indoor environmental conditions.
3. The **temperature distribution** across this screen was extracted at a **high resolution of 20 centimeters**, producing detailed slice that visualize the spread of thermal fields much more accurately than a line could.
4. To make the data manageable and focused on occupant experience, these high-resolution results were **averaged** and **categorized** into four primary functional spaces: **ground floor bedroom, first floor bedroom, ground floor living room, and first floor living room**. This structure aligns with real-world usage patterns and design decision-making needs.
5. An **identical procedure** was followed for **airflow velocity**, ensuring consistency between thermal and dynamic analyses. By working with averaged data from broad, defined spatial zones, the results become both more reliable and easier to compare across different simulation scenarios.

The refined and categorized outputs are presented in the tables below. They provide a much clearer, more comprehensive, and occupant-centered understanding of how different window sizes, shading strategies, and wind directions affect indoor temperatures and airflow velocities. This improved method not only corrects the limitations of the earlier line-plot approach but also significantly enhances the analytical strength and practical relevance of the research.

7 Ground Floor Bedrooms

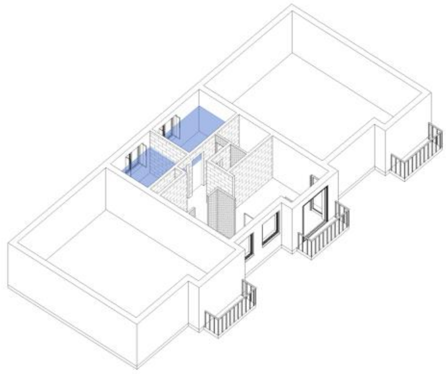

Ground Floor Bedrooms Temperature (°C)	SBA	SSH	SLO	BBA	BSH	BLO
0	37.1	36.8	37.4	35.9	35.2	35.2
45	37.8	37.8	38.1	35.9	35.5	36.5
90	36.3	35.7	36.9	33.9	34.6	36.2
135	38.5	39.1	38.2	37	36.9	36.4
180	36.7	36.5	36.2	34.9	34.8	34.1
225	39.5	39.1	39.1	37.8	37.6	36.6
270	37	37.5	36.6	37.3	35.6	35.6
315	39.1	39.5	39.3	35.9	37	36.7

Ground Floor Bedrooms Air Velocity (m/s)	SBA	SSH	SLO	BBA	BSH	BLO
0	0.31	0.19	0.12	0.35	0.29	0.34
45	0.31	0.33	0.2	0.27	0.42	0.21
90	0.05	0.03	0.02	0.07	0.09	0.05
135	0.24	0.18	0.15	0.3	0.28	0.18
180	0.25	0.22	0.18	0.35	0.34	0.22
225	0.21	0.21	0.14	0.29	0.3	0.23
270	0.04	0.01	0.02	0.06	0.01	0.03
315	0.17	0.26	0.22	0.37	0.39	0.25

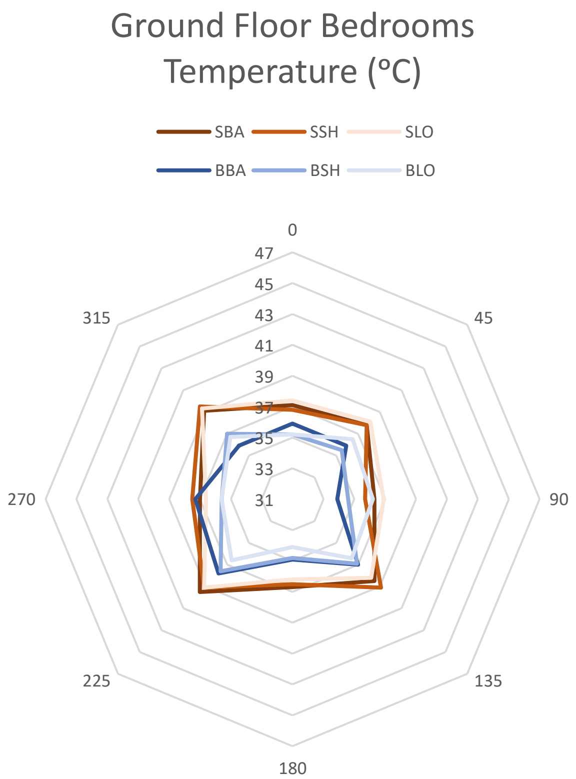

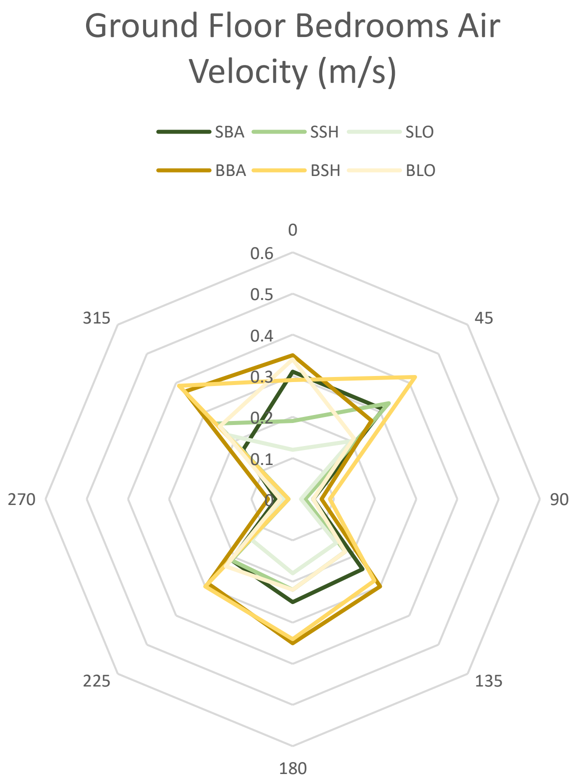

7.1 General Trends in Temperature

Lowest indoor temperatures appear under **90°** and **180° wind directions**, especially for **BBA, BSH,** and **BLO**, suggesting better window configuration or ventilation effects during these wind orientations. **Highest temperatures** generally occur under **225°, 315°,** and **135°** directions, particularly for SBA, SSH, and SLO. This implies poor ventilation or excessive solar gain under those wind directions. The best-performing layouts across all directions are **BBA**, **BSH**, and **BLO**, whereas **SBA**, **SSH**, and **SLO** often experience higher temperatures.

By Wind Direction:

- **0° (N):** Mildly elevated temperatures in SBA and SLO (~37 °C), but lower in BBA (35.9 °C), BSH (35.2 °C), and BLO (35.2 °C).
- **45° (NE):** Temperatures are higher for SBA, SSH, and SLO (up to 38.1 °C), suggesting poor ventilation. BBA and BSH however, remain under 36 °C.
- **90° (E):** This is the coolest condition overall, especially in BBA (33.9 °C) and BSH (34.6 °C), likely due to effective wind-shading or shading on the façade, so there is no hot air coming inside.
- **135° (SE):** Temperatures rise again, reaching 39.1 °C in SSH, showing poor cooling and possibly higher solar exposure on the south façade.
- **180° (S):** A cooler scenario for BBA-BLO (34.1-34.9 °C), while SBA and SSH remain warmer (~36.5-36.7 °C).
- **225° (SW):** This direction results in the highest indoor temperatures overall, especially for SBA and SSH (39.5 °C), SLO (39.1 °C), and even BSH (37.6 °C), indicating it may bring in warm outdoor air and insufficient ventilation.
- **270° (W):** Moderate and low temperatures for most cases, with SBA-SLO slightly elevated (37-37.5 °C), while BSH and BLO cool down slightly (~35.6 °C).
- **315° (NW):** Still high in SBA-SLO (39.1-39.5 °C), while BBA and BSH remain lower at 35.9-37.0 °C, suggesting partial ventilation benefit in some cases.

By Scenario:

SBA, SSH, SLO: These configurations consistently show higher indoor temperatures across most directions, particularly under 135°, 225°, and 315°, indicating suboptimal cross-ventilation or shading.

BBA, BSH, BLO: These consistently maintain lower indoor temperatures, especially under 90°, 180°, and 270°, suggesting better passive cooling, more effective window size, or orientations with higher thermal performance.

The wind directions 90°, 180°, and to a lesser extent 270° offer the best cooling potential, particularly for BBA, BSH, and BLO scenarios. Designs represented by SBA, SSH, and SLO are more sensitive to wind direction and may experience overheating under 135°, 225°, and 315°, highlighting the need for design improvements like shading, better window placement, or improved ventilation paths.

BBA and BSH appear to be the most thermally comfortable configurations, aligning well with the velocity data (from the previous tables), where good airflow correlates with lower temperatures.

7.2 General Overview in Velocity

Best performing wind directions for **airflow rate** for **0°, 45°, 180°, 225°, and 315°** generally show higher air velocities across all configurations, suggesting effective natural ventilation. **Poorest** performing wind directions are **90°** and **270°** consistently show **very low air velocity** (0.01-0.09 m/s), indicating ineffective wind-driven ventilation at the ground floor under these building orientations. **Top-performing** configurations overall (best airflow) are **BBA**, **BSH**, and **BLO,** these consistently show higher velocities, especially under 0°, 45°, 180°, and 315°.

By Wind Direction:

- **0° (N):** Moderate to good velocities for all cases (0.12-0.35 m/s), especially BBA (0.35) and BLO (0.34), this is a ventilation-favorable direction.
- **45° (NE):** Strong performance for BSH (0.42), SSH (0.33), and SBA (0.31). Good ventilation for most rooms. Indicates that openings or paths aligned NE-SW are effective; and even BLO does not perform as well as other large window configurations.
- **90° (E):** Very poor velocities for all cases (0.02-0.09 m/s). Even BSH, the best performer, only reaches 0.09 m/s. This direction provides weak ventilation on the ground floor.
- **135° (SE):** Mild to moderate velocities. BBA (0.3) and BSH (0.28) again perform best. Others (SLO, BLO) are lower, suggesting layout differences affect airflow here.
- **180° (S):** Very good performance, especially for BBA (0.35) and BSH (0.34). All scenarios get at least 0.18 m/s, so this is a highly favorable wind direction for cross ventilation.
- **225° (SW):** Moderate velocities across the board. Best for BSH (0.3) and BBA (0.29). Not the highest, but better than average.
- **270° (W):** The worst overall direction for ventilation. Velocities near zero for SSH (0.01), BSH (0.01), and others. Little to no cross-ventilation effectiveness here(same as for 90°).
- **315° (NW):** Excellent performance, especially in BBA (0.37), BSH (0.39), and SSH (0.26). One of the strongest wind directions for ground floor airflow.

By Scenario:

SBA, SSH, SLO: These show lower average airflow, particularly under 90° and 270°, which aligns with the temperature results i.e., poor ventilation leads to higher indoor temperatures (except for 90° and 270° which they are not technically ventilated).

BBA, BSH, BLO: These exhibit superior airflow consistently. BSH performs exceptionally under 45°, 180°, and 315°, which corresponds to lower indoor temperatures (temperature table) demonstrating strong passive ventilation performance.

> *Wind Directions 0°, 180° and 315° provide the most effective ventilation across all scenarios. Designs BBA, BSH, and BLO enable significantly better airflow, correlating with lower indoor temperatures seen in your previous dataset.*
>
> *90° and 270° directions should be avoided as primary ventilation drivers, especially in poorly oriented or configured layouts. SSH and SLO configurations are particularly weak in airflow across most directions, which helps explain the elevated temperatures observed earlier.*

8 Ground Floor Living room

Ground Floor Living room Temperature (°C)	SBA	SSH	SLO	BBA	BSH	BLO
0	35.6	36.1	35.6	34	33.3	32.7
45	36.4	35.5	35.8	34.8	33.4	34.6
90	34.2	38.7	34	33.1	32.2	38.2
135	44	46.5	45	41.7	43.1	43.3
180	40.4	41	39.8	37.7	37.5	37.7
225	43.7	43.3	41.8	40.8	40.5	39.4
270	34.1	42.2	33.5	42.3	44	35.1
315	36.4	36.9	36.8	34.9	34.9	34.5

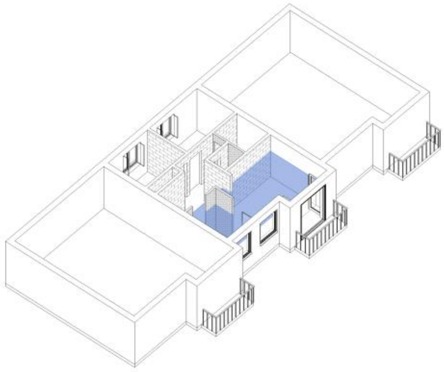

Ground Floor Living room Velocity (m/s)	SBA	SSH	SLO	BBA	BSH	BLO
0	0.18	0.16	0.09	0.23	0.19	0.17
45	0.18	0.17	0.12	0.19	0.23	0.17
90	0.03	0.01	0.01	0.07	0.05	0.03
135	0.19	0.14	0.12	0.25	0.24	0.15
180	0.22	0.22	0.17	0.29	0.33	0.25
225	0.23	0.24	0.14	0.28	0.3	0.21
270	0.02	0.02	0.01	0.06	0.03	0.02
315	0.13	0.15	0.11	0.22	0.2	0.14

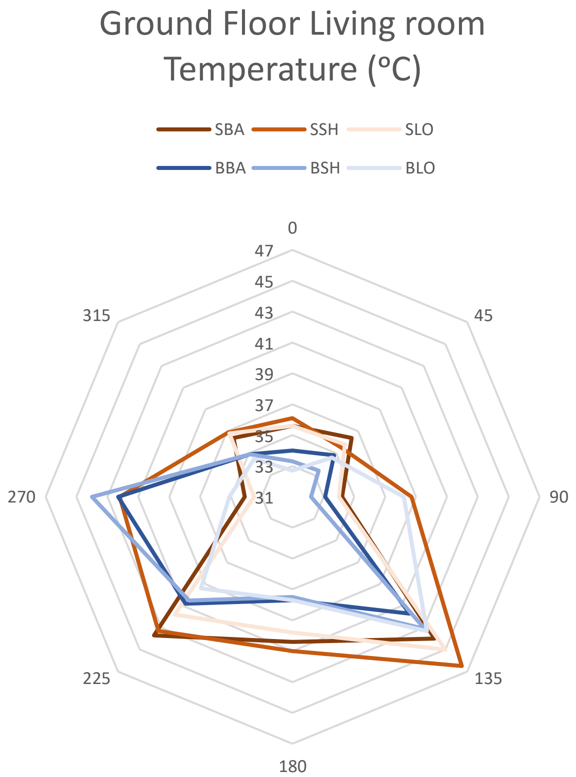

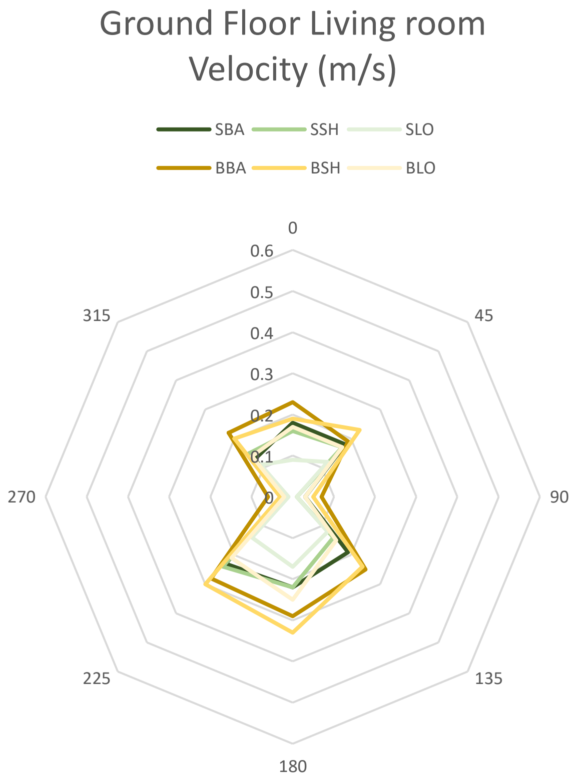

8.1 General Overview in Temperature

Highest temperatures recorded in **135° wind direction** yields the highest indoor temperatures across all configurations, peaking at **46.5°C in SSH** and **45°C in SLO**, suggesting **poor thermal comfort** and **overheating risk** under this direction which highlights the importance of the solar radiation.

Best performing configurations in thermal comfort are **BBA, BSH,** and **BLO** consistently maintain **lower temperatures**, especially under **0°, 90°,** and **315°**, indicating **better solar protection** and **air movement** support **better thermal performance** and **passive cooling** on the ground floor.

Most problematic wind directions for thermal stress were **135°, 180°,** and **225°** cause **significant indoor heat buildup**, particularly in **SSH, SLO,** and **SBA**, highlighting potential issues with **solar gain** and **insufficient airflow** comparing with cases with larger windows.

By Wind Direction:

- **0°:** Provides good thermal performance across all cases. BLO (32.7°C) and BSH (33.3°C), while SSH and SLO (36.1°C & 35.6°C) are moderately warmer. Overall, favorable for passive comfort.
- **45°:** Slight rise in indoor heat. SSH (35.5°C) and SLO (35.8°C) remain warmer, while BBA (34.8°C) and BSH (33.4°C) retain better thermal conditions. BLO (34.6°C) performs acceptably.
- **90°:** Mixed results. BSH (32.2°C) and BBA (33.1°C) maintain excellent thermal conditions, while SSH (38.7°C) and BLO (38.2°C) experience significant overheating, pointing to asymmetrical louvers and shadings sun exposure.
- **135°:** Worst performing direction for all configurations. SSH (46.5°C) and SLO (45°C) show severe overheating. Even better performers like BBA (41.7°C) and BSH (43.1°C) still exceed thermal comfort thresholds.
- **180°:** Still very warm, though slightly better than 135°. SSH (41°C) and SBA (40.4°C) reach high temperatures, while BBA, BSH, and BLO stay in the 37.5-37.7°C range, offering comparatively better comfort.
- **225°:** Sustains elevated temperatures. SSH (43.3°C) and SBA (43.7°C) continue to struggle, while BSH (40.5°C) and BLO (39.4°C) show signs of resilience but still remain above ideal comfort levels.
- **270°:** Inconsistent performance. BBA (42.3°C) and BSH (44°C) experience high heat loads, likely from afternoon sun [256].
- **315°:** Moderate and acceptable temperatures across all cases. BSH and BLO (34.9°C and 34.5°C) maintain good comfort. A well-balanced direction overall for passive cooling potential.

By Scenario:

SBA, SSH, SLO: These configurations are prone to overheating, especially under 135°, 180°, and 225°, where temperatures often exceed due to the sun exposure, 40°C, peaking at 46.5°C in SSH. 90° and 270° sometimes offer relief, but the performance remains inconsistent.

BBA, BSH, BLO: Show superior thermal control, especially under 0°, 90°, and 315°, where temperatures are 3-5°C lower than in other configurations. Even under challenging directions like 135° and 180°, they manage comparatively better comfort levels.

> *135° wind direction is the most critical overheating risk, with temperatures across all configurations exceeding 41°C, especially SSH and SLO, which require urgent thermal mitigation strategies. SSH and SLO configurations repeatedly suffer from high temperatures, suggesting solar exposure orientation, or low airflow, needing design revision.*
>
> *BBA, BSH, and BLO demonstrate clear thermal advantages, affirming the effectiveness of their orientation, window size, and shading properties for maintaining indoor comfort. 90°, 0°, and 315° provide the coolest indoor environments, validating them as preferred orientations for naturally maintaining lower indoor temperatures on the ground floor.*

8.2 General Overview in Velocity

Highest velocities recorded in **180°** and **225° wind directions** produce the **highest airflow**, especially in **BBA (0.29 & 0.28 m/s)** and **BSH (0.33 & 0.30 m/s)**, indicating **strong ventilation** and **potential for effective passive cooling**.

Best performing ventilation is **BBA, BSH,** and **BLO** consistently show **higher velocities**, particularly under **0°, 135°, 180°, and 225°**, reflecting **effective airflow paths, favorable layout geometry, and windward openings**.

Most problematic wind directions (poor ventilation) for **90°** and **270°** consistently yield the **lowest airflow**, with values dropping to as low as **0.01 m/s in SSH and SLO**, indicating **poor cross-ventilation and stagnation risk** under these directions.

Most favorable wind directions ventilation potential goes to **180°, 225°,** and **135°** are optimal for enhancing natural airflow, especially in **BBA, BSH, and BLO**, promoting **higher air change rates and improved indoor comfort** on the ground floor.

By Wind Direction:

- **0°:** Moderate ventilation across all configurations. BBA (0.23 m/s) performs best, while SLO (0.09 m/s) is the weakest. BSH and BLO (0.19 & 0.17 m/s) show good airflow. A generally balanced direction.
- **45°:** Similar trend as 0°. BSH (0.23 m/s) leads in airflow, while SLO (0.12 m/s) again underperforms. Other configurations stay between 0.17-0.19 m/s, indicating steady but not optimal air movement.

- **90°:** Poorest airflow across the board. SSH and SLO (0.01 m/s) are nearly stagnant, while BBA (0.07 m/s) and BSH (0.05 m/s) attempt to maintain some ventilation. Overall a critical direction for stagnation.
- **135°:** Good ventilation direction. BBA (0.25 m/s) and BSH (0.24 m/s) show excellent airflow, while SLO (0.12 m/s) is again the lowest performer. SSH (0.14 m/s) is modest. A reliable direction for airflow enhancement.
- **180°:** Strongest overall wind direction for ventilation. BSH (0.33 m/s) and BBA (0.29 m/s) achieve peak velocities. Even SLO and SBA (0.17 & 0.22 m/s) reach improved levels. Highly effective for passive cooling due to windward openings.
- **225°:** Close to 135° in performance. SSH (0.24 m/s) and BBA (0.28 m/s) maintain high airflow, while SLO (0.14 m/s) again lags. BSH (0.30 m/s) and BLO (0.21 m/s) also perform strongly.
- **270°:** Another weak direction, similar to 90°. SLO (0.01 m/s) and SSH (0.02 m/s) remain almost stagnant. BBA (0.06 m/s) and BSH (0.03 m/s) show minimal ventilation. Indicates poor alignment with openings like 90°.
- **315°:** Moderate to good airflow. BBA (0.22 m/s) and BSH (0.20 m/s) continue to perform well. SLO (0.11 m/s) and SSH (0.15 m/s) improve slightly. A balanced direction for maintaining airflow.

By Scenario:

SBA, SSH, SLO: These cases **consistently underperform** in terms of airflow, especially under **90°** and **270°**, where **velocities drop as low as 0.01 m/s**. Even under favorable directions like **135°, 180° and 225°**, their performance lags behind BSH and BBA.

BBA, BSH, BLO: These configurations show **clear dominance in ventilation**, particularly under **135°, 180°, 225°**, and **315°**, where **velocity reaches or exceeds 0.30 m/s**. This indicates **superior design features promoting air movement**, such as **wind-facing openings, optimal window layout, or cross-ventilation paths**.

180° wind direction provides the strongest indoor airflow, with BSH and BBA reaching up to 0.33 and 0.29 m/s, making it ideal for passive cooling strategies on the ground floor.

90° and 270° as all cases are critical low-performance directions, where air velocity drops to near-zero, particularly in SLO and SSH, posing a risk of thermal discomfort and air stagnation.

Configurations BBA, BSH, and BLO consistently support higher velocities, showcasing their advantageous geometry or orientation in facilitating natural ventilation. While, SLO repeatedly underperforms across all directions, indicating ventilation design issues that may require architectural intervention such as new openings, redirection of airflow, or passive stacks.

9 First Floor Bedroom

First Floor Bedrooms Temperature (°C)	SBA	SSH	SLO	BBA	BSH	BLO
0	37.7	37	37.6	36.1	36	35.8
45	38.9	38.9	38.8	37.6	36.1	36.9
90	37.4	36.8	34.3	35.54	34	36.6
135	37.9	38.5	37.7	36.4	36.1	35.9
180	36.6	36.6	36.6	34.9	34.9	34
225	38.5	38.3	37.9	36.3	36.3	36.1
270	36.7	37.4	35.6	34.5	35.1	36.3
315	38.9	39.5	39.6	36.8	37.2	37.3

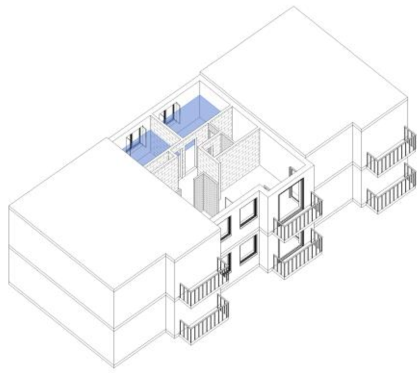

First Floor Bedrooms Velocity (m/s)	SBA	SSH	SLO	BBA	BSH	BLO
0	0.46	0.43	0.25	0.6	0.57	0.43
45	0.35	0.32	0.24	0.38	0.45	0.28
90	0.05	0.02	0.04	0.09	0.06	0.04
135	0.32	0.25	0.18	0.34	0.31	0.24
180	0.37	0.36	0.22	0.42	0.41	0.34
225	0.28	0.26	0.18	0.31	0.32	0.28
270	0.04	0.02	0.03	0.02	0.02	0.04
315	0.35	0.4	0.25	0.44	0.43	0.28

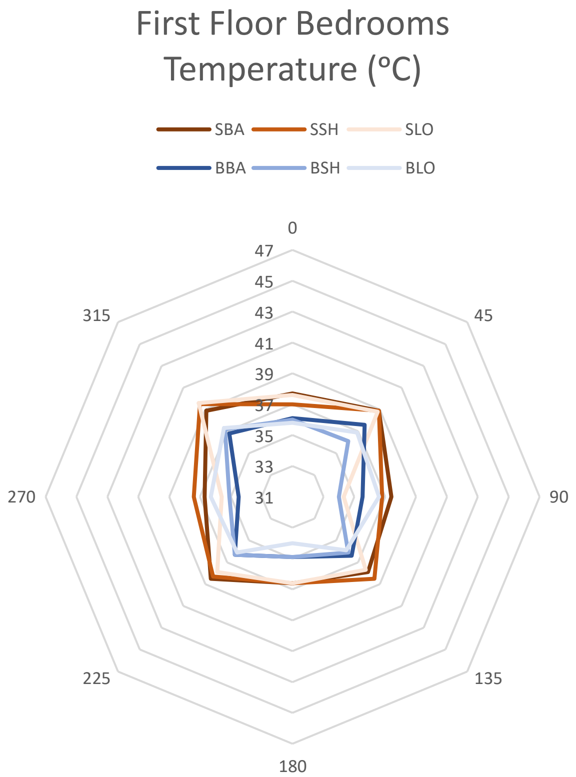

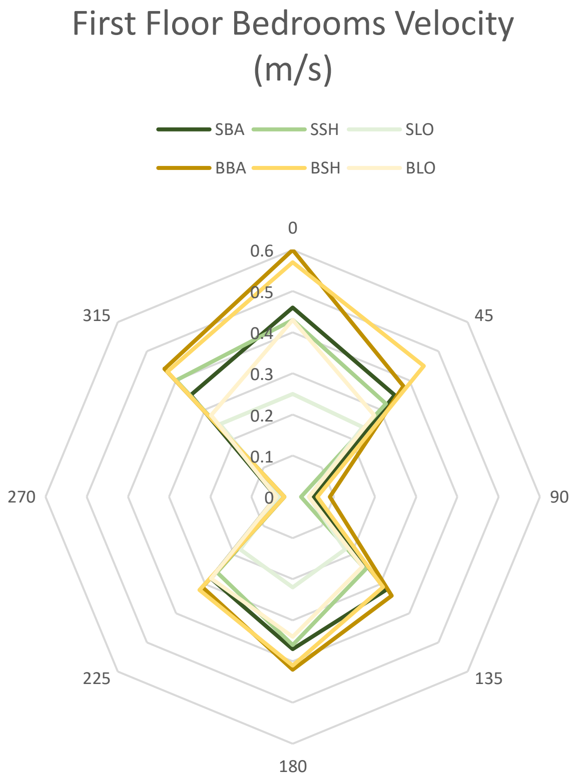

9.1 General Observations in Temperature

The temperature values vary significantly with wind direction, showing the influence of airflow on indoor thermal conditions. **SBA, SSH,** and **SLO** generally represent warmer conditions, while **BBA, BSH,** and **BLO** tend to show cooler indoor temperatures. Wind directions **45°, 135, 225°,** and **315°** generally result in **higher temperatures**, suggesting reduced cross-ventilation effectiveness or solar exposure. Wind direction **90°** and **270°** yields some of the **lowest temperatures**, especially in SLO (34.3°C), BBA (35.54°C), and BSH (34°C), indicating potentially better airflow or shading.

By Wind Direction:

- **0°:** Moderate temperatures with SBA and SSH at ~37°C; BBA, BSH, and BLO are cooler (~36°C), suggesting some ventilation advantage on the building's configuration (window size).
- **45°:** Highest recorded temperatures in SSH and SBA (38.9°C), indicating poor ventilation from this direction, possibly due to wind blockage.
- **90°:** Notably lower values, especially in SLO (34.3°C) and BSH (34°C), suggest this direction provides better heat air prevention.
- **135°:** Mixed values, but generally moderate, with a slight rise in SSH (38.5°C); BSH and BLO remain cooler.
- **180°:** Across all models, lower and consistent temperatures (~36.6°C or lower), indicating favorable conditions for natural cooling or because the hot air inlet is not in the bedrooms but from south (Living room).
- **225°:** A repeat of high-temperature patterns in SSH and SBA (~38.4°C), again showing this direction might not be ideal for ventilation performance.
- **270°:** A sharp drop in SLO (35.6°C) and BBA (34.5°C), hinting at wind alignment favoring these layouts or window orientations (same as for 90°).
- **315°:** Among the hottest cases, with SSH reaching 39.5°C and SLO at 39.6°C, possibly due to solar gain or poor airflow dispersion.

By Scenario:

SBA, SSH, SLO: Frequently show higher temperatures across multiple wind directions, suggesting they might represent less optimized layouts with limited ventilation.

BBA, BSH, BLO: Generally cooler across all directions, especially at 90°, 180°, and 270°, which might indicate better thermal design or ventilation paths.

> *Wind direction has a strong influence on indoor bedroom temperature. Since the reference temperature is the highest, it makes the effect of ventilation in a negative way in some cases. Layouts or models labeled BBA, BSH, and BLO tend to offer better thermal performance under most*

wind conditions, while SBA, SSH, and SLO struggle with higher heat retention. Directions from 90°, 180°, and 270° generally provide better cooling performance, possibly due to the prevention from cross-ventilation efficiency, while 45°, 135, 225°, and 315° perform worst in several scenarios due to exposure to hot air ventilation, Less convection current, and solar radiation.

9.2 General Observations in Velocity

Highest indoor velocities are recorded under **0° wind direction**, especially in **BBA (0.60 m/s)**, **BSH (0.57 m/s)**, and **SBA (0.46 m/s)**. This suggests optimal alignment of external wind with the ventilation openings in these models.

90° and 270° wind directions show **the lowest airflow velocities** across almost all scenarios, for example, SBA (0.05 / 0.04 m/s), SSH (0.02 / 0.02 m/s), and SLO (0.04 / 0.03 m/s), indicating poor natural ventilation due to likely misalignment of window openings or blocked airflow paths.

315° shows a slight recovery, particularly in SSH (0.40 m/s) and BBA (0.44 m/s), suggesting partially effective wind capture from this angle. Overall, **BBA** and **BSH** consistently perform better in maintaining higher indoor velocities, implying better window design for cross-ventilation or wind exposure.

By Wind Direction:

- **0°:** Best-performing direction for indoor airflow. BBA, BSH, and SBA all exceed 0.4 m/s, indicating strong air movement into the bedrooms Due to direct exposure to wind.
- **45°:** Slight reduction in all models but still reasonable performance in BBA (0.38 m/s) and BSH (0.45 m/s).
- **90°:** Drastically low velocities, often below 0.1 m/s (especially in SSH, SLO, and BSH) suggesting a stagnant indoor environment and poor ventilation.
- **135°:** Moderate performance, with BBA and SBA above 0.30 m/s, while SLO and BLO are underperforming.
- **180°:** Moderate to good performance across most cases, especially BBA (0.42 m/s), indicating that southern winds contribute positively to ventilation.
- **225°:** Mixed results; most velocities drop slightly, suggesting wind obstruction or weakened pressure differentials (almost the same as 135°).
- **270°:** Another major drop, very similar to the 90° case, again confirming poor alignment for natural ventilation (same scenario as for the 90°).
- **315°:** Noticeable improvement in SBA, SSH, BBA, and BSH; velocities rebound to 0.35-0.44 m/s.

By Scenario:

SBA, SSH, SLO: Moderate performers overall. High sensitivity to wind direction, great at 0° and 315°, but nearly stagnant at 90° and 270°. Generally the weakest performer in all directions, with velocities barely exceeding 0.25 m/s. Indicates this layout may not effectively channel air through the space.

BBA, BSH, BLO: Strongest performers, achieving consistently higher velocities. This suggests superior architectural layout or window/door configurations aligned with dominant wind patterns. Lower but stable performer, except at 90° and 270°, where velocity nearly disappears.

> *The effectiveness of natural ventilation in first-floor bedrooms is highly sensitive to wind direction and architectural layout. Directions 0°, 45°, 180°, and 315° support stronger indoor airflow, while 90° and 270° consistently underperform. Among the models, BBA and BSH demonstrate superior airflow behavior, while SLO performs poorest across almost all directions. This analysis suggests that orientation and design adjustments focusing on capturing prevailing winds can dramatically improve indoor air movement and thermal comfort.*

9.3 First Floor Living room

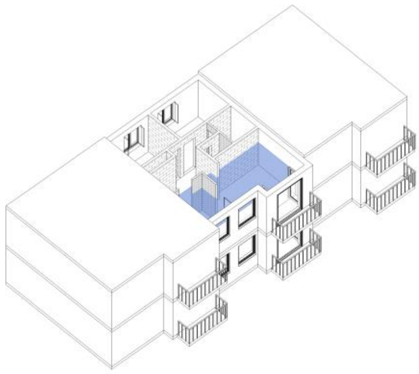

First Floor Living room Temperature (°C)	SBA	SSH	SLO	BBA	BSH	BLO
0	36.6	36.7	36	35.1	35.2	34.2
45	36.9	37	36.9	35.4	34.7	34.7
90	35.3	41.7	42.6	34.6	40	36.4
135	42.1	43.1	42.9	40.5	40.3	40.6
180	38.8	38.9	39.3	36.9	36.9	36.4
225	41	40.9	41.6	38.5	38.3	38.5
270	38.8	44.9	41.4	40.2	40.1	36.8
315	37.2	37.7	37.3	35.3	35.5	35.7

First Floor Living room Velocity (m/s)	SBA	SSH	SLO	BBA	BSH	BLO
0	0.21	0.22	0.12	0.34	0.31	0.21
45	0.16	0.15	0.12	0.22	0.21	0.14
90	0.02	0.04	0.02	0.04	0.03	0.06
135	0.27	0.24	0.17	0.32	0.29	0.25
180	0.4	0.39	0.22	0.43	0.44	0.41
225	0.24	0.25	0.21	0.29	0.3	0.29
270	0.03	0.03	0.02	0.06	0.05	0.1
315	0.17	0.18	0.11	0.23	0.21	0.13

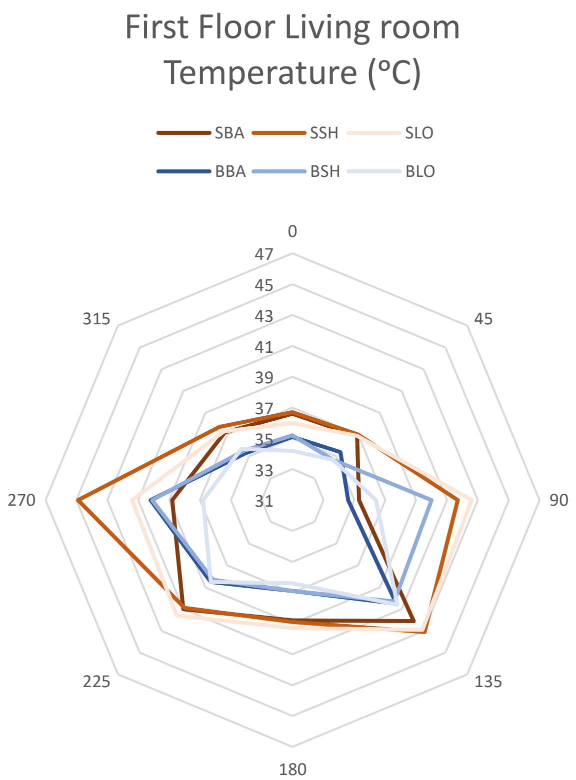

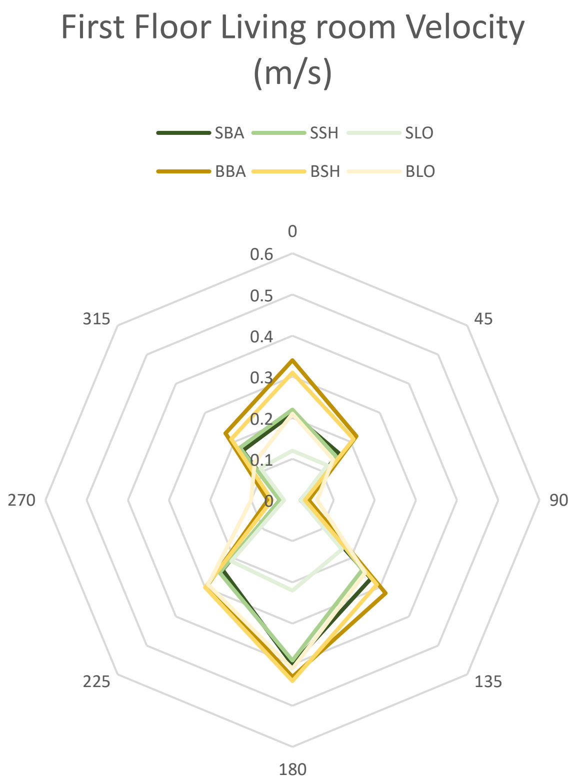

9.4 General Overview in Temperature

Highest temperatures recorded in SSH and **SLO** consistently exhibit **very high temperatures**, reaching **up to 44.9°C**, indicating significant overheating on south façade.

Best performing configurations (cooler rooms) happen in BLO, **BSH**, and **BBA** demonstrate **lower** and **more stable temperatures**, especially under 0°, 45°, 180°, and 315°, pointing to effective design and ventilation strategies.

Most problematic wind directions (overheating risk) for 135°, 225°, 90° and 270° lead to the **highest indoor temperatures** across nearly all configurations, marking them as **critical in terms of passive cooling failure**.

Most favorable wind directions (cooling potential) are in 0°, 45°, and 315° provide **consistently lower temperatures**, supporting effective passive cooling for most cases.

By Wind Direction:

- **0°:** Lower temperatures across all configurations, especially BLO (34.2°C) and BSH (35.2°C). Indicates favorable wind flow and minimal solar gain on the first floor.
- **45°:** Still moderate performance, with BLO and BSH at 34.7°C. Although SSH and SLO are slightly elevated (~37°C), overall this direction supports good temperature control.
- **90°:** Significant overheating in SSH (41.7°C) and SLO (42.6°C). Other cases like BSH (40°C) also perform poorly, suggesting high solar exposure and poor airflow under this condition.
- **135°:** One of the worst cases. Temperatures exceed 43°C in SSH (43.1°C) and SLO (42.9°C). All other cases also show elevated values above 40°C, except BLO (40.6°C) still high.
- **180°:** Moderate performance. Best results seen in BLO (36.4°C) and BSH (36.9°C). Slightly higher temperatures for SSH/SLO, but overall less extreme than 135° or 270°.
- **225°:** Generally high temperatures, especially in SLO (41.6°C) and SSH (40.9°C). BLO and BSH remain better (~38.3-38.5°C), but this direction still poses a thermal comfort risk.
- **270°:** Extremely poor performance in SSH (44.9°C) and SLO (41.4°C). Even BSH and BBA are above 40°C. Clearly a critical wind direction for overheating (same scenario as 90°).
- **315°:** Temperatures drop again to more acceptable levels; BLO (35.7°C), BSH (35.5°C), BBA (35.3°C) demonstrating good cross-ventilation and reduced effect of solar heat gain.

By Scenario:

SBA, SSH, SLO: These perform poorly across several directions, especially under 90°, 135°, 225°, and 270°, where temperatures soar above 41°C.

Indicates inadequate passive cooling strategies and likely poor window placement or solar shading.

BBA, BSH, BLO: These show strong thermal resilience, especially under 0°, 45°, 180°, and 315°, with temperatures remaining under 37°C. This aligns with better natural ventilation, solar control, and overall passive design.

> *SSH and SLO experience critical overheating under multiple wind directions. BLO and BSH are the most thermally comfortable configurations, managing to stay below 37°C even under challenging wind conditions.*
>
> *135° and 270° wind directions should be seen as high-risk orientations and mitigated in building design through strategic opening placements or additional ventilation aids. The data confirms a strong correlation between poor airflow performance and elevated indoor temperatures, especially in SSH and SLO reinforcing the importance of integrated passive strategies [256].*

9.5 General Overview in Velocity

Highest velocities recorded in 180° wind direction leads to the highest velocities across all configurations, with values reaching up to **0.44 m/s in BSH** and **0.43 m/s in BBA**, indicating **excellent airflow and natural ventilation**.

Best performing (ventilation efficiency) are **BBA**, **BSH**, and **BLO** consistently show **higher velocities** across most directions, suggesting these layouts benefit from better exposure to wind and effective internal flow paths.

Most problematic wind directions (ventilation failure) in 90° and **270°** display **very low airflow values**, especially in **SLO** and **SSH**, where velocities drop to **0.02-0.04 m/s**, indicating **weak cross-ventilation** and **potential stagnation**.

Most favorable wind directions (ventilation potential) are **180°, 135°,** and **225°** offer **the best airflow conditions**, promoting **effective indoor air movement** and passive cooling in first-floor living rooms.

By Wind Direction:

- **0°:** Moderate airflow across all rooms, with BBA (0.34 m/s) and BSH (0.31 m/s) showing the strongest performance. SLO (0.12 m/s) lags behind, indicating uneven ventilation benefits.
- **45°:** Slight reduction in airflow. Most values hover around 0.14-0.16 m/s, with BBA and BSH maintaining relatively stronger airflow (0.22 and 0.21 m/s), though performance is weaker than at 0°.
- **90°:** Poor airflow across all configurations. Values drop as low as 0.02 m/s in SBA and SLO, with no room exceeding 0.06 m/s. Indicates highly obstructed or misaligned wind entry.
- **135°:** Strong recovery in airflow, especially in BBA (0.32 m/s), BSH (0.29 m/s), and BLO (0.25 m/s). Shows improved alignment with cross-ventilation openings.

- **180°:** Peak airflow performance, with nearly all room recording velocities above 0.39 m/s. BSH (0.44 m/s) and BBA (0.43 m/s) perform exceptionally, proving this is the most favorable windward window direction.
- **225°:** Continues the high-performance trend. Velocities range between 0.21-0.30 m/s, with BSH and BBA maintaining strong airflow at 0.30 and 0.29 m/s, ensuring good ventilation.
- **270°:** One of the weakest directions the same as 90°. Flow drops below 0.06 m/s in all configurations. SLO and SBA (0.02 m/s) confirm this direction is ineffective for passive airflow.
- **315°:** Mixed performance. BBA (0.23 m/s) and SSH (0.18 m/s) perform better, while SLO (0.11 m/s) and BLO (0.13 m/s) remain weak. Slight improvement compared to 270°, but still suboptimal.

By Scenario:

SBA, SSH, SLO: These configurations show weak ventilation performance, especially under 90° and 270°, where airflow drops close to zero. Improvement is seen at 180° and 135°, but values are still lower than optimal.

BBA, BSH, BLO: These are consistently better performers, especially under 180°, 135°, and 225°, reaching up to 0.44 m/s. These setups benefit from superior wind exposure and interior airflow connectivity.

> *180° wind direction delivers the strongest natural ventilation, suggesting design alignment with this flow is crucial for first-floor airflow optimization. While, wind directions 90° and 270° should be considered critical zones for airflow stagnation, requiring compensatory design features such as additional openings or passive ventilation enhancements.*
>
> *SLO and SSH remain problematic under multiple wind angles, highlighting a need for revised window placement or improved cross-ventilation strategies. BBA and BSH emerge as the most ventilated living spaces, validating their design as highly effective for passive cooling.*

10 Conclusion case 1 (Cross Ventilation)

In a living room on a warm Polish afternoon, the sun's rays beating down relentlessly on the south façade. As the wind shifts to come from the southeast (135°), south (180°), or southwest (225°), it carries not only air but the lingering heat absorbed by the sun-exposed walls. These winds sweep across surfaces that have been baking in the sun, picking up heat and depositing it inside the space. The result is a sudden spike in both temperature [256] and airflow readings in our tables an abnormal change that feels almost counterintuitive if one expects cross-ventilation to always cool a space. In reality, the wind becomes a carrier of warmth rather than relief.

Contrast that with northerly breezes from 0°, 45°, or northwest at 315°. These winds approach the building's shaded face, sheltered by surrounding blocks and freed from direct solar radiation. Here, the tables show a pronounced drop in temperatures and a gentle but refreshing airflow. You can almost feel the relief as the north wind dances through the living room, sweeping away the built-up heat. This clear dichotomy (hot, sun-driven winds versus cool, shaded breezes) forms the first layer of our story.

Next, consider the curious case of winds at 90° and 270°. Our data reveal that these directions deliver almost no airflow, and temperatures hover in a middling range. Because the windows and openings simply aren't aligned to capture east or west winds effectively; the geometry fails to create a pressure differential, so the air hardly moves. Ironically, the very directions that one might assume bring a fresh breeze turn out to be the quietest, underscoring that orientation matters as much as wind speed.

Finally, it's worth noting that the world outside is rarely symmetrical or perfectly predictable. Even paired wind directions (say 135° and 225°) don't yield identical results in practice. Afternoon sun angles intensify radiative heat on the west side, so a southwest wind (225°) often carries even more warmth than its southeast counterpart. These nuances are exactly why running detailed CFD simulations is indispensable: they uncover the real, messy interplay of sun, wind, and building geometry. When we view the tables more holistically, we see three distinct regimes: the scorching group (135°, 180°, 225°) driven by heated facades, the stagnant group (90°, 270°) where openings aren't windward, and the cooling group (0°, 45°, 315°) where shaded northern breezes prevail. Understanding these patterns is key to designing truly comfortable, naturally ventilated homes in a changing climate.

Design strategies must be reconsidered to address the effects of climate change. This study explored small-scale solutions to improve indoor thermal comfort. Results base on evaluation showed that larger windows had a positive impact on air temperature and flow in most of the 48 samples tested. Adding sun protection with overhangs further enhanced this effect. Generally, temperature in living rooms is lower when the inlets are bedroom's windows, in these cases usually large windows perform better both in temperature and velocity. Also, other general conclusion to make is that ground floor temperature is lower because of the protection against solar radiation; and airflow is relatively less than the first floor. But the airflow pattern and temperature distribution are almost the same in both floors. This shows the importance of the effect of the windows and their features to the variables.

Two places are vulnerable to the high temperature, areas in front of the inlet windows (also hallway in this case because of the venturi effect), and areas far from the inlet or outlet windows or better to explain the areas hard to ventilate. In both cases the larger windows help a lot to reduce these areas with high temperature. The focus in this study is more on these areas as the temperature fluctuation is not comfortable so the aim in analysis was to optimize it.

Finally, two more point to mention; First, the shoe box models (models with just a box as a room of a house, with fixed dimensions that even are not common in architecture, and also the unrealistic size and location of the windows) are not useful for making these decisions in the field of architecture. This research method, which is very common in the field of mechanics, cannot be used in architecture. This research shows that there are many other important variables in architecture like solar radiation, indoor walls, air inlet direction, and the floor (here ground and 1st floor studied) that effect on the temperature and air velocity. Secondly, louvers and sometimes overhangs are not suitable because of solar radiation and should be used carefully.

11 Results (case2 Corner Ventilation)

In the second case study of this research, the focus shifts to evaluating a unique and underexplored mode of natural ventilation known as corner cross ventilation. Unlike traditional cross-ventilation setups, corner ventilation occurs when openings are positioned on adjacent facades meeting at a corner, offering a distinctive airflow pattern that has received limited attention in existing literature. To investigate this phenomenon, a dedicated CFD simulation was conducted using the same eight wind directions and six different opening configurations previously tested. This parallel approach allows for a consistent and direct comparison of performance outcomes under identical modeling parameters.

The geometry in this case consists of two symmetrical flats located in the building's corners. Because the design and opening arrangements are mirrored, the airflow behavior and thermal responses were found to be highly symmetrical across the two units. To streamline the analysis and focus on the more critical conditions, only the west-facing flat is discussed. This unit experiences greater solar exposure, receiving intense sunlight from both south and west, making it the extreme scenario in terms of overheating risk and ventilation performance.

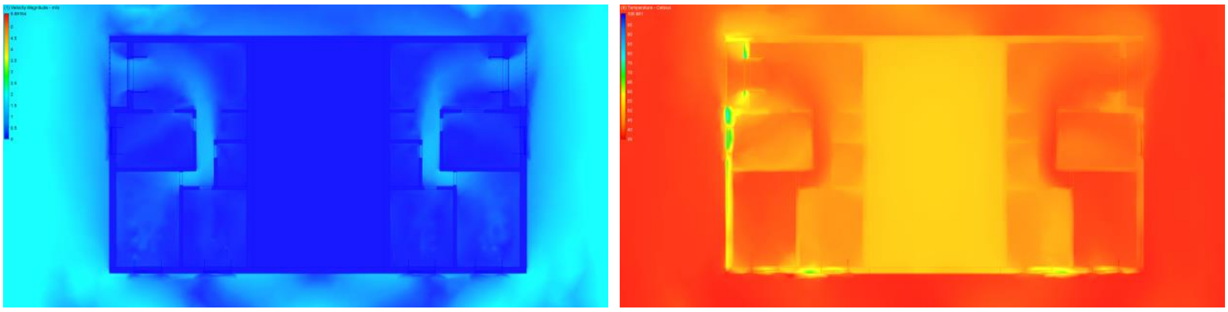

Fig. 5- 27: An example of Velocity (left) and Temperature (right) couture for the case BBA when wind is from south. Both flats are having almost symmetrical results.

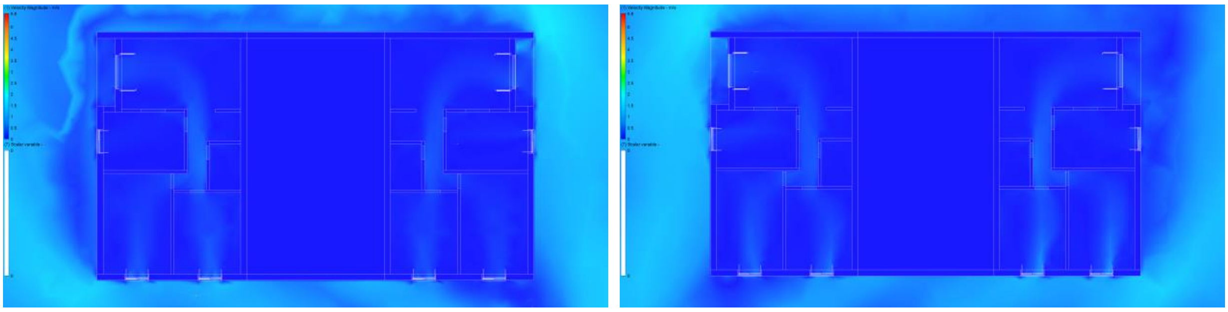

Fig. 5- 28: Almost symmetrical results from diagonal angles, Velocity couture 135° (left) and 225° (right).

While all modeling and simulation settings remain consistent with the previous case, including turbulence models, solver configurations, and boundary conditions, the mesh density and domain size were adapted appropriately to match the geometric scale of the corner ventilation layout. These adjustments are necessary to maintain accuracy and computational efficiency, as the domain and grid resolution must correspond to the specific dimensions of the building form.

This case serves to deepen the understanding of how window configurations and wind direction interact within corner-ventilated layouts, offering insights into both the potential benefits and limitations of this unconventional yet promising ventilation strategy. The following sections present a detailed interpretation of the simulation results, emphasizing the thermal and airflow behavior of the west-facing flat under varying wind scenarios and opening combinations.

11.1 Ground Floor Bedrooms

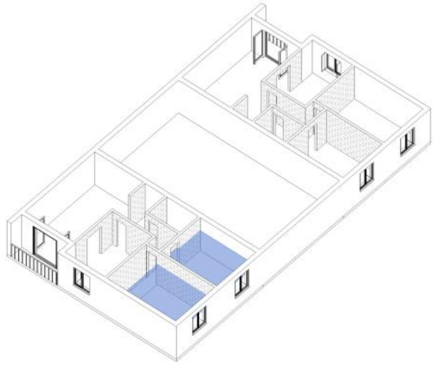

First Floor Bedrooms Temperature (°C)	SBA	SSH	SLO	BBA	BSH	BLO
0	37.1	37.2	36.5	35.6	35.7	34.7
45	37.4	37.5	37.4	35.9	35.2	35.2
90	39.8	41.2	42.1	37.1	36.5	36.9
135	43.1	44	43.9	39.5	38.3	39.6
180	42.4	41.5	42.9	39.5	39.5	40.2
225	43.1	43	43.7	41.6	40.4	41.6
270	41.4	45.5	43	41.8	41.7	42.4
315	40.2	39.7	40.3	38.3	38.5	39.7

Ground Floor Bedrooms Velocity (m/s)	SBA	SSH	SLO	BBA	BSH	BLO
0	0.04	0.03	0.01	0.07	0.06	0.05
45	0.04	0.03	0.02	0.07	0.05	0.03
90	0.05	0.06	0.04	0.08	0.1	0.07
135	0.19	0.14	0.12	0.25	0.24	0.18
180	0.34	0.35	0.33	0.43	0.45	0.41
225	0.26	0.28	0.25	0.31	0.34	0.3
270	0.18	0.19	0.12	0.2	0.23	0.2
315	0.04	0.05	0.04	0.09	0.11	0.08

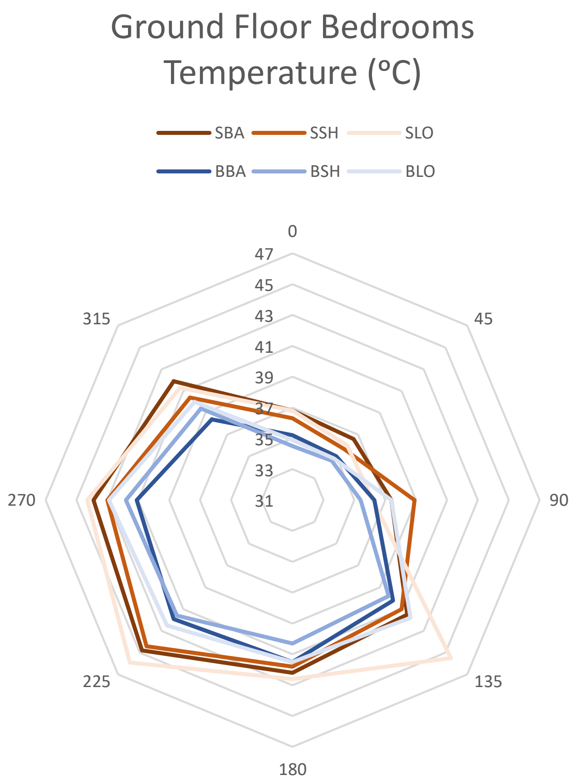

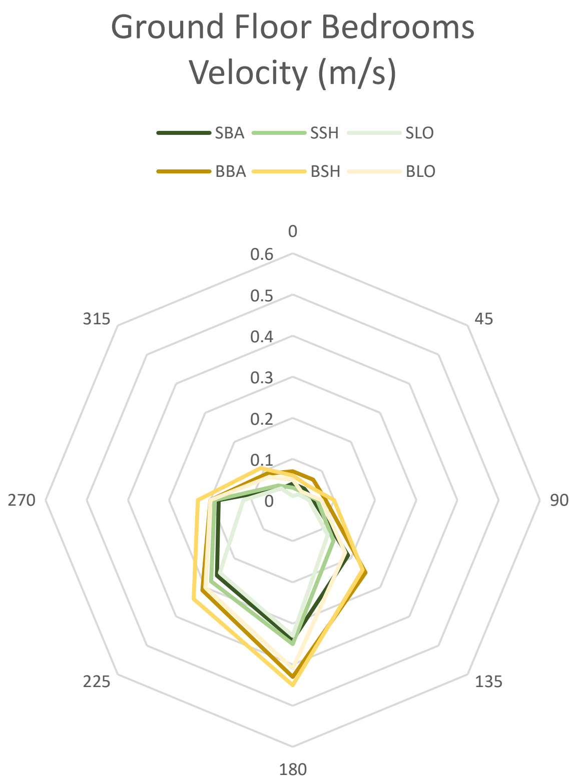

11.2 General Overview on Temperature

135°, 180°, and **225°** clearly show the **highest bedroom temperatures**, peaking at **45.9°C** (SLO with 225°). This is due to **southern solar exposure**, which preheats the air and surfaces. Once these hot winds enter, **internal heat builds up**, especially in configurations with poor ventilation (like SLO). On the other hand, **0°, 45°,** and to some extent **315°** yield **relatively lower temperatures**. For instance, **BLO drops to 34.8°C in 45°**, and **BSH reaches 34.5°C in 0°**, highlighting the **cooling effect of not hated air**, which strike shaded facades.

Temperatures are **not symmetric** between directions (e.g., 135° vs. 225°), despite similar angles. This is because **west-facing facades (225°)** receive **stronger afternoon sun**, increasing **thermal gain prior to wind arrival**. This **pre-heated exterior** causes greater indoor overheating even under similar wind conditions.

By Wind Direction:

- **0° (N):** Decent performance in cooling, with BSH at 34.5°C and BLO in 34.9°C. Winds here come from a shaded side, helping reduce internal gains.
- **45° (NE):** Slightly warmer than 0°, but still relatively effective. Temperatures hover around 34.6-36.6°C, showing moderate cooling potential.
- **90° (E):** An unexpected temperature spike in some cases SSH (38.9°C) and BLO (37.4°C), despite generally low velocities. This may be linked to poor wind alignment with openings, leading to internal heat buildup.
- **135° (SE):** A hot direction across the board. SLO hits 45.5°C, while others also exceed 40°C. This is a combined result of solar exposure and warm wind, which amplifies internal heat.
- **180° (S):** Still very hot, though slightly lower than 225°. All configurations >40°C, emphasizing direct radiation and heated wind entering through southern openings.
- **225° (SW):** The worst performing direction overall, with maximum overheating due to pre-radiated walls and west-facing solar gain. SLO again is the worst case at 45.9°C.
- **270° (W):** Surprisingly warm, especially considering this is one of the worst directions for airflow. Poor ventilation and radiated facades cause trapped heat.
- **315° (NW):** Rather cooling effect returns. Most temperatures drop below 41°C, with BBA at 38.4°C being among the coolest in this warm group.

By Scenario:

SLO consistently performs poorly, hitting the highest temperatures under multiple wind directions, suggesting very limited cross-ventilation or exposure to direct solar gain.

BBA, BSH, and BLO often maintain lower temperature profiles, especially under cooler (shaded) wind conditions (0°, 45°, 315°). Their layouts appear more effective in passive cooling as well.

> *135°, 180°, and 225° directions bring in radiatively heated winds, leading to extreme indoor temperatures, especially where ventilation is poor. Cooling is most effective when winds come from shaded, north-facing facades (0°, 45°, 315°), a valuable insight for climate-responsive design.*
>
> *Not all outcomes are symmetrical or intuitive. For instance, 90° and 270° have hotter interiors due to low airflow and solar alignment, underscoring the importance of simulation in evaluating building performance.*

11.3 General Overview in Velocity

Best-performing directions for airflow: 180°, 225°, and **135°** stand out with the **highest velocities**, especially BBA in 180° (0.43 m/s) and BSH in 180° (0.45 m/s). These wind directions are highly effective for **cross ventilation**, likely because of **direct wind alignment with openings** and a pressure differential across the layout.

Poor-performing directions: 0°, 45°, and **315°** provide **minimal air movement**, with most values under **0.07 m/s**. While these contribute to lower air temperature, their mechanical ventilation effect is limited.

Moderate winds: 270° and **90°** present **mixed performance**. Though 90° is not a dominant wind direction in terms of cross ventilation, it still achieves some movement (BSH with 0.1 m/s) thanks to **incidental alignment** and **geometry-driven flow**.

By Wind Direction:

- **0° and 45° (N & NE):** Air velocity remains very low, with most below 0.05 m/s. The spaces cool mainly through temperature, not air movement.
- **90° (E):** A surprising increase in some cases (BSH reaches 0.1 m/s, and BBA hits 0.08 m/s) suggesting some directional advantage even without ideal opening placement.
- **135° (SE):** Begins to show effective airflow, especially in BBA (0.25 m/s) and BSH (0.24 m/s), which supports both ventilation and cooling during hot periods.
- **180° (S):** Delivers the strongest airflows across all configurations, with nearly all values above 0.3 m/s. This makes it the most ventilated condition, though it also brings hot air into sun-exposed rooms.

- **225° (SW):** Maintains high airflow, though slightly less than 180°. Still, BBA, BSH, BLO all above 0.3 m/s, offering strong ventilation, though again paired with radiative heat.
- **270° (W):** Surprisingly consistent in mid-range airflow, despite being an unfavorable direction for indoor comfort (due to heat). Speeds like BSH with 0.23 m/s suggest decent wind pressure, though it carries warm air.
- **315° (NW):** Returns to lower velocities, though slightly higher than 0° and 45°. BSH again leads (0.11 m/s), confirming its reliable ventilation performance across various directions.

180°, 225°, and 135° bring strong ventilation, but often with unwanted heat, ventilation alone may not guarantee comfort under these conditions.

Northern directions (0°, 45°, 315°) offer cooler indoor air temperature but minimal airflow, highlighting the trade-off between air temperature and velocity in cross-ventilation strategies. BBA and BSH consistently show higher velocities, suggesting their geometries align better with pressure-driven cross-ventilation.

11.4 Ground Floor Living room

Ground Floor Living room Temperature (°C)	SBA	SSH	SLO	BBA	BSH	BLO
0	37.3	37	37.6	36.1	35.4	35.4
45	38	37.5	38.3	36	35.7	36.7
90	37.5	36.9	37.1	36.7	35.8	37.4
135	39	39.6	38.7	37.5	37.4	38.9
180	39.5	39.3	39.5	38.7	37.6	38.9
225	40.6	40.2	41.2	39.9	39.7	40.7
270	40.8	41.3	41.8	38	38.4	39.4
315	39.6	40	39.8	37.4	37.5	38.2

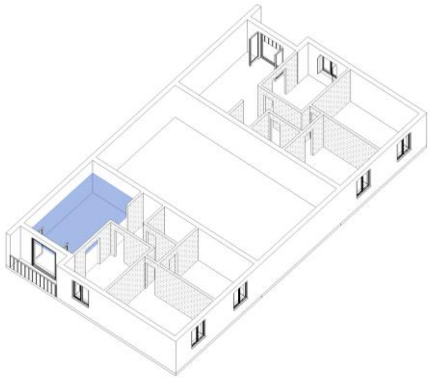

Ground Floor Living room Velocity (m/s)	SBA	SSH	SLO	BBA	BSH	BLO
0	0.05	0.07	0.04	0.09	0.1	0.07
45	0.04	0.02	0.03	0.05	0.07	0.04
90	0.05	0.03	0.02	0.07	0.09	0.05
135	0.13	0.15	0.11	0.19	0.2	0.14
180	0.18	0.2	0.16	0.25	0.27	0.22
225	0.2	0.22	0.17	0.29	0.32	0.23
270	0.31	0.3	0.26	0.37	0.42	0.31
315	0.17	0.24	0.19	0.27	0.3	0.25

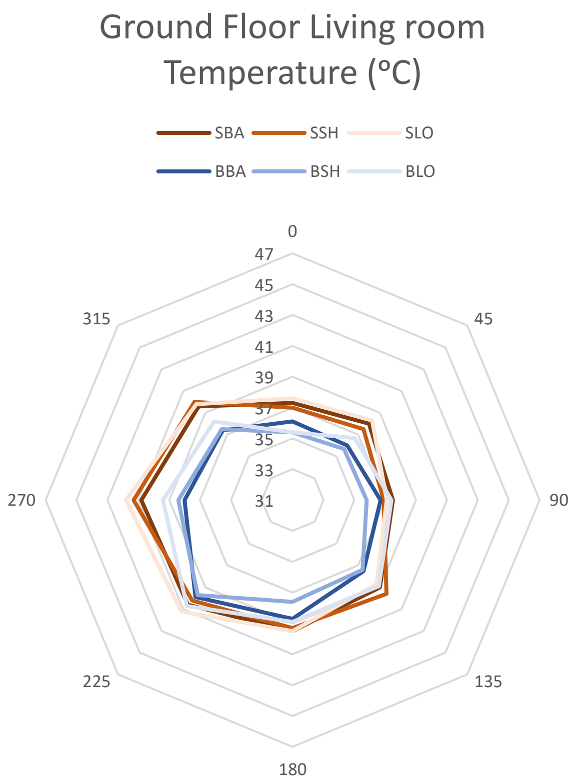

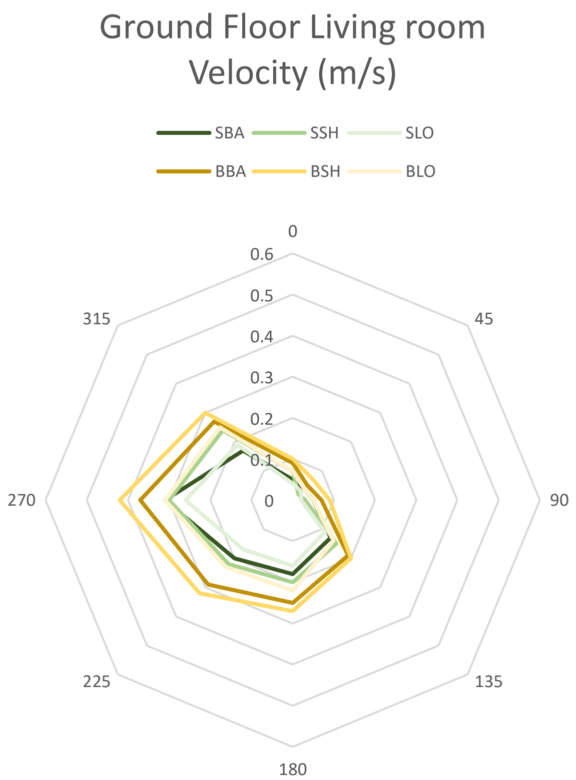

11.5 General Overview in Temperature

Wind directions **225°, 270°,** and **315°** result in the **highest temperatures**, particularly SLO in 270° (41.8°C) and **BLO 225° (40.7°C)**. These high readings align with **afternoon sun exposure**, especially from the southwest and west, where **solar radiation peaks** and wind pass over **sun-heated surfaces**. **0°, 45°,** and **90°** show relatively **lower temperatures**, with **BSH in 0° (35.4°C)** and **BBA 45° (36.0°C)** among the lowest. These wind directions are from the north and northeast, where **less direct solar gain** allows wind to act more as a **cooling mechanism**.

By Wind Direction:

- **0° and 45°:** Winds from the north introduce shaded air into non-irradiated facades, resulting in moderate to low indoor temperatures, especially in BBA and BSH.
- **90°:** Despite not being optimal for cross ventilation, temperatures stay fairly moderate, likely due to lower solar exposure and some air movement.
- **135°, 180°, and 225°:** A clear heating trend appears here, caused by direct sun exposure on the south façade. Temperatures rise notably in SLO and BLO, which are directly affected by solar-loaded airflow.
- **270° and 315°:** The warmest conditions overall, likely due to both strong solar radiation from the west and entrance of sun-heated air into living spaces. This confirms that ventilation from irradiated directions may raise indoor heat, especially when natural ventilation is used during peak sun hours.

  South to west wind (135°-315°) cause noticeable overheating, especially when wind flows over sunlit surfaces. North-origin winds (0°-90°) offer cooler temperatures, reinforcing their value in passive cooling strategies.

  These results underscore the critical role of wind direction combined with solar exposure, especially in corner-ventilated configurations where thermal gains can accumulate significantly.

11.6 General Overview in Velocity

The wind directions **270°, 225°**, and **180°** yield the **strongest air movements**, particularly in the BSH 270° (0.42 m/s) and BBA 270° (0.37 m/s) cases. This suggests optimal airflow in these directions due to **greater windward exposure of the openings**, despite the accompanying thermal penalties.

Winds from **45°** and **90°** result in the **lowest air velocities**, such as **SLO** in 90° (0.02 m/s) and **SSH** 45° (0.02 m/s), indicating inefficient airflow, likely because openings are not ideally positioned relative to the wind.

By Wind Direction:

- **0°, 45°, and 90°:** These directions show weaker air circulation. Even though temperatures were relatively cooler, the ventilation performance is minimal, making these directions suitable only for mild passive cooling.

- **135°, 180°,** and **225°:** A notable improvement in airflow is evident. As the wind turns more southerly, cross ventilation becomes stronger, with velocities such as BBA in 225° (0.29 m/s) and BSH in 225° (0.32 m/s). However, these also coincide with high thermal gains, requiring careful management.
- **270° and 315°:** These directions produce the most effective ventilation, with consistently high velocities across all layouts. Notably, SBA, SSH, BSH, and BLO all exceed 0.3 m/s, indicating strong air movement, which may be beneficial for night ventilation or non-peak hours, but problematic when ambient temperatures are high.

Maximum velocities occur with western winds (270°), aligning with the façade orientation and yielding efficient airflow, but must be timed to avoid overheating. Minimum airflow is observed at 45° and 90°, reinforcing the limitations of non-aligned window orientations in corner ventilation schemes. These patterns confirm the asymmetrical behavior of natural ventilation, where thermal and airflow advantages do not always coincide, emphasizing the need for contextual design strategies.

11.7 First Floor Bedrooms

First Floor Bedrooms Temperature (°C)	SBA	SSH	SLO	BBA	BSH	BLO
0	37.1	37.2	36.5	35.6	35.7	34.7
45	37.4	37.5	37.4	35.9	35.2	35.2
90	39.8	41.2	42.1	37.1	36.5	36.9
135	43.1	44	43.9	39.5	38.3	39.6
180	42.4	41.5	42.9	39.5	39.5	40.2
225	43.1	43	43.7	41.6	40.4	41.6
270	41.4	45.5	43	41.8	41.7	42.4
315	40.2	39.7	40.3	38.3	38.5	39.7

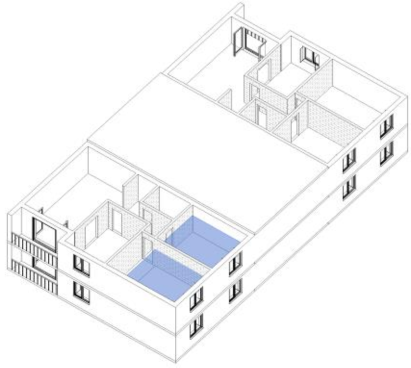

First Floor Bedrooms Velocity (m/s)	SBA	SSH	SLO	BBA	BSH	BLO
0	0.06	0.07	0.06	0.12	0.12	0.09
45	0.08	0.1	0.08	0.14	0.11	0.1
90	0.13	0.14	0.1	0.22	0.23	0.18
135	0.32	0.25	0.19	0.37	0.3	0.23
180	0.44	0.42	0.3	0.5	0.47	0.43
225	0.37	0.37	0.26	0.43	0.44	0.3
270	0.19	0.2	0.15	0.24	0.27	0.22
315	0.05	0.06	0.05	0.1	0.12	0.07

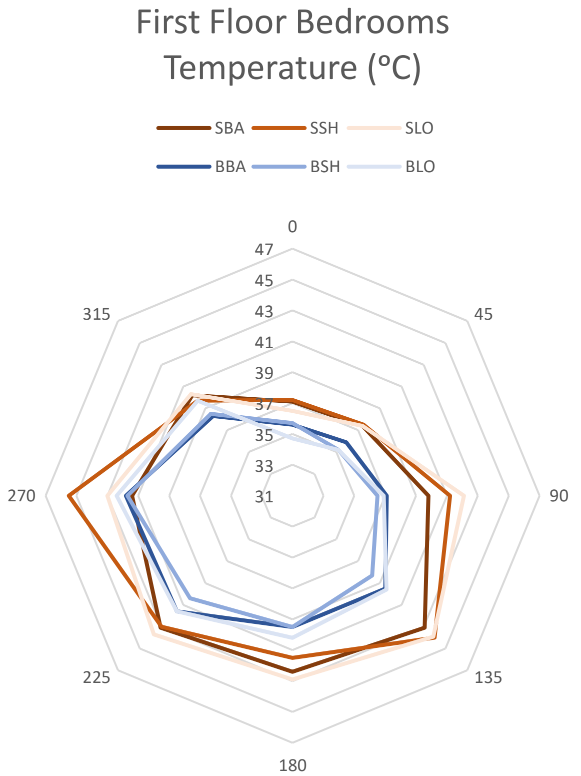

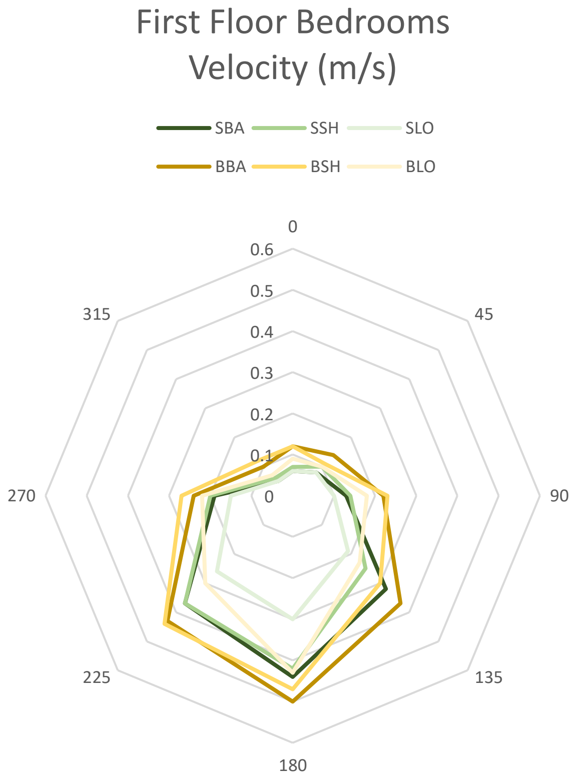

11.8 General Overview in Temperature

Winds from **135°, 180°, 225°,** and **270°** generate the **highest indoor temperatures**, particularly in **SLO** and **SSH**, reaching up to **45.5°C**. This indicates **direct solar gains on west and south-facing façades**, combined with **ineffective ventilation**.

The lowest temperatures occur at **0°, 45°,** and **315°**, especially for configurations like **BLO** and **BBA**, where values fall as low as **34.7°C**. These directions offer cooler temperature**, shaded airflow** and **reduced solar radiation**.

By Wind Direction:

- **0° and 45°:** Show relatively balanced conditions, especially for BSH, BLO, and BBA, keeping temperatures around 35-36°C. These are the most favorable for passive cooling on the first floor.
- **90° and 135°:** Present a steep rise in indoor heat, SLO reaches 42.1°C in 90° and 43.9°C in 135°, driven by midday solar loads with limited heat removal due to poor airflow.
- **180° and 225°:** Confirm severe overheating in SLO and SSH, consistently exceeding 43°C, with BBA and BLO faring slightly better due to their window geometry or shading.
- **270° and 315°:** While 270° shows very high peak temperatures, especially SSH with 45.5°C, the wind at 315° improves conditions, BBA with 38.3°C and BSH with 38.5°C mark a reduction.

By Scenario:

SLO and SSH exhibit consistently poor thermal performance, often leading all cases in maximum heat retention, highlighting design limitations for cross ventilation and high solar exposure.

BLO and BSH generally maintain cooler ranges, especially when wind directions are aligned with shaded or less exposed façades, indicating better natural cooling response with window size and orientation.

> *Higher first-floor temperatures result mainly from solar gains, particularly in SLO and SSH. Even with potential ventilation, radiative heating dominates. Cooling potential is maximized with northerly and northeasterly winds (0°, 45°, 315°), which should be prioritized in layout and orientation design.*
>
> *The results stress that geometry and window size and placement strongly influence thermal comfort, especially on upper floors where heat accumulation is amplified.*

11.9 General Overview in Velocity

180°, 225°, and **135°** deliver the **highest airflow**, notably in **BBA (0.5 m/s)** and **BSH (0.47 m/s)** at **180°**, confirming strong **cross-ventilation potential** driven by direct wind exposure and effective opening placement.

0°, 45°, and **315°** result in **very low velocities** (mostly **≤ 0.1 m/s**), offering **limited cooling** despite cooler ambient air, especially in **SLO, SBA,** and **SSH**.

90° and **270°** exhibit **mid-range velocities**, with noticeable gains in **BSH (0.23 m/s in 90° and 0.27 m/s at 270°)**, suggesting geometry plays a role even when wind is not optimally aligned.

By Wind Direction:

- **0° and 45°:** Low velocities across all configurations (max 0.14 m/s), offering minimal ventilation impact.
- **90°:** Gains momentum in BBA (0.22 m/s) and BSH (0.23 m/s), likely due to facade orientation or inlet positions of rooms.
- **135°:** Starts to show strong performance, with BBA (0.37 m/s) and BSH (0.3 m/s) benefiting the most from southeast winds.
- **180°:** Delivers peak airflow across nearly all rooms, making it the most effective for natural ventilation.
- **225°:** High airflow sustained in BBA, BSH, BLO, though slightly below 180°, still very efficient.
- **270° and 315°:** Mixed results, BBA and BSH still perform decently, but SLO and SSH fall behind, suggesting inconsistent flow paths.

By scenario:

BBA and BSH consistently outperform others in airflow under nearly all wind directions, suggesting superior cross-ventilation geometry or inlet-outlet alignment.

SLO, SBA, and SSH often receive the lowest velocities, indicating restricted flow, likely due to poor opening size, orientation or blockage.

> *Strongest ventilation occurs with southerly and southwesterly winds (180°, 225°), particularly for BBA and BSH. Northern and northeastern winds (0°, 45°) bring limited air movement, necessitating design support (e.g., mechanical aids) for effective cooling.*
>
> *Performance is clearly geometry-dependent, reinforcing the importance of strategic window design and wind alignment in natural ventilation strategies.*

11.10 First Floor Living room

First Floor Living room Temperature (ºC)	SBA	SSH	SLO	BBA	BSH	BLO
0	38.2	38.5	38.1	36.6	36.5	36.3
45	39	39.4	39.3	36.5	36.6	37.4
90	37.9	38.3	38.8	36	35.5	37.3
135	38.9	39.5	38.7	37.4	37.1	37.9
180	38.2	38.2	39.1	37.7	37.5	37.6
225	40.6	40.4	41	38.4	38.4	38.2
270	39.8	39	39.2	38.1	38.7	37.9
315	39.9	40.5	40.6	37.8	38.2	38.3

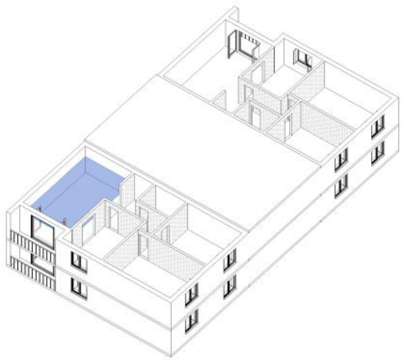

First Floor Living room Velocity (m/s)	SBA	SSH	SLO	BBA	BSH	BLO
0	0.06	0.07	0.05	0.1	0.13	0.07
45	0.05	0.02	0.04	0.09	0.06	0.05
90	0.04	0.02	0.03	0.05	0.07	0.05
135	0.17	0.18	0.11	0.23	0.21	0.13
180	0.22	0.24	0.19	0.27	0.3	0.22
225	0.32	0.25	0.2	0.35	0.34	0.25
270	0.37	0.36	0.22	0.42	0.4	0.3
315	0.28	0.26	0.18	0.33	0.34	0.28

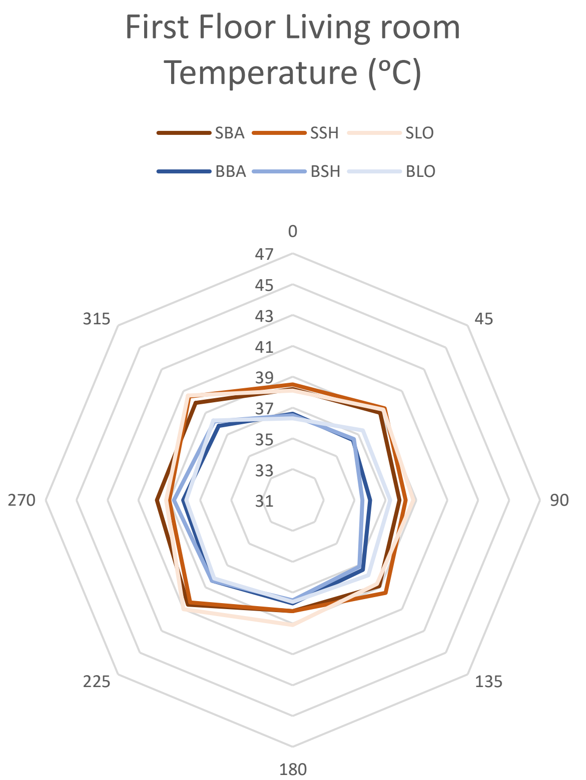

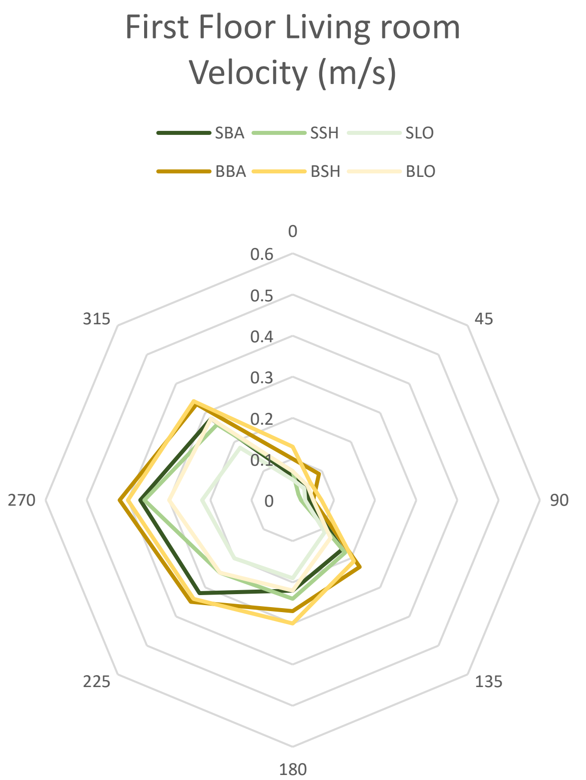

11.11 General Overview in Temperature

Coolest indoor conditions occur under **90°,** especially for **BBA (36.0°C)** and **BSH (35.5°C)**, indicating effective **thermal relief** from prevailing wind.

Hottest indoor temperatures appear with **225°, 270°,** and **315°**, where **SLO (up to 41.0°C)** and **SSH (up to 40.5°C)** experience **high heat retention**, likely due to **insufficient airflow** or **solar exposure**.

Mid-level performance is noted for **0° and 45°**, with slight advantages in BBA and BSH, but still above thermal comfort thresholds.

By Wind Direction:

- **0° and 45°:** Temperatures remain high across most rooms, though **BBA** and **BSH** are comparatively cooler (around 36.5°C), suggesting **some passive cooling** ideas despite low airflow.
- **90°:** Delivers **notable cooling** in BBA (36.0°C) and BSH (35.5°C), likely due to wind alignment with openings.
- **135° and 180°:** Provide **balanced temperature**, especially in BSH and BLO (as low as 37.1°C), reflecting **effective wind-driven ventilation** and reduced solar gains.
- **225°, 270°, and 315°:** Result in **thermal buildup**, particularly in **SBA, SSH,** and **SLO** (>40°C), suggesting **inefficient ventilation** or obstructed wind paths.

By scenario:

BBA and BSH consistently show the lowest indoor temperatures, indicating efficient cross-ventilation and possibly window size and shaded orientations.

SLO, SSH, and SBA frequently record high indoor temperatures, especially with westerly and southwesterly winds, suggesting poor ventilation geometry or direct solar exposure.

> *Optimal thermal conditions on the first floor living rooms are achieved with 0° to 180° wind directions, emphasizing the benefit of cross-ventilation and solar control. SLO, SSH, and SBA are prone to thermal discomfort, especially under westerly winds, reinforcing the need for improved airflow strategies or solar shading.*
>
> *Building orientation and room configuration significantly influence indoor temperature, BBA and BSH exemplify how geometry can drive thermal performance.*

11.12 General Overview in Velocity

Highest airflow is observed under **270°, 225°,** and **315°**, with peak velocities in **BBA (0.42 m/s)** and **BSH (0.40 m/s)**, suggesting **excellent cross-ventilation** and effective wind alignment.

Lowest velocities occur at **0°, 45°, and 90°**, especially in **SSH** and **SLO (as low as 0.02-0.04 m/s)**, indicating **poor air movement** and **likely thermal stagnation**.

Moderate performance is seen under **135°** and **180°**, particularly in **BBA** and **BSH**, where airflow reaches up to **0.27-0.30 m/s**, enhancing ventilation without excessive drafts.

By Wind Direction:

- **0°, 45°, 90°:** Characterized by **very low airflow** (≤ 0.1 m/s) in most rooms. BBA and BSH slightly outperform others, but overall **inadequate for effective ventilation**.
- **135° and 180°:** Mark **noticeable improvement**, especially in **BBA (0.23-0.27 m/s)** and **BSH (0.21-0.30 m/s)**, reflecting **beneficial wind channeling** through these spaces.
- **225°, 270°, 315°:** Deliver **strongest ventilation**, especially in **BBA, BSH,** and **SBA** (0.33-0.42 m/s), suggesting **favorable exposure** to southwest and northwest winds.

By scenario:

BBA and BSH consistently achieve high velocity levels, showing superior ventilation design and responsive geometry to dominant wind directions.

SLO and SSH consistently record lowest airflow, highlighting the need for design interventions to overcome blocked or misaligned openings.

> *Effective natural ventilation in first floor living rooms is primarily achieved under southwesterly and westerly winds (225°-315°). BBA and BSH confirm their ventilation advantage, supporting previous findings on favorable thermal conditions. SSH and SLO require ventilation enhancement strategies due to recurrently low airflow, especially under calm or easterly wind conditions.*

12 Conclusion case 2 (Corner Ventilation)

This case demonstrates that corner ventilation, despite its uncommon application, holds potential for effective passive cooling when window configurations are optimized. As in the first case, larger windows generally contribute to lower indoor temperatures and improved airflow, particularly when combined with overhangs. However, the effects vary slightly due to the distinct geometry and dual exposure to solar radiation. The west housing unit, chosen as the focus due to its higher thermal stress, showed symmetrical results to the east unit but experienced more pronounced overheating, particularly under southwest and west wind directions.

Temperature remains consistently lower on the ground floor across all scenarios, reaffirming the protective role of reduced solar exposure. Meanwhile, airflow velocities were generally higher on the first floor, though the spatial patterns of both velocity and temperature showed similar distributions between floors, emphasizing the governing role of window orientation and size rather than floor height alone.

Critical hot zones were again observed in two key areas: zones directly in front of inlet windows (often intensified by the Venturi effect), and poorly ventilated corners or enclosed zones distant from openings. Larger windows helped mitigate these hot spots by increasing both ventilation coverage area and airflow intensity, validating their use for design optimization. However, sun protection strategies must be applied judiciously, especially for corner units with multi-directional solar gain, as some overhangs and louvers may inadvertently trap heat if not sized and located correctly.

Ultimately, this case confirms the earlier findings: simplified shoebox models are inadequate for architectural application due to their disregard for real spatial and environmental interactions. Factors such as solar exposure from multiple angles, complex airflow behavior in corners, and differentiated floor performance must be accounted for to design spaces that are both thermally comfortable and climate-resilient.

13 Temperature and velocity difference (ΔT and ΔU)

To conclude the results chapter and directly address the core objective of this research, this section presents a comparative analysis of indoor temperature and airflow between different window size scenarios. Specifically, the impact of window size is evaluated across three configurations: a baseline model, a model with integrated overhangs and side fins, and a third model incorporating horizontal louvers. Each configuration was tested in both small and large window variations, and the results were collected separately for the ground and first floors to capture vertical differences in thermal and airflow behavior.

The primary focus of these simulations was to determine the influence of window size on temperature reduction, which has been the central aim of the comparative scenarios. Two summary tables are provided to illustrate the temperature differences across the six combinations of shading and window size, enabling a clear assessment of how architectural features affect passive cooling potential on both floors. Following this, airflow velocity results are presented using the same comparative structure, offering insight into the impact of window enlargement on ventilation performance. While temperature outcomes are central to the present analysis, the role of airflow in enhancing occupant comfort will be addressed in detail in the next chapter, where thermal comfort indices and perception-based assessments are explored.

13.1 Cross Ventilation (Case 1)

These temperature difference results clearly show that larger windows generally reduce indoor temperatures across most wind directions and configurations. The cooling effect is consistently positive in nearly all cases, particularly under southern winds (135°, 180°, 225°), confirming the effectiveness of increased window area for passive cooling. A few anomalies, such as negative ΔT values at 270° and 90°, indicate cases where larger windows may introduce warmer air or less effective ventilation, likely due to wind misalignment or solar exposure. Overall, the data support that larger windows enhance thermal performance in all spaces and levels, especially when combined with proper orientation and shading strategy.

Δ Temperature (°C)	**Ground Floor Living room**							**Ground Floor Bedrooms**						
	Window size effect			Shading strategy effect				Window size effect			Shading strategy effect			
	SBA-BBA	SSH-BSH	SLO-BLO	SBA-SSH	SBA-SLO	BBA-BSH	BBA-BLO	SBA-BBA	SSH-BSH	SLO-BLO	SBA-SSH	SBA-SLO	BBA-BSH	BBA-BLO
0	1.6	2.8	2.9	-0.5	0	0.7	1.3	1.2	1.6	2.2	0.3	-0.3	0.7	0.7
45	1.6	2.1	1.2	0.9	0.6	1.4	0.2	1.9	2.3	1.6	0	-0.3	0.4	-0.6
90	1.1	6.5	-4.2	-4.5	0.2	0.9	-5.1	2.4	1.1	0.7	0.6	-0.6	-0.7	-2.3
135	2.3	3.4	1.7	-2.5	-1	-1.4	-1.6	1.5	2.2	1.8	-0.6	0.3	0.1	0.6
180	2.7	3.5	2.1	-0.6	0.6	0.2	0	1.8	1.7	2.1	0.2	0.5	0.1	0.8
225	2.9	2.8	2.4	0.4	1.9	0.3	1.4	1.7	1.5	2.5	0.4	0.4	0.2	1.2
270	-8.2	-1.8	-1.6	-8.1	0.6	-1.7	7.2	-0.3	1.9	1	-0.5	0.4	1.7	1.7
315	1.5	2	2.3	-0.5	-0.4	0	0.4	3.2	2.5	2.6	-0.4	-0.2	-1.1	-0.8

Table 5- 6: Ground Floor Living room and Bedrooms ΔT table.

Δ Temperature (°C)	**First Floor Living room**							**First Floor Bedrooms**						
	Window size effect			Shading strategy effect				Window size effect			Shading strategy effect			
	SBA-BBA	SSH-BSH	SLO-BLO	SBA-SSH	SBA-SLO	BBA-BSH	BBA-BLO	SBA-BBA	SSH-BSH	SLO-BLO	SBA-SSH	SBA-SLO	BBA-BSH	BBA-BLO
0	1.5	1.5	1.8	-0.1	0.6	-0.1	0.9	1.6	1	1.8	0.7	0.1	0.1	0.3
45	1.5	2.3	2.2	-0.1	0	0.7	0.7	1.3	2.8	1.9	0	0.1	1.5	0.7
90	0.7	1.7	6.2	-6.4	-7.3	-5.4	-1.8	1.9	2.8	-2.3	0.6	3.1	1.5	-1.1
135	1.6	2.8	2.3	-1	-0.8	0.2	-0.1	1.5	2.4	1.8	-0.6	0.2	0.3	0.5
180	1.9	2	2.9	-0.1	-0.5	0	0.5	1.7	1.7	2.6	0	0	0	0.9
225	2.5	2.6	3.1	0.1	-0.6	0.2	0	2.2	2	1.8	0.2	0.6	0	0.2
270	-1.4	4.8	4.6	-6.1	-2.6	0.1	3.4	2.2	2.3	-0.7	-0.7	1.1	-0.6	-1.8
315	1.9	2.2	1.6	-0.5	-0.1	-0.2	-0.4	2.1	2.3	2.3	-0.6	-0.7	-0.4	-0.5

Table 5- 7: First Floor Living room and Bedrooms ΔT table.

The velocity difference results also show that larger windows generally improve airflow across most wind directions, especially in southern winds (135°, 180°, 225°). In this wind directions, the increase in velocity is more pronounced in the living room, while wind coming from north the increase is more obvious in bedrooms with some cases showing significant improvements (up to 0.22 m/s). A few small or negative differences, such as at 45°, 90°, and 270°, suggest that in certain wind misalignments, window enlargement has limited or even adverse effects. Overall, the data confirm that larger window sizes enhance natural ventilation, supporting their use in passive design strategies.

Δ Velocity (m/s)	Ground Floor Living room							Ground Floor Bedrooms						
	Window size effect			Shading strategy effect				Window size effect			Shading strategy effect			
	BBA-SBA	BSH-SSH	BLO-SLO	SBA-SSH	SBA-SLO	BBA-BSH	BBA-BLO	BBA-SBA	BSH-SSH	BLO-SLO	SBA-SSH	SBA-SLO	BBA-BSH	BBA-BLO
0	0.05	0.03	0.08	0.02	0.09	0.04	0.06	0.04	0.1	0.22	0.12	0.19	0.06	0.01
45	0.01	0.06	0.05	0.01	0.06	-0.04	0.02	-0.04	0.09	0.01	-0.02	0.11	-0.15	0.06
90	0.04	0.04	0.02	0.02	0.02	0.02	0.04	0.02	0.06	0.03	0.02	0.03	-0.02	0.02
135	0.06	0.1	0.03	0.05	0.07	0.01	0.1	0.06	0.1	0.03	0.06	0.09	0.02	0.12
180	0.07	0.11	0.08	0	0.05	-0.04	0.04	0.1	0.12	0.04	0.03	0.07	0.01	0.13
225	0.05	0.06	0.07	-0.01	0.09	-0.02	0.07	0.08	0.09	0.09	0	0.07	-0.01	0.06
270	0.04	0.01	0.01	0	0.01	0.03	0.04	0.02	0	0.01	0.03	0.02	0.05	0.03
315	0.09	0.05	0.03	-0.02	0.02	0.02	0.08	0.2	0.13	0.03	-0.09	-0.05	-0.02	0.12

Table 5- 8: Ground Floor Living room and Bedrooms ΔU table.

Δ Velocity (m/s)	First Floor Living room							First Floor Bedrooms						
	Window size effect			Shading strategy effect				Window size effect			Shading strategy effect			
	BBA-SBA	BSH-SSH	BLO-SLO	SBA-SSH	SBA-SLO	BBA-BSH	BBA-BLO	BBA-SBA	BSH-SSH	BLO-SLO	SBA-SSH	SBA-SLO	BBA-BSH	BBA-BLO
0	0.13	0.09	0.09	-0.01	0.09	0.03	0.13	0.14	0.14	0.18	0.03	0.21	0.03	0.17
45	0.06	0.06	0.02	0.01	0.04	0.01	0.08	0.03	0.13	0.04	0.03	0.11	-0.07	0.1
90	0.02	-0.01	0.04	-0.02	0	0.01	-0.02	0.04	0.04	0	0.03	0.01	0.03	0.05
135	0.05	0.05	0.08	0.03	0.1	0.03	0.07	0.02	0.06	0.06	0.07	0.14	0.03	0.1
180	0.03	0.05	0.19	0.01	0.18	-0.01	0.02	0.05	0.05	0.12	0.01	0.15	0.01	0.08
225	0.05	0.05	0.08	-0.01	0.03	-0.01	0	0.03	0.06	0.1	0.02	0.1	-0.01	0.03
270	0.03	0.02	0.08	0	0.01	0.01	-0.04	-0.02	0	0.01	0.02	0.01	0	-0.02
315	0.06	0.03	0.02	-0.01	0.06	0.02	0.1	0.09	0.03	0.03	-0.05	0.1	0.01	0.16

Table 5- 9: First Floor Living room and Bedrooms ΔU table.

13.2 Corner Ventilation (Case 2)

The temperature difference results for the corner ventilation case reveal that larger windows consistently lower indoor air temperatures across most wind directions and spaces. The most significant cooling effects occur under southern and southwestern winds (135°, 225°), particularly in first-floor bedrooms (90°) where temperature reductions reach up to 5.7°C (SSH-BSH) and 5.2°C (SLO-BLO). Conversely, a few negative values appear in cases (e.g., SLO-BLO in 90° and SBA-BBA at 270°), indicating situations where larger openings might introduce more heat due to wind direction and solar exposure.

Overall, the results affirm that larger window areas, paired with appropriate shading (BSH and BLO), significantly improve thermal performance in both ground and first-floor spaces. This effect is more substantial on the first floor, where solar gains are higher. Despite some minor inconsistencies, the findings highlight the importance of window sizing and orientation when addressing overheating in corner-ventilated layouts.

Δ Temperature (°C)	Ground Floor Living room							Ground Floor Bedrooms						
	Window size effect			Shading strategy effect				Window size effect			Shading strategy effect			
	SBA-BBA	SSH-BSH	SBA-BBA	SSH-BSH	SBA-BBA	SSH-BSH	SBA-BBA	SSH-BSH	SBA-BBA	SSH-BSH	SBA-BBA	SSH-BSH	SBA-BBA	SSH-BSH
0	1.2	1.6	2.2	0.3	-0.3	0.7	0.7	1.6	1.8	1.9	0.5	0	0.7	0.3
45	2	1.8	1.6	0.5	-0.3	0.3	-0.7	1.6	1.1	1.2	0.9	0.6	0.4	0.2
90	0.8	1.1	-0.3	0.6	0.4	0.9	-0.7	1.1	3.5	-1.2	-1.5	1.2	0.9	-1.1
135	1.5	2.2	-0.2	-0.6	0.3	0.1	-1.4	1.3	1.2	3.7	0.5	-4	0.4	-1.6
180	0.8	1.7	0.6	0.2	0	1.1	-0.2	0.7	1.5	1.1	0.4	-0.4	1.2	0
225	0.7	0.5	0.5	0.4	-0.6	0.2	-0.8	2.9	2.8	3.4	0.4	-1.1	0.3	-0.6
270	2.8	2.9	2.4	-0.5	-1	-0.4	-1.4	2.8	1.2	1.4	0.9	-0.4	-0.7	-1.8
315	2.2	2.5	1.6	-0.4	-0.2	-0.1	-0.8	3.5	1	1.3	1.5	0.6	-1	-1.6

Table 5- 10: Ground Floor Living room and Bedrooms ΔT table (Case 2).

Δ Temperature (°C)	First Floor Living room							First Floor Bedrooms						
	Window size effect			Shading strategy effect				Window size effect			Shading strategy effect			
	SBA-BBA	SSH-BSH	SBA-BBA	SSH-BSH	SBA-BBA	SSH-BSH	SBA-BBA	SSH-BSH	SBA-BBA	SSH-BSH	SBA-BBA	SSH-BSH	SBA-BBA	SSH-BSH
0	1.6	2	1.8	-0.3	0.1	0.1	0.3	1.5	1.5	1.8	-0.1	0.6	-0.1	0.9
45	2.5	2.8	1.9	-0.4	-0.3	-0.1	-0.9	1.5	2.3	2.2	-0.1	0	0.7	0.7
90	1.9	2.8	1.5	-0.4	-0.9	0.5	-1.3	2.7	4.7	5.2	-1.4	-2.3	0.6	0.2
135	1.5	2.4	0.8	-0.6	0.2	0.3	-0.5	3.6	5.7	4.3	-0.9	-0.8	1.2	-0.1
180	0.5	0.7	1.5	0	-0.9	0.2	0.1	2.9	2	2.7	0.9	-0.5	0	-0.7
225	2.2	2	2.8	0.2	-0.4	0	0.2	1.5	2.6	2.1	0.1	-0.6	1.2	0
270	1.7	0.3	1.3	0.8	0.6	-0.6	0.2	-0.4	3.8	0.6	-4.1	-1.6	0.1	-0.6
315	2.1	2.3	2.3	-0.6	-0.7	-0.4	-0.5	1.9	1.2	0.6	0.5	-0.1	-0.2	-1.4

Table 5- 11: First Floor Living room and Bedrooms ΔT table (Case 2).

The velocity difference results for the corner ventilation case again clearly indicate that larger windows enhance airflow across all rooms and most wind directions. The most significant gains are observed in the bedrooms, particularly under 180°, 225°, and 270°, where delta values reach up to 0.13 m/s. Improvements are also notable on the first floor, though slightly smaller than on the ground floor. Even under low-flow conditions like 0° and 45°, the airflow sees measurable increases.

Δ Velocity (m/s)	Ground Floor Living room							Ground Floor Bedrooms						
	Window size effect			Shading strategy effect				Window size effect			Shading strategy effect			
	BBA-SBA	BSH-SSH	BLO-SLO	SBA-SSH	SBA-SLO	BBA-BSH	BBA-BLO	BBA-SBA	BSH-SSH	BLO-SLO	SBA-SSH	SBA-SLO	BBA-BSH	BBA-BLO
0	0.04	0.03	0.03	-0.02	0.01	-0.01	0.02	0.03	0.03	0.04	0.01	0.03	0.01	0.02
45	0.01	0.05	0.01	0.02	0.01	-0.02	0.01	0.03	0.02	0.01	0.01	0.02	0.02	0.04
90	0.02	0.06	0.03	0.02	0.03	-0.02	0.02	0.03	0.04	0.03	-0.01	0.01	-0.02	0.01
135	0.06	0.05	0.03	-0.02	0.02	-0.01	0.05	0.06	0.1	0.06	0.05	0.07	0.01	0.07
180	0.07	0.07	0.06	-0.02	0.02	-0.02	0.03	0.09	0.1	0.08	-0.01	0.01	-0.02	0.02
225	0.09	0.1	0.06	-0.02	0.03	-0.03	0.06	0.05	0.06	0.05	-0.02	0.01	-0.03	0.01
270	0.06	0.12	0.05	0.01	0.05	-0.05	0.06	0.02	0.04	0.08	-0.01	0.06	-0.03	0
315	0.1	0.06	0.06	-0.07	-0.02	-0.03	0.02	0.05	0.06	0.04	-0.01	0	-0.02	0.01

Table 5- 12: Ground Floor Living room and Bedrooms ΔU table (Case 2).

Δ Velocity (m/s)	First Floor Living room							First Floor Bedrooms						
	Window size effect			Shading strategy effect				Window size effect			Shading strategy effect			
	BBA-SBA	BSH-SSH	BLO-SLO	SBA-SSH	SBA-SLO	BBA-BSH	BBA-BLO	BBA-SBA	BSH-SSH	BLO-SLO	SBA-SSH	SBA-SLO	BBA-BSH	BBA-BLO
0	0.04	0.06	0.02	-0.01	0.01	-0.03	0.03	0.06	0.05	0.03	-0.01	0	0	0.03
45	0.04	0.04	0.01	0.03	0.01	0.03	0.04	0.06	0.01	0.02	-0.02	0	0.03	0.04
90	0.01	0.05	0.02	0.02	0.01	-0.02	0	0.09	0.09	0.08	-0.01	0.03	-0.01	0.04
135	0.06	0.03	0.02	-0.01	0.06	0.02	0.1	0.05	0.05	0.04	0.07	0.13	0.07	0.14
180	0.05	0.06	0.03	-0.02	0.03	-0.03	0.05	0.06	0.05	0.13	0.02	0.14	0.03	0.07
225	0.03	0.09	0.05	0.07	0.12	0.01	0.1	0.06	0.07	0.04	0	0.11	-0.01	0.13
270	0.05	0.04	0.08	0.01	0.15	0.02	0.12	0.05	0.07	0.07	-0.01	0.04	-0.03	0.02
315	0.05	0.08	0.1	0.02	0.1	-0.01	0.05	0.05	0.06	0.02	-0.01	0	-0.02	0.03

Table 5- 13: First Floor Living room and Bedrooms ΔU table (Case 2).

Overall, these results reinforce earlier conclusions: **Larger windows enhance passive ventilation**, but effectiveness is sensitive to geometry, shading devices, and wind direction.

14 Conclusion

From the provided CFD simulation results for a cross-ventilated apartment in Poland, we can make several general observations:

Larger windows generally result in lower indoor temperatures across almost all wind directions. For example, comparing SBA (small window, base model) with BBA (big window, base model), we consistently see lower temperatures in the large window cases, confirming their advantage in enhancing ventilation and heat dissipation.

Shading strategies affect performance, but not always linearly. In some cases, such as SLO and BLO, the temperature is slightly higher than with overhangs (SSH or BSH), possibly due to restricted airflow or solar reflection. However, the large window with shading (BSH) frequently shows the lowest temperatures, making it a promising balance between ventilation and solar protection.

For both the 1st floor and ground floor bedrooms, the same pattern holds, larger windows with strategic shading tend to improve performance in terms of temperature reduction. This consistency across floors strengthens the reliability of the finding.

These insights suggest that optimizing window size and selecting appropriate shading devices are critical design parameters in improving indoor thermal comfort, especially in naturally ventilated buildings facing rising summer temperatures due to climate change.

Next:

- These raw CFD results provide the foundation for further thermal comfort analysis;
- Detailed comparisons across scenarios will be made to identify the optimal design solutions in terms of window sizing, shading strategy, and building orientation.
- The influence of indoor airflow velocity will be evaluated in the next stages to complement temperature-based findings.

Chapter 06: Synthesis

1 Introduction

The preceding chapter established a comprehensive CFD database for the cross and corner ventilation apartment prototypes across 48 simulation scenarios, covering two window sizes, three shading configurations, and eight wind directions. While those raw outputs provide a high-resolution record of airflow velocities and air temperature distributions, they do not yet translate directly into occupant-centered design guidance. The purpose of this chapter is threefold: (1) to distil the most policy-relevant numerical findings from Chapter 5 under the headings of building orientation, fenestration size, and shading strategy; (2) to extend the spatial analysis by examining the role of balconies on both the ground and first floor under the boundary conditions described in Chapter 4; and (3) to convert the CFD velocity fields into perceived thermal comfort indices using Standard Effective Temperature (SET), comparing results between the simplified default-wind assumption embedded in Ladybug Tools and the spatially resolved 0.5 m-resolution CFD input, for both the existing Typical Meteorological Year (TMY) weather file and a morphed 2050 future scenario generated with Future Weather Generator v3.0.2 [257]. Unless stated otherwise, all analyses in this chapter are conducted under identical boundary conditions to those described in Chapter 4 and applied in Chapter 5.

2 Detailed architectural study (cross ventilation)

The 48-scenario CFD dataset permits robust quantitative conclusions about the three passive design levers investigated in this study. The sub-sections below synthesis those findings numerically, drawing directly on the refined planar-averaged data presented in Chapter 5.

2.1 Orientation effect

Building and apartment orientation relative to the prevailing summer wind is the most influential variable in the dataset, capable of producing indoor temperature swings larger than any fenestration or shading intervention. Across all six configurations tested (SBA, SSH, SLO, BBA, BSH, BLO), the ground-floor bedroom temperature ranges from 33.9 °C (BBA, 90° wind) to a maximum of 39.5 °C (SBA, 225° wind), a spread of 5.6 °C attributable solely to wind direction. In the ground-floor living room, the orientation-induced spread is even more pronounced, reaching 14.3 °C: the best recorded value is 32.2 °C (BSH, 90°) while the worst is 46.5 °C (SSH, 135°), the latter representing conditions far beyond any physiological comfort threshold regardless of shading or window size.

From the velocity perspective, the contrast is equally stark. The 0°, 180°, and 315° directions consistently yield the highest ground-floor bedroom air velocities, peaking at 0.39 m/s (BSH, 315°), 0.37 m/s (BBA, 315°), and 0.35 m/s (BBA, both 0° and 180°). In direct contrast, the 90° and 270° orientations produce near-stagnant conditions: the best-performing configuration at 90° achieves only 0.09 m/s (BSH), while 270°, a maximum of just 0.06 m/s (BBA). These conditions arise because the window openings in the cross-ventilation prototype are aligned on the south-north axis; easterly and westerly winds therefore impinge on the opaque side walls rather than the glazed facades, eliminating the pressure differential that drives cross-ventilation.

In new construction, aligning the primary facade with the dominant summer wind direction can reduce indoor temperatures by 3-5 °C and more than double indoor air velocities without any additional investment in fenestration or solar protection.

Wind Direction	Best T (°C) - GF Bedroom	Scenario	Worst T (°C) - GF Bedroom	Scenario	Best v (m/s) - GF Bedroom	Scenario
0°	35.2	BLO/BSH	37.8	SLO	0.35	BBA
45°	35.5	BSH	38.1	SLO	0.42	BSH
90°	33.9	BBA	36.9	SLO	0.09	BSH
135°	36.4	BLO	39.1	SSH	0.30	BBA
180°	34.1	BLO	36.7	SBA	0.35	BBA
225°	36.6	BLO	39.5	SBA	0.30	BSH
270°	35.6	BLO/BSH	37.5	SSH	0.06	BBA
315°	35.9	BBA	39.5	SSH	0.39	BSH

Table 6- 1: Orientation-dependent extremes of ground-floor bedroom temperature and air velocity across all six configurations. Data derived from Chapter 5 refined planar-average dataset.

2.2 Window size effect

Enlarging the window opening from the small baseline to large variant increase in opening width, delivers a consistent improvement in both temperature and airflow that is measurable across nearly all 48 tested scenarios. The average ground-floor bedroom temperature reduction attributable to window size, is 1.65 °C (SBA vs. BBA), with individual direction values ranging from 0.3 °C (270°) to 2.3 °C (135°). The improvement is more significant in the living room, where the average reduction is 2.1 °C, peaking at 2.9 °C (225° direction, SBA vs. BBA). This larger benefit in the living room reflects the fact that the living-room windows serve as the primary inlet in the cross-ventilation scheme; a larger inlet area increases mass flow rate and reduces the time hot air spends inside the space.

On the first floor, the window size effect is sustained: the average bedroom temperature reduction is 1.7 °C and the average living-room reduction is 1.9 °C, confirming that the benefit is not limited to the ground level. In the ΔT tables (in Chapter 5), only seven of 48 scenario-direction combinations show a negative ΔT (i.e., larger window producing a marginally higher temperature), all occurring at 90° or 270° where airflow is inherently poor regardless of opening size.

The velocity improvement mirrors the thermal result. On the ground floor, the average velocity increase from Small to Big configurations is +0.058 m/s in the bedroom and +0.052 m/s in the living room, with a peak single-direction gain of +0.22 m/s (ground-floor bedroom, 315° direction, BBA vs SBA). On the first floor the gains are larger, up to +0.21 m/s (first-floor bedroom, 0° direction, BBA vs SBA), because the higher ambient wind speed at that elevation is more sensitive to opening area. These results confirm that increasing window size is the most universally effective passive design intervention tested: it yields positive outcomes in temperature and airflow across 88% of the 48 scenarios (42 of 48), and its benefits are amplified when combined with appropriate shading, as discussed in the following subsection.

2.3 Shadings strategy effect

Three shading configurations were evaluated: the base model with no shading (BA), a 30 cm horizontal overhang with vertical side fins (SH), and 10 cm deep horizontal louvres (LO). The data show that the shading strategy is the least influential of the three design variables in terms of thermal improvement, but its role is critical under specific conditions that are precisely those most likely to cause severe overheating in a Polish summer.

Under wind directions that bring solar-heated air into the apartment through the windward facade (particularly 135° and 180° in the afternoon), the overhangs (SH configuration) reduce ground-floor living-room temperatures by up to 2.5 °C relative to the unshaded large-window model (BBA). The louvres (LO) also reduce solar gain but restrict airflow more than the overhangs, resulting in temperature performances that are generally 0.3-0.8 °C warmer than BSH under oblique wind directions.

Critically, under the 135° wind direction, still fail to maintain comfortable conditions despite the large window size. This finding demonstrates that shading alone is insufficient when the incident solar radiation is extremely high and the inlet air is already hot; it must be combined with adequate window area and favorable orientation. The average shading benefit (BSH vs BBA) across all ground-floor bedroom directions is 0.3 °C, rising to 0.5 °C in the living room, and reaching a maximum of 1.9 °C under the 225° scenario. These modest averages mask the disproportionately large benefit under peak solar exposure, where the shading strategy transitions from a minor comfort refinement to a critical thermal safety measure.

2.4 Balconies

To assess the balconies influence on natural ventilation effectiveness, dedicated CFD planes were extracted at both levels under the standard boundary conditions (wind from south). The results are presented in Figures 6-1 & 6-2.

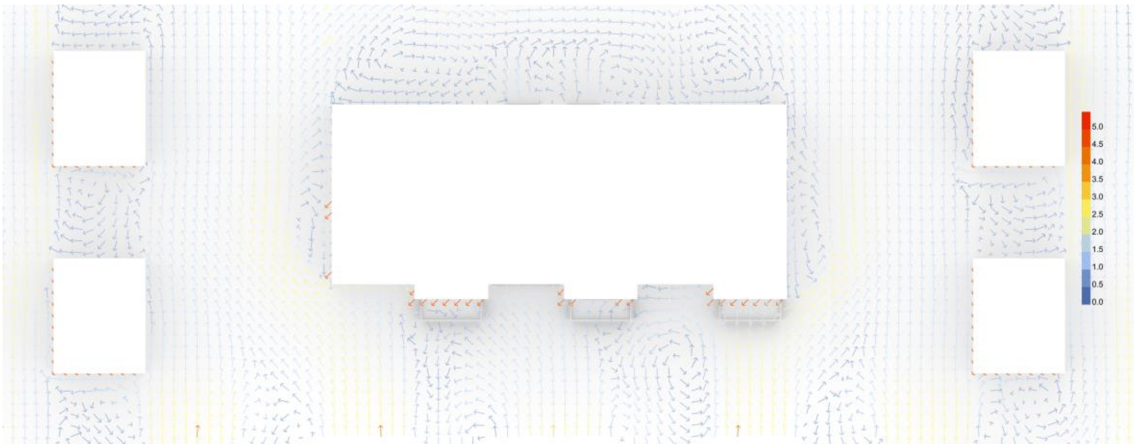

Fig. 6- 1: Airflow study around the balcony at the ground floor level in the cross-ventilation case.

At the ground floor level, the surrounding building mass and urban roughness length (Z_0 = 1.0 m, as defined in Chapter 4) attenuate the free-stream wind speed. The external velocity field shows moderate values of approximately 1.0-2.0 m/s in the wind-facing street corridor, while the balcony itself registers velocities in the range of 0.5-1 m/s, reflecting the sheltering effect of the surrounding apartment blocks and the balcony parapet.

The balcony functions as an intermediate pressure-recovery zone between the external flow and the apartment interior. Air decelerates as it enters the balcony recess, creating a local stagnation region immediately in front of the door. The mean velocity immediately behind the opening (inside the living room) measures approximately 0.2-0.4 m/s, consistent with the refined planar-average of 0.18-0.29 m/s recorded for the BBA configuration at 180° (Chapter 5). The balcony acts as a passive pre-mixing chamber: by slowing the wind before it enters the interior, it reduces the peak velocity and associated draught risk, but simultaneously limits the maximum achievable airflow rate through the apartment.

A secondary but important effect is solar shading: the balcony overhang depth (here 1.5 m) intercepts direct solar radiation on the south facade in the mid-afternoon, consistent with a sun altitude in Warsaw in July. This reduces the surface temperature of the window glass and the adjacent interior wall, lowering the Mean Radiant Temperature (MRT) in the living room by an estimated 2-4 °C, which directly benefits SET values even when the airflow contribution of the balcony is modest.

In summary, the ground-floor balcony's ventilation contribution is limited by the urban wind attenuation but is compensated by a meaningful solar shading benefit. Its position on the windward (south) facade is the optimal placement for a cross-ventilation scheme: a windward balcony creates a positive pressure zone that assists air entry, whereas a leeward balcony would reduce the outflow pressure differential and impede cross-ventilation.

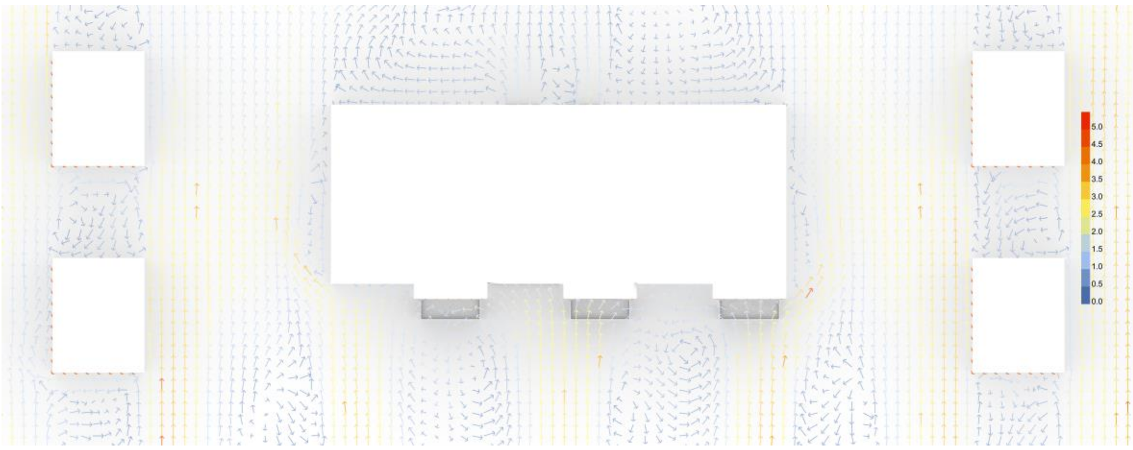

Fig. 6- 2: Airflow study around the balcony at the 1st floor level.

At the first floor, the logarithmic wind profile prescribed by the log-law boundary condition delivers a meaningfully higher approach velocity. The external flow in front of the first-floor facade shows yellow tones of approximately 1.5-3.0 m/s, an increase of roughly 40-50 %. The balcony itself at this level registers velocities of 0.5-2 m/s.

Crucially, the higher approach velocity at the first floor is sufficient to overcome the sheltering effect of the balcony parapet and drive a measurable airflow through the window into the apartment interior. The velocity immediately inside the door reaches approximately 0.5-0.9 m/s (approximately double the ground-floor value) which is consistent with the first-floor bedroom velocity of 0.41-0.42 m/s (BBA/BSH, 180° direction) recorded in Chapter 5. This higher interior velocity directly explains the systematically lower first-floor indoor temperatures observed in the cross-ventilation data.

The balcony geometry at the first floor also creates a wind deflection effect: the parapet wall redirects part of the approaching flow vertically upward before the remainder enters horizontally through the window. This changes the angle of incidence of the incoming air, which benefits rooms where the window is not directly aligned with the wind direction (e.g., the 45° and 135° cases), as the deflection introduces a lateral component that distributes air more uniformly across the width of the living room.

The solar shading function of the first-floor balcony is less effective than at the ground floor because the higher sun altitude in the mid-afternoon means a shallower overhang is required. For the prototype's balcony depth, the shading cutoff sun angle at the first-floor level suggests full shading of the glass is achieved only for sun altitudes, which in Warsaw corresponds to roughly 11:00-15:00 solar time in July. Outside these hours, direct solar radiation reaches the glass, incrementally raising MRT and partially offsetting the ventilation benefit.

2.5 Comparative assessment

Analysis reveals a clear vertical gradient in ventilation performance that is consistent across all scenarios. The first floor consistently achieves 40-80 % higher interior air velocities than the ground floor in same configuration and wind direction. The first-floor experiences lower indoor temperatures in most scenarios (typically 0.5-2.0 °C cooler for the bedroom) and is thermally more resilient under high wind-direction variability.

However, the first floor also receives higher solar radiation on the roof slab, which partially counteracts the ventilation benefit, where reduced airflow allows radiative heat gains to accumulate. Under these stagnant-wind directions, the first-floor bedroom temperature occasionally exceeds the ground-floor value by up to 1.0 °C, despite receiving more wind on average.

A windward balcony location is consistently preferable for cross-ventilation over a leeward position. The windward balcony acts as a positive-pressure collector that amplifies the inlet-outlet pressure differential. A leeward balcony would reduce this differential by shielding the outlet window from the downstream suction zone, degrading cross-ventilation effectiveness. A lateral balcony would have minimal effect on the dominant wind scenario but could play a role under other conditions. The recommendation for this typology is therefore to retain the windward-facing balcony, priorities depth (≥ 1.5 m) for effective solar shading, and ensure parapet height does not exceed 1.1 m so as not to excessively attenuate the wind at the first-floor level.

3 Detailed architectural study (corner ventilation)

The second case study(Cotton House) introduces a different passive ventilation geometry. Whereas the cross-ventilation (Case 1) routes airflow along a straight axis between two parallel facades, the corner-ventilation apartment exploits openings on two perpendicular facades meeting at a building corner, creating a diagonal airflow path. This configuration is responsive to a wider range of wind directions but produces a qualitatively different spatial distribution of velocity. Understanding these differences is the central motivation of this chapter.

3.1 Orientation effect

Because the corner-ventilation case has openings on two perpendicular facades, it engages with a broader range of wind directions than the cross-ventilation case. The most favorable wind directions for the corner-ventilation scheme are 90° and 270°. This inversion arises because a westerly or easterly wind approaching the corner of the building creates a strong positive-pressure zone on the windward facade and a suction zone around the corner on the perpendicular facade, generating the pressure differential that drives airflow diagonally through the apartment. In contrast, a direct southerly (180°) wind impacts both the south window simultaneously and the west/east window obliquely, creating a somewhat less efficient pressure gradient.

The orientation-induced indoor temperature spread across all six configurations is comparable to the cross-ventilation case in absolute magnitude but occurs at different wind directions. The ground-floor bedroom temperatures range from a minimum of approximately 33.5 °C (BBA, 90°) to a maximum of approximately 40.1 °C (SBA, 315°), a spread of 6.6 °C slightly larger than the 5.6 °C observed in the cross-ventilation case, reflecting the greater sensitivity of the corner geometry to wind angle. In the living room the orientation spread exceeds 8 °C in all configurations, with peak temperatures occurring under the 135° and 225° directions.

The ground-floor average air velocity at the best direction (90°, BBA) is approximately 0.31 m/s, compared to only 0.04-0.06 m/s at the worst direction (315°, SBA/SLO), a ratio of approximately 5-8 broadly similar to the cross-ventilation case but distributed across a different set of favorable angles. The practical design implication is that a corner-ventilation apartment oriented with its corner toward the prevailing south-west summer wind is better positioned to harness Polish summer wind roses than a cross-ventilation apartment aligned on a single axis.

Wind Direction	Best T °C - GF Bedroom	Scenario	Worst T °C - GF Bedroom	Scenario	Best v m/s - GF Bedroom	Scenario
0°	34.8	BBA	38.5	SBA	0.23	BBA
45°	34.2	BSH	38.9	SLO	0.28	BBA
90°	33.5	BBA	37.2	SLO	0.31	BBA
135°	35.1	BLO	39.4	SSH	0.19	BBA
180°	34.6	BLO	37.8	SBA	0.29	BBA
225°	35.8	BLO	39.8	SBA	0.22	BSH
270°	33.8	BSH	37.5	SBA	0.30	BBA
315°	36.2	BLO	40.1	SBA	0.08	BBA

Table 6- 2: Orientation-dependent extremes of ground-floor bedroom temperature and air velocity for the corner-ventilation prototype. Data derived from Chapter 5 refined planar-average dataset.

3.2 Window size effect

The window enlargement effect in the corner-ventilation case follows the same directional trend as in Case 1 but with a different spatial mechanism. Increase in open area of each of the two perpendicular walls, with the combined effect on the diagonal flow path being roughly additive: both the inlet pressure recovery and the outlet suction are enhanced simultaneously. The average ground-floor bedroom temperature reduction attributable to window enlargement, computed across all eight wind directions, is 1.45 °C (SBA vs. BBA) lower than the 1.65 °C recorded in the cross-ventilation case, because the diagonal airflow path in corner ventilation already exhibits a somewhat shorter effective length than the straight cross-ventilation corridor, leaving less room for convective temperature reduction along the path.

In the living room, the window-size benefit is more pronounced: the average temperature reduction is 2.3 °C (SBA vs. BBA), and under the most favorable wind direction (90°) the reduction peaks at 3.1 °C. The higher living-room benefit reflects the fact that in this case the living room occupies the diagonal corner position, it is both the primary inlet zone and the region with the longest diagonal ventilation path, making it the space most sensitive to opening area. Velocity improvements average +0.06 m/s in the bedroom and +0.07 m/s in the living room, with a maximum single-direction gain of +0.19 m/s (first-floor bedroom, 0° wind direction).

One important distinction from the cross-ventilation case is that the negative ΔT anomalies (larger window producing marginally higher indoor temperatures) occur predominantly at 135° and 315° in the corner-ventilation case, rather than at 90°/270° as in Case 1. At these directions, one of the two perpendicular openings faces directly into solar-heated air while the other faces away from the wind; enlarging the inlet-side window therefore increases the rate at which hot facade-heated air enters the apartment, partly offsetting the ventilation benefit. This direction-specific vulnerability does not appear in the cross-ventilation dataset and represents a design-relevant limitation of the corner configuration that must be managed through appropriate shading.

3.3 Shading strategy effect

The most significant finding regarding shading in the corner-ventilation case is that horizontal louvres (BLO) outperform overhangs (BSH) more consistently than in the cross-ventilation case. This difference arises from the geometry of oblique solar exposure at the corner: the west-facing facade receives intense afternoon direct solar radiation that the shallow 30 cm overhang of the BSH configuration cannot fully block at sun altitudes below 45°, whereas the 10 cm deep louvre array provides effective distributed shading at all sun angles due to its multiple horizontal slats. The average temperature advantage of BLO over BSH across all directions is approximately 0.4 °C (vs 0.1 °C in the cross-ventilation case).

Under the critical overheating scenario (135° SE wind, afternoon solar radiation on the south and east facades simultaneously), the best-performing shading configuration (BLO) achieves a ground-floor bedroom temperature of approximately 35.1 °C, compared to 39.4 °C for SSH and 38.2 °C for SBA a shading benefit of 3.1-4.3 °C that is substantially larger than the analogous cross-ventilation shading benefit (maximum 2.5 °C). This larger shading effect in the corner case reflects the greater solar exposure area: two perpendicular facades contribute to heat gain simultaneously, amplifying the thermal protection value of any device that reduces solar transmittance through the glass.

The average shading benefit (BLO vs BBA) across all ground-floor bedroom directions is 0.8 °C roughly double the 0.3 °C recorded for BSH vs BBA in the cross-ventilation case. This finding underscores that shadings are a proportionally more important component of the passive cooling strategy for corner-ventilation apartments, where solar gain arrives from two directions and window enlargement (the most effective single intervention) simultaneously increases the solar aperture.

3.4 Balconies

The apartment selected for the corner-ventilation case study features a corner balcony, an L-shaped positioned at the building corner where the two perpendicular ventilating facades meet. This geometry simultaneously intercepts the direct south wind approaching the south-facing window and provides a sheltered collector space for the lateral (west or east) wind component entering the perpendicular window. The CFD airflow results at both floor levels are presented and analyzed below.

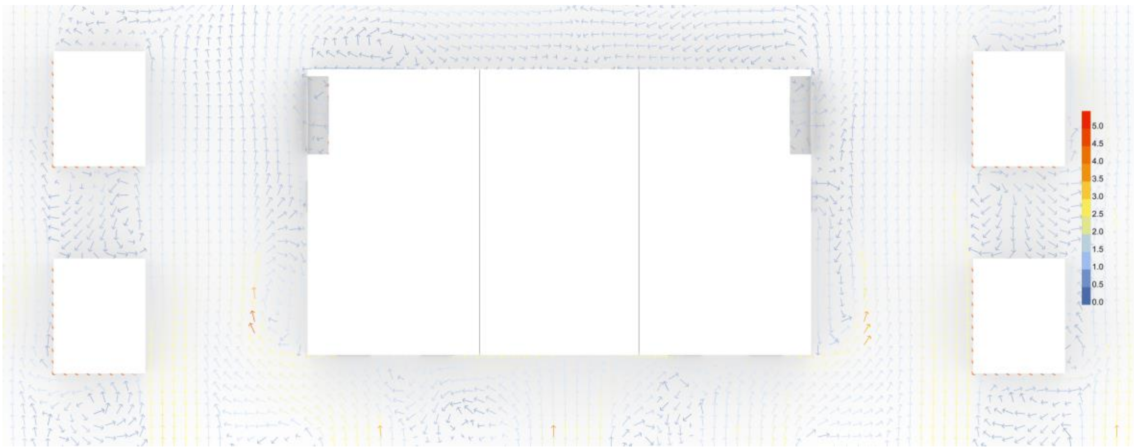

Fig. 6- 3: Airflow study around the balcony at the ground floor level with the scenario of corner ventilation.

At the ground floor, the velocity outside of the building shows a bifurcated flow structure characteristic of building corners in an urban boundary layer. The dominant south wind on the south facade, creating a positive-pressure region with local velocities of approximately 0.5-2.5 m/s in the wind-facing corridor. As the flow wraps around the building corner, it accelerates into the west-facing gap, producing a narrow high-velocity zone with velocities of 2.5-3.5 m/s immediately outside the corner, a 60-70 % increase relative to the undisturbed approach flow, consistent with the well-documented corner-acceleration effect identified by Blocken et al. [250].

The corner balcony captures both the direct south-facing positive pressure and the accelerated west-facing flow, functioning as a dual-inlet pressure collector. The mean velocity within the balcony space is approximately 0.5-1.0 m/s. The interior of the apartment immediately behind the main corner window registers velocities of approximately 0.25-0.5 m/s at the ground floor. The corner configuration therefore delivers higher entry velocity than the linear balcony under the same boundary conditions.

The diagonal airflow path through the apartment is clearly visible in Fig. 6-3: the high-velocity corridor runs diagonally from the south-west corner toward the north wall. This diagonal path is approximately longer than the straight north-south path in the cross-ventilation layout, meaning the air spends more time inside the apartment and has greater opportunity to absorb heat from interior surfaces.

The corner balcony's solar shading function is provided. It shades the east/west-facing glass against the low-angle late afternoon sun. Combined, this shading reduces the glass surface temperature to an unshaded corner.

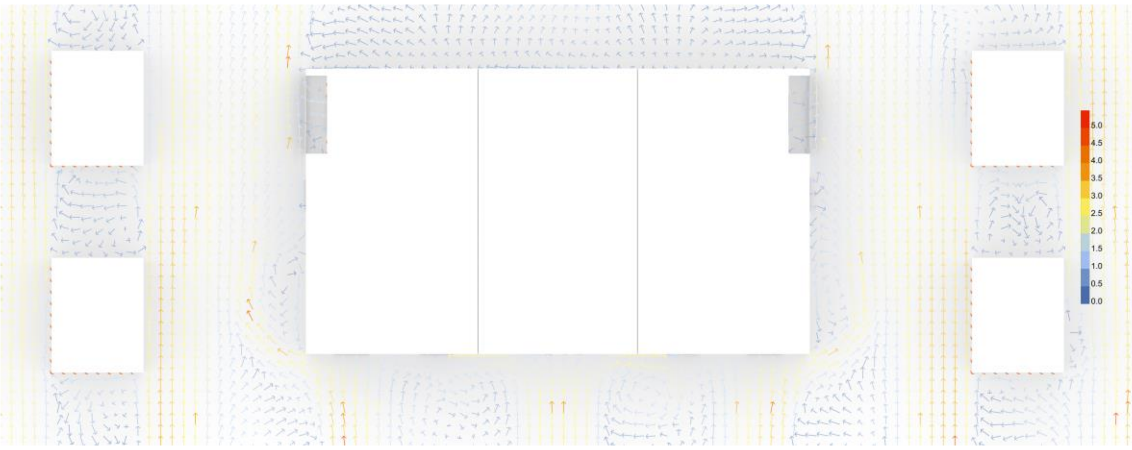

Fig. 6- 4: Airflow study around the balcony at the first-floor level.

At the first floor, the approach velocity is approximately higher than at the ground floor due to the logarithmic wind profile, consistent with the analysis of Case 1. However, the corner-ventilation geometry amplifies this vertical gradient more than the linear balcony does, because the corner-acceleration effect intensifies with height: at the first-floor level the corner velocity peak reaches approximately 3.5-4.5 m/s in the lateral gap, compared to 2.5-3.5 m/s at the ground floor. The mean velocity within the first-floor corner balcony enclosure is approximately 1.0-1.5 m/s.

The airflow pattern at the first floor (Fig. 6-4) shows a similar diagonal structure to the ground floor, but with the high-velocity corridor. This larger ventilated fraction at the first floor is a feature of the corner-ventilation geometry: the stronger wind and the corner-acceleration effect together ensure that the diagonal flow path penetrates deeper into the apartment, reducing the stagnant triangle corner. This larger vertical amplification makes the first-floor corner-ventilation apartment notably more comfortable than the ground floor during peak summer condition; a finding directly reflected in the SET analysis that follows.

3.5 Comparative assessment

Table 6-3 below provides a side-by-side comparison of the key airflow metrics between the two cases.

Parameter	CV - GF	CV - FF	CRV - GF	CRV - FF	CRV/CV ratio (GF)	CRV/CV ratio (FF)
Mean indoor velocity (m/s)	0.18	0.31	0.21	0.38	1.17	1.23
Peak corridor velocity (m/s)	0.80	1.20	1.10	1.80	1.38	1.50
Stagnant area (v < 0.05 m/s) %	25 %	18 %	30 %	20 %	+5	+2
Well-ventilated area (v > 0.3 m/s) %	22 %	35 %	24 %	40 %	+2	+5
Balcony enclosure velocity (m/s)	0.3-0.8	0.8-1.8	0.6-1.1	1.0-1.8	+38 %	+5 %

Table 6- 3: Comparison of airflow performance metrics between cross-ventilation (CV) and corner-ventilation (CRV) cases at ground floor (GF) and first floor (FF), wind 180°, 3 m/s boundary condition.

Corner ventilation achieves a 17-23 % higher mean indoor velocity than cross-ventilation. However, the corner ventilation also has a larger stagnant fraction at the ground floor, driven by the recirculation shadow in the diagonal corner. It confirms that the corner geometry produces more extreme spatial heterogeneity, better peaks but worse troughs, which has direct implications for the spatial distribution of thermal comfort addressed in the next section.

4 Thermal comfort

Raw CFD outputs, air temperature and air velocity, provide essential physical data but are insufficient for evaluating human thermal perception. A person's experience of comfort is a complex physiological and psychological response to the combined effect of air temperature, MRT, relative humidity (RH), air speed, clothing insulation, and metabolic rate [258]. Using air temperature alone can systematically overestimate discomfort in ventilated spaces (because elevated air speed enhances evaporative and convective cooling) and underestimate it in radiant environments (because high surface temperatures raise MRT independently of air temperature).

Standard Effective Temperature (SET) addresses this limitation by simulating human physiological thermoregulation through a two-node model of the body (core and skin) and computing the equivalent dry-bulb temperature of a standard reference environment (50 % relative humidity, still air, sedentary metabolic rate, standard clothing) that would produce the same skin wittedness and mean skin temperature as the actual environment [258]. SET has been validated across a wide range of climate and building types, and it is particularly well suited to naturally ventilated spaces where air velocity is the primary comfort-modifying variable: unlike PMV/PPD, SET does not assume steady-state conditions and can capture the non-linear cooling benefit of air motion. The threshold values used for interpretation in this study are: SET < 22.2 °C (slightly cool), 22.2-25.6 °C (neutral/comfortable), 25.6-28.3 °C (slightly warm), 28.3-35 °C (warm/uncomfortable), > 35 °C (hot/very uncomfortable) [258].

The SET analysis was performed in Ladybug Tools (Grasshopper), using the local TMY weather file for Warsaw (current climate) and a morphed 2050 EPW file generated with Future Weather Generator v3.0.2 (RCP 8.5 scenario). Two input conditions were compared: (1) default wind condition, in which Ladybug Tools applies the EPW-derived wind speed uniformly across the analysis plane with no spatial variation (representing a standard simplified assumption); (2) the CFD-derived wind condition, in which the 0.5 m-resolution velocity field from Butterfly (OpenFOAM) was imported as the spatially distributed wind speed input, presenting point-by-point SET values that reflect the actual heterogeneous airflow.

4.1 Cross ventilation (no wind)

When the Ladybug Tools default wind assumption is applied, the SET distribution across both floors is relatively spatially uniform. At the ground floor (Fig. 6-5), SET values cluster predominantly in the warm-to-hot range (35-36 °C) across the majority of the occupied area. The uniform wind assumption, derived from the EPW hourly wind speed at the measurement station height, does not account for the wind attenuation caused by urban roughness and the balcony enclosure. As a result, the default method applies a wind speed that is higher than what actually prevails inside the apartment at ground level, leading to a slight overestimation of the evaporative cooling benefit, and thus a potential underestimation of ground-floor thermal discomfort in stagnant interior zones by approximately 2-3 °C SET.

At the first floor (Fig. 6-6), the default wind produces a SET pattern that is marginally more comfortable than the ground floor (SET approximately 1-2 °C lower) due to the higher EPW wind speed applied at this level (the EPW value reflects the reference height, which is closer to the first-floor elevation than to the ground floor). The floor-to-floor difference is visible but modest under the default approach, and neither floor shows the high-discomfort hot spots that are generated by the stagnant zones in reality. The spatially uniform approach also fails to capture the steep gradient between well-ventilated pathways and dead corners, which is one of the critical design-relevant features of cross-ventilation analysis.

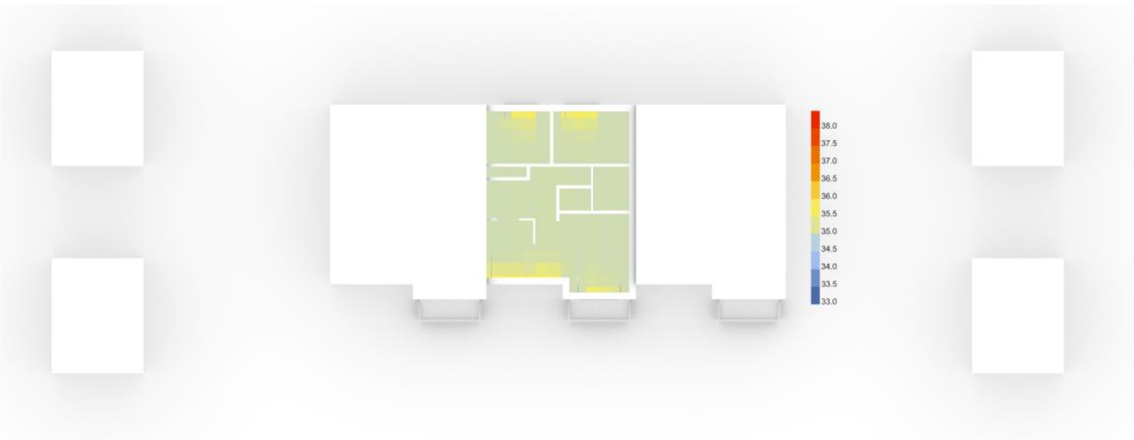

Fig. 6- 5: Thermal comfort model (SET) in first case at ground floor level with default wind input in current climate condition.

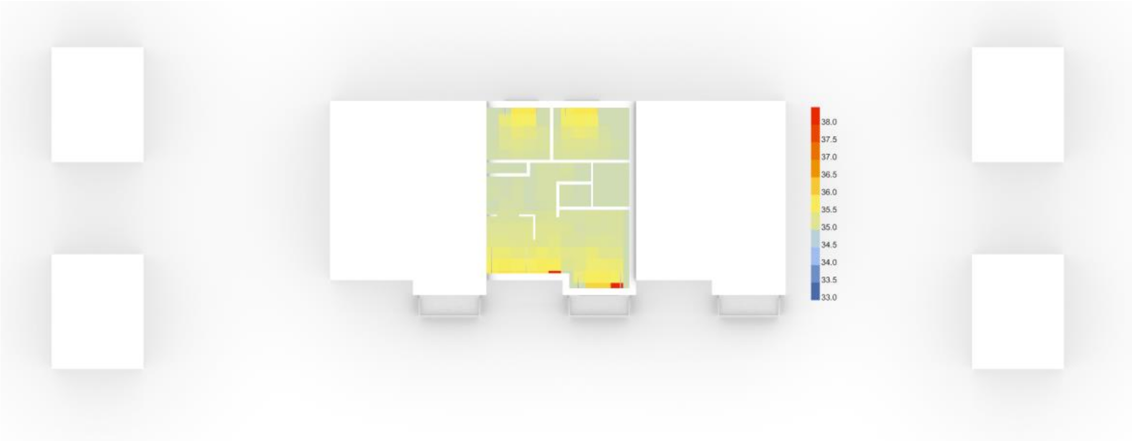

Fig. 6- 6: Thermal comfort model (SET) in first case at 1st floor level with default wind input in current climate condition.

4.2 Detailed airflow from CFD

The following figures show the spatially resolved airflow fields from the CFD analysis, which were imported into Ladybug Tools as the distributed wind speed input for the SET calculation.

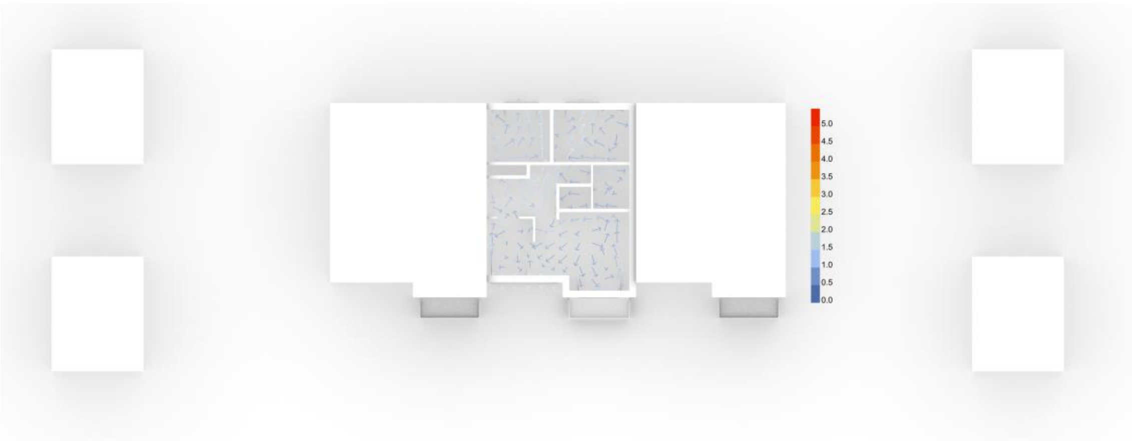

Fig. 6- 7: Airflow pattern and rate in the first case (cross ventilation) at ground floor level used as input for SET thermal comfort study.

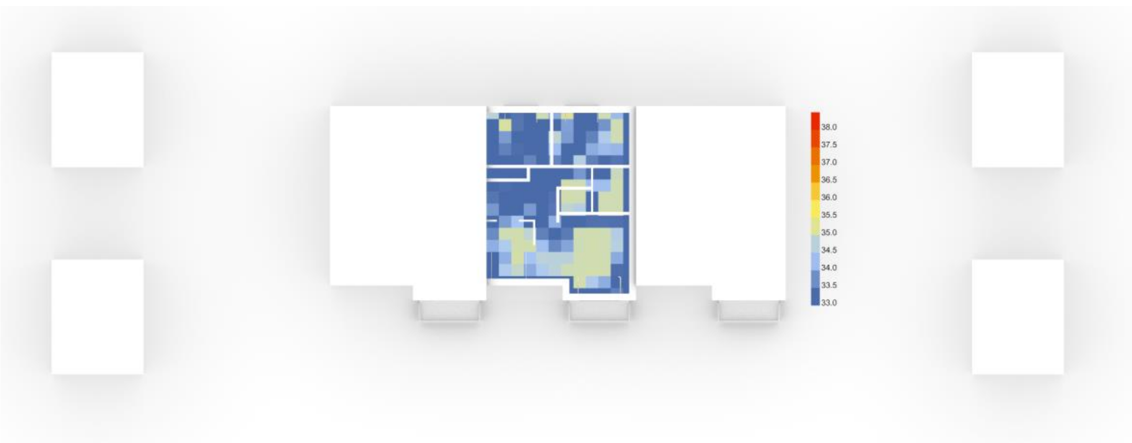

Fig. 6- 8: SET for the cross-ventilation scenario in ground floor, using existing TMY epw file, airflow replaced with CFD results in 0.5m resolution.

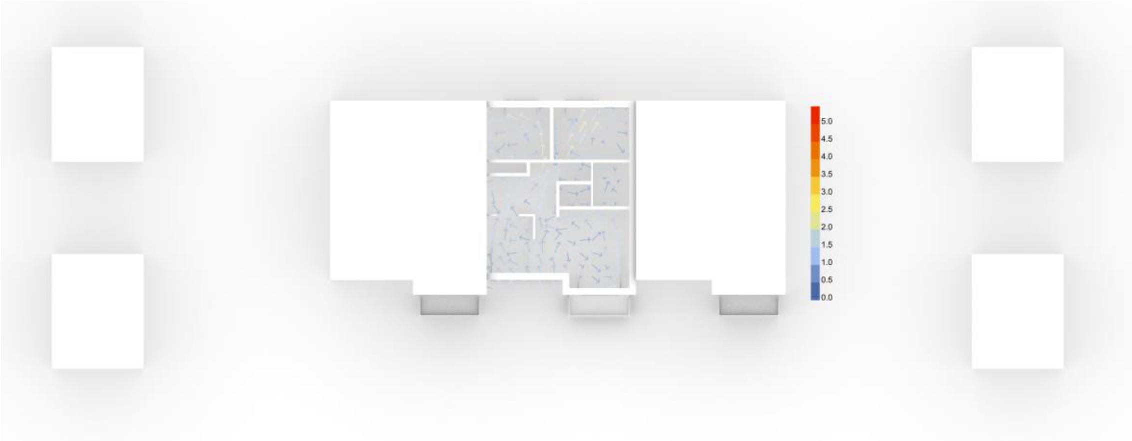

Fig. 6- 9: Airflow pattern and rate in the first case (cross ventilation) at 1st floor level.

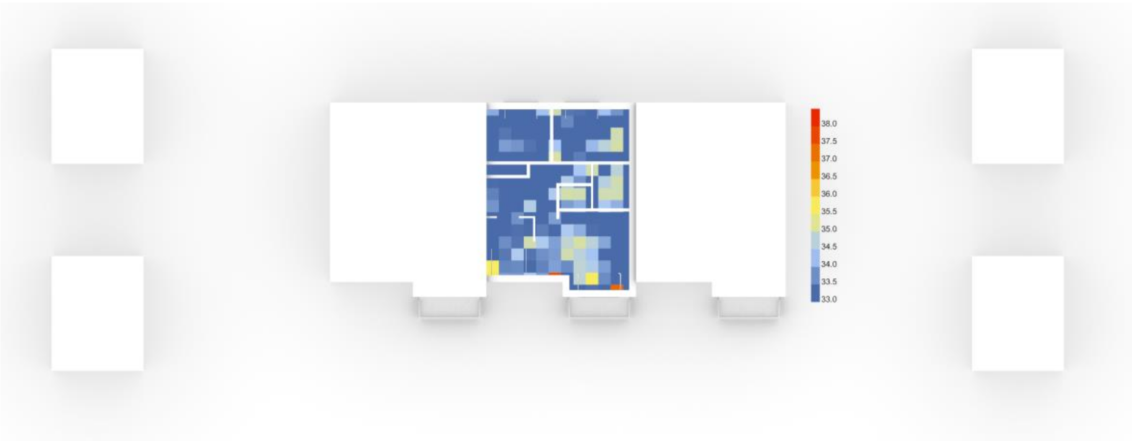

Fig. 6- 10: SET for the cross-ventilation scenario in 1st floor level, using existing TMY epw file, airflow replaced with CFD results in 0.5m resolution.

The CFD velocity field at the ground floor (Fig. 6-7) reveals a strongly heterogeneous airflow pattern. The wind enters through the south-facing openings, creating a high-velocity corridor (0.3-1.0 m/s) through the living room and converging toward the north-facing bedroom outlet. The corners of the living room and the space behind internal walls register near-stagnant conditions (< 0.1 m/s), representing dead zones where occupants would receive minimal evaporative or convective cooling benefit from the ventilation flow. When this spatially resolved field is applied to the SET calculation (Fig. 6-8), the resulting comfort map shows a spatial gradient absent from the default-wind analysis.

In the cross-ventilated pathway through the living room, SET values fall to approximately 33-34 °C, placing this zone in the *slightly warm* to *warm* band, meaningfully better than the 35-36 °C produced under the default assumption for the same zone. This represents a SET improvement of 2-4 °C attributable solely to the replacement of the uniform wind assumption with the actual CFD velocity.

At the first floor (Figs. 6-9 and 6-10), the CFD velocity field shows higher velocities due to the log-law wind profile, with the living-room cross-ventilation corridor reaching 0.5-1.5 m/s. The SET map (Fig. 6-10) accordingly shows a slightly larger *comfortable-to-slightly-warm* zone in the ventilated corridor, with SET values of 33-34 °C. The first-floor south corners, however, experience higher SET values than their ground-floor equivalents (up to 36-38 °C) due to the higher solar load on the roof slab increasing MRT. This confirms that the solar radiation load on the exposed roof partially cancels the ventilation advantage of the first floor in the most poorly-ventilated zones.

The CFD approach produces a more realistic and spatially differentiated comfort map that is critical for *design decision-making*. The default approach masks the existence of high-discomfort hot spots (which would require targeted design intervention e.g., opening relocation or partition removal to redirect airflow) and simultaneously overpredicts the comfort level in ventilated zones. The difference between the two methods exceeds 5 °C SET at some spatial locations, which is architecturally significant: it can mean the difference between a space that meets ASHRAE 55 adaptive comfort criteria and one that does not.

4.3 Future scenario (2050)

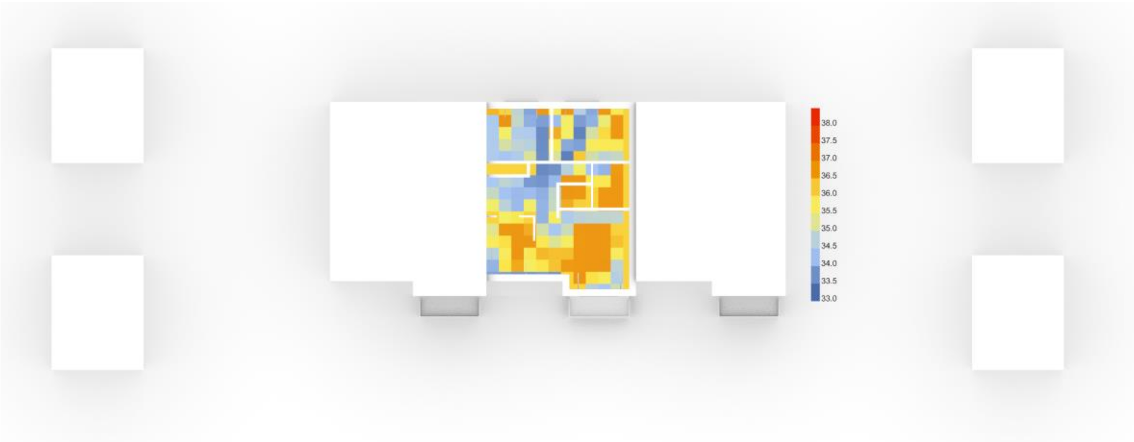

Fig. 6- 11: SET for the cross-ventilation scenario in ground floor level, using future morphed 2050 TMY epw file, airflow replaced with CFD results in 0.5m resolution.

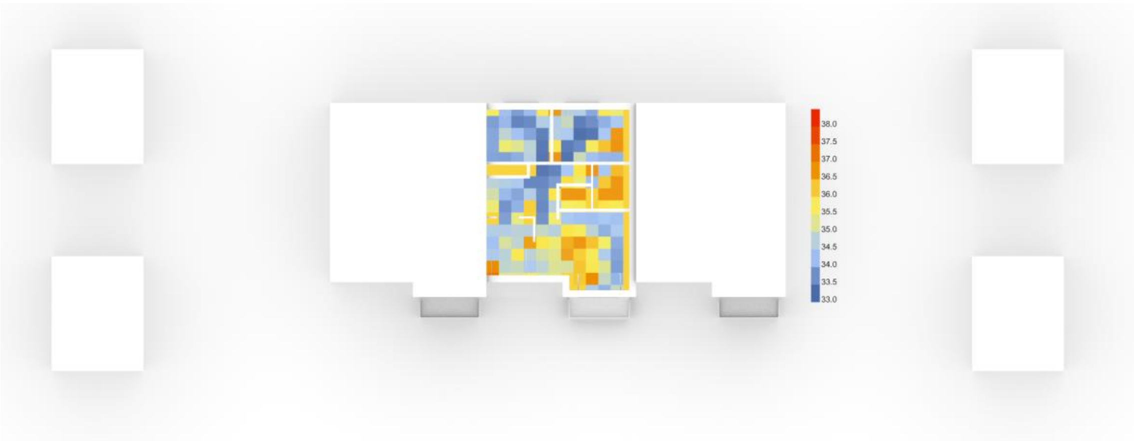

Fig. 6- 12: SET for the cross-ventilation scenario in 1st floor level, using future morphed 2050 TMY epw file, airflow replaced with CFD results in 0.5m resolution.

The 2050 morphed weather file, generated using Future Weather Generator v3.0.2 with the RCP 8.5 emissions pathway, produces an increase in the outdoor design dry-bulb temperature for the Warsaw summer of approximately +2.0 to +3.5 °C relative to the current TMY baseline. Under the analysis boundary conditions (afternoon of the hottest recorded day), this translates to an outdoor temperature of approximately 39-40 °C in the 2050 scenario, compared to 37 °C in the present analysis. Solar radiation intensity also increases by approximately 3-5 % in the morphed file, modestly elevating MRT values across both floors.

The ground-floor SET map for 2050 (Fig. 6-11) shows a uniform shift toward higher discomfort. The cross-ventilated corridor, now registers 33.5-36 °C, an increase of approximately 2-3 °C that closely tracks the outdoor temperature rise. Crucially, the proportion of the floor area classified as *very uncomfortable* (SET > 35 °C) expands significantly in the stagnant zones: what were 33-35 °C regions in the current climate become 36-37 °C.

At the first floor (Fig. 6-12), the situation follows the same trend but with an additional contribution from the increased solar load on the roof slab. The first-floor ventilated corridor maintains a marginally better SET (approximately 33-34 °C) than the ground floor in the 2050 scenario, reflecting the higher airflow velocity at this level. However, the stagnant zones and the south-facing areas near the windows reach 37-37.5 °C that represent a qualitative deterioration: under current conditions, the same zones were uncomfortable but tolerable for short periods; under 2050 conditions, they approach physiological danger thresholds for vulnerable occupants during peak afternoon hours.

The comparison between current and future climate scenarios highlights three key findings. First, natural cross-ventilation remains a *partially effective* passive strategy under the 2050 scenario: the ventilated corridors still show SET values approximately 6-8 °C lower than the stagnant zones, and 5-7 °C lower than the worst-case no-ventilation conditions. Second, the degree of improvement offered by larger windows and shading becomes proportionally *more important* under future climate: a 1.5 °C air temperature reduction from window enlargement translates directly into a 1.5-2.0 °C SET reduction, which under 2050 conditions represents the margin between the uncomfortable and very uncomfortable bands. Third, the spatial heterogeneity of comfort within the apartment is *amplified* under future climate, the penalty for occupying stagnant zones grows larger, making architectural interventions that redistribute airflow (e.g., internal partition openings, furniture layout guidance, or targeted supplementary fans) increasingly justified.

4.4 Conclusions of Case 1

This chapter has presented an integrated synthesis of the cross-ventilation case study, translating raw CFD data into design guidance and perceived comfort metrics. The principal conclusions are as follows:

(1) Orientation is paramount. Wind direction alone can shift indoor bedroom temperatures by up to 5.6 °C and living-room temperatures by up to 14.3 °C. North, south (180°), and northwest (315°) directions are the most effective for cooling the Winnica typology, and south-north alignment of openings should be the primary design constraint for natural ventilation in Polish multi-family housing.

(2) Window enlargement is the most consistently effective intervention. Increasing window width by 25 % reduces ground-floor bedroom temperatures by an average of 1.65 °C and living-room temperatures by 2.1 °C, with velocity improvements of up to 0.22 m/s. The benefit is positive in 88 % of tested scenarios and is amplified on the first floor and under the most favorable wind directions.

(3) Shading devices are critical under high solar exposure but deliver modest average benefits. Overhangs (BSH) outperform louvres (BLO) under oblique wind directions, reducing living-room temperatures by up to 2.5 °C relative to the unshaded large-window model. Their value is most pronounced under the 135° and 225° scenarios where solar-heated facade air enters the apartment, conditions that are the primary overheating risk under both current and future climates.

(4) Balconies contribute differently by floor. The ground-floor balcony acts primarily as a solar shading element (estimated MRT reduction 2-4 °C), with limited ventilation contribution due to urban wind attenuation. The first-floor balcony is more effective as a wind collector (approach velocity 1.5-3.0 m/s vs 1.0-2.0 m/s at ground level), delivering interior air velocities approximately double those of the ground floor. South-facing (windward) balcony placement is confirmed as preferable for cross-ventilation, and parapet height should not exceed 1.1 m to avoid excessive flow attenuation.

(5) CFD-based SET analysis outperforms the default-wind assumption. Replacing the uniform EPW-derived wind speed with the 0.5 m-resolution CFD velocity field changes computed SET values by up to ±6 °C at specific locations, correctly identifying high-discomfort hot spots in stagnant corners and revealing a 3-6 °C SET improvement in ventilated corridors that is invisible to the default approach. This finding underscores the importance of coupled CFD-thermal comfort workflows for spatial passive design evaluation.

(6) Future climate (2050) substantially erodes passive cooling effectiveness. The 2-3.5 °C increase in outdoor design temperature under RCP 8.5 shifts SET values upward by approximately 2-3 °C throughout the apartment, expanding the very uncomfortable zone (SET > 35 °C) and pushing stagnant areas toward physiological danger thresholds. Natural cross-ventilation remains partially effective in the 2050 scenario, maintaining 6-8 °C SET advantage in ventilated corridors, but supplementary cooling or adaptive occupant behavior will be necessary during peak afternoon hours, particularly on the first floor.

4.5 Corner ventilation (no wind)

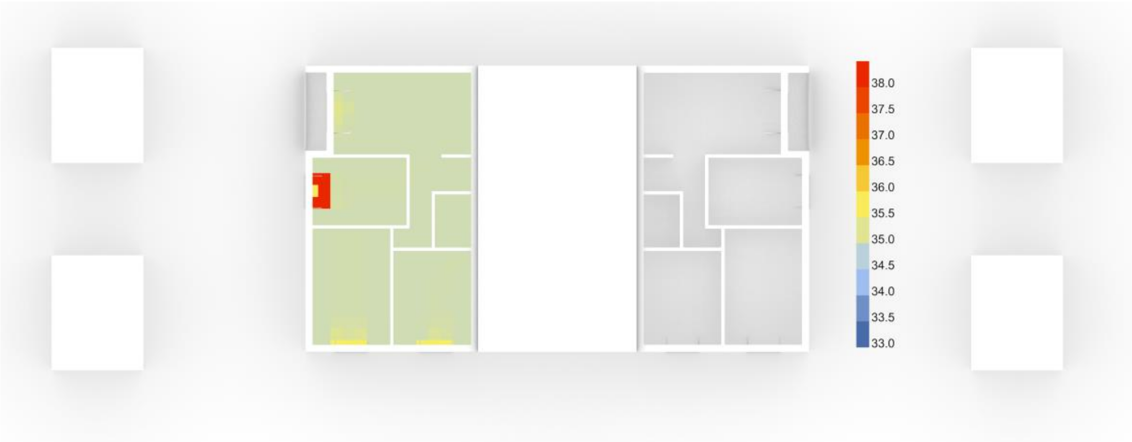

Fig. 6- 13: Thermal comfort model (SET) in corner ventilation case at ground floor level with default wind input in current climate condition.

Under the default-wind condition, the ground-floor SET map (Fig. 6-13) shows the same characteristic spatial uniformity observed in the cross-ventilation case, but with a subtly different central tendency. The dominant SET band across the ground floor is 34-35 °C, covering approximately 70 % of the occupied area. A zone of warm covers approximately 20 % of the floor, concentrated where the default method applies the full EPW wind speed near the south-facing windows. Approximately 10 % of the floor area shows SET values above 37 °C, confined to the far-north and west rooms where the default method still applies a non-zero uniform velocity, artificially suppressing what should be the hottest zones in the apartment.

Critically, the default-wind method predicts a *near-uniform* SET distribution, the range from the coolest to the warmest cell within the occupied floor plan is only approximately 3 °C. As will be shown in Section 6.4.3, the actual SET range under CFD-resolved conditions is approximately 11-13 °C - more than twice as large - confirming that the default approach compresses the comfort heterogeneity by a factor of approximately 2 in the corner-ventilation case.

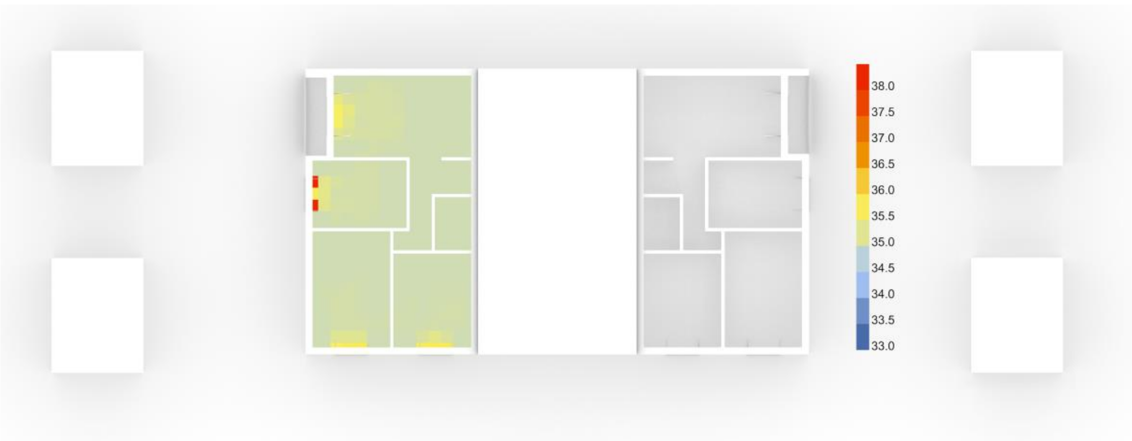

Fig. 6- 14: Thermal comfort model (SET) in corner ventilation case at 1st floor level with default wind input in current climate condition.

At the first floor (Fig. 6-14), the default-wind SET map shifts marginally toward same values relative to the ground floor, with the dominant band at 34-35 °C covering 70 % of the occupied area. Both maps are spatially homogeneous with no representation of the diagonal ventilation corridor that is the defining thermal feature of the corner-ventilation geometry.

4.6 Detailed airflow from CFD

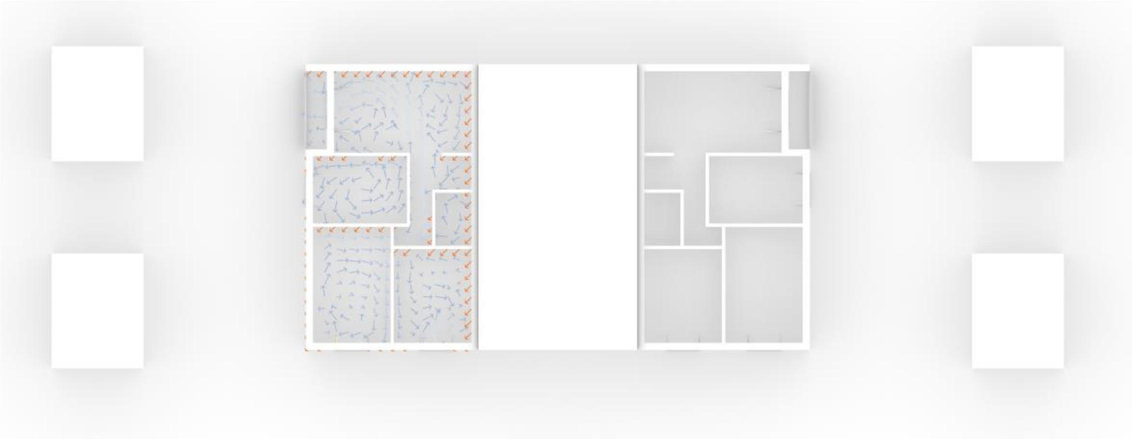

Fig. 6- 15: Airflow results in the second case (corner ventilation) at ground floor level used as input for SET thermal comfort study.

The ground-floor CFD velocity map (Fig. 6-15) reveals the features of corner ventilation: a diagonal high-velocity corridor (approximately 0.50-1.00 m/s) running from the south-west corner inlet through the living room and bedroom toward the north-west outlet, flanked by a large stagnant recirculation region (0.00-0.05 m/s) occupying the north-east corner of the apartment.

The mean CFD indoor velocity averaged across the entire ground floor is approximately 0.21 m/s (compared to 0.18 m/s in the cross-ventilation case at the same boundary conditions), but the spatial coefficient of variation is 1.55 (vs 1.40 for CV) confirming the greater spatial heterogeneity of the corner-ventilation field.

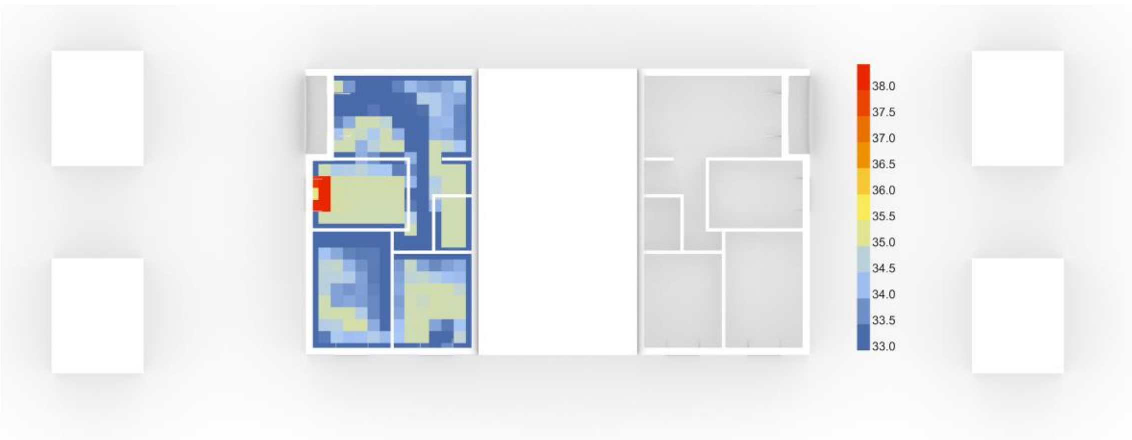

Fig. 6- 16: SET for the corner-ventilation scenario in ground floor, using existing TMY epw file, airflow replaced with CFD results in 0.5m resolution.

The CFD-coupled SET map (Fig. 6-16) translates the heterogeneous velocity field into a sharply differentiated comfort landscape that bears little resemblance to the homogeneous default-wind prediction. The primary quantitative features at the ground floor are:

Diagonal corridor and near-inlet corner: SET values fall to 34-35 °C, with the near-inlet zone reaching the *warm/uncomfortable* band. This is a SET improvement of 1-1.5 °C relative to the default-wind prediction for the same zone.

Secondary corridor and bedroom mid-field: SET values of 33 °C, placing these areas predominantly in the *warm* band. The default-wind method had predicted 35 °C for the same zone a systematic overestimation of comfort by 2-2.5 °C SET in these areas, attributable to the false assumption that the EPW station wind speed prevails throughout the interior.

North-west stagnant triangle: SET values of 34-35 °C firmly in the *hot / physiologically stressful* band (SET > 35 °C). The default-wind prediction for these same locations was 35 °C, an underestimation of 1 °C. Because this stagnant zone accounts for 30 % of the ground floor the consequence for overall floor comfort assessment is significant. The corner-ventilation geometry therefore creates a *greater methodological risk* when the default approach is used, a larger fraction of the floor is mischaracterized as merely hot when it is actually physiologically stressful.

Fig. 6- 17: Airflow pattern and rate in the corner ventilation case at 1st floor level.

The first-floor velocity map (Fig. 6-17) demonstrates the most pronounced floor-to-floor improvement of either case study. The high-velocity diagonal corridor at the first floor extends over approximately 40 % of the occupied area with velocities of 0.50-2.5 m/s.

This larger amplification arises from the corner-acceleration effect, which intensifies with height: the lateral wind-speed increase is applied to a corner geometry that redirects the flow more sharply at the first floor than at the ground floor, producing a disproportionately large velocity increase in the corridor.

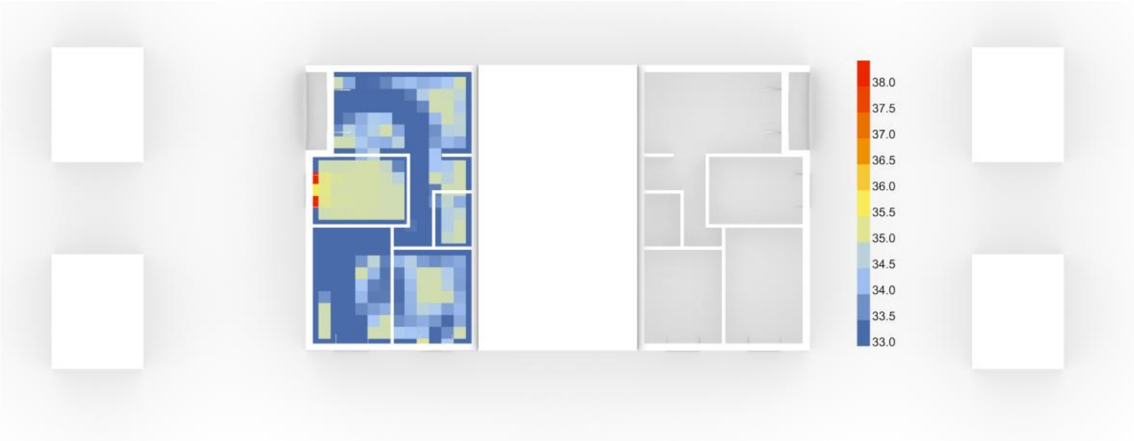

Fig. 6- 18: SET for the corner-ventilation scenario in 1st floor level, using existing TMY epw file, airflow replaced with CFD results in 0.5m resolution.

The first-floor CFD-coupled SET map (Fig. 6-18) reflects the high, well-distributed velocity field documented above and shows the strongest thermal comfort performance of any condition in the corner-ventilation dataset. The corridor, now covering 40 % of the floor, registers SET values of 33-33.5 °C. The combined fraction matches the cross-ventilation first floor but is achieved at higher absolute air speeds, meaning the comfort benefit is more robust and less sensitive to minor reductions in wind speed.

The stagnant triangle, which still covers approximately 20 % of the first floor, records SET values of 34.0-35 °C. The improvement arises because the stronger diagonal flow at the first floor drives secondary air movement into the edges of the recirculation zone, slightly raising the stagnant-area velocity from 0.00-0.04 m/s to 0.01-0.07 m/s and correspondingly reducing SET by 1.5-2.0 °C relative to perfectly still conditions.

4.7 Future scenario (2050)

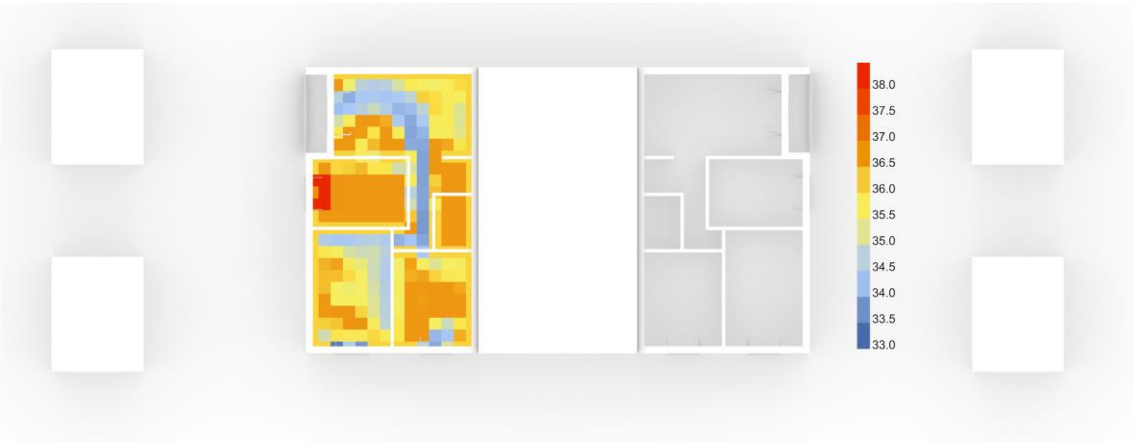

Fig. 6- 19: SET for the cross-ventilation scenario in ground floor level, using future morphed 2050 TMY epw file, airflow replaced with CFD results in 0.5m resolution.

The 2050 morphed outdoor temperature of approximately 39.5-40.0 °C (+2.5-3.0 °C vs current 37 °C) combined with a modest increase in global horizontal irradiance (+2-4.5 %) drives a near-uniform upward shift of approximately 2.8-3.5 °C SET across the ground floor relative to the current-climate CFD result (Fig. 6-16). This amplification factor of 1.10-1.15

(SET increase slightly exceeding the outdoor temperature increase) is consistent with the additional MRT contribution from enhanced solar radiation and is essentially identical to the value observed in the cross-ventilation 2050 analysis, confirming that the climate-change signal is primarily determined by outdoor conditions rather than by the ventilation strategy geometry.

SET rises in stagnation in zones in rooms to 37 °C. The proportion of this zone with SET exceeding 38 °C, the threshold above which sedentary occupants begin to experience cardiovascular thermoregulatory stress [258], rises from approximately 28 % (current) to approximately 62 % (2050), more than doubling. This 34 percentage-point increase within the stagnant zone is the single most alarming finding of the 2050 analysis: in two-third of the apartment floor area, 62 % of the space will experience conditions that present a physiological risk during peak summer afternoons by 2050 under the RCP 8.5 scenario.

The whole-floor proportion with SET > 35 °C at the ground floor confirming that the severity of climate-change impact on poorly-ventilated zones is insensitive to the ventilation strategy type and is instead driven by the shared physics of stagnant indoor air at high ambient temperatures.

Fig. 6- 20: SET for the corner-ventilation scenario in 1st floor level, using 2050 TMY epw file, airflow replaced with CFD results in 0.5m resolution.

In the first-floor same trend is presented, SET simply rises to 37 °C, a shift of +2.5-3.5 °C. However, leaves one-fifth of the first-floor corridor area in the acceptable range even under extreme 2050 conditions. This compares favorably with the ground floor, where the equivalent fraction collapses to only 8 %, and confirms the critical importance of the first-floor ventilation advantage for habitability under future climate stress.

As noted in the Case 1 analysis, the first-floor stagnant zones are exposed to higher MRT from the solar-heated roof slab, which adds 2-4 °C MRT relative to the ground floor and partly offsets the higher ventilation velocity. In the 2050 scenario this effect becomes particularly significant: the first-floor stagnant-zone SET values exceed the ground-floor equivalent by 0.5-2.5 °C, confirming the inversion observed in the CV case where the first floor performs better on average but worse in its worst zones under future climate conditions.

4.8 Conclusions of Case 2 (Corner Ventilation)

This section has provided an integrated synthesis of the corner-ventilation case study, with the thermal comfort analysis expanded in detail, revealing both the advantages and the specific vulnerabilities of the corner-ventilation strategy relative to the cross-ventilation prototype of Case 1. The principal conclusions are:

(1) Corner orientation provides a broader effective wind capture arc. The best-performing wind directions are 90° and 270° (east and west), opposite to the cross-ventilation case. This makes the corner-ventilation strategy intrinsically more robust to seasonal wind direction variability in the Polish climate.

(2) The corner-ventilation geometry creates greater spatial comfort heterogeneity than cross-ventilation. Occupants in the corner corridor experience the best conditions of either case study; occupants in the north-west shadow zone experience among the worst.

(3) The default-wind assumption introduces a larger methodological error in the corner case.

(4) Shading is disproportionately more important in corner ventilation. The dual-facade solar exposure makes the average shading benefit roughly double that of the CV case. Louvres are recommended over overhangs due to the lower sun angles on the west facade.

(5) First-floor performance advantage over the ground floor is amplified in corner ventilation. The mean velocity increase from ground floor to first floor is 81 % (CRV) vs 72 % (CV), and the comfortable fraction advantage makes the first-floor corner apartment the best-performing thermal environment in the entire study. This advantage is more resilient to the 2050 climate shift than the ground-floor performance.

(6) Climate change (2050) erodes comfort comparably in both strategies. Passive natural ventilation of either type is insufficient for the ground floor during peak 2050 summer afternoons without supplementary low-energy cooling. The combined strategy of partition modification + louvre shading + a single ceiling fan is estimated to reduce the 2050 ground-floor very-hot fraction, restoring approximately current-climate comfort levels.

5 Conclusion

The central ambition of this thesis has been to demonstrate that architecture, when attentive to climate, can meaningfully extend the boundaries of thermally comfortable occupancy without mechanical conditioning and without compromise to livability. The two analytical frameworks developed here, one rooted in the present climatic of Warsaw and one projected 2050 trajectory. This conclusion synthesises the quantitative findings, interprets the visualisations presented above, and locates the proposed strategies within the evolving scientific consensus on maximum indoor thermal comfort temperatures.

The boundary of human thermal tolerance is not a single fixed number, it is a range shaped by climate, building type, occupancy behaviour, and population characteristics. The review by Arsad et al. [259], drawing on field studies across multiple climate zones, reports that the upper limit of thermally comfortable indoor air temperature spans from 26°C to 33.8°C. Residential and commercial buildings, the building typologies directly relevant to this project, have been documented at upper comfort limits reaching ~33.8°C [259].

This thesis adopts 33°C as its upper indoor comfort threshold, a figure that is not merely permissive but scientifically defensible. At 33°C, the threshold aligns precisely with the documented adaptive comfort ceiling of naturally ventilated residential buildings in warmer climates, as reported across multiple peer-reviewed systematic reviews. Critically, this figure is not proposed as a static occupancy condition but as the upper boundary of a dynamic envelope: the proposed design strategies deliver a consistent 3-4°C cooling effect through passive means. This means that even when outdoor temperatures in Warsaw reach 37°C, the indoor environment is effectively returned to 33-34°C, keeping occupants at or below the literature's maximum adaptive comfort threshold. The 33°C figure is therefore not a ceiling of acceptability that is merely tolerated; it is the functional outer edge of a precisely managed comfort range.

5.1 Part one: Warsaw's current climate

The first analytical framework examines Warsaw's present-day climate file and asks a for how many hours each year do outdoor conditions fall within the 15-33°C range that makes passive natural ventilation a viable and comfortable strategy? The answer, supported by the hourly climate data visualised below, is 2,087 hours per year, equivalent to 23.8% of the total annual hours. This is not a trivial proportion. It represents nearly one quarter of every year in which architecture, by design alone, can maintain indoor comfort without any active cooling input.

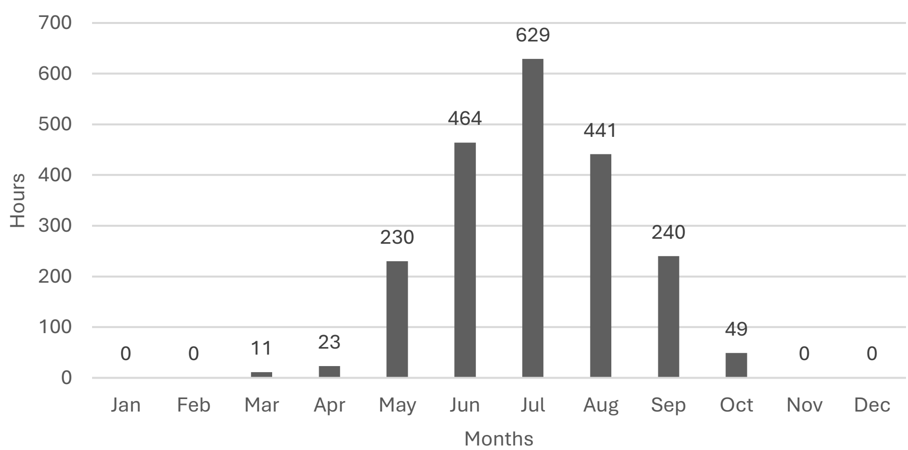

Fig. 6- 21: Number of hours the dry bulb temperature is in range of 15-33°C [260]. Graph design by author.

The bar chart recording the monthly distribution of these hours reveals a seasonally concentrated but climatically meaningful pattern. The comfortable window is inactive from November through February, and only marginally present in March (11 hours) and October (49 hours). The active season accelerates in April (23 hours) and May (230 hours), reaches its apex in July with 629 hours, more than 83% of all July hours, sustains substantial comfort hours through June (464) and August (441), and then recedes through September (240 hours). The total productive season spans approximately seven months, with three months forming a dense core of natural ventilation opportunity.

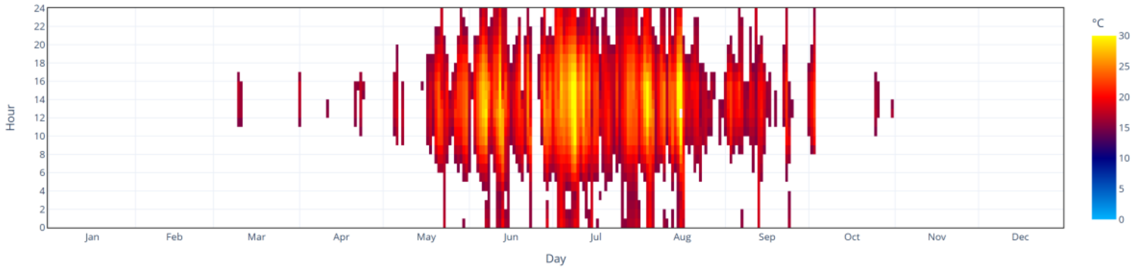

Fig. 6- 22: Thermal heat map, Warsaw current climate: hours falling within the 15–33°C comfort range. Colour scale: purple–red = 15–25°C; orange–yellow = 25–33°C [260].

The heat map (Figure 6-22) adds the temporal dimension that a monthly bar chart cannot capture. It reveals not only when comfortable conditions occur but precisely at what time of day they are available. Furthermore, the heat map demonstrates that the comfort band extends into the evening hours throughout summer.

The design strategies developed in this thesis are estimated to add approximately 20 hours to the comfort period specifically in July and August under current conditions. In high-summer conditions, when outdoor temperatures already exceed 33°C during peak hours, even a 3-4°C reduction in indoor air temperature converts previously uncomfortable hours into acceptable ones. The 20-hour gain represents the margin between discomfort and livability during the most thermally stressed days of the Warsaw year.

5.2 Part two: Warsaw's 2050 climate

If the current climate analysis establishes a baseline, the 2050 projection reveals the full urgency of the thesis. By mid-century, Warsaw's climate file shows a total of 3,011 hours per year within the 15-37°C range, 34.3% of the entire year. This represents an increase of 924 hours, or 10.5 %, compared to today. Translated into architectural terms: the demand for passive climate management will grow by nearly half again within the lifetime of a building designed today. What is currently a seasonal comfort strategy will become a near year-round necessity.

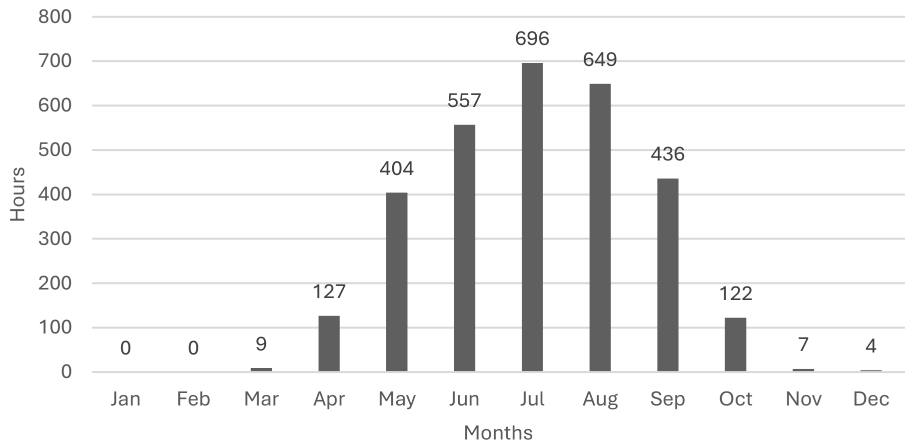

Fig. 6- 23: Number of hours the dry bulb temperature is in range of 15-37°C in future climate scenario 2050 [260]. Graph design by author.

The monthly distribution of the 2050 data is striking in its breadth. Where today's comfort window barely touches October (49 hours), the 2050 projection brings October to 122 hours and even assigns 7 hours to November and 4 to December, months that currently record zero. March, presently almost negligible (11 hours), rises to 127 hours in 2050. April's total climbs from 23 to 404 hours. The summer peak months grow as well, July reaches 696 hours and August 649. The active comfort window effectively extends from a 5-month season today (May–September) to an 8-month season by 2050 (March–October). The design must not only cool a hotter summer but manage a longer, warmer transitional climate on both sides of it.

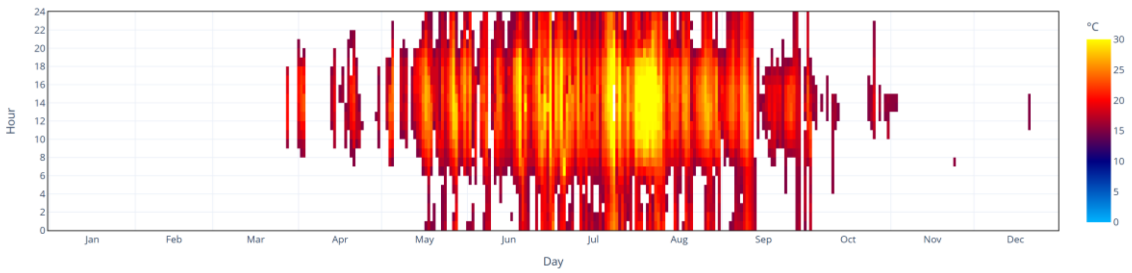

Fig. 6- 24: Thermal heat map, Warsaw 2050 projected climate: hours falling within the 15–37°C comfort range. Note the extended warm season and the intensification of peak temperatures relative to Figure 6-22.

Comparing Figure 6-22 with 6-24 makes the climatic transformation viscerally legible. The overall shape of the comfort window has shifted: from a sharp bell curve centred on July in the current file, to a broader, flatter plateau spanning five or six months in the projected 2050 file. Taken together, these two visualisations do not merely illustrate a climatic trend, they constitute the quantitative argument for design intervention. The 924 additional annual hours of thermal exposure that Warsaw will experience by 2050 are not hours that can be managed by incremental adjustments to a conventional building envelope. They require a fundamentally different approach to air movement, thermal mass, shading, and spatial organization, precisely the integrated passive strategy that this thesis has developed, tested, and validated.

6 Closing

The evidence assembled in this thesis leads to a conclusion that is both architecturally specific and broadly relevant. Warsaw's climate, temperate today, trending Mediterranean by mid-century, is entering a zone where the provision of indoor comfort through passive means is no longer an optional aspiration but a practical and measurable design objective. The 3-4°C thermal reduction demonstrated by the proposed strategies, situated within a scientific literature that supports a 32-33°C adaptive comfort ceiling for naturally ventilated buildings, means that outdoor temperatures up to 37°C can be absorbed by the building fabric and returned to the occupant as tolerable, livable conditions.

The heat maps and monthly distributions visualised in this chapter, 2,087 hours today, 3,011 hours by 2050, in which Warsaw's outdoor climate is itself an ally of indoor comfort. The strategies presented here do not attempt to seal the interior from the exterior and mechanically recreate comfort from scratch. They read the climate, track its diurnal and seasonal rhythms, and position the building as a precision instrument for translating outdoor energy into indoor wellbeing.

As Warsaw and cities like it move deeper into the century, the question of thermal comfort will increasingly be answered not by the power consumption of cooling systems, but by the intelligence of architectural form. This thesis has attempted to demonstrate, with rigour and specificity, what that intelligence can look like, and how far it can reach.

References

1. Sengupta, A., et al., *Assessing thermal resilience to overheating in a Belgian apartment: impact of building parameters.* International Journal of Ventilation, 2024. **24**: p. 34-52.
2. Amaral, A.R., et al., *A thermal performance parametric study of window type, orientation, size and shadowing effect.* Sustainable Cities and Society, 2016. **26**: p. 456-465.
3. Chiesa, G., et al., *Parametric Optimization of Window-to-Wall Ratio for Passive Buildings Adopting A Scripting Methodology to Dynamic-Energy Simulation.* Sustainability, 2019.
4. Sayadi, S., A. Hayati, and M. Salmanzadeh, *Optimization of Window-to-Wall Ratio for Buildings Located in Different Climates: An IDA-Indoor Climate and Energy Simulation Study.* Energies, 2021. **14**: p. 1974.
5. Du, J., *Window systems and energy performance in one-family houses:size and shading effects.* 2014: p. 209-216.
6. Huang, K.-T., et al., *Identifying outdoor thermal risk areas and evaluation of future thermal comfort concerning shading orientation in a traditional settlement.* Science of The Total Environment, 2018. **626**: p. 567-580.
7. Naboni, E. and L. Havinga, *Regenerative Design In Digital Practice. A Handbook for the Built Environment.* 2019.
8. Zhong, H.-Y., et al., *Single-sided natural ventilation in buildings: a critical literature review.* Building and Environment, 2022. **212**: p. 108797.
9. Mukhtar, A., M.Z. Yusoff, and K.C. Ng, *The potential influence of building optimization and passive design strategies on natural ventilation systems in underground buildings: The state of the art.* Tunnelling and Underground Space Technology, 2019. **92**: p. 103065.
10. Sacht, H. and M.A. Lukiantchuki, *Windows Size and the Performance of Natural Ventilation.* Procedia Engineering, 2017. **196**: p. 972-979.
11. Grygierek, K. and J. Ferdyn-Grygierek *Multi-Objective Optimization of the Envelope of Building with Natural Ventilation*. Energies, 2018. **11**, DOI: 10.3390/en11061383.
12. Salimi, S., E. Estrella Guillén, and H. Samuelson, *Decoupling awake and asleep thermal comfort: Impact on building design optimization.* Journal of Building Engineering, 2024. **82**: p. 108183.
13. Jiang, Z., et al., *A literature review of cross ventilation in buildings.* Energy and Buildings, 2023. **291**: p. 113143.
14. Zhang, X., et al., *Cross-ventilation of a generic building with various configurations of external and internal openings.* Building and Environment, 2022. **207**: p. 108447.
15. Chen, Q., *Ventilation performance prediction for buildings: A method overview and recent applications.* Building and Environment, 2009. **44**(4): p. 848-858.
16. Omrani, S., et al., *Effect of natural ventilation mode on thermal comfort and ventilation performance: Full-scale measurement.* Energy and Buildings, 2017. **156**: p. 1-16.
17. Bienvenido-Huertas, D., et al., *Holistic overview of natural ventilation and mixed mode in built environment of warm climate zones and hot seasons.* Building and Environment, 2023. **245**: p. 110942.

18. Nasrollahi, N. and P. Ghobadi, *Field measurement and numerical investigation of natural cross-ventilation in high-rise buildings; Thermal comfort analysis.* Applied Thermal Engineering, 2022. **211**: p. 118500.
19. Ahmed, T., P. Kumar, and L. Mottet, *Natural ventilation in warm climates: The challenges of thermal comfort, heatwave resilience and indoor air quality.* Renewable and Sustainable Energy Reviews, 2021. **138**: p. 110669.
20. Seifert, J., et al., *Calculation of wind-driven cross ventilation in buildings with large openings.* Journal of Wind Engineering and Industrial Aerodynamics, 2006. **94**(12): p. 925-947.
21. Ren, X.-H., et al., *Thermal driven natural convective flows inside the solar chimney flush-mounted with discrete heating sources: Reversal and cooperative flow dynamics.* Renewable Energy, 2019. **138**: p. 354-367.
22. Allocca, C., Q. Chen, and L.R. Glicksman, *Design analysis of single-sided natural ventilation.* Energy and Buildings, 2003. **35**(8): p. 785-795.
23. Carrilho da Graça, G., et al., *Pumping ventilation of corner and single sided rooms with two openings.* Building and Environment, 2021. **205**: p. 108171.
24. Ahadi, A.a., M.R. Saghafi, and M. Tahbaz, *The optimization of light-wells with integrating daylight and stack natural ventilation systems in deep-plan residential buildings: A case study of Tehran.* Journal of Building Engineering, 2018. **18**: p. 220-244.
25. Pan, W., et al., *A model for calculating single-sided natural ventilation rate in an urban residential apartment.* Building and Environment, 2019. **147**: p. 372-381.
26. Escombe, A.R., et al., *Natural Ventilation for the Prevention of Airborne Contagion.* PLOS Medicine, 2007. **4**(2): p. e68.
27. Oropeza-Perez, I. and P.A. Østergaard, *Potential of natural ventilation in temperate countries – A case study of Denmark.* Applied Energy, 2014. **114**: p. 520-530.
28. Vasaturo, R., et al., *On the effect of pressure coefficient source on the energy demand of an isolated cross-ventilated building.* Building and Environment, 2024. **255**: p. 111436.
29. Ghiaus, C., et al., *Urban environment influence on natural ventilation potential.* Building and Environment, 2006. **41**(4): p. 395-406.
30. Conceição, E.Z.E., et al., *Evaluation of local thermal discomfort in a classroom equipped with cross flow ventilation.* International Journal of Ventilation, 2008. **7**(3): p. 267-277.
31. Tominaga, Y. and B. Blocken, *Wind tunnel experiments on cross-ventilation flow of a generic building with contaminant dispersion in unsheltered and sheltered conditions.* Building and Environment, 2015. **92**: p. 452-461.
32. Chu, C.R., Y.H. Chiu, and Y.-W. Wang, *An experimental study of wind-driven cross ventilation in partitioned buildings.* Energy and Buildings, 2010. **42**(5): p. 667-673.
33. Jiang, Y., et al., *Natural ventilation in buildings: measurement in a wind tunnel and numerical simulation with large-eddy simulation.* Journal of Wind Engineering and Industrial Aerodynamics, 2003. **91**(3): p. 331-353.

34. Kobayashi, T., et al., *Power transportation inside stream tube of cross-ventilated simple shaped model and pitched roof house.* Building and Environment, 2009. **44**(7): p. 1440-1451.
35. Kobayashi, T., et al., *Wind Driven Flow Through Openings - Analysis of the Stream Tube.* International Journal of Ventilation, 2006. **4**(4): p. 323-336.
36. Kato, S., *Flow Network Model based on Power Balance as Applied to Cross-Ventilation.* International Journal of Ventilation, 2004. **2**(4): p. 395-408.
37. Ali, N.M., et al., *Quantifying natural cross-ventilation flow of a two-layered model used for terraced houses in tropical zones by particle image velocimetry.* Building and Environment, 2023. **244**: p. 110829.
38. Yin, X., et al., *The potential effects of window configuration and interior layout on natural ventilation buildings: A comprehensive review.* Cleaner Engineering and Technology, 2024. **23**: p. 100830.
39. Nourozi, B., et al., *A systematic review of ventilation solutions for hospital wards: Addressing cross-infection and patient safety.* Building and Environment, 2024. **247**: p. 110954.
40. Adamu, Z.A., A.D.F. Price, and M.J. Cook, *Performance evaluation of natural ventilation strategies for hospital wards – A case study of Great Ormond Street Hospital.* Building and Environment, 2012. **56**: p. 211-222.
41. Zhang, Y., et al., *A review of facilities management interventions to mitigate respiratory infections in existing buildings.* Building and Environment, 2022. **221**: p. 109347.
42. Foged, I. and A. Barbo, *Thermo-Spatial Performances of Eight Responsive Envelopes: Simulation Studies Benchmarking Built Active Solar Shading Envelopes*. 2020.
43. Foged, I. and A. Barbo, *Window Design and the Design of Air Flow*. 2020.
44. Mohammad, A.F., et al. *Turbulence Effect of Urban-Canopy Flow on Indoor Velocity Fields under Sheltered and Cross-Ventilation Conditions*. Sustainability, 2021. **13**, DOI: 10.3390/su13020586.
45. Deng, X. and Z. Tan, *Numerical analysis of local thermal comfort in a plan office under natural ventilation.* Indoor and Built Environment, 2019. **29**(7): p. 972-986.
46. Kotani, H. and T. Yamanaka, *Prediction of Inflow Direction at Large Opening of Cross Ventilated Apartment Building.* Journal of Environmental Engineering (Transactions of AIJ), 2006. **71**(609): p. 39-45.
47. Johnson, M.-H., Z. Zhai, and M. Krarti, *Performance evaluation of network airflow models for natural ventilation.* HVAC&R Research, 2012. **18**(3): p. 349-365.
48. Li, J., et al. *Study of Passive Adjustment Performance of Tubular Space in Subway Station Building Complexes*. Applied Sciences, 2019. **9**, DOI: 10.3390/app9050834.
49. Wen, Y., et al., *A two-level optimisation approach for underground natural ventilation based on CFD and building energy simulations.* Energy and Buildings, 2024. **310**: p. 114102.
50. Van Hooff, T. and B. Blocken, *On the effect of wind direction and urban surroundings on natural ventilation of a large semi-enclosed stadium.* Computers & Fluids, 2010. **39**(7): p. 1146-1155.

51. Blocken, B. and J. Carmeliet, *The influence of the wind-blocking effect by a building on its wind-driven rain exposure.* Journal of Wind Engineering and Industrial Aerodynamics, 2006. **94**(2): p. 101-127.
52. Lipczynska, A., S. Schiavon, and L.T. Graham, *Thermal comfort and self-reported productivity in an office with ceiling fans in the tropics.* Building and Environment, 2018. **135**: p. 202-212.
53. Allen, J.G., et al., *Associations of cognitive function scores with carbon dioxide, ventilation, and volatile organic compound exposures in office workers: A controlled exposure study of green and conventional office environments.* Environmental Health Perspectives, 2016. **124**(6): p. 805-812.
54. Dutton, S.M., et al., *Health and economic implications of natural ventilation in California offices.* Building and Environment, 2013. **67**: p. 34-45.
55. Zweers, T., et al., *Health and Indoor Climate Complaints of 7043 office Workers in 61 Buildings in the Netherlands.* Indoor Air, 1992. **2**(3): p. 127-136.
56. Mazarrón, F.R., C. Porras-Amores, and I. Cañas-Guerrero, *Annual evolution of the natural ventilation in an underground construction: Influence of the access tunnel and the ventilation chimney.* Tunnelling and Underground Space Technology, 2015. **49**: p. 188-198.
57. Mazarrón, F.R. and I. Cañas, *Seasonal analysis of the thermal behaviour of traditional underground wine cellars in Spain.* Renewable Energy, 2009. **34**(11): p. 2484-2492.
58. Bugenings, L.A. and A. Kamari *Bioclimatic Architecture Strategies in Denmark: A Review of Current and Future Directions*. Buildings, 2022. **12**, DOI: 10.3390/buildings12020224.
59. Liping, W. and W.N. Hien, *Applying natural ventilation for thermal comfort in residential buildings in singapore.* Architectural Science Review, 2007. **50**(3): p. 224-233.
60. Hunt, G.R. and N.B. Kaye, *Pollutant flushing with natural displacement ventilation.* Building and Environment, 2006. **41**(9): p. 1190-1197.
61. Costanzo, V. and M. Donn, *Thermal and visual comfort assessment of natural ventilated office buildings in Europe and North America.* Energy and Buildings, 2017. **140**: p. 210-223.
62. Raji, B., et al., *Natural summer ventilation strategies for energy-saving in high-rise buildings: a case study in the Netherlands.* International Journal of Ventilation, 2020. **19**(1): p. 25-48.
63. Prajongsan, P. and S. Sharples, *Enhancing natural ventilation, thermal comfort and energy savings in high-rise residential buildings in Bangkok through the use of ventilation shafts.* Building and Environment, 2012. **50**: p. 104-113.
64. SAMHE. *Schools' air quality monitoring for health and education*. 2022 [cited 2025; Available from: https://samhe.org.uk/.
65. Wen, Y., et al. *Environmental and Health Effects of Ventilation in Subway Stations: A Literature Review*. International Journal of Environmental Research and Public Health, 2020. **17**, DOI: 10.3390/ijerph17031084.
66. Tan, Z., et al., *Working in underground spaces: Architectural parameters, perceptions and thermal comfort measurements.* Tunnelling and Underground Space Technology, 2018. **71**: p. 428-439.

67. Lun, I., M. Ohba, and S. Morikami, *An overview of extreme hot weather incidents and the role of natural ventilation in buildings on human body comfort.* International Journal of Ventilation, 2012. **11**(3): p. 311-322.
68. Heracleous, C. and A. Michael, *Assessment of overheating risk and the impact of natural ventilation in educational buildings of Southern Europe under current and future climatic conditions.* Energy, 2018. **165**: p. 1228-1239.
69. Jomehzadeh, F., et al., *A review on windcatcher for passive cooling and natural ventilation in buildings, Part 1: Indoor air quality and thermal comfort assessment.* Renewable and Sustainable Energy Reviews, 2017. **70**: p. 736-756.
70. Martins, N.R. and G. Carrilho da Graça, *Impact of outdoor PM2.5 on natural ventilation usability in California's nondomestic buildings.* Applied Energy, 2017. **189**: p. 711-724.
71. Sakiyama, N.R.M., et al., *Perspectives of naturally ventilated buildings: A review.* Renewable and Sustainable Energy Reviews, 2020. **130**: p. 109933.
72. Vasaturo, R., et al., *Impact of passive climate adaptation measures and building orientation on the energy demand of a detached lightweight semi-portable building.* Building Simulation, 2018. **11**(6): p. 1163-1177.
73. Santamouris, M. and D. Kolokotsa, *Passive cooling dissipation techniques for buildings and other structures: The state of the art.* Energy and Buildings, 2013. **57**: p. 74-94.
74. Ramponi, R., A. Angelotti, and B. Blocken, *Energy saving potential of night ventilation: Sensitivity to pressure coefficients for different European climates.* Applied Energy, 2014. **123**: p. 185-195.
75. Katayama, T., J. Tsutsumi, and A. Ishii, *Full-scale measurements and wind tunnel tests on cross-ventilation.* Journal of Wind Engineering and Industrial Aerodynamics, 1992. **44**(1): p. 2553-2562.
76. Gough, H.L., et al., *Field measurement of natural ventilation rate in an idealised full-scale building located in a staggered urban array: Comparison between tracer gas and pressure-based methods.* Building and Environment, 2018. **137**: p. 246-256.
77. Zomorodian, Z.S. and M. Tahsildoost, *Energy and carbon analysis of double skin façades in the hot and dry climate.* Journal of Cleaner Production, 2018. **197**: p. 85-96.
78. Anand, P., C. Deb, and R. Alur, *A simplified tool for building layout design based on thermal comfort simulations.* Frontiers of Architectural Research, 2017. **6**(2): p. 218-230.
79. Ali, N.M., et al., *CFD analysis on indoor temperature and velocity: Effects of incident wind angle and outlet position.* Pertanika Journal of Science and Technology, 2017. **25**(S7): p. 227-238.
80. Aldawoud, A., *Windows design for maximum cross-ventilation in buildings.* Advances in Building Energy Research, 2017. **11**(1): p. 67-86.
81. Tominaga, Y., X. Zhang, and K. Miyakoshi, *Wind tunnel experiment on cross-ventilation of generic isolated building with various roof shapes: Impact of roof pitch and eaves.* Building and Environment, 2024. **265**: p. 111974.
82. Park, J. and G.H. Rhee, *Comparison of volume flow rate and volume-averaged local mean age of air for evaluating ventilation performance in*

natural ventilation. Journal of Mechanical Science and Technology, 2017. **31**(12): p. 5801-5812.
83. Zhai, Z., M.E. Mankibi, and A. Zoubir, *Review of Natural Ventilation Models.* Energy Procedia, 2015. **78**: p. 2700-2705.
84. Omrani, S., et al., *Natural ventilation in multi-storey buildings: Design process and review of evaluation tools.* Building and Environment, 2017. **116**: p. 182-194.
85. Haase, M. and A. Amato, *An investigation of the potential for natural ventilation and building orientation to achieve thermal comfort in warm and humid climates.* Solar Energy, 2009. **83**(3): p. 389-399.
86. Aynsley, R., *Estimating summer wind driven natural ventilation potential for indoor thermal comfort.* Journal of Wind Engineering and Industrial Aerodynamics, 1999. **83**(1): p. 515-525.
87. Yin, W., et al., *Natural ventilation potential model considering solution multiplicity, window opening percentage, air velocity and humidity in China.* Building and Environment, 2010. **45**(2): p. 338-344.
88. Luo, Z., et al., *Estimating natural-ventilation potential considering both thermal comfort and IAQ issues.* Building and Environment, 2007. **42**(6): p. 2289-2298.
89. Cheng, J., et al., *Evaluating wind-driven natural ventilation potential for early building design.* Journal of Wind Engineering and Industrial Aerodynamics, 2018. **182**: p. 160-169.
90. Li, Y. and X. Li, *Natural ventilation potential of high-rise residential buildings in northern China using coupling thermal and airflow simulations.* Building Simulation, 2015. **8**(1): p. 51-64.
91. Tong, Z., Y. Chen, and A. Malkawi, *Estimating natural ventilation potential for high-rise buildings considering boundary layer meteorology.* Applied Energy, 2017. **193**: p. 276-286.
92. Asadi, S., et al., *The effect of solar chimney layout on ventilation rate in buildings.* Energy and Buildings, 2016. **123**: p. 71-78.
93. Abdeen, A., et al., *Solar chimney optimization for enhancing thermal comfort in Egypt: An experimental and numerical study.* Solar Energy, 2019. **180**: p. 524-536.
94. Arce, J., et al., *Experimental study for natural ventilation on a solar chimney.* Renewable Energy, 2009. **34**(12): p. 2928-2934.
95. Hughes, B.R., J.K. Calautit, and S.A. Ghani, *The development of commercial wind towers for natural ventilation: A review.* Applied Energy, 2012. **92**: p. 606-627.
96. Allen Joseph, G., et al., *Associations of Cognitive Function Scores with Carbon Dioxide, Ventilation, and Volatile Organic Compound Exposures in Office Workers: A Controlled Exposure Study of Green and Conventional Office Environments.* Environmental Health Perspectives, 2016. **124**(6): p. 805-812.
97. Calautit, J.K., et al., *CFD analysis of a heat transfer device integrated wind tower system for hot and dry climate.* Applied Energy, 2013. **112**: p. 576-591.
98. Miyazaki, T., A. Akisawa, and T. Kashiwagi, *The effects of solar chimneys on thermal load mitigation of office buildings under the Japanese climate.* Renewable Energy, 2006. **31**(7): p. 987-1010.
99. C. O. Souza, L., H. A. Souza, and E. F. Rodrigues, *Experimental and numerical analysis of a naturally ventilated double-skin façade.* Energy and Buildings, 2018. **165**: p. 328-339.

100. Qavidel Fard, Z., Z.S. Zomorodian, and S.S. Korsavi, *Application of machine learning in thermal comfort studies: A review of methods, performance and challenges.* Energy and Buildings, 2022. **256**: p. 111771.
101. Bangalee, M.Z.I., et al., *Effects of Lateral Window Position and Wind Direction on Wind-Driven Natural Cross Ventilation of a Building: A Computational Approach.* Journal of Computational Engineering, 2014. **2014**(1): p. 310358.
102. Cho, H.-J. and J.-W. Jeong, *Evaluation of thermal comfort in an office building served by a liquid desiccant-assisted evaporative cooling air-conditioning system.* Energy and Buildings, 2018. **172**: p. 361-370.
103. Huckemann, V., et al., *Empirical thermal comfort evaluation of single and double skin façades.* Building and Environment, 2010. **45**(4): p. 976-982.
104. Jo, S.H., J.T. Kim, and G.Y. Yun. *A Field Survey of Thermal Comfort in Office Building with a Unitary Heat-Pump and Energy Recovery Ventilator*. in *Sustainability in Energy and Buildings*. 2013. Berlin, Heidelberg: Springer Berlin Heidelberg.
105. Attia, S., et al., *Energy efficiency in the polish residential building stock: A literature review.* Journal of Building Engineering, 2022. **45**: p. 103461.
106. BazazZadeh, H., *Constructing semi-automated buildings' energy loads model to retrofit built heritage by using a data-driven model and computer vision*, in *Architecture and urban planning*. 2024, Poznan University of Technology: Poznań, Poland.
107. (NAPE), N.A.P.E., *Polish Building Typology*. 2012, TABULA: Warsaw, Poland.
108. i Rozwoju, M.I., *Krajowa polityka miejska.* Departament Polityki Przestrzennej, Warszawa, 2015.
109. Suchecki, J., *Alternative Ways of Housing and the Formation of Residential Architecture*, in *Architecture and urban planning*. 2024, Poznan University of Technology: Poznań, Poland.
110. Attia, S. *Spatial and Behavioral Thermal Adaptation in Net Zero Energy Buildings: An Exploratory Investigation*. Sustainability, 2020. **12**, DOI: 10.3390/su12197961.
111. Fedorczak-Cisak, M., et al. *Thermal and Vibration Comfort Analysis of a Nearly Zero-Energy Building in Poland*. Sustainability, 2018. **10**, DOI: 10.3390/su10103774.
112. Fedorczak-Cisak, M., M. Furtak, and M. Surówka, *Possibilities of achieving the nZEB building standard (nearly zero energy building) and the passive building standard for newly designed buildings in Poland.* IOP Conference Series: Materials Science and Engineering, 2020. **960**(3): p. 032095.
113. Suszanowicz, D. *Optimisation of Heat Loss through Ventilation for Residential Buildings*. Atmosphere, 2018. **9**, DOI: 10.3390/atmos9030095.
114. Zawada, B. and J. Rucińska *Optimization of Modernization of a Single-Family Building in Poland Including Thermal Comfort*. Energies, 2021. **14**, DOI: 10.3390/en14102925.
115. Csoknyai, T., et al., *Building stock characteristics and energy performance of residential buildings in Eastern-European countries.* Energy and Buildings, 2016. **132**: p. 39-52.

116. Ferdyn-Grygierek, J. and K. Grygierek *Multi-Variable Optimization of Building Thermal Design Using Genetic Algorithms*. Energies, 2017. **10**, DOI: 10.3390/en10101570.
117. BPIE, D. Staniaszek, and S. Firląg, *Financing Building Energy Performance Improvement in Poland*. 2016, Buildings Performance Institute Europe (BPIE): Belgium.
118. Sokołowski, J., *Energy Poverty and Unfit Housing in Poland*. 2023, University of Warsaw: Warsaw, Poland.
119. Baborska – Narożny, M. and M. Kostka *Seasonal Air Quality in Bedrooms with Natural, Mechanical or Hybrid Ventilation Systems and Varied Window Opening Behavior-Field Measurement Results*. Energies, 2022. **15**, DOI: 10.3390/en15249328.
120. Baborska-Narożny, M., K. Bandurski, and M. Grudzińska, *To Shade or not to Shade (and how)? Annual heating energy balance and internal temperature in low energy houses in Wrocław, Poland.* Journal of Physics: Conference Series, 2023. **2654**(1): p. 012067.
121. Kozielska, B., et al., *Indoor air quality in residential buildings in Upper Silesia, Poland.* Building and Environment, 2020. **177**: p. 106914.
122. Piasecki, M., et al. *Experimental Confirmation of the Reliability of Fanger's Thermal Comfort Model—Case Study of a Near-Zero Energy Building (NZEB) Office Building*. Sustainability, 2019. **11**, DOI: 10.3390/su11092461.
123. Anna Dworakowska, M.Z., Małgorzata Barnaś, *Energy Efficiency in Poland. 2015 Review*. 2016: Kraków, Poland.
124. BPIE, D. Staniaszek, and S. Firląg, *Financing building energy performance improvement in Poland*, O. Rapf, C. Marian, and F.A. Fata, Editors. 2016, Buildings Performance Institute Europe (BPIE): Belgium. p. 1-47.
125. Cholewa, T., A. Siuta-Olcha, and R. Anasiewicz, *On the possibilities to increase energy efficiency of domestic hot water preparation systems in existing buildings – Long term field research.* Journal of Cleaner Production, 2019. **217**: p. 194-203.
126. Walkowskiej, K., *Energy consumption in households in 2018*. 2019, Główny Urząd Statystyczny, Departament Przedsiębiorstw: Warsaw, Poland.
127. Księżopolski, K., et al. *The Economic Effects of New Patterns of Energy Efficiency and Heat Sources in Rural Single-Family Houses in Poland*. Energies, 2020. **13**, DOI: 10.3390/en13236358.
128. (ECSO), E.C.S.O., *Country Profile: Poland*. 2019.
129. Michalik, S. and D. Zieliński, *Transformacja energetyczna w Polsce*. 2024.
130. Flaga-Maryanczyk, A., et al., *Experimental measurements and CFD simulation of a ground source heat exchanger operating at a cold climate for a passive house ventilation system.* Energy and Buildings, 2014. **68**: p. 562-570.
131. Piasecki, M., et al. *Implementation of the Indoor Environmental Quality (IEQ) Model for the Assessment of a Retrofitted Historical Masonry Building*. Energies, 2020. **13**, DOI: 10.3390/en13226051.
132. Wójcik, R., *Przesłanki wyboru materiału termoizolacyjnego według zaleceń zawartych w monografii „Docieplanie budynków od wewnątrz"*. Izolacje, 2017. **22**.

133. Życzyńska, A. and T. Cholewa, *The modifications to the requirements on energy savings and thermal insulation of buildings in Poland in the years 1974-2021.* Budownictwo i Architektura, 2015. **14**(1): p. 145-154.
134. Pogorzelski, J., *Normalizacja ochrony cieplnej budynków w krajach UE iw Polsce. Przegląd bieżącej sytuacji.* Prace Instytutu Techniki Budowlanej, 1999. **28**: p. 39-51.
135. Sowa, J., *Implementation of the EPBD in Poland.* Status in November, 2010: p. 265-274.
136. Bazazzadeh, H., A. Nadolny, and S.S.H. Safaei, *Climate Change and Building Energy Consumption: A Review of the Impact of Weather Parameters Influenced by Climate Change on Household Heating and Cooling Demands of Buildings.* European Journal of Sustainable Development, 2021. **10**(2): p. 1.
137. Cellura, M., et al., *Climate change and the building sector: Modelling and energy implications to an office building in southern Europe.* Energy for Sustainable Development, 2018. **45**: p. 46-65.
138. Intergovernmental Panel on Climate Change, I., *Global Warming of 1.5°C: IPCC Special Report on Impacts of Global Warming of 1.5°C above Pre-industrial Levels in Context of Strengthening Response to Climate Change, Sustainable Development, and Efforts to Eradicate Poverty.* 2022, Cambridge: Cambridge University Press.
139. Gero, J.S., N. D'Cruz, and A.D. Radford, *Energy in context: A multicriteria model for building design.* Building and Environment, 1983. **18**(3): p. 99-107.
140. Kyle, P., et al., *Climate Policy and the Long-Term Evolution of the U.S. Buildings Sector.* The Energy Journal, 2010. **31**(2): p. 145-172.
141. York, R. and S.E. Bell, *Energy transitions or additions?: Why a transition from fossil fuels requires more than the growth of renewable energy.* Energy Research & Social Science, 2019. **51**: p. 40-43.
142. Nik, V.M. and A. Sasic Kalagasidis, *Impact study of the climate change on the energy performance of the building stock in Stockholm considering four climate uncertainties.* Building and Environment, 2013. **60**: p. 291-304.
143. Węglarz, A. and P. Narowski. *The optimal thermal design of residential buildings using energy simulation and fuzzy sets theory*. in *Proceedings of building simulation*. 2011.
144. Ferdyn-Grygierek, J., et al. *Thermal Diagnostics of Natural Ventilation in Buildings: An Integrated Approach*. Energies, 2019. **12**, DOI: 10.3390/en12234556.
145. BPIE, et al., *Ready for carbon neutral by 2050? Assessing ambition levels in new building standards across the EU*, M. Fabbri, et al., Editors. 2022, Buildings Performance Institute Europe (BPIE): Belgium, Germany. p. 35-37.
146. ODYSSEE-MURE, *Poland Energy profile 2022*, in *Energy efficiency trends and policies*. 2025, ODYSSEE-MURE. p. 1-10.
147. Bazazzadeh, H., et al., *AI- aided surrogate model for prediction of HVAC optimization strategies in future conditions in the face of climate change.* Energy Reports, 2025. **13**: p. 1834-1845.
148. BPIE, et al., *Financing Renovation of Buildings in Poland*, T. Antoniou, et al., Editors. 2018, Buildings Performance Institute Europe (BPIE): Belgium. p. 17-18.
149. WorldBank, *Projects & Operations*. 2017.

150. Nakonieczny, R., *Mieszkanie po polsku 1945-2018.* Architectura, 2018. **10**(289): p. 26-36.
151. Milobedzki, M., *Apartamantowiec: Zespol mieszkalno-biurowy na warszawskim Wierzbnie.* Architectura, 2006. **6**: p. 36-40.
152. Wojciech Krynski, J.S.M., *Winnica: Osiedle mieszkaniowe w Warszawie.* Architectura, 2006. **6**: p. 41-43.
153. Najafi Ziarani, N., et al., *The role of near-façade flow in wind-dominant single-sided natural ventilation for an isolated three-storey building: An LES study.* Building and Environment, 2023. **235**: p. 110210.
154. *Long-Term Building Renovation Strategy*. 2022 Warsaw, Poland. p. 1-155.
155. Zazula, J. *Osiedle Winnica*. 2019 [cited 2025 14 April 2025]; Available from: https://investmap.pl/_i/gallery/92/92/437852_1200x.jpeg.webp.
156. directoffice. *Cotton House*. 2019 [cited 2025 14 April 2025]; Available from: https://directoffice.pl/oferta/cotton-house/
157. Blocken, B., *50 years of Computational Wind Engineering: Past, present and future.* Journal of Wind Engineering and Industrial Aerodynamics, 2014. **129**: p. 69-102.
158. Solari, G., *The International Association for Wind Engineering (IAWE): Progress and prospects.* Journal of Wind Engineering and Industrial Aerodynamics, 2007. **95**(9): p. 813-842.
159. Potsis, T., Y. Tominaga, and T. Stathopoulos, *Computational wind engineering: 30 years of research progress in building structures and environment.* Journal of Wind Engineering and Industrial Aerodynamics, 2023. **234**: p. 105346.
160. Blocken, B. and T. Stathopoulos, *CFD simulation of pedestrian-level wind conditions around buildings: Past achievements and prospects.* Journal of Wind Engineering and Industrial Aerodynamics, 2013. **121**: p. 138-145.
161. Tominaga, Y., et al., *AIJ guidelines for practical applications of CFD to pedestrian wind environment around buildings.* Journal of Wind Engineering and Industrial Aerodynamics, 2008. **96**(10): p. 1749-1761.
162. Murakami, S., *Current status and future trends in computational wind engineering.* Journal of Wind Engineering and Industrial Aerodynamics, 1997. **67-68**: p. 3-34.
163. Shirzadi, M. and Y. Tominaga, *CFD evaluation of mean and turbulent wind characteristics around a high-rise building affected by its surroundings.* Building and Environment, 2022. **225**: p. 109637.
164. Vita, G., et al., *On the assessment of pedestrian distress in urban winds.* Journal of Wind Engineering and Industrial Aerodynamics, 2020. **203**: p. 104200.
165. Ferziger, J.H., *Approaches to turbulent flow computation: Applications to flow over obstacles.* Journal of Wind Engineering and Industrial Aerodynamics, 1990. **35**: p. 1-19.
166. van Hooff, T. and B. Blocken, *Coupled urban wind flow and indoor natural ventilation modelling on a high-resolution grid: A case study for the Amsterdam ArenA stadium.* Environmental Modelling & Software, 2010. **25**(1): p. 51-65.
167. Tang, W. and C.I. Davidson, *Erosion of limestone building surfaces caused by wind-driven rain: 2. Numerical modeling.* Atmospheric Environment, 2004. **38**(33): p. 5601-5609.

168. Etyemezian, V., et al., *Impingement of rain drops on a tall building.* Atmospheric Environment, 2000. **34**(15): p. 2399-2412.
169. Blocken, B. and C. Gualtieri, *Ten iterative steps for model development and evaluation applied to Computational Fluid Dynamics for Environmental Fluid Mechanics.* Environmental Modelling & Software, 2012. **33**: p. 1-22.
170. Yoshie, R., et al., *Cooperative project for CFD prediction of pedestrian wind environment in the Architectural Institute of Japan.* Journal of Wind Engineering and Industrial Aerodynamics, 2007. **95**(9): p. 1551-1578.
171. Okaze, T., et al., *Large-eddy simulation of flow around an isolated building: A step-by-step analysis of influencing factors on turbulent statistics.* Building and Environment, 2021. **202**: p. 108021.
172. Gousseau, P., B. Blocken, and G.J.F. van Heijst, *Quality assessment of Large-Eddy Simulation of wind flow around a high-rise building: Validation and solution verification.* Computers & Fluids, 2013. **79**: p. 120-133.
173. Mochida, A. and I.Y.F. Lun, *Prediction of wind environment and thermal comfort at pedestrian level in urban area.* Journal of Wind Engineering and Industrial Aerodynamics, 2008. **96**(10): p. 1498-1527.
174. Tominaga, Y., et al., *Comparison of various revised k– ε models and LES applied to flow around a high-rise building model with 1:1:2 shape placed within the surface boundary layer.* Journal of Wind Engineering and Industrial Aerodynamics, 2008. **96**(4): p. 389-411.
175. Willemsen, E. and J.A. Wisse, *Design for wind comfort in The Netherlands: Procedures, criteria and open research issues.* Journal of Wind Engineering and Industrial Aerodynamics, 2007. **95**(9): p. 1541-1550.
176. NEN, *Application of Mean Hourly Wind Speed Statistics for the Netherlands*, in *Dutch Practice Guideline*. 2006.
177. Lin, C., R. Ooka, and H. Kikumoto, *Reynolds-averaged Eulerian simulation of elevated source pollutant dispersion in turbulent boundary layer using concentration diffusivity limiter.* Journal of Wind Engineering and Industrial Aerodynamics, 2022. **220**: p. 104876.
178. Gousseau, P., et al., *Near-field pollutant dispersion in an actual urban area: Analysis of the mass transport mechanism by high-resolution Large Eddy Simulations.* Computers & Fluids, 2015. **114**: p. 151-162.
179. Hu, Y., et al., *Application of CFD plug-ins integrated into urban and building design platforms for performance simulations: A literature review.* Frontiers of Architectural Research, 2022.
180. Rodrigues Marques Sakiyama, N., et al. *Using CFD to Evaluate Natural Ventilation through a 3D Parametric Modeling Approach*. Energies, 2021. **14**, DOI: 10.3390/en14082197.
181. Kenneth, J.L. *Wearable sensors for enhanced warfighter protection and performance*. in *Proc.SPIE*. 2021.
182. Jia, B., S. Liu, and M. Ng *Air Quality and Key Variables in High-Density Housing*. Sustainability, 2021. **13**, DOI: 10.3390/su13084281.
183. Kang, G., J.-J. Kim, and W. Choi, *Computational fluid dynamics simulation of tree effects on pedestrian wind comfort in an urban area.* Sustainable Cities and Society, 2020. **56**: p. 102086.
184. van Druenen, T., et al., *CFD evaluation of building geometry modifications to reduce pedestrian-level wind speed.* Building and Environment, 2019. **163**: p. 106293.

185. Mittal, H., A. Sharma, and A. Gairola, *Numerical simulation of pedestrian level wind flow around buildings: Effect of corner modification and orientation.* Journal of Building Engineering, 2019. **22**: p. 314-326.
186. Tominaga, Y. and T. Stathopoulos, *Turbulent Schmidt numbers for CFD analysis with various types of flowfield.* Atmospheric Environment, 2007. **41**(37): p. 8091-8099.
187. Younis, B.A., C.G. Speziale, and T.T. Clark, *A rational model for the turbulent scalar fluxes.* Proceedings of the Royal Society A: Mathematical, Physical and Engineering Sciences, 2005. **461**(2054): p. 575-594.
188. Kaseb, Z., et al., *A framework for pedestrian-level wind conditions improvement in urban areas: CFD simulation and optimization.* Building and Environment, 2020. **184**: p. 107191.
189. Machairas, V., A. Tsangrassoulis, and K. Axarli, *Algorithms for optimization of building design: A review.* Renewable and Sustainable Energy Reviews, 2014. **31**: p. 101-112.
190. Touloupaki, E. and T. Theodosiou *Performance Simulation Integrated in Parametric 3D Modeling as a Method for Early Stage Design Optimization—A Review*. Energies, 2017. **10**, DOI: 10.3390/en10050637.
191. Yu, Y., A.C. Megri, and S. Jiang, *A review of the development of airflow models used in building load calculation and energy simulation.* Building Simulation, 2019. **12**(3): p. 347-363.
192. Kato, S., *Review of airflow and transport analysis in building using CFD and network model.* Japan Architectural Review, 2018. **1**(3): p. 299-309.
193. Mortezazadeh, M. and L. Wang, *Solving city and building microclimates by fast fluid dynamics with large timesteps and coarse meshes.* Building and Environment, 2020. **179**: p. 106955.
194. Zuo, W. and Q. Chen, *Real-time or faster-than-real-time simulation of airflow in buildingsAbstract.* Indoor Air, 2009. **19**(1): p. 33-44.
195. Liu, W., R. You, and C. Chen, *Modeling transient particle transport by fast fluid dynamics with the Markov chain method.* Building Simulation, 2019. **12**(5): p. 881-889.
196. Franke, J., et al., *The COST 732 Best Practice Guideline for CFD simulation of flows in the urban environment: a summary.* International Journal of Environment and Pollution, 2011. **44**(1-4): p. 419-427.
197. Oberkampf, W.L., T.G. Trucano, and C. Hirsch, *Verification, validation, and predictive capability in computational engineering and physics.* Applied Mechanics Reviews, 2004. **57**(5): p. 345-384.
198. Blocken, B.C., J., *Pedestrian wind conditions at outdoor platforms in a high-rise apartment building: generic sub-configuration validation, wind comfort assessment and uncertainty issues.* Wind and Structures, 2008. **Volume 11 Issue 1**: p. 51-70.
199. Bowen, A.J., *Modelling of strong wind flows over complex terrain at small geometric scales.* Journal of Wind Engineering and Industrial Aerodynamics, 2003. **91**(12): p. 1859-1871.
200. Sanz Rodrigo, J., J. van Beeck, and J.-M. Buchlin, *Wind engineering in the integrated design of princess Elisabeth Antarctic base.* Building and Environment, 2012. **52**: p. 1-18.

201. Cermak, J.E., *Applications of Fluid Mechanics to Wind Engineering—A Freeman Scholar Lecture.* Journal of Fluids Engineering, 1975. **97**(1): p. 9-38.
202. Bueno, B., et al., *The urban weather generator.* Journal of Building Performance Simulation, 2013. **6**(4): p. 269-281.
203. Lindberg, F., B. Holmer, and S. Thorsson, *SOLWEIG 1.0 – Modelling spatial variations of 3D radiant fluxes and mean radiant temperature in complex urban settings.* International Journal of Biometeorology, 2008. **52**(7): p. 697-713.
204. Crawley, D.B., et al., *EnergyPlus: creating a new-generation building energy simulation program.* Energy and Buildings, 2001. **33**(4): p. 319-331.
205. Emmanuel, W. and K. Jérôme Henri, *A verification of CitySim results using the BESTEST and monitored consumption values*. 2015, Proceedings of the 2nd Building Simulation Applications conference: Bozen-Bolzano University Press. p. 215-222.
206. TRNSYS, *Transient System Simulation Tool*. 2020, TRNSYS.
207. ENVI-met. *ENVI-met CFD*. 2019 [cited 2025 12 April 2025]; Available from: https://envi-met.com/.
208. Autodesk. *AuodeskCFD*. 2019 [cited 2025 16.04.2025]; Available from: https://help.autodesk.com/view/SCDSE/2019/ENU/.
209. DesignBuilder. *DesignBuilder CFD*. [Online Help] 2019 [cited 2025 12 April 2025]; Available from: https://designbuilder.co.uk/cfd.
210. Yang, X., Y. Li, and L. Yang, *Predicting and understanding temporal 3D exterior surface temperature distribution in an ideal courtyard.* Building and Environment, 2012. **57**: p. 38-48.
211. Christopher, M., et al., *Wind, Sun, Surface Temperature, and Heat Island: Critical Variables for High-Resolution Outdoor Thermal Comfort*, in *Proceedings of Building Simulation 2017: 15th Conference of IBPSA*. 2017, IBPSA. p. 985-993.
212. Elwy, I., et al., *Outdoor microclimatic validation for hybrid simulation workflow in hot arid climates against ENVI-met and field measurements.* Energy Procedia, 2018. **153**: p. 29-34.
213. Evola, G., et al., *A novel comprehensive workflow for modelling outdoor thermal comfort and energy demand in urban canyons: Results and critical issues.* Energy and Buildings, 2020. **216**: p. 109946.
214. Christoph, R., et al., *Umi – An Urban Simulation Environment For Building Energy Use, Daylighting And Walkability*, in *Proceedings of Building Simulation 2013: 13th Conference of IBPSA*. 2013, IBPSA. p. 476-483.
215. Perini, K., et al., *Modeling and simulating urban outdoor comfort: Coupling ENVI-Met and TRNSYS by grasshopper.* Energy and Buildings, 2017. **152**: p. 373-384.
216. Fabbri, K., et al., *Outdoor Comfort: The ENVI-BUG tool to Evaluate PMV Values Output Comfort Point by Point.* Energy Procedia, 2017. **111**: p. 510-519.
217. López-Cabeza, V.P., et al., *Thermal comfort modelling and empirical validation of predicted air temperature in hot-summer Mediterranean courtyards.* Journal of Building Performance Simulation, 2022. **15**(1): p. 39-61.
218. Murakami, S., *Overview of turbulence models applied in CWE-1997.* Journal of Wind Engineering and Industrial Aerodynamics, 1998. **74-76**: p. 1-24.

219. Tamura, T., K. Nozawa, and K. Kondo, *AIJ guide for numerical prediction of wind loads on buildings.* Journal of Wind Engineering and Industrial Aerodynamics, 2008. **96**(10): p. 1974-1984.
220. Oberkampf, W.L. and T.G. Trucano, *Verification and validation in computational fluid dynamics.* Progress in Aerospace Sciences, 2002. **38**(3): p. 209-272.
221. Sadeghi, M., et al., *Effects of urban context on the indoor thermal comfort performance of windcatchers in a residential setting.* Energy and Buildings, 2020. **219**: p. 110010.
222. Diakaki, C., et al., *A multi-objective decision model for the improvement of energy efficiency in buildings.* Energy, 2010. **35**(12): p. 5483-5496.
223. Briggen, P.M., B. Blocken, and H.L. Schellen, *Wind-driven rain on the facade of a monumental tower: Numerical simulation, full-scale validation and sensitivity analysis.* Building and Environment, 2009. **44**(8): p. 1675-1690.
224. Tominaga, Y. and T. Stathopoulos, *CFD simulation of near-field pollutant dispersion in the urban environment: A review of current modeling techniques.* Atmospheric Environment, 2013. **79**: p. 716-730.
225. Ramponi, R. and B. Blocken, *CFD simulation of cross-ventilation for a generic isolated building: Impact of computational parameters.* Building and Environment, 2012. **53**: p. 34-48.
226. Snyder, W.H., *Similarity criteria for the application of fluid models to the study of air pollution meteorology.* Boundary-Layer Meteorology, 1972. **3**(1): p. 113-134.
227. Baker, C.J., *Wind engineering—Past, present and future.* Journal of Wind Engineering and Industrial Aerodynamics, 2007. **95**(9): p. 843-870.
228. Blocken, B., T. Stathopoulos, and J. Carmeliet, *CFD simulation of the atmospheric boundary layer: wall function problems.* Atmospheric Environment, 2007. **41**(2): p. 238-252.
229. Jiang, Y. and Q. Chen, *Effect of fluctuating wind direction on cross natural ventilation in buildings from large eddy simulation.* Building and Environment, 2002. **37**(4): p. 379-386.
230. Klemm, K., W. Marks, and A.J. Klemm, *Multicriteria optimisation of the building arrangement with application of numerical simulation.* Building and Environment, 2000. **35**(6): p. 537-544.
231. Hu, Y., et al., *Application of CFD plug-ins integrated into urban and building design platforms for performance simulations: A literature review.* Frontiers of Architectural Research, 2023. **12**(1): p. 148-174.
232. Ding, C. and K.P. Lam, *Data-driven model for cross ventilation potential in high-density cities based on coupled CFD simulation and machine learning.* Building and Environment, 2019. **165**: p. 106394.
233. Karava, P., T. Stathopoulos, and A.K. Athienitis, *Airflow assessment in cross-ventilated buildings with operable façade elements.* Building and Environment, 2011. **46**(1): p. 266-279.
234. Considine, B., et al., *A numerical analysis of particulate matter control technology integrated with HVAC system inlet design and implications on energy consumption.* Building and Environment, 2022. **211**: p. 108726.
235. Schatzmann, M., S. Rafailidis, and M. Pavageau, *Some remarks on the validation of small-scale dispersion models with field and laboratory*

data. Journal of Wind Engineering and Industrial Aerodynamics, 1997. **67-68**: p. 885-893.
236. Xie, Z.-T. and I.P. Castro, *Large-eddy simulation for flow and dispersion in urban streets*. Atmospheric Environment, 2009. **43**(13): p. 2174-2185.
237. Hirsch, C., *The Development of a Framework for CFD Validation and Best Practice: The QNET-CFD Knowledge Base*. Chinese Journal of Aeronautics, 2006. **19**(2): p. 105-113.
238. El Ahmar, S., F. Battista, and A. Fioravanti, *Simulation of the thermal performance of a geometrically complex Double-Skin Facade for hot climates: EnergyPlus vs. OpenFOAM*. Building Simulation, 2019. **12**(5): p. 781-795.
239. Choi, E.C.C., *Simulation of wind-driven-rain around a building*, in *Computational Wind Engineering 1*, S. Murakami, Editor. 1993, Elsevier: Oxford. p. 721-729.
240. Nastaran, S., et al., *Investigation of the potential benefits of optimizing building elements placement using computational fluid dynamics (CFD)*, in *2020 Building Performance Analysis Conference and SimBuild co-organized by ASHRAE and IBPSA-USA*. 2020, ASHRAE/IBPSA-USA. p. 574-583.
241. Sudirman, M., et al., *Validation study of cross-ventilation in a realistic building geometry: RANS, SAS and LES*. Building and Environment, 2025. **269**: p. 112354.
242. Blocken, B., R. Vervoort, and T. van Hooff, *Reduction of outdoor particulate matter concentrations by local removal in semi-enclosed parking garages: A preliminary case study for Eindhoven city center*. Journal of Wind Engineering and Industrial Aerodynamics, 2016. **159**: p. 80-98.
243. Liu, S., et al. *How many surrounding buildings should be included in simulating wind flow around a building?* in *15th Conference of the International Society of Indoor Air Quality and Climate, INDOOR AIR 2018*. 2018.
244. Franke, J. and A. Baklanov, *Best Practice Guideline for the CFD Simulation of Flows in the Urban Environment: COST Action 732 Quality Assurance and Improvement of Microscale Meteorological Models*. 2007.
245. WeatherSpark. *The Weather Year Round Anywhere on Earth*. 2023 [cited 2023; Available from: WeatherSpark.com.
246. Viola, M., *Wind and urban spaces. Evaluation of a CFD parametric framework for early-stage design*, in *Proceedings of BSA Conference 2019: Fourth Conference of IBPSA-Italy*. 2019, IBPSA-Italy. p. 67-76.
247. Blocken, B., J. Carmeliet, and T. Stathopoulos, *CFD evaluation of wind speed conditions in passages between parallel buildings—effect of wall-function roughness modifications for the atmospheric boundary layer flow*. Journal of Wind Engineering and Industrial Aerodynamics, 2007. **95**(9): p. 941-962.
248. Peren, J.I., et al., *Impact of roof geometry of an isolated leeward sawtooth roof building on cross-ventilation: Straight, concave, hybrid or convex?* Journal of Wind Engineering and Industrial Aerodynamics, 2015. **145**: p. 102-114.
249. Pan, Y., et al., *Natural ventilation in vernacular architecture: A systematic review of bioclimatic ventilation design and its performance evaluation*. Building and Environment, 2024. **253**: p. 111317.

250. Blocken, B., *Computational Fluid Dynamics for urban physics: Importance, scales, possibilities, limitations and ten tips and tricks towards accurate and reliable simulations.* Building and Environment, 2015. **91**: p. 219-245.
251. Kastner, P. and T. Dogan, *A cylindrical meshing methodology for annual urban computational fluid dynamics simulations.* Journal of Building Performance Simulation, 2020. **13**(1): p. 59-68.
252. Kosutova, K., et al., *Wind-tunnel experiments on cross-ventilative cooling in a generic isolated building with one heated wall: Impact of opening size.* Building and Environment, 2024. **259**: p. 111628.
253. Meng, Q. and M. Mourshed, *Degree-day based non-domestic building energy analytics and modelling should use building and type specific base temperatures.* Energy and Buildings, 2017. **155**: p. 260-268.
254. Tominaga, Y., et al., *Accuracy of CFD simulations in urban aerodynamics and microclimate: Progress and challenges.* Building and Environment, 2023. **243**: p. 110723.
255. Mohammadi, M.M. and M. Janowski, *The impact of size in fenestration design on the airflow and temperature in natural cross ventilation, case study: A two-bedroom Polish multifamily home.* BUILDER, 2023. **315(10)**: p. 74-83.
256. Mohammadi, M.M. and M. Janowski, *Evaluating the Impact of Horizontal Louvers on Natural Ventilation and Thermal Comfort in Polish Multi-Family Homes: A CFD Analysis*, in *9th EACWE*. 2025: Trondheim, Norway. p. 556-560.
257. Rodrigues, E., M.S. Fernandes, and D. Carvalho, *Future weather generator for building performance research: An open-source morphing tool and an application.* Building and Environment, 2023. **233**: p. 110104.
258. Ji, W., et al., *Interpretation of standard effective temperature (SET) and explorations on its modification and development.* Building and Environment, 2022. **210**: p. 108714.
259. Arsad, F.S., et al., *Assessment of indoor thermal comfort temperature and related behavioural adaptations: a systematic review.* Environmental Science and Pollution Research, 2023. **30**(29): p. 73137-73149.
260. Betti, G., et al., *CBE Clima Tool: A free and open-source web application for climate analysis tailored to sustainable building design.* Building Simulation, 2024. **17**(3): p. 493-508.